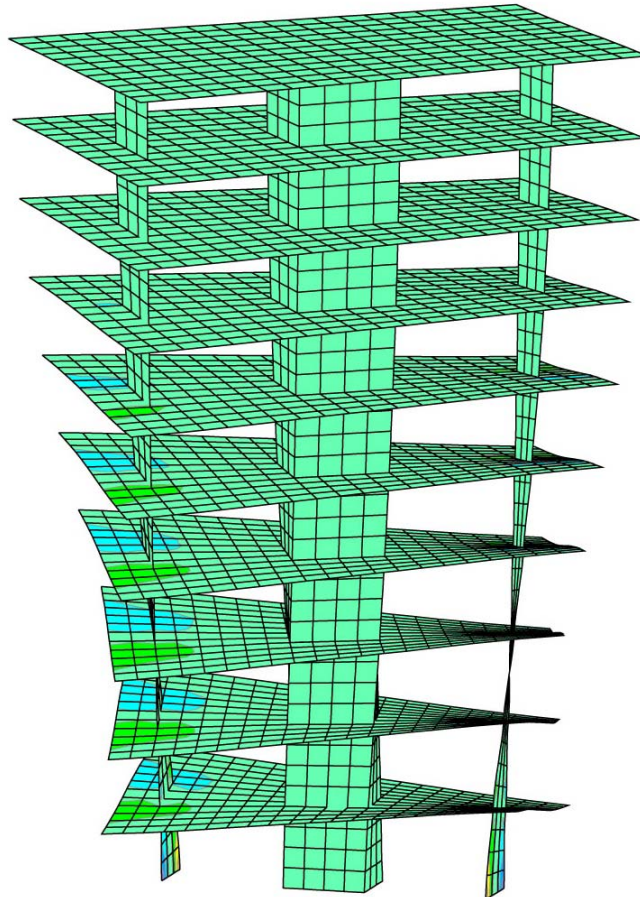


CHALMERS



Stability of Tall Buildings

DAVID GUSTAFSSON & JOSEPH HEHIR

Department of Civil and Environmental Engineering
Division of Structural Engineering
Concrete Structures
CHALMERS UNIVERSITY OF TECHNOLOGY
Göteborg, Sweden 2005

Master's Thesis 2005:12

MASTER'S THESIS 2005:12

Stability of Tall Buildings

DAVID GUSTAFSSON & JOSEPH HEHIR

Department of Civil and Environmental Engineering
Division of Structural Engineering
Concrete Structures

CHALMERS UNIVERSITY OF TECHNOLOGY

Göteborg, Sweden 2005

Stability of Tall Buildings

DAVID GUSTAFSSON & JOSEPH HEHIR

© DAVID GUSTAFSSON & JOSEPH HEHIR, 2005

Master's Thesis 2005:12

Department of Civil and Environmental Engineering

Division of *Structural Engineering*

Concrete Structures

Chalmers University of Technology

SE-412 96 Göteborg

Sweden

Telephone: + 46 (0)31-772 1000

Cover:

Deformation figure from a FE-analysis of a multi storey structure subjected to twisting.

Reproservice / Department of Civil and Environmental Engineering

Göteborg, Sweden 2005

Stability of Tall Buildings

DAVID GUSTAFSSON & JOSEPH HEHIR

Department of Civil and Environmental Engineering

Division of *Structural Engineering*

Concrete Structures

Chalmers University of Technology

ABSTRACT

The methods used for stability calculations of columns, solid shear walls, pierced shear walls, coupled and uncoupled components, cores, single storey structures and multi storey structures have been examined. The examination performed in order to ascertain short comings or advantages for different stabilising components and systems.

Analyses were made of deflection and buckling combining bending and shear for columns, solid shear walls and pierced shear walls. Calculation methods for single and multi storey structures concerning deflection and buckling due to translation, rotation or a combination of the two are analysed and the results are compared with finite element analyses results. The importance of pure torsion is somewhat neglected in these methods and therefore a method was devised for including a components torsional resistance in the calculations.

The calculation methods are computer assisted through the use of Matlab, Mathcad and Excel. Comparisons of results are made between the calculation methods and Finite Element Analysis performed with a programme called SOLVIA.

Vianello's method for calculating critical buckling loads, of columns and solid shear walls, due to bending has proven its worthiness. The method for calculating stability of pierced shear walls, according to studied, has proven itself to be in need of improvements. The use of the polar moment of inertia has proven to give inaccurate results. The result comparison of the single storey structures concerning translation, rotation and combined rotation and translation show that the calculation methods are satisfactory. Concerning multi storey structures subjected to translation or rotation a question arose concerning the interaction between the stabilising components and the floor slabs. The inclusion of a central cores own torsional resistance into the calculation methods led to improved results.

The results showed that further investigation of the calculation methods concerning stability of tall buildings is advisable and that specifically methods for determining the interactive behaviour of stabilising systems joined by floor slabs should be researched.

Key words: *Tall buildings; Stability; 2nd order effects; Global buckling; Vianello; Shear angle; Stiffness; Torsion; Warping;*

Contents

1	INTRODUCTION	1
1.1	Background	1
1.2	Aim and scope	1
1.3	Scientific approach	1
1.4	Methods presented	2
1.5	Limitations	2
2	TALL BUILDINGS	3
2.1	Evolution of tall buildings through the ages	3
2.2	Loads	10
2.2.1	Load distribution	11
2.2.2	Estimates concerning loads, environment and material	17
2.2.3	Loading assumptions	18
2.2.4	1 st and 2 nd order theory	20
2.3	Buckling and torsional phenomena	20
2.3.1	Bending and shear	20
2.3.2	Torsion	21
2.4	Principles for stabilisation of tall buildings	26
2.4.1	Stabilising components	26
2.4.1.1	Columns	26
2.4.1.2	Towers	26
2.4.1.3	Shear walls	27
2.4.2	Situating of stabilising components	28
2.4.3	Guidelines for choosing stabilising systems	30
2.5	Reality versus model	32
2.5.1	Theory of linear elasticity	32
2.5.2	Young's modulus	34
2.5.3	Long term effects	34
2.6	Problems concerning tall buildings	35
2.6.1	Comfort	36
2.6.2	Pierced shear walls	36
2.6.3	Load distribution	36
2.6.4	Twisting and open cross sections	37
2.6.5	Interaction between the soil and the foundation	37
2.6.6	Methods	38
2.6.7	Summation of the effect from approximation	39
3	CALCULATION METHODS FOR STABILISING COMPONENTS	40
3.1	Solid components – Columns and shear walls	40
3.1.1	Buckling load through bending – General calculations	40
3.1.2	Bending contribution of cantilever columns	43
	CHALMERS , <i>Civil and Environmental Engineering</i> , Master's Thesis 2005:12	III

3.1.3	Shear contribution of cantilever columns	44
3.1.4	Combined bending and shear	45
3.1.5	Derivation of magnification factor	46
3.2	Pierced shear walls	48
3.2.1	Derivation of buckling load	49
3.2.1.1	Bending in the transversal part	50
3.2.1.2	Bending in the vertical part	50
3.2.1.3	Shear in the transversal part	51
3.2.1.4	Shear in the vertical part	51
3.2.2	Calculation method for deflection	52
3.3	Vianello's method	55
3.4	Elastic restraint	64
4	CALCULATION METHODS FOR STABILISING SYSTEMS	67
4.1	Single storey system acting in a plane	67
4.1.1	Assumptions	67
4.1.2	Stiffness number	68
4.1.3	System of columns acting in one plane	69
4.1.4	Stiffness number for a non-stabilising unit	70
4.1.5	Horizontal load distribution among columns in a plane	71
4.1.6	Calculation method of moments on a single storey one plane system	72
4.1.7	Numerical example - Columns in one plane	75
4.2	Stabilisation systems – Buckling in space	79
4.2.1	General expression of translation and rotation	79
4.2.2	Derivation of critical buckling load through rotation	80
4.2.3	Calculation methods for establishing critical buckling load	82
4.2.3.1	Stiffness due to influence from shear	82
4.2.3.2	Location of the rotation centre	83
4.2.3.3	Simplification of stiffness numbers	83
4.2.3.4	Non stabilising units	84
4.2.3.5	Buckling load for single storey building – summation	85
4.2.3.6	Buckling load - Multi-storey expressions	86
4.2.4	Numerical example - Single storey structure	88
4.2.4.1	Buckling load through translation	89
4.2.4.2	Buckling load through rotation	91
4.2.5	Numerical example - Multi storey structure	93
4.3	Dimensioning forces and moments	96
5	INVESTIGATIONS	101
5.1	FE-analyses of solid shear walls	101
5.1.1	Check of FE-model	102
5.1.1.1	Modelling - Deflection of solid shear walls	102
5.1.1.2	Modelling - Buckling of solid shear walls	105
5.1.2	Results	108
5.1.2.1	Deflection	108
5.1.2.2	Buckling	109

5.2	Investigation of the Vianello method	110
5.2.1	Case 1: Even load, uneven stiffness	111
5.2.2	Case 2: Uneven load, uneven stiffness	113
5.2.3	Case 3: Slender wall - Uneven load, uneven stiffness	115
5.2.4	Case 4: Robust wall - Uneven load, uneven stiffness	117
5.2.5	Results	118
5.3	Investigation of pierced shear walls	119
5.3.1	Results of deflection and buckling load	121
5.3.2	Improvements for buckling load results	122
5.3.2.1	Altering the deformable length of the transversal	123
5.3.2.2	Shear factors	128
5.3.2.3	Shear angles	133
5.3.3	Stress distribution	136
5.3.3.1	Hand calculation methods	136
5.3.3.2	Results	139
5.3.4	Conclusions and recommendations	143
5.4	Investigation of the polar moment of inertia	144
5.5	Force distribution in single storey structures.	149
5.5.1	FE-model	149
5.5.2	Case 1 – Study of translation	150
5.5.3	Case 2 – Study of rotation	151
5.5.4	Case 3 – Study of combined translation and rotation	154
5.6	Study of the overall stiffness equation	158
5.6.1	Coupled and uncoupled approach	160
5.6.2	Case 1 - Coupled approach	161
5.6.3	Case 2 – Uncoupled approach	164
5.6.4	Conclusions	166
5.7	Force distribution in a multi storey structure	167
5.7.1	Modelling	167
5.7.2	Study of translation	169
5.7.2.1	Case 1a - Walls at the extremities	170
5.7.2.2	Case 1b - Walls close to RC	172
5.7.3	Study of twisting	174
5.7.3.1	Case 2a – Walls at the extremities	177
5.7.3.2	Case 2b – Walls close to the RC	179
5.7.3.3	Discussion	182
5.7.4	Torsional resistance in cores	183
5.7.4.1	Expression for including torsional stiffness of cores	185
5.7.4.2	Case 1 – U-shaped core	189
5.7.4.3	Case 2 – Closed rectangular core, load on top floor	190
5.7.4.4	Case 3 – Closed rectangular core, load on all ten floors	192
5.7.4.5	Results	193
5.7.5	Warping effects	194
6	CONCLUSIONS AND RECOMMENDATIONS	200
6.1	Conclusions	200
6.2	Recommendations	201

6.3	Further studies	202
7	REFERENCES	203
APPENDIX A	VIANELLO ITERATIONS	
APPENDIX B	RESULTS - PIERCED SHEAR WALLS	
APPENDIX C	FORCE DISTRIBUTION - SINGLE STOREY STRUCTURES	
APPENDIX D	FORCE DISTRIBUTION - MULTI STOREY STRUCTURES	
APPENDIX E	EQUATIONS FOR COUPLED COMPONENTS	
APPENDIX F	CALCULATION OF BUCKLING LOADS IN MATHCAD	

Preface

This thesis is the culmination of 4½ arduous years of study at Chalmers University of Technology, Sweden. It has been produced through the cooperation of Reinertsen Sverige AB and the Division of Structural Engineering at the Department of Civil and Environmental Engineering of Chalmers University of Technology.

Professor Björn Engström, the examiner, has provided continued assistance and invaluable insights on stability during the production of this work. Morgan Johansson, PhD, of Reinertsens has supervised this endeavour diligently. Morgan has helped considerably through his clarity, enthusiasm and his unselfish willingness to assist while directing this project.

Assistance, for which we are very thankful, with the FE-programme SOLVIA has been provided by Ginko Gueorguiev of Reinertsens.

Our opponents, Morgan Mathiasson & Nicklas Karlsson, have continually assisted with the development of this thesis and we thank them wholeheartedly. Good luck to both of you for the future.

Finally, but certainly not least, we wish to thank our families who have persevered with us through our studies at Chalmers. Without their love, patience, commitment and understanding this thesis would never have been completed. Maria, Anja, Erik, Sasha and Bonnie, we thank you for enduring with us.

Göteborg February 2005

David Gustafsson & Joseph Hehir

Notations

Roman upper case letters

A	Cross sectional area, constant depending on load application
B	Constant depending on shape of the 2 nd order vertical load, bimoment
B_x	Stiffness value due to influence of shear in the x -direction
B_y	Stiffness value due to influence of shear in the y -direction
C	Overall stiffness value
C_{DIR}	Directional coefficient
CG	Centre of gravity
C_{TEM}	Seasonal coefficient
C_{ALT}	Altitude coefficient
E	Young's modulus
E_{ef}	Young's modulus due to long term effects
G	Shear modulus
H	Horizontal force
$H_{inclination}$	Horizontal force due to unintended inclination
I	Moment of inertia
I_p	Polar moment of inertia
I_t	Moment of inertia in transversal part of pierced shear walls
I_v	Moment of inertia in vertical part of pierced shear walls
K	Factor used for determining deflections in pierced shear walls
$K_{1,2,3,4}$	Factors for determining warping conditions
K_v	Torsional stiffness cross section factor
K_w	Warping stiffness cross section factor
L	Height of a member
L_b	Length of beam
L_c	Buckling length
L_h	Total height of building or structure
L_{sec}	Storey/section height
M	Moment
M_0	Initial bending moment (1 st order)
M_d	Total bending moment (2 nd order included)
M_{er}	Restraint moment
M_{tot}	Total moment (local moment included)
$M_{twist,S}$	St. Venant moment contribution
$M_{twist,V}$	Vlasov moment contribution
$M_{twist,x}$	Total torsional moment
N	Axial force
$N_{cr,B}$	Critical buckling load, considering bending

$N_{cr,col}$	Critical buckling load considering a single column
$N_{cr,elrest}$	Critical buckling load considering elastic restraint
$N_{cr,S}$	Critical buckling load considering shear
$N_{cr,sys}$	Critical buckling load for a system in one plane without shear
$N_{cr,tot}$	Critical buckling load, considering both bending and shear
RC	Centre of rotation
V	Shear force

Roman lower case letters

a	Length of floor slab
b	Breadth of floor slab, distance between the centres of each vertical part in a pierced shear wall
b_0	Total breadth of pierced shear wall
c	Deformable length of the transversal part of a pierced shear wall
c_0	Width of gap in pierced shear walls
e	Eccentricity
h_t	Height of transversal in pierced shear walls
j	Stiffness number
k	Factor concerning bending
k_E	Euler parameter concerning bending
k_V	Vianello parameter concerning bending
m	Torque per unit height
n	Number of storeys
q_h	Distributed horizontal load
q_v	Distributed vertical load
q_{ref}	Reference wind velocity pressure
r^{-1}	Curvature of deflection
r_0^{-1}	Initial curvature
r_{Δ}^{-1}	2 nd order curvature
t	Thickness, time
w	Displacement
x	Distance from the structure's rotational centre to the individual unit's rotational centre in the x -direction
x_{RT}	x -coordinate that describes the position of the rotational centre of the structure
$x_{RT,unit}$	Coordinate that describes the position of the rotational centre of a stabilising unit in relation to the defined origin, in the x -direction
x_T	Displacement of the structures rotational centre to the centre of gravity in the x -direction

y	Deflection, distance from the structure's rotational centre to the individual unit's rotational centre in the y -direction
y_0	1 st order deflection, total deflection used in Vianello's method
y_{RT}	y -coordinate that describes the position of the rotational centre of the structure
$y_{RT,unit}$	Coordinate that describes the position of the rotational centre of a stabilising unit in relation to the defined origin, in the y -direction
y_{tot}	Total deflection (2 nd order effects included)
y_T	Displacement of the structures rotational centre to the centre of gravity in the y -direction
y'	Angle of deflection (slope)
y''	Curvature of deflection
v_{ref}	Reference wind velocity
$v_{ref,0}$	Initial reference wind velocity
v_{tot}	Total deflection (2 nd order effects included)

Greek upper case letters

ΔM	Secondary moment (2 nd order)
Δy	2 nd order deflections
$(\Sigma N)_{cr}$	Total critical buckling load
$(\Sigma N)_{cr,B}$	Total critical load, considering bending
$(\Sigma N)_{cr,elrest}$	Total critical load, considering elastic restraint
$(\Sigma N)_{cr,S}$	Total critical load, considering shear

Greek lower case letters

α	General symbol for angles, variable used in calculating deflections in pierced shear walls
α_m	Inclination factor
α_s	Angle of deflection due to shear
β	Shape factor for magnification factor (A/B)
β_c	Factor describing development of creep
β_s	Factor describing development of strain
γ_{er}	Angle describing elastic restraint
$\gamma_{t,bend}$	Component of shear angle concerning bending in the transverse part of a pierced shear wall
$\gamma_{t,shear}$	Component of shear angle concerning shear in the transverse part of a pierced shear wall
$\gamma_{v,bend}$	Component of shear angle concerning bending in the vertical part of a pierced shear wall

$\gamma_{v, shear}$	Component of shear angle concerning shear in the vertical part of a pierced shear wall
γ_{tot}	Total shear angle for pierced shear walls
ε	Strain
ε_{cs}	Shrinkage strain
$\varepsilon_{ce,0}$	Notational shrinkage coefficient
ξ	Shear reduction factor
σ	Stress
σ_W	Warping stress
τ_b	Shear in partially connecting beam of a stabilising core
μ	Variable used in calculating deflections, shear friction coefficient
φ	Change of angle, angle
φ_0	Notional creep coefficient
φ_{ef}	Creep factor
θ	Twisting angle per unit height
χ	Rotation of the beam's cross section
ψ	Angle of rotation
ω	Sectorial coordinate

Other indexes, such as *left*, *right* and *centre*, exist in this thesis in order to identify the situation of a specific parameter. Directions are represented by the subtexts *x*, *y* and *z*.

1 Introduction

1.1 Background

The increased demand for taller structures requires that a structural engineer is familiar with the buckling phenomena that can occur in such a building and so complete competent calculations. The engineer must have an understanding of workable calculation methods for designing this type of structure and must also be confident in using them.

Reinertsen Sverige AB were interested in instigating a Masters Thesis on this subject and The Division of Structural Engineering at The Department of Civil and Environmental Engineering at Chalmers University of Technology, Gothenburg, Sweden obliged. This thesis would provide the company with a deeper understanding of the phenomena that are involved in stability calculations and hopefully a workable method for future calculations.

1.2 Aim and scope

The aim of this thesis is to provide a concise and usable method for analysing stability of tall structures. The respective calculation methods published by Westerberg (1999) and Lorentsen *et al.* (2000) are standard works in Sweden which have been chosen for investigation. A basic understanding of the parameters involved in the calculations shall be provided. These existing calculation methods will be presented and analysed in order to identify discrepancies that may exist in the methods. Analytical calculations of components, individual and in combinations shall be demonstrated and FE-analysis will be performed to compare the results and in order to ascertain how much the results concur. This thesis is produced in a pedagogical format in order for it to be used educationally.

1.3 Scientific approach

A substantial literary study has been completed while obtaining relevant information on calculation methods for designing for stability in tall buildings. Numerical examples; of calculating buckling loads for single and multi storey structures; of deflections and buckling in solid shear walls; of deflections, buckling and stress distributions of pierced shear walls; of force distributions in single storey structures; of coupled and uncoupled approach to calculating U-shaped core elements; of force distribution in a multi storey structure, are presented and compared with FE-results in order to draw conclusions on the reliability of the calculation methods.

1.4 Methods presented

Westerberg (1999) and Lorentsen (2000) approaches for considering the contribution from 2nd order effects for calculating stability on single and multi storey structures are examined.

The Vianello method for calculating critical buckling loads due to bending is introduced and compared with the approximate method and FE-analyses.

Regarding pierced shear walls, two methods are presented. One method is utilised for establishing the buckling load for the wall and a second method is used for deriving the top deflection of the wall subjected to a horizontal distributed load. Both methods are taken from Lorentsen *et al.* (2000)

Two methods concerning the calculation of a complete structure are investigated. One approach regards only the calculation of the critical buckling load for the whole structure. The second method is used for one storey structures and is more accurate as the load distribution is taken into account in a more exact manner.

A method for including torsional resistance in the stability calculations is devised by the authors of this thesis.

1.5 Limitations

Stability analysis of tall buildings is a huge subject which requires years of active study in order to attain a relatively complete understanding. In order to contain the thesis to a workable size it has been decided to limit the study to linear analysis. All of the concrete elements in this thesis are assumed to be uncracked and the effects of temperature, creep and shrinkage are not taken into account. Non-linear analysis may be investigated by a follow up group of graduate engineers. Dynamics is an advanced field of theory which shall not be dealt with here. This work shall concentrate on static problems. Stabilising systems consisting of frameworks, façades and tubes, are mentioned and their functionality is ascertained while calculations, on these types of stabilising elements, are not pursued. Methods concerning treatments of connections are not included in this thesis but the problems are brought up.

In this thesis the limitations has been drawn to study problems or inaccuracy concerning stabilising structures consisting of shear walls, towers and columns. Problems concerning detailing, such as joints and connecting details, for transferring loads between different parts through a building are not studied in detail. Some of these problems are discussed as they are important to consider especially in cases where twisting occurs.

2 Tall buildings

To define a tall building it is best to decide from whose perspective one is looking. A bureaucrat may decide that anything over 5 storeys is a tall building and from this decision he may categorise accordingly and be very satisfied. For a structural engineer it is not so simple. A tall building is, from a structural engineer's perspective, to be considered tall when, due to its height, the lateral forces suffered by the structure play a significant role in the design. [Smith and Coull (1991)]

2.1 Evolution of tall buildings through the ages

The great metropolises of the world share common dilemmas. Increased population densities due to the migration of people from the countryside to the cities, combined with the rising price of developable land and the environmental politics of the day provide the city councillors with no better solution than to build higher. Human nature also compels us to achieve that which has previously not been accomplished and all through history, from The Tower of Babel to The Empire State Building, has man endeavoured to reach the sky.

From an historical point of view it has been defence, power and religion that have driven humanity to build high. Defensive fortifications had to be high and robust in order to be effective. Figure 2.1 shows an Irish Round Tower, built by Christian Monks around 1000 AD, which stretched 30 metres into the sky and was used as a refuge for when the Vikings would come plundering. The material used is granite stones joined by mortar. Great respect is due the monks who built this tower because they built a stable structure using little structural engineering knowledge and only using materials that were ready at hand. The choice of design is worth noting because these monks opted for a structure which is both aerodynamic and resistant to torsion, because of its uniform form. [Ireland Mid-West (2004)]



Figure 2.1: Kilmacduagh Round Tower Ireland, 30 metres high (circa 1000 AD). [Interactive Interpretative Centre of the Burren (2004)]

Building tall to display power can be exemplified by the biblical story of the Tower of Babel, Figure 2.2, and how the descendents of Noe built a tower in the land of Sennar (modern day Iraq) in order to reach the skies and so show God how mighty they had become. Of course God was not happy about this and demolished the Tower and scattered the descendents of Noe across the globe. This was in prehistoric times, about 5,500 BC, so no real records survive. King Nebuchadnezzar II of Babylon (605 – 562 BC) is reputed to have built a tower on the foundations of the original. His tower is historically verifiable and he managed to build a tower 90 metres high using only baked bricks made of mud and straw, joined by a mortar made of bitumen, which is a mixture of tar like hydrocarbons which are derived from petroleum. [Global Security (2004)]. Great rulers had to build great monuments to show how powerful they were. The victories of Nelson and Napoleon inspired the inauguration of tall monuments to show the world how great these men, and how powerful the nations they defended, were. Even today there is a certain respect given to the countries that can build the highest in that their ability to build high represents their might.



Figure 2.2: *Bruegel's depiction of The Tower of Babel. [Museum of unnatural mystery (2004)]*

Religion has always inspired people to build tall structures. The pyramids of Egypt and Mexico are fine examples of this. The building of cathedrals in Europe, pagodas in Japan, mosques in The Middle East and temples in India have brought forth the ingenuity of the builders and have shone as beacons to their respective worshippers. Looking at a wonderfully huge, graceful and artfully carved structure the believers were filled with awe for the power of the respective God/Gods who inspired the edifice. In Europe the construction of cathedrals led to the establishment of a quasi-religious status for the masons who were designing these amazing structures. Cologne Cathedral was begun in 1248, Figure 2.3, and the masons used their knowledge to build a structure that must have installed awe in all who looked upon her. They were

very secretive of their calculation methods, their chemical compositions of mortar and their methods of construction. The finances to build high came from the church but the knowledge came from the masons/engineers.



Figure 2.3: Cologne Cathedral, 156 metres high. [Service t-online (2004)]

Considering the buildings constructed for the common people it is best to start with the Romans. Before Nero's fire of 64 AD, Rome had a multitude of four storey tenements built of wood. After the fire, the four storey wooden tenements were replaced by tenements built with new brick and concrete materials which were used to form arches and curved dome structures. Over the centuries there were no great leaps in material science so timber and masonry were the norm. The timber structures were not strong enough to build over five storeys and they were very susceptible to fire. The masonry possessed high compressive strength and it was fire resistant but its lower supports could not take the weight of very high buildings. Most cities in Europe have experienced catastrophic fires because their buildings were mostly made of wood. The great fire of London in 1666 led to a possibility to rebuild the city in brick. A similar fire occurred in Chicago in 1871 which also made way for construction in brick. The best that could be done, height wise, with masonry was achieved in 1891, in Chicago, when the 16 storey Monadok Building was erected by the engineers Burnham and Root. To build this structure the bottom floor had to have 2 m thick walls which quite depleted the usefulness of that floor. [Smith and Coull (1991)]

To build higher than this it was necessary for new materials to be produced and their properties examined. The industrial revolution provided the materials wrought iron and steel and also provided the social impetus for building higher as more workers from the countryside were required to work in the factories, so houses had to be provided for them. The necessity of having workers near at hand to the factories and that land was in short supply led to the solution of building higher. The term high-rise began to be used to describe tall buildings and with the development in steel production more and more, ever higher, buildings were being built. The first steel frame structure, Rand-McNally Building in Chicago Figure 2.4, was built in 1889 by Burnham and Root and was 10 storeys high. (Smith, Coull 1991)



Figure 2.4: Rand-McNally Building Chicago, 10 storeys, 1889. [American Institute of steel construction (2004)]

A mile stone was reached in 1891 when diagonal bracings, used to form vertical trusses, were used in the 22 storey Masonic Temple, Chicago Figure 2.5. This is the forefather of today's shear wall and braced frame constructions. The engineers, Burnham and Root, decided on introducing the above mentioned diagonal bracings above the 10th floor. They chose steel for the rigid frames and wrought iron as the material for the bracings. This building remained the tallest in Chicago until the 1920's because the city council enacted height restrictions after its inauguration. [Smith and Coull (1991)]

One further important factor in building higher was the invention of the elevator. One could not expect people to spend time and energy climbing stairs and the rents for the top floors were actually lower than rents for the lower floors, so the elevator had to be incorporated into designs. The first elevator was installed in The Equitable Life Insurance Building in New York in 1870, designed by Gilman, Kendell and Post, led to the landlords being able to charge equal rents for the lower and upper floors as they were now equally accessible. The invention of the electric elevator in 1890 made it possible for landlords to build even higher buildings without having to worry about if they could effectively rent out the floor space on the higher floors. [Smith and Coull (1991)]

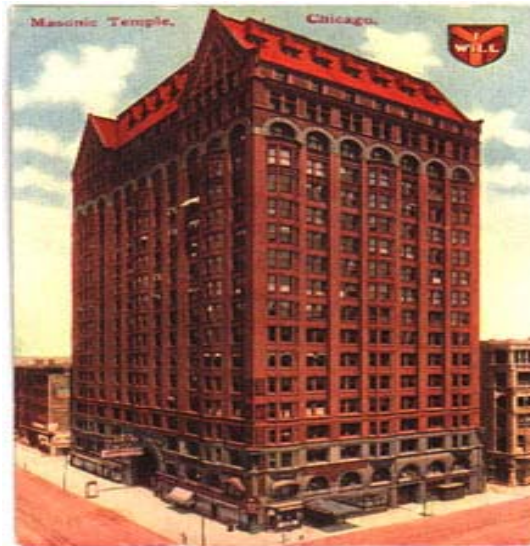


Figure 2.5: *Masonic Temple, Chicago, 22 storeys, 1891. [The skyscraper museum (2004)]*

Design methods became more sophisticated and construction techniques were refined until in 1913 The Woolworth Building in New York, Figure 2.6, designed by Cass Gilbert (architect) and Gunvald Aus (structural engineer), reached a height of 58 storeys. This building remained the tallest building in the world until 1930. The structure was built to withstand winds of up to 360 km/h, it contained thirty elevators and it was the first building to have its own steam turbines installed. When building such a huge structure it is very important to envisage the foundation required for a soil consisting of alluvial mud and sand for depth of 30 m. Gunvald Aus chose pneumatic caissons (French for big box), which use air pressure to expel water, for founding the 66 concrete piers that would connect the structure to the ground. A caisson is a large hollow box, made of steel, which is driven into the ground, excavated and then filled with concrete. The basements themselves began at 16.5 m below ground level. In order to withstand the 360 km/h winds that the building was designed for Gunvald decided to have different stabilising systems in different parts of the building. The lower stories employed a portal system of braces, that is a combination of struts and ties which lie in the plane of the inclined braces, were used to transfer wind pressure from the upper parts of the trusses to an abutment. The tower construction was more complicated and girder and knee brace stiffening was chosen. Two design solutions, for the tower, that could have been better thought out were that the wall columns did not get direct column support from below and were therefore carried by girders and that where the columns were counterbalanced, the transfer of wind shear in the outer faces of the tower must have been made through the floor. [Smith and Coull (1991)] [The skyscraper museum (2004)]



Figure 2.6: The Woolworth Building, New York, 1913. [Kent State University (2004)]

The end of the skyscraper era was heralded by the building of The Empire State Building in New York (1931). A steel riveted frame was used and the building reached a height of 102 storeys which wasn't surpassed until the raising of the first tower of the World Trade Centre in 1973. As The Empire State Building was the largest project undertaken up to that time, three structural engineering companies were employed. The structure was so well designed that, in 1945, it withstood the impact of a B-25 bomber on the 79th floor. Fourteen people were killed when one of the engines passed through the entire building but the structure held, only sustaining damage to the outer wall. [Emporis (2004)]

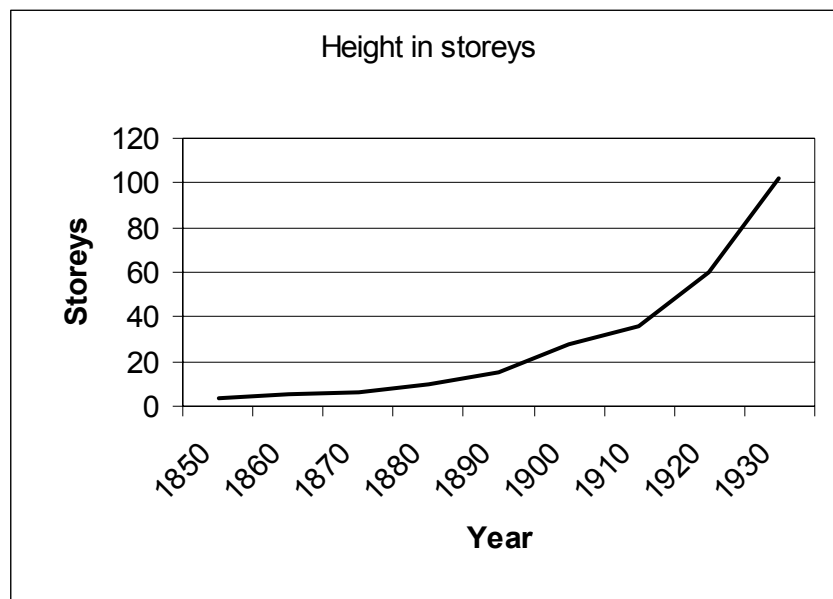


Figure 2.7: Time line of structure height in storeys.

Figure 2.7 shows how building height increased from 1850 to 1930 in the USA. After 1931 and the construction of The Empire State Building, the United States fell into a depression and the consecutive commencement of World War II meant that further increase in building height was halted until 1973, when the first tower of The World Trade Centre was erected. [Smith and Coull (1991)]

The World Trade Centre, 110 storeys, used an innovative structural model designed by John Skilling and Les Robertson who chose a system that was simplistic but effective. This building was the first to use no brick or stonework. They used the steel façade as a wind bracer to provide the stability while the central core took all the self weight. The wind bracing façade, made of closely spaced steel columns, was attached to the central core by steel floor trusses. The central core itself contained the elevator shafts which were specially designed. The engineers were worried about the air pressure which could lead to buckling of the shafts, so the elevator designers created a system of elevators that was divided between a local and an express system. A traditional system would have meant that half the area of the lower stories would have been taken up by elevator shafts so stop off points for the elevators were installed on the 44th and the 78th floor. After the aeroplane collisions of the 11th of September 2001 it is widely assumed that the steel trusses connecting the façade to the central core over heated and lost their rigidity leading to a progressive collapse of the structure. It is although notable that the structures did withstand the impact of the passenger planes. [Department of Civil Engineering, University of Sydney (2004)]

After the cessation of combat in World War I reinforced concrete was used to imitate steel forms. The full potential of reinforced concrete had not been fully realised although The Exchange Building in Seattle, 1930, did reach 23 storeys. It was not until after World War II that radically new structural and architectural solutions were propagated through the realisation that reinforced concrete can be easily formed in order to satisfy architectural specifications and structural integrity. [Smith and Coull (1991)]

In the past, city councils have commissioned land on the outskirts of their cities for development but the advances in environmental science over the last decades have recognised the vital importance, for the atmosphere, of maintaining land in its natural state, plus the importance of arable farming for providing fresh provisions for the cities. The availability of fresh produce may not be so problematic in the western world, because of the advanced infrastructure, but the developing nations see this as a major quandary. The tides of human migration are as unstoppable as population growth but the cities of developing lands have to decide whether to commandeer more arable land or to build higher. Here, in the West, are many large urban areas that are slowly eating up the natural land which exists around them. Large conurbations such as the Ruhrgebiet in Germany and the Lille area of Northern France are facing health problems due to their difficulties in holding down pollution levels. One can especially look to South-East Asia where cities such as Hong Kong, Shanghai and Singapore have chosen to build higher, in order to accommodate their citizens, instead of succumbing to urban sprawl. *Table 2.1* gives the heights achieved depending on the usage of the building in order to show that tall structures are not only office buildings. [Emporis (2004)]

Table 2.1: The current highest buildings according to usage, and some Swedish buildings.

Usage	Name	City	Height (m)	Floors	Year
Offices	Taipei 101	Taipei	509	101	2004
Lodging	Ryugyoug Hotel*	Pyongyang	330	105	1992
Residential	21st Century Tower	Dubei	269	55	2003
Education	Moscow University	Moscow	240	36	1953
Hospital	Guy's Tower	London	143	34	1974
Offices	Kista Tower	Stockholm	128	32	2001
Residential	Turning Torso	Malmö	190	54	2004
Lodging	Gothia Tower W.	Gothenburg	70	23	2001

* Structurally complete but not yet in use.

It is evident, due to the existence of tall buildings, like Kista Tower, that the skills and knowledge to build higher do exist in Sweden. Gothenburg is not as crowded as the cities of South-East Asia but it is hoped that the City Fathers are beginning to see the advantages of constructing taller buildings. To build further on the outskirts of Gothenburg means that more farm land and more forest will be lost. Gothenburg is still experiencing an increase in population due to economic migration of workers and so shall further accommodation, to work, to play and to live, be required. Obviously people who work in the city may also want to live near to their place of work in the city. This involves the economic aspect of supply and demand, where if there are enough customers who are willing to pay then industry will find a way to provide for them.

2.2 Loads

This chapter will discuss how loads are applied, the estimations and assumptions that have to be studied and the implications of 2nd order effects. The use of codes will be explained and the assumptions used for implementing service limit state, SLS, and ultimate limit state, ULS, will be clarified.

2.2.1 Load distribution

With tall buildings it is important to understand how and which loads are applied where on the building. The loads can be divided very simply between vertical and horizontal burdens. The vertical loads are the weight of the building, imposed load and snow load. The horizontal loads are wind and the unintended inclinations.

The vertical loads are taken up by the bearing walls, columns or towers and are led to the foundations. The loads occurring from the wind are first taken by the façades and are then further distributed to the slabs.

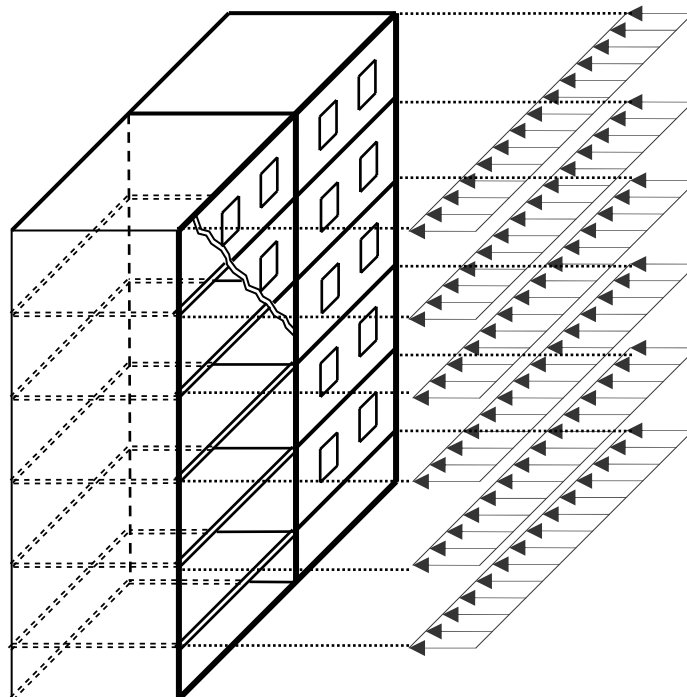


Figure 2.8: Multi-storey structure with applied wind load.

The floor slabs act as diaphragms and are often considered to be stiff in their plane and deformations in its plane is usually disregarded. The slabs are connected to the stabilising units, such as shear walls, towers or stabilising columns. Figure 2.8 shows a multi storey building with the wind loads applied as they are interpreted to be.

Some facades also have columns attached directly to them and in these cases the loads are first transferred to the columns resulting in concentrated loads on the floor slabs. See Figure 2.9.

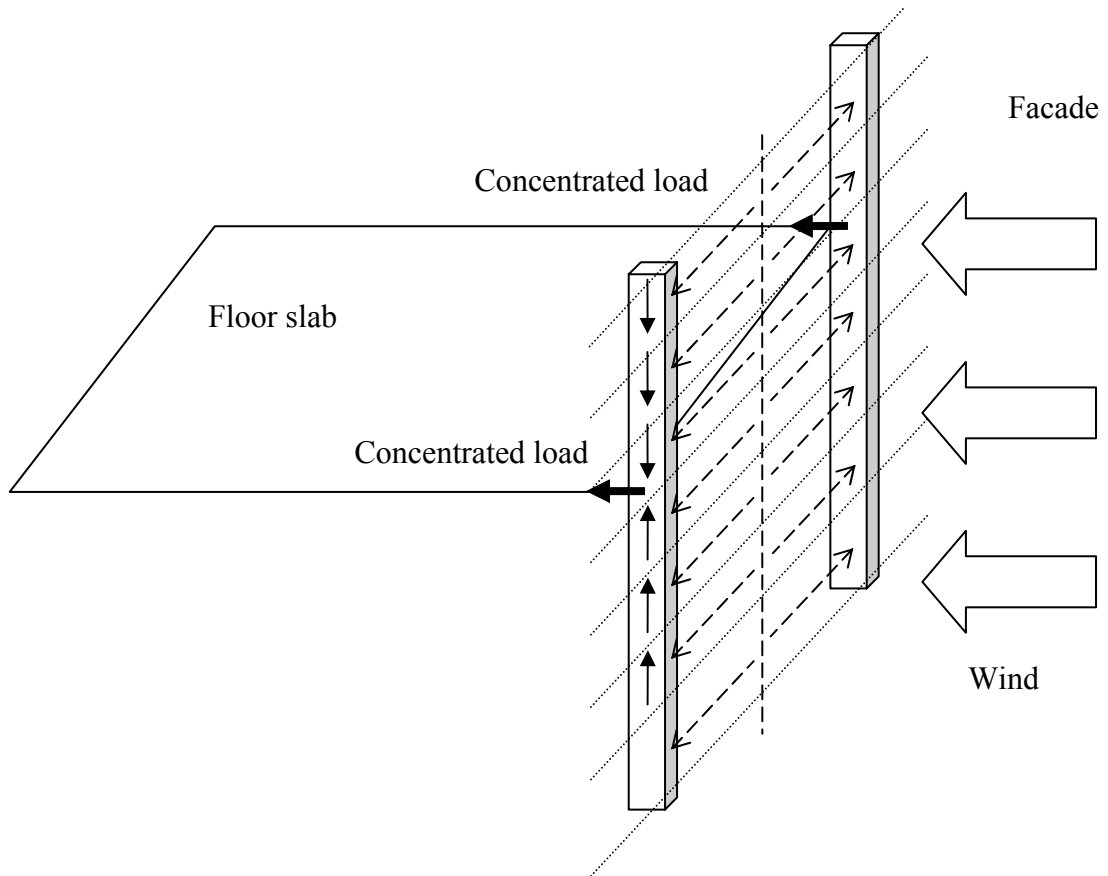


Figure 2.9: Wind load on facade causing concentrated loads in a floor slab.

If the façade which takes the wind load is supported by the floor slabs, then the floor slabs will be subjected to a distributed load, see Figure 2.10. Compared to Figure 2.9 the different load application causes a different stress distribution in the slab. The stress distributions have to be dealt with through careful planning of how the slabs and the facade are connected. Floor slabs are often considered to be stiff, and the horizontal load distribution through the building is due to the stiffness of the different stabilising components. If the floor slab is not stiff enough, or slip occurs in joints between slab elements in the same plane, then the displacement of the floor slab will not be the same along the loaded side of the floor slab, as in Figure 2.9. Stress distribution in floors depends on both loads and supports.

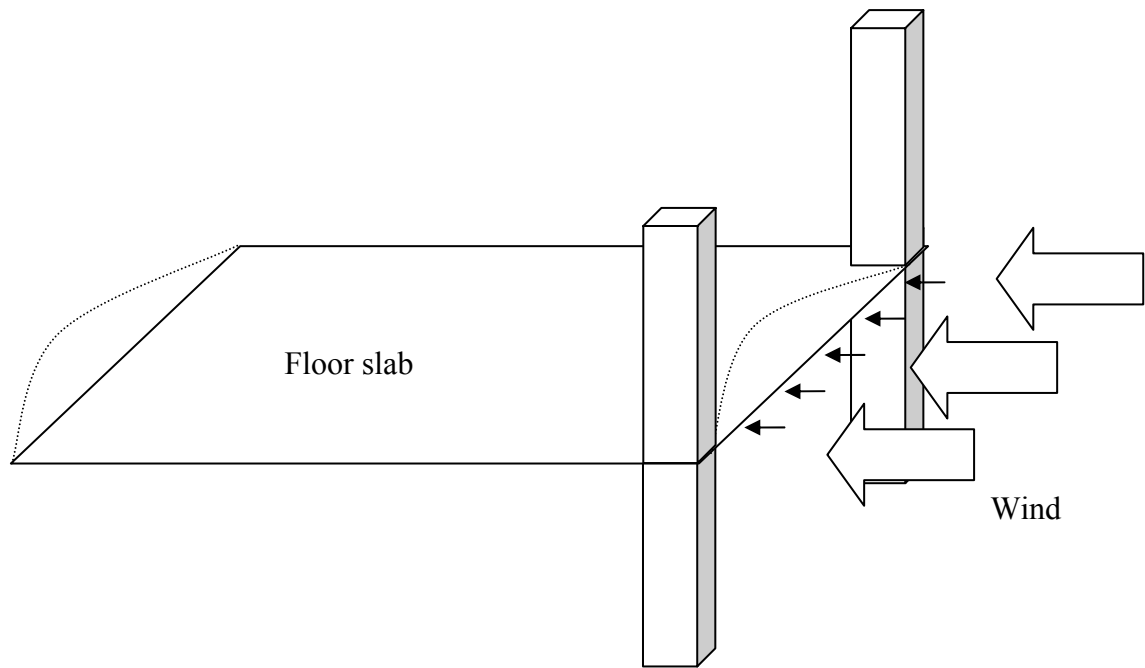


Figure 2.10: Façade attached directly on the floor slab.

How the floor slab will react to a distributed load is shown in Figures 2.11 and 2.12. If the slab is assumed to be stiff then the load is distributed according to the stiffnesses of the stabilising units i.e. stiffer units will attract a greater part of the applied force than weaker units. Figure 2.11 describes a load case which assumes a uniform lateral movement seen from the top of the structure. The dotted line represents the original position of the slabs and the shear walls. This load situation can be compared to a stiff beam standing on spring supports and if the supports have equal stiffness then the load will be evenly divided among them, see Figure 2.11.

Figure 2.12 shows a load case where the slab is not assumed to be completely rigid and bending occurs due to the distributed load. Now a system is presented where the load distribution along the three supports is not only dependent on the stiffness of the supports. With normal beam theory it is assumed that the supports are endlessly stiff and the load is distributed among the supports according to elastic theory. In a case with 3 supports the middle support will attract $10/8 qL$ of the load and the outer supports will attract $3/8 qL$. L refers to the span between the supports. Figure 2.12 shows a situation where the load distribution is hard to establish or predict. Here there is a combination of load distribution depending on both the stiffness of the supporting walls and the bending in the slab due to elastic theory.

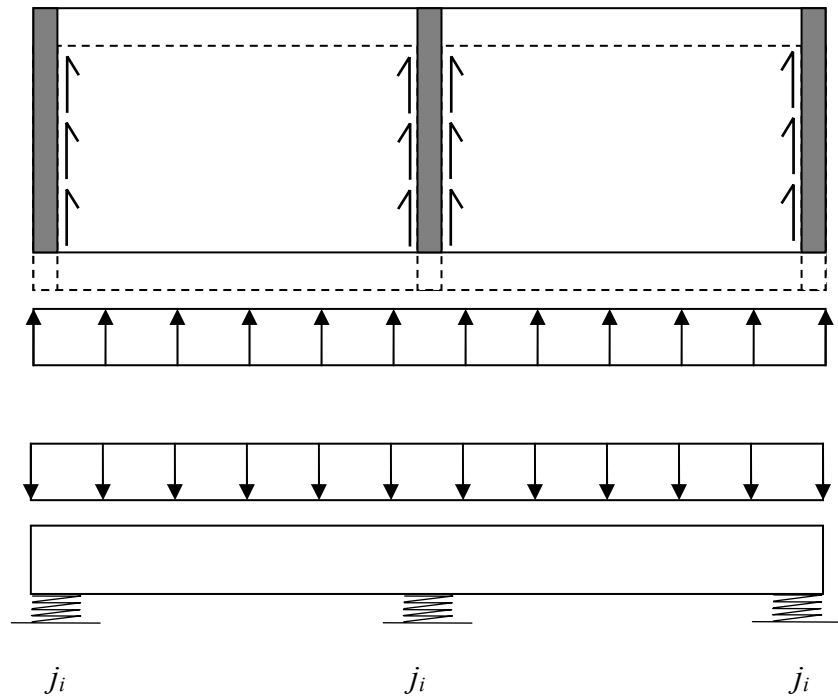


Figure 2.11: Load case which assumes a uniform lateral movement of the slab.

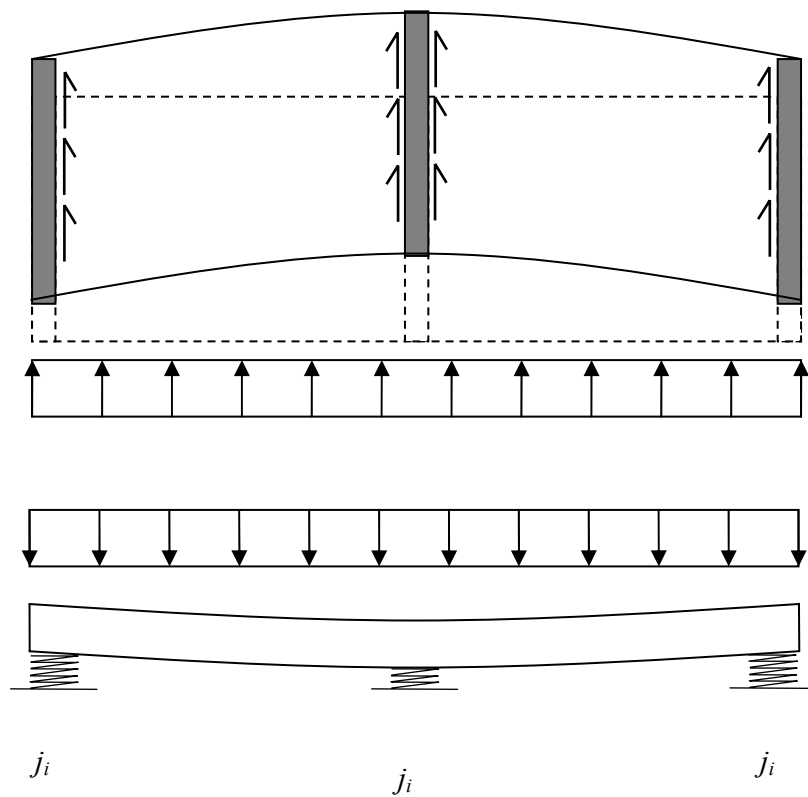


Figure 2.12: Load case where the slab is not assumed to be completely rigid and bending occurs due to the distributed load.

If the floor slabs are assumed to be stiff and the case shown in Figure 2.11 presents a model resembling the real structure, it is of vital importance to ascertain that bending does not occur in the slabs themselves. In Figure 2.12 it is shown that the middle wall is subjected to greater deflections than the outer walls, subtracting greater forces than it is dimensioned for.

The floor is supported by the stabilising units through a shear force distributed along the width of the wall. The walls are subjected to both bending and shear deformations but in low robust walls the bending contribution is negligible. See Figure 2.13. If slender units are used for stabilising then bending mainly occurs and shear deformation is negligible.

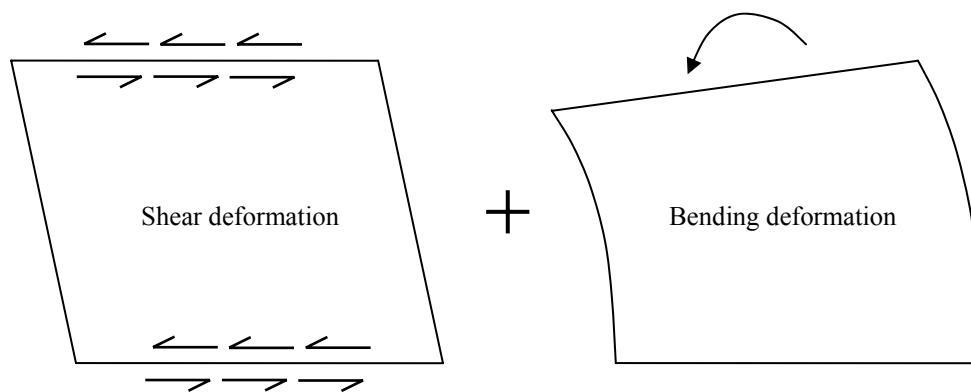


Figure 2.13: Bending and shear deformations.

When the entire structure is considered, even though shear walls are considered as low and robust in each floor, the shear wall becomes more slender in taller structures. It is therefore necessary to consider both bending and shear when calculating on tall buildings. Figure 2.14 presents shear and bending deformation of a tall shear wall subjected to a distributed load along the height. The deformation from bending is curved in the opposite direction to the shear deformation. The deformation from shear is due to the shear forces applied through the floor slabs in each storey. As the loads accumulate and increase through the building the largest singular deformation occurs at the first floor for the shear contribution. Figure 2.15 shows a FE-analysis representation of a pierced shear wall subjected to both bending and shear.

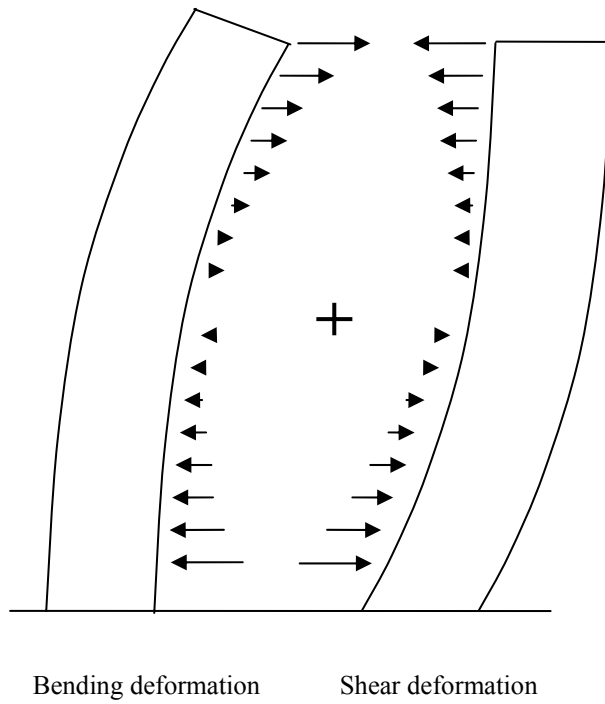


Figure 2.14: Shear and bending deformation of a tall shear wall subjected to a distributed load along the height.

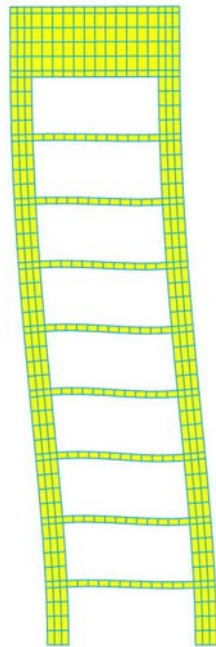


Figure 2.15: FE-analysis representation of a pierced shear wall subjected to both bending and shear.

2.2.2 Estimates concerning loads, environment and material

Considering how accurately the stability of a tall building can be calculated, concerning functionality during the entire projected service life of the structure, one must make certain assumptions concerning the external and the internal environment, degradation of the material and accidental impacts or loadings, and natural disasters.

External climate conditions will affect the stability of a structure through wind, humidity, rain and temperature variation. The treatment of wind loads, specifically in tall buildings, is very well documented in Eurocode (1991). [Zalka (1992)]

First a reference wind velocity is ascertained:

$$v_{ref} = C_{DIR} \cdot C_{TEM} \cdot C_{ALT} \cdot v_{ref,0} \quad (2.1)$$

The value $v_{ref,0}$ is defined as the 10 minute mean wind velocity at 10 metres above the ground of terrain category II (urban terrain) having a mean return period of 50 years. Different terrains have different factors depending on if the structure will be on a shore line, urban, countryside or suburban. The value itself is derived from the extensive records that are kept on wind conditions in each country. From this value it can be plainly seen that stronger winds may occur and especially for tall buildings where wind loading is vital, this value will have to be altered. Coefficients of direction, C_{DIR} , season, C_{TEM} , and altitude, C_{ALT} , will be taken in to account to derive a reference wind velocity. This value will be used to attain the reference wind velocity pressure.

$$q_{ref} = \frac{\rho}{2} \cdot v_{ref}^2; \quad \rho = \text{air density} \quad (2.2)$$

This value will be further altered through coefficients for exposure, topography, roughness, gust wind response, aerodynamics, external pressure and also specifically for tall buildings the structure will be divided into different heights where different roughness and exposure factors will be applied. While determining the load cases, consideration must also be given to suction that will occur on walls and roofs due to the wind. All of these factors are based on intense investigation but are still models of reality and extreme buildings have to take into account even more extreme conditions which lead to the design engineers of extremely tall buildings having to sometimes develop their own extreme factors. [Eurocode (1991)]

The effects of rain, humidity and temperature variation on a structure which has stability components on the outer shell may be hazardous over a long period of time. The engineer has to establish a relevant period of time before reparations to the structural components have to be made. Here again the engineer has to rely on weather statistics developed over the last century and then further take into account the extreme conditions that may occur. Again the engineer has to work with a model of reality.

The internal environment of a building is controlled by the heating and ventilation systems. The stability components of the structure should be isolated against internal

influences and there should not really be a problem concerning the internal environment. What the engineer has to be careful with here is the materials that are used for protecting the stability components. Whether it is paint, wood or concrete the engineer has to be aware of their material values concerning for example permeability which could, under extreme conditions, allow damaging moisture to reach the material of the stabilising components. Service life analysis of these materials would be necessary in order to determine maintenance episodes and so protect the stability system. Assumptions are again made while determining for example humidity or water spillage.

2.2.3 Loading assumptions

The loads on a building are modelled through investigating the buildings usage, situation and dimensions. Concerning dimensions there are no assumption made as all dimensions are real. On the other hand the usage of the building and the situation of the building require a closer look. The engineer has access to codes which describe specifically how load combinations are calculated using factors, considering situation and usage, in order to ascertain loading values for Service Limit State, SLS and Ultimate Limit State, ULS. Considering usage it is important for the engineer to pay considerable attention to the imposed loads. For this the engineer has access to codes which give values per m² of floor space for different activities and also factors to be used when establishing load cases. All of these factors and values are based on assumptions which are designed to always keep the engineers calculations on the safe side. [Eurocode (1991)]

Considering the calculations of load cases concerning SLS and ULS one must first look at the engineering community and how it works. As mentioned previously, a structural engineer's primary concern is safety. The engineering community today tends to produce specialised engineers who are not experts in all the fields of study required to build a safe building, but rather produces engineers who are specialised in for example materials, climate control, structural integrity and geotechnics. This requires that the engineering team are able to understand the assumptions made by each other. Ideally the engineers will use the most appropriate design and construction techniques, the best available materials and the most up to date environmental data. On top of this, safety factors will be applied in order to insure that the calculations will be pessimistic and so shall the building be considered safe. [Zalka (1992)]

Consider a building where the designer knew exactly the material properties of the components, knew exactly how they would behave under the projected life time of the building, knew exactly how the building would be serviced and also had access to exact data concerning internal/external environment and the projected loading histories of the building. This building would require no safety factors. Because of these discrepancies the structural engineer is required to incorporate partial factors into his/her design calculations at an early stage. These factors are multiplied to the basic variables in order to give pessimistic values concerning the variables performance. [Zalka (1992)]

It is analytical theory based on elastic and non-elastic behaviour that has led to the development of load conditions i.e. SLS and ULS. In the beginning of the design

process the structural engineer will directly reduce the material property values of the components by using partial factors which are applied to either ULS or SLS. It seems logical to assume that a structure designed for SLS should by definition be safe; meaning that it will not collapse, because in order for the building to be serviceable it must be safe, but this is not the case because it is ULS that considers collapse. Should the engineer then wholly disregard SLS and only calculate in ULS?

ULS considers ultimate loading in different load combinations. It is not possible to evaluate a specific safety factor which describes the safety margin that exists between SLS and ULS. The way the theory of SLS and ULS works is that the loading factors applied in ULS describe initially an assumed structural behaviour of the building, not if it will actually fail or not. Reality is not the same as the model. [Zalka (1992)]

Loads have to be assigned load-paths. These are determined through establishing how the loads are applied, how the loads will transfer through the stabilising system and finally how these loads will be taken up by the foundations. A relationship exists where the number of potential load-paths and the number of stabilising elements is related to the number of potential load-carrying mechanisms within the elements and the joints between them. A particular loading case will only initiate a certain number of the load paths available. Interdependence must exist between each path in order for a structure to retain stability while each successive mechanism comes into effect. To increase the possibility of sustaining a system of load-paths it is advised to insure that the load-paths are intertwined meaning that the more integrated the stabilising system is the better the system will absorb loads. [Zalka (1992)]

A further affect on loading is obtained through the unintentional inclination of supporting elements. Inclinations, of columns, that may exist in the building are assumed through using the factor α_m in the equation below which determines the horizontal load due to inclination, $H_{inclination}$.

This value is derived through the equation below where n is the number of columns above the storey being examined.

$$\alpha_m = 0.0003 + \frac{0.012}{\sqrt{n}} \quad (2.3)$$

$$H_{inclination} = \Sigma N \cdot \alpha_m \quad (2.4)$$

It is often regular for the engineer to assume that the stabilising components of a structure are fully fixed. This assumption implies that the stabilising component in question and the ground it is anchored in react in union. This assumption assumes that the ground itself is solid and does not have elastic properties. This assumption is fine for structures anchored in the bedrock but those anchored in soil present more difficulties. Anchorage in soil leads to it being necessary to calculate with elastic restraint included. This requires that the soil properties of the ground in question have to be examined and it is well known that it is difficult to determine soil properties exactly. It is therefore important for the engineer to remember that the restraint values determined by the geological investigation are in error to a degree of 30%. [Lorentsen *et al.* (2000)]

2.2.4 1st and 2nd order theory

In order to understand stability one has to first understand the theory that is utilised while calculating. When calculating with columns, shear walls and towers one has to take into account both 1st and 2nd order theory. 1st order theory explains the direct results of actions, moments and deflections. 2nd order theory takes into account the additional moments that occur because of the 1st order deflections combined with axial loads. [Westerberg (1999)]

A transverse load is applied at the centre of the column, Figure 2.16. From this load, a deflection y_0 and a moment M_0 occur. With the application of an axial load is gained a further deflection Δy and a compliment moment ΔM . M_0 and y_0 are 1st order effects and ΔM and Δy are 2nd order effects. See chapter 3.1.5 on the derivation of the magnification factor. The 2nd order effects are due to axial loads combined with the 1st order deflection

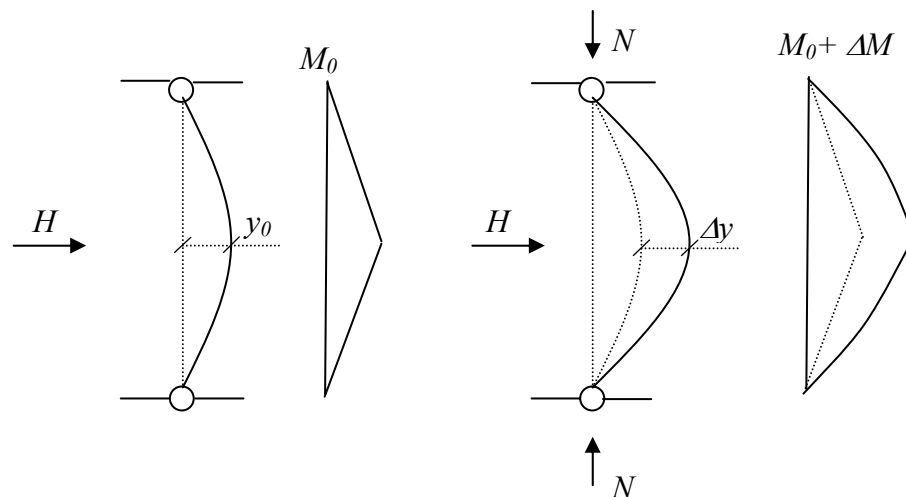


Figure 2.16: 1st and 2nd order deflections and moments. Based on Westerberg (1999).

2.3 Buckling and torsional phenomena

2.3.1 Bending and shear

Buckling is a phenomenon which occurs when a structure is subjected to axial load suffers uncontrolled large displacement, transverse to the load. Transversal buckling, i.e. in plane, has two contributions, bending and shear. The bending deformation causes a curved shape. The shear deformation results in straight inclined shape. Combined they result in the critical buckling mode displayed in Figure 2.17.

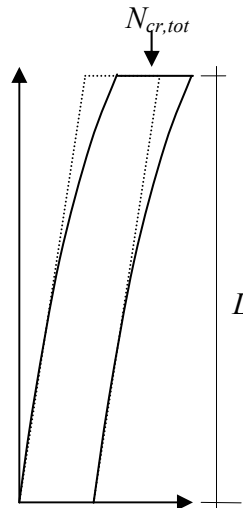


Figure 2.17: Combined bending and shear.

2.3.2 Torsion

The occurrence of torsional buckling in tall buildings is a well studied phenomenon which is generally not adequately applied by structural engineers. [Smith and Coull (1991)] Torsion involves a twisting action, due to applied vertical or horizontal loads. When a vertical load is applied buckling through translation may be replaced by a first buckling mode due to twisting. Observe in Figure 2.18a how the torque about the rotation centre occurs. Here is shown a stabilising component which does not have a coinciding centre of gravity and rotational centre. The applied vertical load results in a torsional action about the centre of rotation, behind the tower where the rotation centre is situated. Figure 2.18b shows how a cross section of the stabilising component is influenced by tension and compression occurring because of the stresses due to the torsion. Displacement due to twisting will occur. The bottom end of the element is assumed to be fixed to the ground.

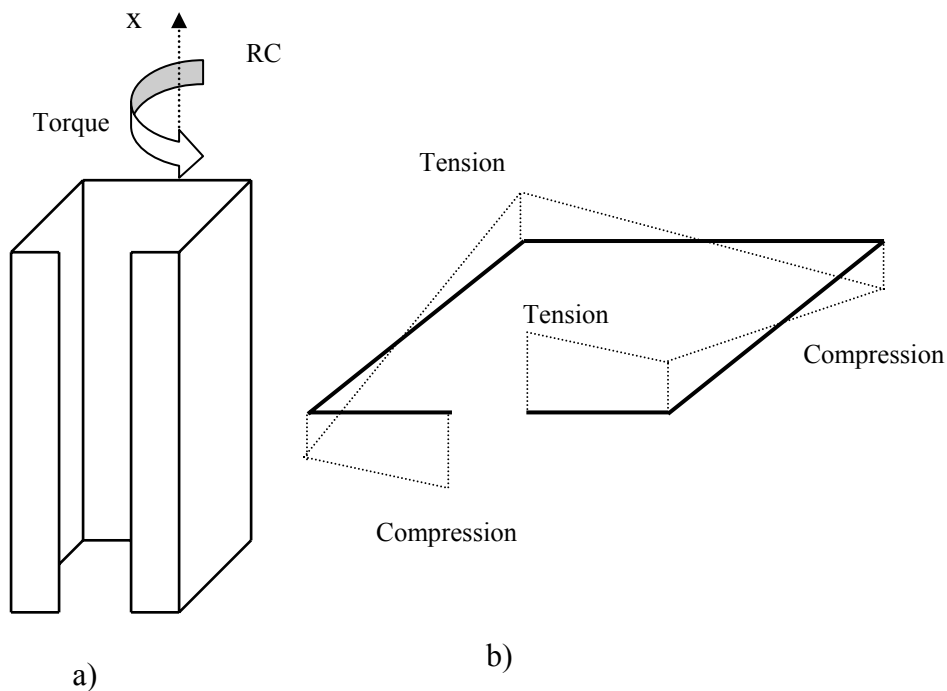


Figure 2.18: Core showing how applied torque on the rotational centre causes tensions and compressions in the cross section.

Eccentric horizontal loading of a stabilising element leads to torsion and sectional torsional moments along the length of the element. In order to calculate the torsional moment at a specific point in the stabilising component it is necessary to consider two contributing factors. The equation below shows the relationship.

$$M_{twist} = M_{twist,S} + M_{twist,V} = GK_v \theta - EK_w \theta'' \quad (2.5)$$

M_{twist} = Torsional moment around the x axis

$M_{twist,S}$ = St. Venant component of torsional moment

$M_{twist,V}$ = Vlasov component of torsional moment

G = Shear modulus

K_v = Twisting stiffness cross-sectional factor

K_w = Warping stiffness cross-sectional factor

θ = Twist per unit height

Figure 2.19 below shows how the patterns of shear flow due to torsion occur in different stabilising element forms. Observe how the closed cross-section b) has an overall closed shear flow while example c) shows a dramatic change in the shear flow

due to the cross section being open. Example a) shows how the shear flow in an I-girder is mapped.

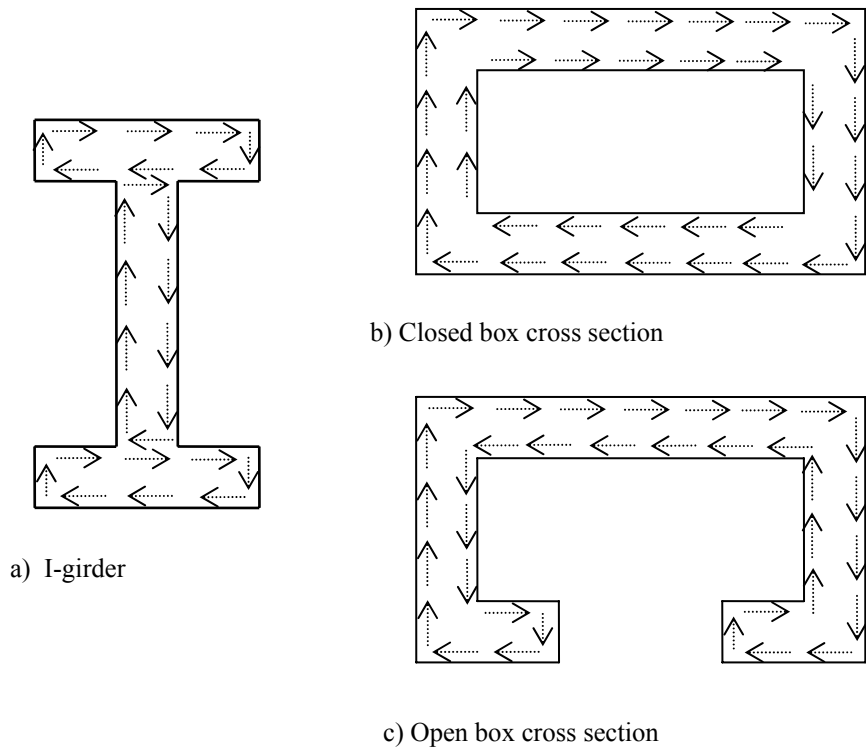


Figure 2.19: Shear flow due to torsion in three cross sections.

St. Venant torsion is observed when the torsional cross-sectional moments are entirely taken up by the shear stresses. If axial stresses occur then they participate in taking up the torsional moment through warping resistance. This effect is called Vlasov torsional resistance. Observe Equation (2.5) and how the St. Venant and the Vlasov components combined make up the total torsional moment. How this equation is developed is explained in Samuelsson and Wiberg (1993).

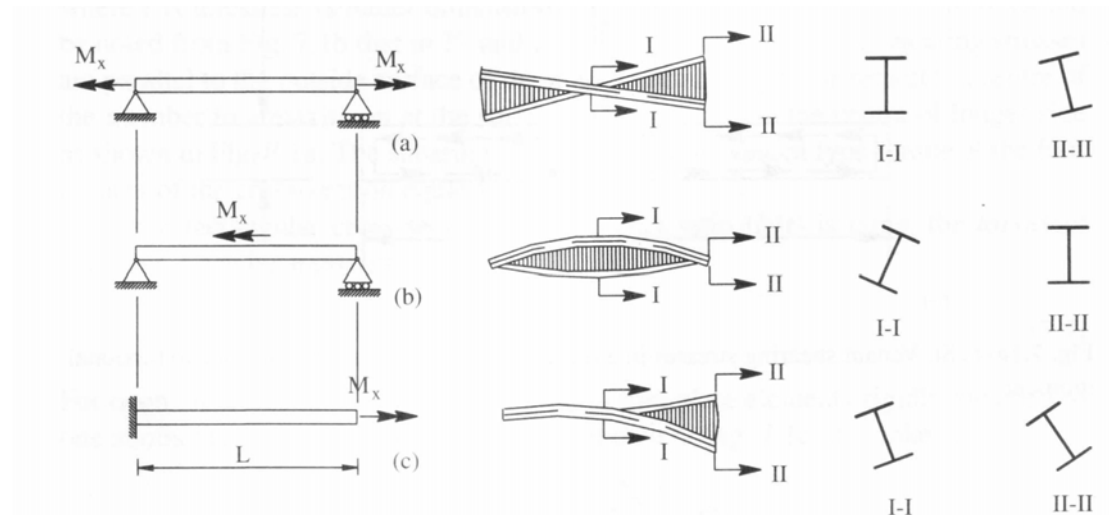


Figure 2.20: Torsional moment distortions [Gambhir (2004)]

Figure 2.20 shows three girders subjected to different torsional moments. The first girder, marked a) is simply supported and torque is applied from both ends. Observe that rotation about the x -axis is allowed which means that the girder is not restrained and therefore has no warping displacement which leads to the conclusion that no warping stresses exist. Uniform torsion is observed, which induces only St. Venant stresses. This means that the flanges will remain straight. [Gambhir (2004)]

The second girder, marked b), is restrained with pronged supports at the ends and a torque is applied at the centre. Now the girder can not rotate about the x -axis which leads to the development of warping stresses; hence shall the flanges not remain straight. Observe that, due to symmetry, the St. Venant contribution is highest at the ends and abate towards the centre while the Vlasov contribution is at its maximum in the centre and diminish towards the ends. This symmetry causes the elimination of warping displacements at the centre. [Gambhir (2004)]

The third girder, marked c) is a cantilever which actually represents half the girder represented in case b). Here the girder is fixed at one end and the torque is applied at the end. Here we see the occurrence of warping. The Vlasov stresses are highest at the top and the St. Venant stresses are highest at the fixed end. [Gambhir (2004)]

If this girder is placed in the vertical, then a core in a tall building is represented, see Figure 2.21. The displacement of the flanges due to warping causes points a) and c) descend while the points b) and d) ascend. This axial displacement is due to Vlasov stresses. Observe that in this example the rotational centre is positioned at the centre of the web. This is due to the double symmetry that exists in an I-girder with flanges of equal length.

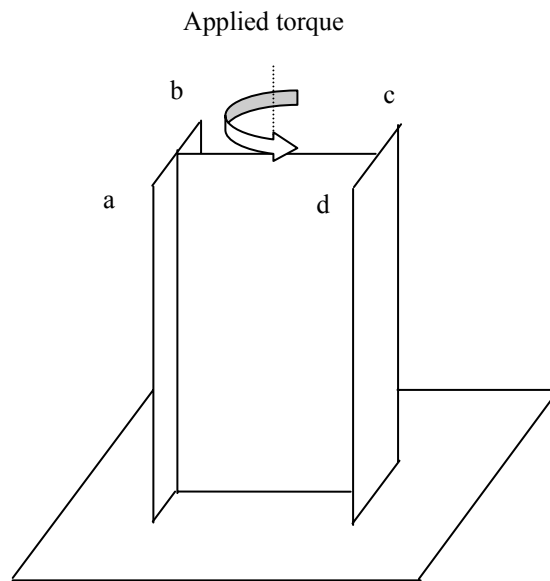


Figure 2.21: Torque in an I-shaped core due to Vlasov unrestrained stresses.

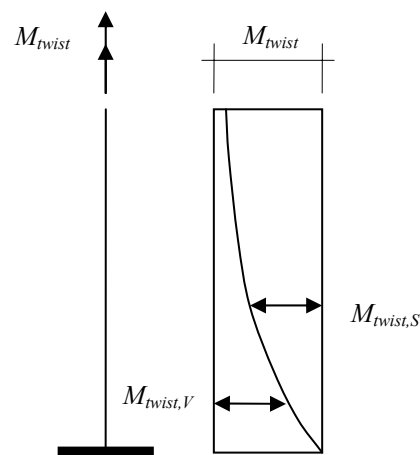


Figure 2.22: St. Venant and Vlasov contributions to the twisting moment.

Figure 2.22 shows how torsional moments are divided along an I-girder. The Vlasov contribution is greatest at the fixed end and least at the free end. The opposite is true for the St. Venant contribution.

These phenomena are not only reserved for steel girders. When concrete walls of composite form i.e. T-shaped, U-shaped, H-shaped and so on, are utilised in tall buildings then St. Venant and Vlasov stresses can occur. How to deal with the warping phenomenon is generally not well known to structural engineers and specific investigation of its occurrence is advised for all stability calculations. [Smith and Coull (1991)]

2.4 Principles for stabilisation of tall buildings

2.4.1 Stabilising components

This section intends to describe and explain the stabilising components: columns, towers and shear walls. Stabilising components are assumed to be fully fixed at the base and hinged at the top. Non-stabilising units are assumed to be hinged at both ends and therefore, since they must be braced by stabilising elements, have a negative contribution to stabilisation.

2.4.1.1 Columns

A linear structural member which takes vertical loads can generally be called a column. They consist of steel, wood or concrete depending on the strength and/or the aesthetics required. Columns are found mainly in structures in order to provide support for beams or slabs. When calculating stability in a structure with columns it is essential to ascertain if the column is stabilising or not. This means that non stabilising elements have to be held up by the stabilising elements so they have a certain negative effect on the over all stiffness of the system. Section, 4.1.3 explains this phenomenon.

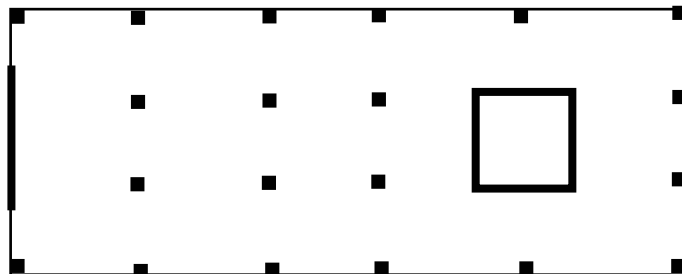


Figure 2.23: A shear wall paired with a tower which combined takes care of stability.

Figure 2.23 shows a stabilising system. The columns are used to take the load from the floors but may still have a positive or negative effect on stability depending on their rigidity, placement and connections.

2.4.1.2 Towers

Towers, reinforced concrete for this thesis, are rigid cores situated inside tall buildings. Usually a tower will exist with another tower or combined with shear walls and/or with columns. The combined effect will give rise to a greater resistance to torsion depending on how the units are situated in relation to each other. Ideally they are situated as far apart as possible for creating a torsional resistance. A disadvantage with using a single tower, on its own, is that it is susceptible to torsion and must therefore be heavily dimensioned in order to resist torque.

The use of towers is favourable in that they can be used not only as stabilising units but also as elevator shafts or stairwells. Funnelling of ventilation shafts, water pipes and electric cables can also be hidden within the tower giving the architect more manoeuvrability and the client more effective use of the space provided.

Towers which have open cross sections, for example U-shaped or H-shaped, have less resistance to torsion than closed sections and should in general be combined with other stabilising components.

2.4.1.3 Shear walls

Shear walls, made of reinforced concrete, are used in modern buildings because of their effectiveness in maintaining stability and for the freedom they offer the architect who is designing. A shear wall's position in a building is often initially decided by the architect. The architect is trained to design for the buildings function and appearance and not for its stability so when a structural engineer is not involved in the first phase of design, it may lead to the shear walls being situated in non-favourable positions. Also, while choosing reinforced concrete walls as partition walls, the architect can be unintentionally gaining stabilising elements. Pierced shear walls are described as shear walls with holes. These holes can be windows or doors that are necessary for access or lighting for the building.

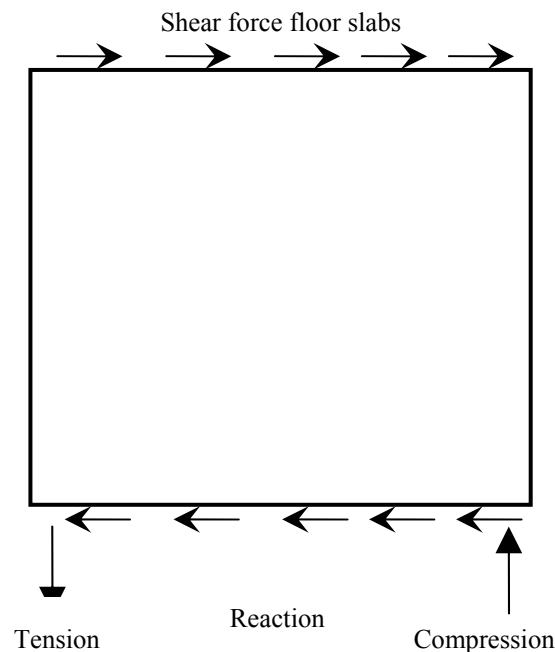


Figure 2.24: A shear wall with horizontal load applied.

Figure 2.24 shows how a typical shear wall functions. The force from the horizontal wind load results in shear forces which act within the wall and tension and compression resulting at the ground.

2.4.2 Situating of stabilising components

Stabilising walls may also be placed in certain positions in a building to help with sound isolation. An apartment tower block may have a stabilising wall system resembling Figure 2.25 in order to divide effectively against sound intrusion from the neighbouring apartments. The central stairwell or lift shaft, marked *S*, will be pierced because of door openings for accessing the apartments, while the four stabilising walls will be solid and will effectively isolate the occupants from each other.

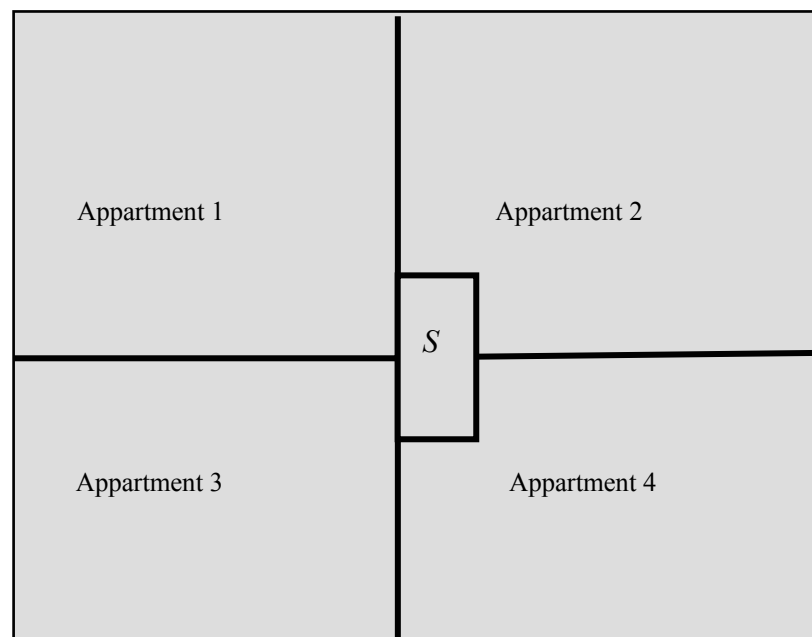


Figure 2.25: Stabilising system when walls are required to also act as sound isolators.

In modern buildings it is fashionable to have an open foyer on the ground floor. This open, spacious and welcoming area does cause problems for the structural engineer because the stabilising walls have to be discontinued for this floor. Here it is advisable to have shear walls or pierced shear walls on the side of the building so that stability can be assured and the architectural integrity of creating open spaces can be maintained.

This thesis does not consider façades but rather towers, shear walls, columns, and combinations of these three stabilising components. Observe that the use of one stabilising component, such as a concrete core tower at the centre of a building, on its own, is not recommended as it can be susceptible to torsion but it can be usable if the component is designed with very high torsional stiffness. The placing of the rotational centre at the centre of the building is advised because it exceedingly reduces the buildings susceptibility to twisting due to evenly distributed horizontal loads. The placing of shear walls as far from the centre of gravity as possible is advisable in order to increase the resistance to torque. Figure 2.26 shows some examples.

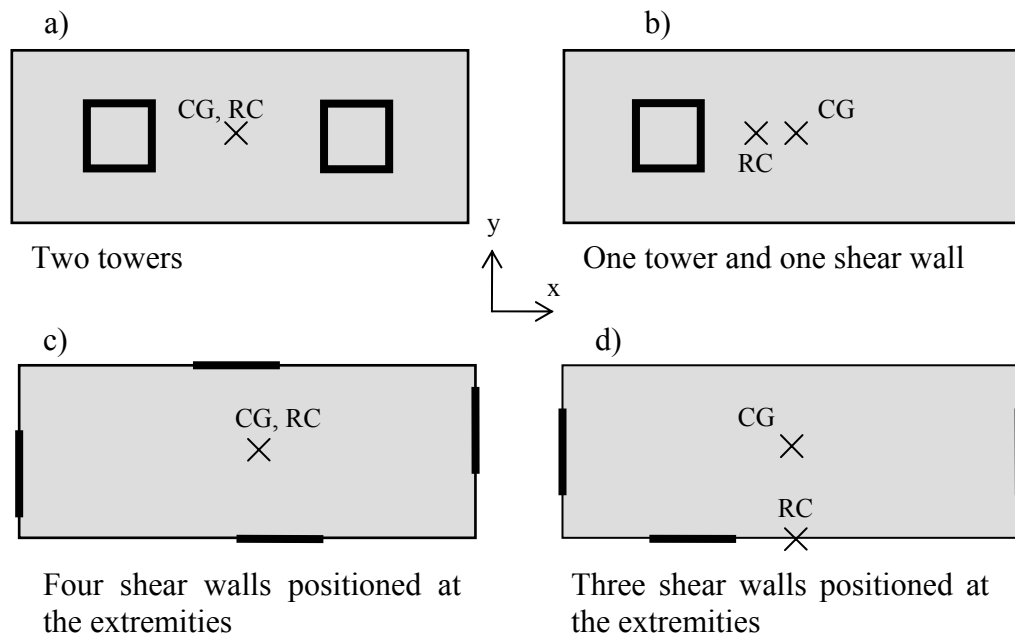


Figure 2.26: Examples of locations of stabilising units.

Observe that in Figure 2.26 the buildings have no central core tower that acts independently and that the shear walls are situated at the extremities.

Observe the difference between the four walled and the three walled examples. The three walled example, Figure 2.26d, is referring a case where the minimum stability is attained. To obtain minimum stability there has to be at least one wall in each direction for stabilising through translation. To also attain stability through rotation the structure requires at least two walls stabilising in one direction. It can be observed, in the last picture, Figure 2.26d, that a distributed horizontal force in the x direction will lead to the occurrence of a large twisting in the structure. Figure 2.26c has a fourth wall which help to achieve a better stability, especially for distributed load cases.

2.4.3 Guidelines for choosing stabilising systems

The choice of frame is important while developing concepts of tall buildings. Fazlur Kahn, an engineer who designed many skyscrapers in USA, has stated that “I strive for structural simplicity.... The technical man mustn't be lost in his own technology”. He means that the supporting structure does not need to be complicated and he developed principles in the selection of stability system considering the height of the building. [Lorentsen *et al.* (2000)]

- 15 storeys: A framework of fully fixed columns and beams, consisting of stiff joints which are able to take up moments. Both pictures marked *a)* in Figure 2.27 and 2.28.
- 25 storeys: A framework of pinned columns and beams which are connected to a central tower consisting of concrete or vertical trusses. Both pictures marked *b)* in Figure 2.27 and 2.28.
- 40 storeys: Fully or partially fixed columns and beams with shear walls or vertical trusses situated at the extremities of the building. Picture *c)* from Figure 2.27 and a combination of pictures *a)* and *b)* from Figure 2.28.
- 60 storeys: The same as for 40 storeys but complemented with additional strategically placed horizontally trusses, encircling the top and then more further down. Picture *d)* from Figure 2.27.
- 80 storeys: Façade columns between themselves connected to façade beams to make a framework. The façades have a united action so that they together function as a rectangular tube restrained in the foundations. Pictures *e)* and *f)* from Figure 2.27.
- 100 storeys: Façade walls consisting of combined frameworks and trusses. The façades have a united action so that they together function as a rectangular tube restrained in the foundations. Pictures *e)* and *f)* from Figure 2.27 and picture *f)* from Figure 2.28.
- 110 storeys: Here the building is divided into many rectangular tubes so that each inner column has a direct cooperation with the façades. The tubes each reach a different height in the building so as that the wind loads influence is reduced to the minimum. Picture *f)* from Figure 2.27.
- 120 storeys: An outer façade, acting as a tube, combined with large trusses attached for increased stability. Picture *g)* from Figure 2.27.

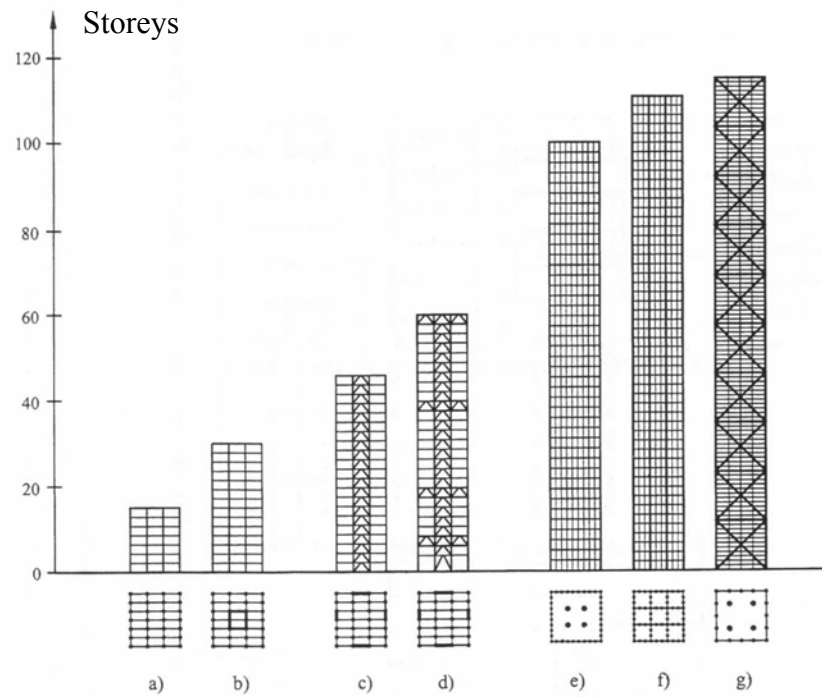


Figure 2.27: Stabilising systems depending on the number of storeys. [Lorentsen et al. (2000)]

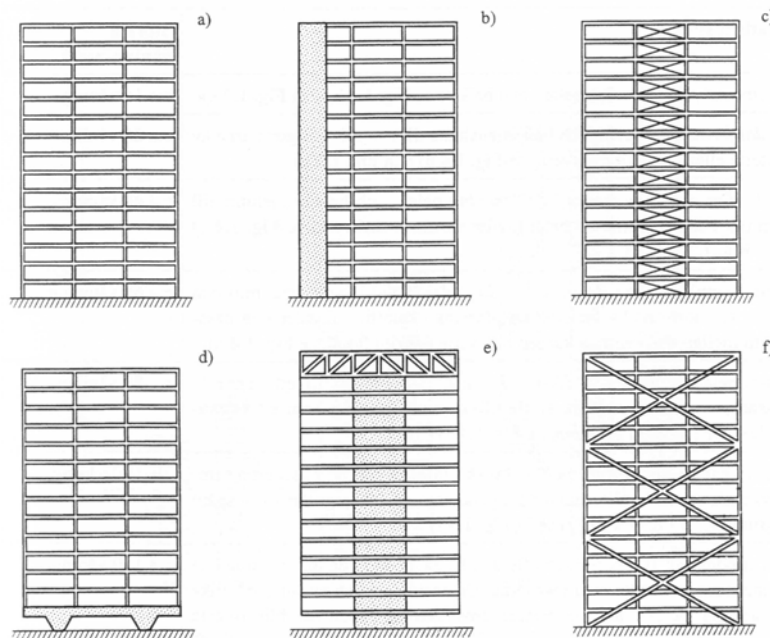


Figure 2.28: Examples of stabilising systems. [Lorentsen et al. (2000)]

Fazlur Kahn's recommendations are usable but, because of architectural influences, the engineer is often given a very complicated stabilizing system to calculate.

Especially here in Sweden it is suspected that engineers tend to enter the design phase at a late stage. Perhaps introducing engineers at an earlier stage will give the engineers more chance to influence the final design and so keep to Fazlur Kahn's principle of simplicity.

2.5 Reality versus model

This Section will attempt to describe specifically the difference between the model the engineer creates, in order to design for stability, and the actual reality that exists. All the various estimations that the engineer has to deal with and some assumptions that he/she has to make will be extensively explained and hopefully present an understanding of how much the engineer relies upon his/her own understanding of the factors applied in order to eventually produce a model that is as near to reality as is required.

An engineer models a structure through attempting to imitate as the reality that exists for the structure being designed. Considering stability of a building it is the robustness of a structure during its service life and its ability to resist loads which requires modelling. The engineer must construct a model of how the loads should be transported to the ground and how the stabilising elements interact. The engineer must consider the stiffness values of the individual stabilising elements and the combined system concerning translation and rotation; how the relative load cases are calculated concerning SLS or ULS. The service life of the structure has to be considered and how the assumptions on interior/exterior climatic impact, degradation of materials and natural disasters or accidental impacts can be quantified. All of these considerations have to be intelligently modelled using assumptions and partial factors to resemble as the reality that exists for that specific structure. [Zalka (1992)]

Recently, engineers have recognised the advantages of developing data on reliability margins through using probability theory. This is because, outside the modelled world of the engineer there are always random variations of many elements comprising the structure/environment system. By using the statistical procedures developed into probability theory the engineer can deal with the occurring variations in a rational manner. Through assembling a large body of data on each respective material property and then establishing clear unequivocal rules for the quantification of individual factors, can the engineer develop a system of safety factors specific to each individual project and so produce calculations which more realistically represent reality. [Zalka (1992)]

2.5.1 Theory of linear elasticity

The theory in this thesis is based on the assumption of linear elasticity. Combined with Euler-Bernoulli beam theory, a differential equation which describes the relationship between the load, the stiffness of the unit and the displacement is acquired.

$$\frac{d^2}{dx^2} \left[EI \frac{d^2 w}{dx^2} \right] = q \quad (2.6)$$

w = displacement; q = distributed load

This equation describes how a beam displaces itself considering an even stiffness along the beam. Euler-Bernoulli theory assumes that each cross section retains its size and form. The basic equation above is derived through four distinct subsets of beam theory; kinematics, constitutive, resultants and equilibrium.

$$\text{Kinematics} \Rightarrow \chi = -\theta = \frac{dw}{dx} \quad (2.7)$$

$$\text{Constitutive} \Rightarrow \sigma_x(x, y) = E \cdot \varepsilon_x(x, y) \quad (2.8)$$

$$\begin{aligned} \text{Resultants} \quad & \Rightarrow M(x) = \iint y \cdot \sigma(x, y) \cdot dy \cdot dz \\ & \Rightarrow V(x) = \iint \sigma_{xy}(x, y) \cdot dy \cdot dz \end{aligned}$$

$$\begin{aligned} \text{Equilibrium} \quad & \Rightarrow \frac{dM}{dx} = V \\ & \Rightarrow \frac{dV}{dx} = -q \end{aligned}$$

To obtain the relationship between the displacement w and the distributed load q , the equations above are combined. The two equations of equilibrium are first combined in order to eliminate the shear force V .

$$\frac{d^2 M}{dx^2} = -q$$

Then M is replaced through the resultant equations.

$$\frac{d^2}{dx^2} \cdot \left[\iint y \cdot \sigma \cdot dy \cdot dz \right] = -q$$

The constitutive relationship is used to replace stress σ with the strain ε . Then the kinematics is used to replace the strain ε with the displacement w .

$$\frac{d^2}{dx^2} \left[E \iint y \cdot \varepsilon \cdot dy \cdot dz = -q \right] \text{ och } \frac{d^2}{dx^2} \left[E \cdot \frac{d\chi}{dx} \iint y^2 \cdot dy \cdot dz \right] = -q$$

$$\frac{d^2}{dx^2} \left[E \cdot \frac{d^2 w}{dx^2} \iint y^2 \cdot dy \cdot dz \right] = q$$

Next step involves recognizing that the integral over y^2 is defined of the beam's moment of inertia, I .

$$I = \iint y^2 \cdot dy \cdot dz \quad (2.9)$$

Finally the Euler-Bernoulli equation is achieved.

$$\frac{d^2}{dx} \left[EI \frac{d^2 w}{dx^2} \right] = q \quad (2.6)$$

The kinematics relationship builds on the theory that the normals (lines perpendicular to the beam's neutral plane embedded in the beam's cross sections) do not bend, do not elongate and always make a right angle to the neutral plane. This is a theory designed to enable the engineer to make a model of reality and does not actually represent exactly how beams react to loads.

All of the assumptions and estimations described in this section are the engineer's tool for interpreting reality into a workable model. It is essential that an engineer is aware of how this model is derived and implemented so that its use will lead to intelligent interpretations of how the physical world actually works. Designing stability systems for extremely tall structures could require the engineer to develop extreme factors which requires the engineer to further quantify effectively the existing assumptions and estimations.

2.5.2 Young's modulus

Young's modulus, E , is the modulus of elasticity. It is described as the ratio of stress to strain on the loading plane along the loading direction.

$$E = \frac{\sigma}{\varepsilon} \quad (2.10)$$

Stress and strain values are acquired, for different materials, through testing. As the tension or compression increases so does the strain. During this testing process the relationship will show itself not be linear. Young's modulus is determined through calculating the slope of the relationship between the stress and strain shown in a stress/strain diagram. Young's modulus is also influenced by other factors, such as temperature changes, humidity, plastification, i.e. material hardening due to high stresses and time. It is therefore important to understand that due to these influences Young's modulus can change during a material's life time.

2.5.3 Long term effects

Long term effects on stabilising structures depend on creep and shrinkage. Creep is the increase in strain, over time, under a constant stress. Creep increases with increasing water-cement ratio and decreases with an increase in relative humidity. Creep can be accounted for by simply reducing Young's modulus, E ; by a creep factor obtained through codes.

$$E_{ef} = \frac{E}{(1 + \varphi_{ef})} \quad (2.11)$$

E_{ef} is the altered modulus of elasticity affected by the creep factor φ_{ef} . The creep factor itself can be determined through Equation (2.11) but there are other models that can be used.

$$\varphi_{ef} = \varphi_0 \cdot \beta_c(t - t_0) \quad (2.12)$$

φ_0 is the notional creep coefficient which takes into account the relative humidity, the mean compressive strength of concrete at 28 days and factors related to the effect of concrete strength and age at first loading. $\beta_c(t - t_0)$ describes the development of creep with time after loading where t is the considered time and t_0 is the time at first loading.

Shrinkage is a time dependant phenomenon which considers strains which are independent of stresses and result in deformations. The shrinkage value $\varepsilon_{cs}(t)$ is dependent on time and is formulated as

$$\varepsilon_{cs}(t - t_s) = \varepsilon_{cs,0} \cdot \beta_s(t - t_s) \quad (2.13)$$

Where t is the age to be calculated on and t_s is the age when shrinkage began. The notational shrinkage coefficient, $\varepsilon_{cs,0}$, is derived through the mean compressive strength of the concrete at 28 days and coefficients depending on concrete type, relative humidity and effect of concrete strength on shrinkage.

2.6 Problems concerning tall buildings

While dimensioning a tall building the engineer has to foresee the problems that may arise. The primary concern for the engineer is that the building will provide a safe and harmonious place for recreation, for working and for living. The secondary concern is that the client will receive the most cost effective design.

The engineer must design with failure in mind. For example, if one stabilising component fails due to impact, fire or accident, the buildings other components have to be able to take up the weight, i.e. collapse has to be prohibited. Concerning specifically fire, the building has to hold up for the period required for people to evacuate the building before collapse. In order to ensure that the client is content, the engineer must design a building that is optimal for its purpose. This means that the structure will not be over dimensioned for exceptional safety, and the client shall not have material costs that are unnecessary.

2.6.1 Comfort

Concerning comfort, some tall buildings may experience vibrating sway, which is the back and forth movement of a building due to wind loads. Such sway can lead to cracking in the concrete and further weakening of the structure due to fatigue, if the sway is considerably strong and frequent. This sway may also cause the users of the building to experience motion sickness which causes nausea. A building with uncomfortable movements may even be uninhabitable. An engineer can hinder these effects through creating an aerodynamic structure which is less affected by the winds, through designing the structure with attention to strengthening against sway and through avoiding critical resonance frequencies. [Postgraduate medicine online (1999)] [Vibration data (2002)]

There exists a certain frequency range that is uncomfortable for people. Most people feel the affects of motion sickness in the frequency range 0.1 – 1.0 Hz. Calculations should be made to determine the structures eigenfrequencies, transverse and lateral, and damping should be applied when necessary. [University of Sydney (2004)]

2.6.2 Pierced shear walls

Concerning solid stabilising components, such as shear walls, forces and moments are relatively easy to establish. The stiffness is the same throughout the wall and linear behaviour can be assumed as long as the unit is uncracked. The estimating of force distribution for pierced shear walls is on the other hand less predictable. Depending on the hole dimensions in relation to the height and the breadth of the wall, the behaviour is different. Walls with small holes have a strong connection between the vertical parts deriving an almost full interaction between them. These walls can be treated as solid walls as the behaviour is almost the same. Walls with big holes, in this thesis mentioned as walls with slender verticals or transversals, have almost no interaction between the verticals and can be treated as two separate walls disregarding the contribution from the transversal parts. Considering all walls, with varying hole dimensions in combination with asymmetry and more than one section of holes, it is obvious that the behaviour and the force distribution is hard to predict. A flexible method adaptable for all kinds of pierced walls is therefore to be preferred if possible.

2.6.3 Load distribution

The interaction between stabilising components in a building depends on many factors. All parts in a complete structure play a significant role on influencing the force paths, i.e. transferring the loads from the subjected surfaces down through the building to the foundations. In most calculations it is assumed that the floor slabs are fully stiff and do not bend in their plane, and that no slip occurs in the joints. The floor slabs are connected to the vertical stabilising members and play a significant role for distributing the load between the stabilising components. The floor slabs are usually the components that are subjected at the beginning of the load path taking the load directly from the facades. If the assumed stiffness of the slabs does not

correspond to a real slab, the problem for establishing a correct force distribution begins already with this first assumption. This uncertainty in combination with an unsymmetrical load, subjecting the building to twisting, leads to there being a force distribution which will be even harder to predict, especially for tall buildings.

2.6.4 Twisting and open cross sections

There are different methods for stabilising a building. Tall buildings often use a combination of stabilising systems and a stabilising tower is common to be positioned at the centre of a building, i.e. a core. In load cases where only translation occurs, the behaviour and the stress distribution of the core is seldom a problem to predict. For open cross section, such as U-shape, L-shape etc., subjected to twisting, the shear stresses which develop in the opened tower are uneven and an unpredicted warping effect may occur. This effect is often neglected or is not always understood by engineers. [Smith and Coull (1991)] The effect is considered to be quite small in low rise buildings but in tall structures the rotation angle, along the height, will cause a greater rotation and the warping effect causes the extremities, the flanges, to displace in the axial and lateral directions. These displacements are often partly prevented due to the connected floor slabs which are acting as connecting beams between the opened flanges, creating a closed or partly closed cross section. This means that the slab is now subjected to considerable tensile forces for preventing the opened cross section of the tower from displacing. These forces have a different intensity and force direction in the slabs than the slabs are normally dimensioned for. [Smith and Coull (1991)]

2.6.5 Interaction between the soil and the foundation

Tall buildings that are connected to solid bedrock are the only form of foundation that should be considered as a fully fixed. This assumption is still commonly used in design and the calculation processes for establishing buckling loads and dimensional forces and moments. Foundations resting on a layer of clay are considered as a structure *partly fixed* at the base. In the calculating process this could be taken into account by using the method of *elastic restraint*.

This method is transforming the unpredictable soil into an elastic spring and so making it possible for an interpretation of this phenomenon into the calculations. The knowledge of the soil is first of all a very uncertain subject and in combination with the approximation made for making the effect applicable in calculation the model will probably not agree very well with the real behaviour.

The problems related to the soil properties is also an issue for structures resting on piles drilled through the layer of clay bonded into the bedrock. The lateral resistance in the soil, preventing the piles from lateral displacement, is not to be treated as a compact non movable mass. Especially for tall buildings subjected to vibrating sway the clay will be frequently compressed and released from the dynamic forces causing the piles to move in a lateral direction compressing the soil. The upper part of the soil

is the most sensitive and the loss of interaction between soil and the piles has to be considered for dimensioning a stable structure.

2.6.6 Methods

The way tall buildings are designed and treated is different depending on which country one is in and which codes are utilised. The codes do not include everything, and relying only on the restrictions printed is not enough. It is noticed that the way a building is checked or designed differs between engineering companies even though the same code is followed. Even the restrictions in the codes are interpreted differently. [Johansson (2005)]

It is observed in different literatures different methods for calculating stability. Different tables are often used to achieve fast results but the basic theory is often the same i.e. based upon the theory of elasticity. Which methods the engineers are using is not an important issue but it is important how deep an understanding the engineer has of how the methods used were derived. Without knowledge of the assumptions the methods are based upon, it can be difficult to draw conclusions as to whether the calculations are good estimations of the structure or not. For complicated structures it is preferable to use FE-analyses in addition to hand calculations for achieving comparisons and a better prediction of the structure's behaviour. Even though a calculation program such as an FE-program is used, the effects of the interpretation of the FE-model, such as boundary conditions, load application, material properties etc., has to be observed as the FE-method is also a *model* of the real structure. In some cases a non linear analysis has to be considered.

The calculation methods used for pierced shear walls are described in Westerberg (1991) and Lorentsen *et al.* (2000). Both methods used for calculating on pierced shear walls are based upon an elastic behaviour with unified material properties through the whole wall. The method used for establishing the buckling load involves many assumptions and it is therefore suspected that the model will not resemble a real wall.

In the hand calculation method, for establishing the top deflection of the wall, the load is interpreted as a distributed horizontal load acting along the height of the wall. The real wall is actually subjected to shear forces along the breadth of the wall on each storey through the connections of the floor slabs. The method used does not therefore resemble the real load case. In that case where the loads are applied (distributed along the breadth of the wall) the wall may have to be strengthened causing non uniform material properties through the structure. If these parts are weak, cracking may occur and the stiffness of the wall will be reduced causing a lower interaction between the verticals. The real wall is then a completely different wall than the one interpreted in to the hand calculation.

The approaches for calculating on complete structures, involve several assumptions such as, evenly distributed columns and the vertical load distribution. Regarding the vertical load distribution, the method uses a simplified expression assuming that the evenly distributed columns are taking all the vertical loads while the stabilising components are assumed not to be bearing. A problem with using this method occurs

especially for buildings such as residential buildings which seldom utilise columns but instead use stabilising walls for taking all the vertical loads combined with stabilising the building. The method does not therefore resemble a real structure.

2.6.7 Summation of the effect from approximation

It is worth mentioning that engineers who are used to calculate on low rise buildings often do not need to consider many of the problems mentioned in this section. With an increasing height of a building, the effect of all the assumptions and approximation made by the engineer will increase and in some cases a bad estimation can cause a weak building showing an unpredictable behaviour. It is therefore to be noted that the same approach used in low rise buildings should not be used for dimensioning tall buildings. The 2nd order effect is here greatly influenced by the approximations made in the design process. If the problems which are brought up in this section are disregarded the real building may behave unpredictably and the building may succumb to unwanted deformations. The 2nd order contribution may greatly increase due to the greater deflections. Cracking may occur in parts where it is not predicted and in these parts the stiffness is reduced and the capacity for taking forces is also reduced. The force distribution will then be different than the building is designed for and other stabilising units will be overly subjected causing cracking. Even though the building does not collapse the reduced stiffness can cause the building to become uncomfortable and the use of the building may eventually be prohibited.

3 Calculation methods for stabilising components

This chapter will describe the methods for calculating the buckling load due to bending through using the Vianello method, Euler buckling factors or through deriving a k -value. The shear contribution to buckling will also be clearly explained and derived. How the contributions of shear and bending are combined to produce the critical buckling load is shown and how to use the magnification factor for determining 2nd order effects is used for obtaining the design moment.

A calculation method for pierced shear walls is presented and the assumptions used for this type of modelling are clearly described. Vianello's method for determining the bending contribution to buckling is described through the building up of an iteration process in order to effectively explain the theory behind the method and how it is used.

3.1 Solid components – Columns and shear walls

The buckling criterion of a component, or a whole structure, is vital when considering the calculation of stability. When the critical buckling load is established it is used frequently in comparison with the actual load on the structure. It is also of importance concerning the estimation of second order effects. The contribution of second order effects is included in the calculations through using quotients of the actual load and the critical buckling load. The critical buckling load depends on deformations from both bending and shear. The contributions from each part can differ, and in some structures, for example for high slender stabilising components, the shear deformation is negligible in comparison with the bending deformations and therefore is generally ignored. This chapter will show the derivations of the critical buckling load for a cantilever column as this model is closest to the actual application, i.e. fully fixed at the base.

3.1.1 Buckling load through bending – General calculations

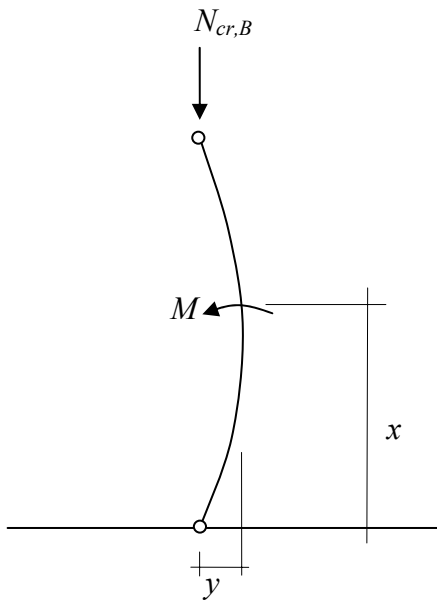
The Euler expression for bending is often used in estimating the critical buckling load for a single component subjected to a concentrated load at the top. In a complete stabilising structure, for example a building, an expression for the structures buckling load takes a more simplified expression using a single factor, k_V , and the complete height of the structure, L_h . The k_V -value is based upon the amount of storeys the building has, or in other terms, the amount of vertical load applied along the structure. This value can be established through Vianello's method explained in Section 3.3.

The k -value derived below is for a single column subjected to a vertical load on the top and note well that this k -value should not be confused with Vianello's k_V .

$$N_{cr,B} = k^2 \cdot EI \quad \text{or as the known Euler expression}$$

$$N_{cr,B} = \frac{\pi^2 EI}{L_c^2} \quad (3.1)$$

$$k = \frac{\pi}{L_c}$$



Establishing the moment at a certain point along the column, assuming an imperfection with a sinus shape.

$$M_x = N_{cr,B} \cdot y(x)$$

$$M_x = -EI \cdot y''(x)$$

Figure 3.1: Buckling load through bending.

Combining the two expressions above a differential equation is acquired.

$$y''(x) + \frac{N_{cr,B}}{EI} \cdot y(x) = 0 \quad (3.2)$$

Solution:

$$y(x) = A \sin kx + B \cos kx \quad (3.3)$$

$$y'(x) = Ak \cos kx - Bk \sin kx$$

$$y''(x) = -Ak^2 \sin kx - Bk^2 \cos kx$$

$$y''(x) = -k^2 (A \sin kx + B \cos kx) \quad (3.4)$$

Combining Equation 3.3 and 3.4 a second expression for \$y''\$ is acquired.

$$y''(x) = -k^2 \cdot y$$

This leads to the determining of the critical buckling load due to bending with the help of a factor \$k\$.

$$y''(x) = -\frac{N_{cr,B}}{EI} \cdot y(x) \quad \Rightarrow \quad k^2 = \frac{N_{cr,B}}{EI} \quad \Rightarrow \quad N_{cr,B} = k^2 \cdot EI$$

$$k = \frac{\pi}{L_c}$$

L_c is the so called buckling length. L_c is different depending on how the behaviour of the column is interpreted according to the boundary conditions. In some literature the Euler expression uses a k_E as a multiplication factor which gives the buckling length L_c .

$$N_{cr} = \frac{\pi^2 EI}{(k_E \cdot L)^2} \quad (3.5)$$

$$L_c = k_E \cdot L \text{ (Buckling length)} \quad k_{E,cantilever}=2$$

Figure 3.2 below presents different k_E values for different boundary conditions.

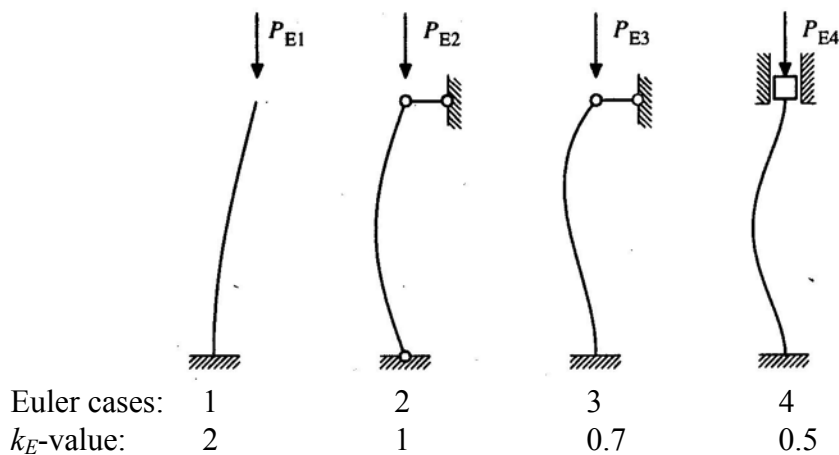
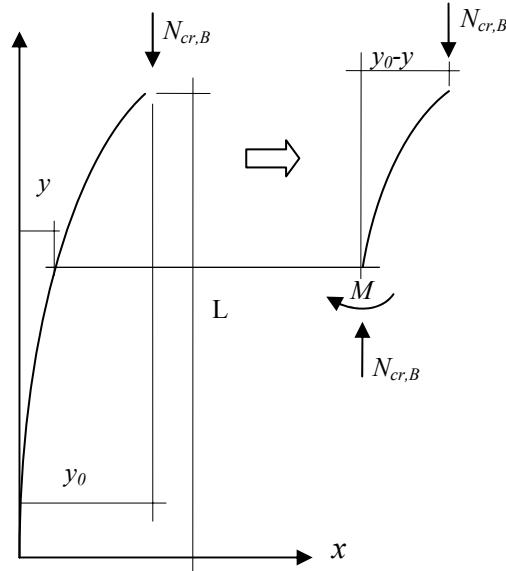


Figure 3.2: Euler buckling modes.

3.1.2 Bending contribution of cantilever columns



$$M = N_{cr,B}(y_0 - y) \quad (3.6)$$

$$M = -EIy'' \quad (3.7)$$

Assumed linear response; EI constant along the length \Rightarrow

$$y'' + \frac{N_{cr,B}}{EI}y = N_{cr,B}y_0 \quad (3.8)$$

Figure 3.3: Bending of a cantilever column

To establish the value of k for a cantilever column, the boundary conditions are interpreted into the solution of the differential equation mentioned in the previous chapter. The displacement, which contributes to the moment, is here $(y_0 - y)$ where y varies along the column, see Figure 3.3.

$$y = A \sin kx - B \cos kx + y_0 \quad (3.9)$$

$$y' = Ak \cos kx - Bk \sin kx \quad (3.10)$$

As y represents the variable deflection along the column, y' expresses the slope at a certain point along the column, i.e. dy/dx .

Boundary conditions:

Both the displacement y and the slope y' are zero at the bottom and at the top the variables are given the maximum values.

$$x = 0 \Rightarrow y = 0 \quad y' = 0 \Rightarrow A = 0$$

$$x = L \Rightarrow y = y_0 \Rightarrow B \cos kL + y_0 = y_0 \Rightarrow \cos kL = 0 \Rightarrow k = \pi/2L, 3\pi/2L, \dots$$

$$k = \frac{\pi}{2L} \Rightarrow k^2 = \frac{\pi^2}{(2L)^2}$$

The cantilever column, because of the boundary conditions, has the highest value due to the fact that the deflected column has the shape of a half buckling mode, see Figure 3.2.

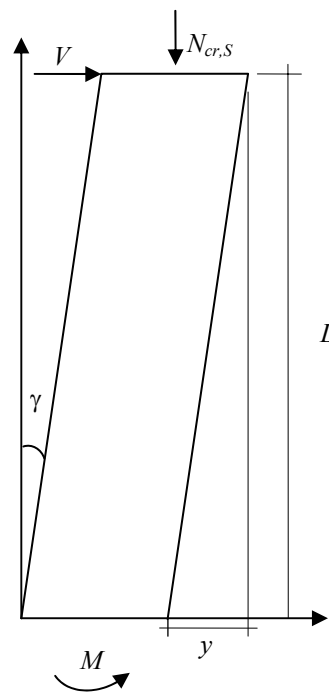
3.1.3 Shear contribution of cantilever columns

The critical buckling load, only regarding shear, is derived from the shear modulus and the cross sectional area of the column. See Figure 3.4.

$$N_{cr,S} = G \cdot A \quad (3.11)$$

GA is the shear stiffness of the member and the shear modulus G for a concrete member is assumed to be 40% of Young's modulus. This value is derived from Poisson constant $\nu = 0.25$, the estimation for concrete. [Lorentsen *et al.* (2000)]

$$G = \frac{E}{2(1+\nu)} = \frac{1}{2.5} E = 0.4E \quad (3.12)$$



$$M = N_{cr,S} \cdot y$$

$$y = \gamma \cdot L \quad (\text{for small angles})$$

Observe that the shear force, V , is a fictional force. It represents a force that gives the same deflection which occurs from the critical buckling load when the structure is failing.

$$M = V \cdot L$$

$$N_{cr,S} = \frac{M}{y} = \frac{VL}{y} = \frac{VL}{\gamma L} = \frac{\gamma GA \cdot L}{\gamma L} = GA$$

$$\text{Observe that } \gamma = \frac{1}{GA} \quad (3.13)$$

Figure 3.4: Shear buckling of a column.

The stress distribution from shear is not uniformly distributed in large cross sections. To obtain a more representative value for the whole cross section the shear capacity is reduced with a value $\xi = 1.2$.

$$N_{cr,S} = \frac{GA}{\xi} \quad (3.14)$$

3.1.4 Combined bending and shear

Both bending and shear deformations contribute to the deflection and the critical buckling load. The final curvature of the deflection is therefore established through the sum of the curvatures from each contribution, see Figure 3.5.

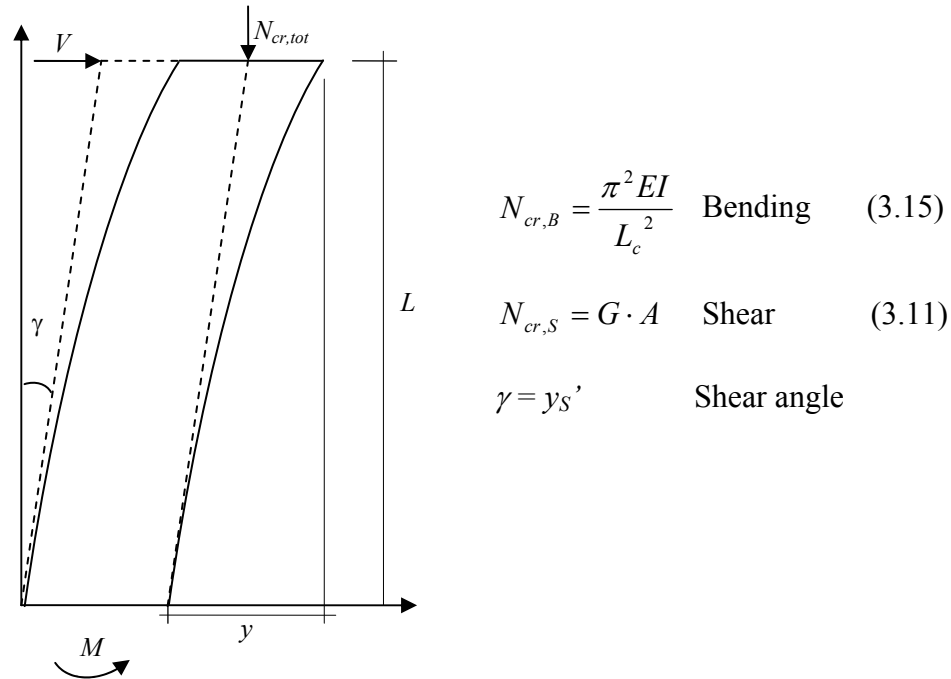


Figure 3.5: Buckling due to bending and shear.

$$\text{Curvature from Shear: } y_S' = \frac{V}{GA} = \frac{N_{cr,tot} y'}{GA} \Rightarrow y_S'' = \frac{N_{cr,tot} y''}{GA} \quad (3.16)$$

$$\text{Curvature from Bending: } y_B'' = \frac{-M}{EI} = \frac{N_{cr,tot} (y_0 - y)}{EI} \quad (3.17)$$

Combining both of the components the equations below are achieved.

$$y'' = y_B'' + y_S'' = \frac{N_{cr,tot} y''}{GA} + \frac{N_{cr,tot} (y_0 - y)}{EI} \Rightarrow y'' = \frac{N_{cr,tot}}{1 - \frac{N_{cr,tot}}{GA}} \cdot \frac{(y_0 - y)}{EI}$$

It is important to distinguish between $N_{cr,B}$, $N_{cr,S}$ and $N_{cr,tot}$. $N_{cr,tot}$ is the critical load that is to be derived. The last part of Equation (3.17) can be compared with the curvature for bending.

$$y'' = \frac{N_{cr,B} (y_0 - y)}{EI} \quad (3.18)$$

A new expression is derived and gives a more simplified expression for the combined buckling load, $N_{cr,tot}$.

$$N_{cr,B} = \frac{N_{cr,tot}}{1 - \frac{N_{cr,tot}}{GA}} \Rightarrow N_{cr,tot} = \frac{1}{\frac{1}{N_{cr,B}} + \frac{1}{N_{cr,S}}} \quad (3.19)$$

3.1.5 Derivation of magnification factor

To establish the total moment, occurring both from horizontal load and the second order contribution, a so called *magnification factor* is introduced. The total moment can be expressed as the following:

$$M_d = M_0 \cdot \left(1 + \frac{\beta}{\frac{N_{cr}}{N} - 1} \right) \quad (3.20)$$

$$M_d = M_0 \cdot \text{magnification factor}$$

$$M_d = M_0 + \Delta M$$

As one can see from the expressions above, there is a relationship between the 1st and the 2nd order moment. The 2nd order moment occurs from the deflection caused by the 1st order moment combined with the vertical load. The deflection is related to the stiffness of the component and weak components will therefore develop large second order deflections.

The second order moment depends on the vertical load and the deflection. The deriving of the magnification factor is here based on the deflections.

$$M_d = M_0 + \Delta M = M_0 + N \cdot y; \quad y = y_0 + \Delta y$$

Where y_0 is the 1st order deflection. The deflection can also be written as the curvature times the length in square.

$$y = y' \cdot L \quad \text{resp.} \quad y' = y'' \cdot L \Rightarrow y = y'' \cdot L^2 = \frac{1}{r} \cdot L^2$$

When a sinus formed curvature is assumed. When different types of load act on a column, the *shape* of the curvature also changes. Both the horizontal load and the vertical load affect the buckling shape and the expression for the curvature above has to be altered by a *distribution factor* for each load case.

$$y = y_0 + \Delta y \Rightarrow y = \frac{1}{r_0} \cdot \frac{L^2}{A} + \frac{1}{r_\Delta} \cdot \frac{L^2}{B} \Rightarrow y = \frac{M_0}{EI} \cdot \frac{L^2}{A} + \frac{\Delta M}{EI} \cdot \frac{L^2}{B} \Rightarrow$$

$$y = \frac{\frac{M_0 B}{NA}}{\frac{B \cdot EI}{L^2 \cdot N} - 1} \quad (3.21)$$

A is the distribution factor related to the load distribution from the 1st order moment, while B refers to the shape occurring when the column deflects under the vertical load. The second order moment can now be rewritten as the following:

$$\Delta M = N \cdot y = M_0 \cdot \frac{B/A}{\frac{(B \cdot EI/L^2)}{N} - 1} \quad (3.22)$$

As the factor B refers to the shape due to the second order contribution, the curvature along the column is similar to a sinus curve. B is therefore often assumed to be equal to π^2 . The expression $(B \cdot EI/L^2)$ is then identified as the critical buckling load for bending. On the other hand, the factor A differs depending on whether there is a point load or a distributed load etc. applied on the column or a 1st order eccentricity of the vertical load, see *Figure 3.6*. The quotient B/A is called a *shape factor* and is replaced by the symbol β .

$$M_d = M_0 \cdot \left(1 + \frac{\beta}{\frac{N_{cr}}{N} - 1} \right) \quad (3.20)$$

It is also notable that $\beta = \frac{B}{A} = \frac{\pi^2}{\pi^2} = 1$, for an axially loaded column with factor $A = \pi$ representing the imperfection and factor $B = \pi$ representing the 2nd order effect, see *Figure 3.6*.

When β is equal to 1, the expression becomes simplified to

$$M_d = M_0 \cdot \left(\frac{1}{1 - \frac{N}{N_{cr}}} \right) \quad (3.23)$$

To calculate the total moment shown above, the critical buckling load has to be established first. *Figure 3.6* presents some A and B values which are used for establishing the shape factor β .

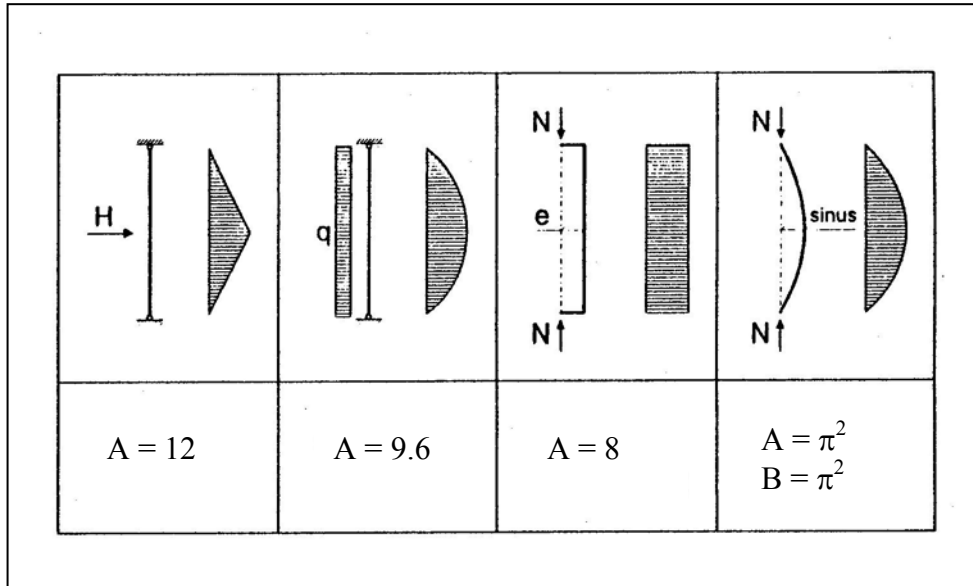


Figure 3.6: A and B values for deriving the β value. [Westerberg (1999)]

3.2 Pierced shear walls

Through Section 3.1.1 to 3.1.4 buckling of columns or shear walls is explained for solid units. In this section a hand calculation method taken from Lorentsen *et al.* (2000), is used to derive the critical buckling load for *pierced* shear walls. As described earlier shear deformation is often neglected in tall stabilising units because bending is dominant. When stabilising elements are pierced, shear deformation can not be neglected. Calculation is more complicated compared with the solid units. The calculations are based on the establishment of the *shear angle* γ . The shear angle consists of contributions from deformations occurring from both bending and shear deformations in the vertical and horizontal components of a representative section at the base of the wall. See Figure 3.7 where L_{sec} is the height of one storey. The calculated value of the shear angle γ expresses the angle when the shear force, V , is equal to 1.

$$N_{cr,s} = \frac{GA}{\xi} = \frac{\xi}{\gamma} \quad (3.24)$$

$$\gamma = \gamma_{t,bend} + \gamma_{v,bend} + \gamma_{t,shear} + \gamma_{v,shear} \quad (3.25)$$

v stands for the vertical parts and t represents the transversal parts of the wall.

$$\gamma_{t,bend} = \frac{L_{sec}^3 c^3}{12b^2 EI_t} \quad (3.26)$$

$$\gamma_{v,bend} = \frac{L_{sec}^2}{24EI_v} \quad (3.27)$$

$$\gamma_{t, shear} = \xi \frac{L_{sec} c}{b^2 G A_t} \quad (3.28)$$

$$\gamma_{v, shear} = \frac{\xi}{2 G A_v} \quad (3.29)$$

3.2.1 Derivation of buckling load

The reason the formula is split up into different parts is to reveal how much each part contributes to the total shear angle. The derivations are all based upon the equation of the elastic line and uniformity is assumed throughout the wall.

In order to calculate, the wall is modelled as a framework positioned in the centre of the components of the shear wall, See Figure 3.7. The connection between the vertical parts and the transversal part is assumed to be rigid, see Figure 3.8.

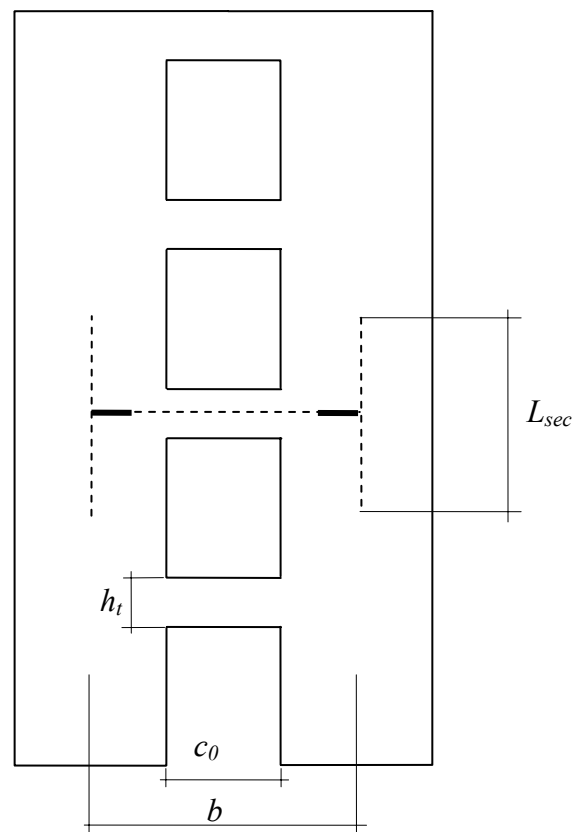


Figure 3.7: Pierced shear wall.

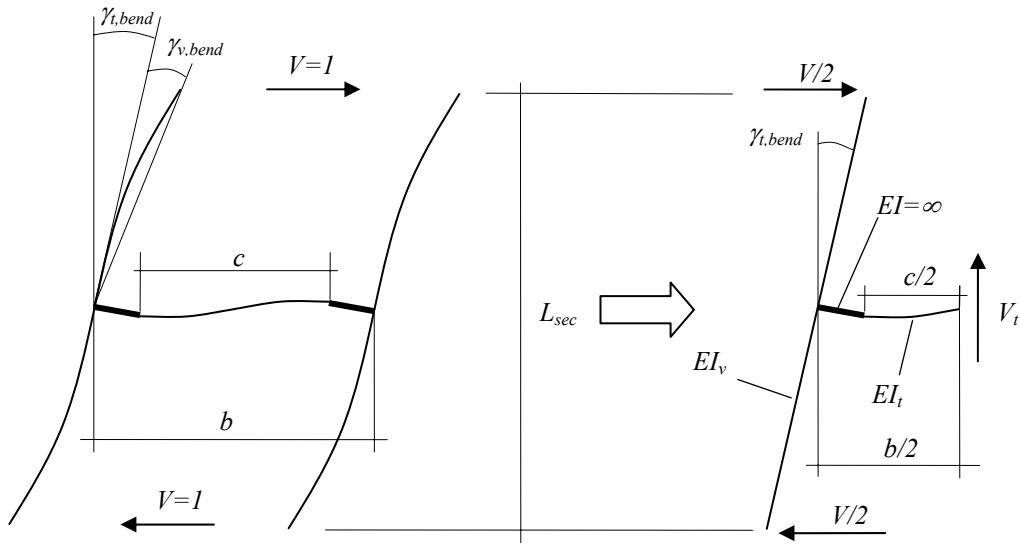


Figure 3.8: Representative section of a pierced shear wall.

3.2.1.1 Bending in the transversal part

Bending in the transversal part is expressed in Equation (3.26).

$$\gamma_{t,bend} = \frac{L_{sec} c^3}{12b^2 EI_t} \quad (3.26)$$

The contribution from bending of the transversal part is caused by a shear force bending the length $c/2$ in Figure 3.8. The presumptions are that the inflexion point is in the middle and that the inner part has $EI = \infty$. The length of the deformable transversal part is assumed to have the length $c = h_t + c_0$, i.e. the length is influenced by the thickness and the length of the transversal part. See Figure 3.8.

3.2.1.2 Bending in the vertical part

The bending in the vertical part is expressed in Equation (3.27).

$$\gamma_{v,bend} = \frac{L_{sec}^2}{24EI_v} \quad (3.27)$$

Bending of the vertical part with the length $L_{sec}/2$ has the same derivation as the previous component. Only the length and the shear force differ. $y =$ deflection.

$$y = \frac{1}{2} \left(\frac{L_{sec}}{2} \right)^3 \cdot \frac{1}{3EI_v} \quad y = \frac{L_{sec}}{2} \cdot \gamma_{v,bend} \quad \Rightarrow \quad \gamma_{v,bend} = \frac{y}{\frac{L_{sec}}{2}} = \frac{L_{sec}}{24EI_v}$$

3.2.1.3 Shear in the transversal part

As Figure 3.9 illustrates, the angle γ_t is caused by a shear force in the vertical direction.

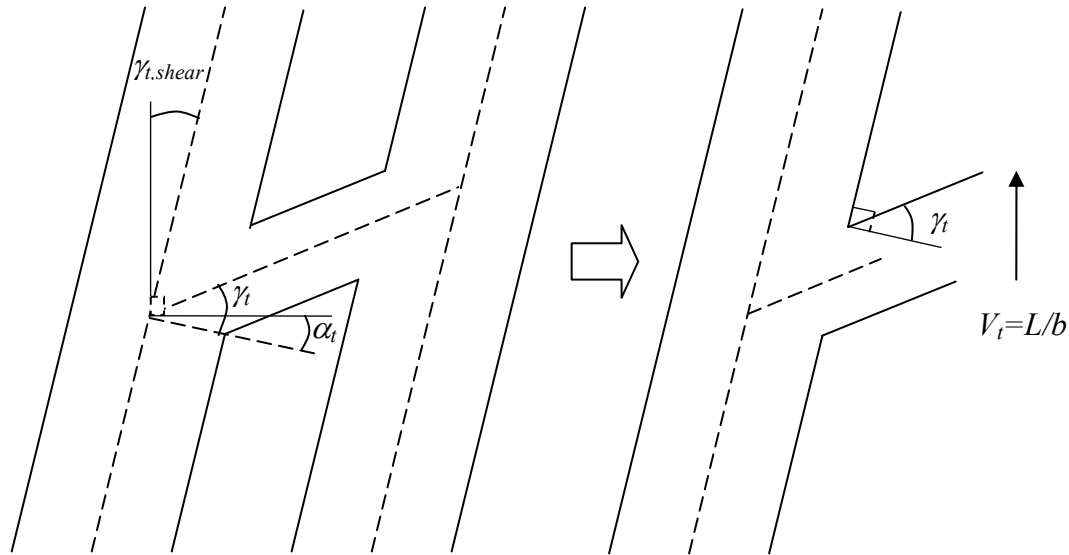


Figure 3.9: Shear deformation.

$$V_t \frac{b}{2} = V \frac{L_{\text{sec}}}{2} \Rightarrow V_t = \frac{L_{\text{sec}}}{b} \cdot V; \text{ and } V=I \Rightarrow \gamma_t = \frac{\xi V_t}{GA_t}$$

To transform γ_t to the contribution $\gamma_{t,\text{shear}}$, the angles are compared from Figure 3.9.

$$\alpha_t \frac{b}{2} = \gamma_t \frac{c}{2} \Rightarrow \alpha_t = \gamma_t \frac{c}{b}$$

$$\gamma_{t,\text{shear}} = \alpha_t = V_t \frac{\xi}{GA_t} \frac{c}{b} = \xi \frac{L_{\text{sec}} c}{b^2 GA_t} \quad (3.28)$$

3.2.1.4 Shear in the vertical part

The shear contribution from the vertical part is expressed through Equation (3.29).

$$\gamma_{v,\text{shear}} = \frac{V}{2} \frac{\xi}{GA_v} \quad V=I \Rightarrow \gamma_{v,\text{shear}} = \frac{\xi}{2GA_v} \quad (3.29)$$

The derived theory will be used in Section 5.3 where different cross sections will be calculated and compared with results from FE analyses. It will then be clearer how the contributions from the different parts will vary and affect the total shear angle, and finally the critical buckling load.

3.2.2 Calculation method for deflection

When calculating deflection of pierced shear walls the approach is different from the establishing of the buckling load. The shear part of the buckling load is based upon a shear angle that represents the state when the shear capacity or the critical buckling load is reached. This angle does not represent the angle for the whole structure. The vertical loads are decreasing with the height of the building which leads to different angles on each floor.

Deflections of pierced shear walls are complicated to establish and involve advanced derivations to obtain a usable expression. This derivation is not taken up here in detail but the basics are presented. The method is explained in Smith and Coull (1991).

The method of calculating deflection of pierced walls is based upon a modification of the shear angle.

$$y' = \frac{\xi}{GA} V = \gamma \cdot V \quad \text{Represent the angle that occurs for a shear force } V. \quad (3.30)$$

$$\gamma = \frac{\xi}{GA} \quad \text{Represent the shear angle, i.e. the angle when } V=I. \quad (3.31)$$

The modification of the angle in Equation 3.30 takes into account that a part of the shear force is carried by vertical parts. The angle y' is therefore reduced.

$$\begin{aligned} y'' &= -\frac{M}{EI_v} \Rightarrow V = EI_v y''' \\ y'_s &= \gamma(V - 2(-EI_v y''')) = \gamma \cdot V + 2\gamma EI_v (y''''_B + y''''_s) \\ y''''_B &= -\frac{V}{EI} \Rightarrow y'_s = \gamma \cdot V + 2\gamma \cdot y EI_v \frac{V}{EI} + 2\gamma EI_v y''''_s \\ \Rightarrow y''''_s - y'_s \frac{1}{\gamma 2EI_v} &= -\frac{V}{2EI_v} \left(1 - \frac{2EI_v}{EI}\right) \end{aligned}$$

To obtain a simpler expression two new variables are established. [Loretsen *et al.* (2000)]

$$\alpha^2 = \frac{1}{\gamma 2EI_v} \quad (3.32)$$

$$\mu = \frac{1}{1 - \frac{2EI_v}{EI}} \quad (3.33)$$

$$\Rightarrow \frac{y''''_s}{\gamma} - \frac{y'_s}{\gamma} \alpha^2 = -\alpha^2 V \frac{1}{\mu}$$

The variables α and μ are used to simplify the final expression for the top deflection of a pierced shear wall subjected to a distributed horizontal load.

$$y_{\max} = K \frac{qL_h^4}{8E2I_v} \quad (3.34)$$

$$K = \left[1 - \frac{1}{\mu} - \frac{8}{\mu} \left(\frac{\alpha L_h \sinh(\alpha L_h) - \cosh(\alpha L_h) + 1}{(\alpha L_h)^4 \cosh(\alpha L_h)} - \frac{1}{2(\alpha L_h)^2} \right) \right] \quad (3.35)$$

The derivation of the factor K is not presented here and further information can be found in Lorentsen *et al.* (2000).

The expression for the deflection is derived from the theory of linear elasticity and stands for the top deflection of two combined solid members subjected to a distributed horizontal load. The stiffness EI_v represents the stiffness of one member. The factor K is then established to take into account the effect of the holes.

The variables α and μ can be rewritten to simplify the calculation.

$$\alpha^2 = \frac{1}{\gamma 2EI_v} = \frac{12I_t}{\Sigma I_v} \left(\frac{b}{c} \right)^3 \frac{\mu}{bL_{\text{sec}}} \quad (3.36)$$

$$\mu = \frac{1}{1 - \frac{2EI_v}{EI}} = 1 + \frac{\Sigma A_v}{A_{v,1}A_{v,2}} \frac{\Sigma I_v}{b^2} \quad (3.37)$$

L_{sec} is the storey height. b , c and I_t are presented in Section 3.2.1.

This method is also applicable for shear walls with more than one section of holes.

For a wall with two vertical sections with holes, the same approach explained above can be used. Only the sum of the cross section area and the sum of the moment of inertia is added with a third contribution from the extra vertical part.

For a shear wall with one vertical row of holes:

$$\Sigma I_v = I_{v,1} + I_{v,2} \quad \Sigma A_v = A_{v,1} + A_{v,2}$$

The factor K can be taken from the graph in Figure 3.10 which shows functions based on Equation 3.35.

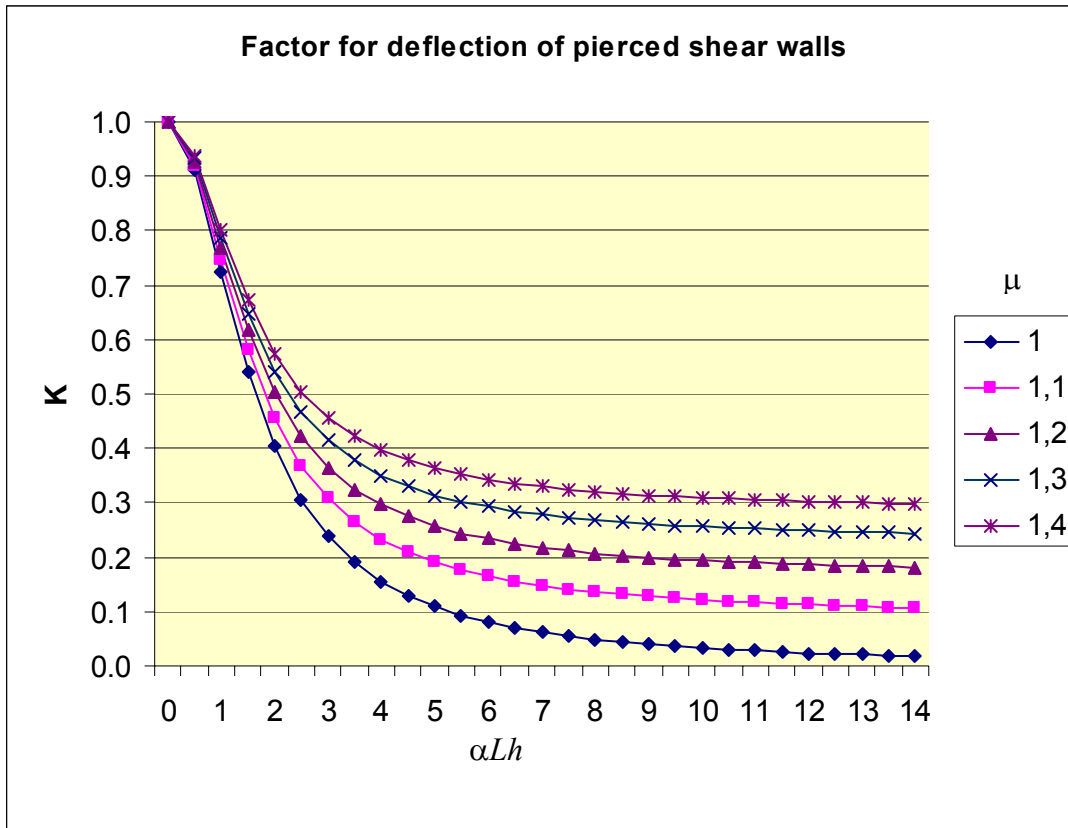


Figure 3.10: Graph for determining the K factor.

3.3 Vianello's method

In the last years of the 19th century, an Italian mathematician named Vianello devised an iterative procedure which could effectively be used to calculate critical buckling loads concerning the bending contribution. The Vianello iteration is especially effective for establishing critical buckling load, concerning bending, in members with non uniform stiffness throughout their height. Learning how to use Vianello's Method is a lengthy and methodical process which requires plenty of time in order to gain a usable understanding. Literature is sparse so the only three sources studied are Westerberg (1999), Lorentsen *et al.*(2000) and Petersson and Sundquist (2002).

The point of using a Vianello iteration is to calculate a k -value to be used in Equation (3.38), for calculating the critical buckling load regarding bending.

$$N_{cr,B} = k_V \cdot \frac{EI}{L_h^2} \quad (3.38)$$

This is the critical load due to bending, where L_h is the total height of the structure. The iteration uses the differential equation of equilibrium of the system and can be seen in Equation (3.8). See Section 3.1.1.

$$y'' = \frac{-M}{EI} = \frac{N_{cr,B} \cdot y_0}{EI} \left[1 - \left(\frac{x}{L} \right)^2 \right] \quad (3.39)$$

y_0 = maximum bending deflection:

The method is capable of calculating both discrete elements, meaning individual, and continuous systems, meaning a system of combined components. The best way to explain how the method is used is to perform an actual iteration. For this individual member the load is applied at the top and the stiffness is constant through the column.

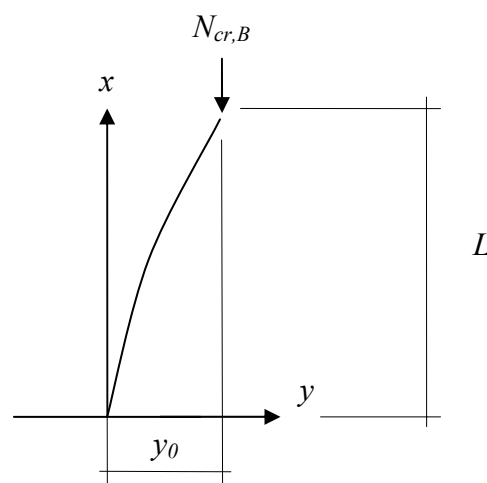


Figure 3.11: A column with a vertical force N .

The problem is shown in Figure 3.11. In order to calculate the critical buckling load a Vianello table is assembled. The x/L shows the level in the column where the calculations are valid. The y_a is the initial estimation of deflection. Observe the differential Equation (3.39) where $(x/L)^2$ is found. It is from this equation that the first estimation of y_a is set to be equal to $(x/L)^2$.

Table 3.1: First step

$\frac{x}{L}$	y_a	y''	y'	y_b	$\frac{y_a}{y_b}$
1	1				
0.9	0.81				
0.8	0.64				
0.7	0.49				
0.6	0.36				
0.5	0.25				
0.4	0.16				
0.3	0.09				
0.2	0.04				
0.1	0.01				
0	0				
	y_0	$\frac{N_{cr,B} \cdot y_0}{EI}$	$\frac{N_{cr,B} \cdot y_0}{EI} \cdot \Delta x$	$\frac{N_{cr,B} \cdot y_0}{EI} \cdot \Delta x^2$	

The first step involves setting up a table, Table 3.1, and inserting the x/L -values and assuming the y_a -values through squaring x/L , where the numbers in the column y_a are factors of y_0 .

$$y'' = \frac{-M}{EI} = (y_0 - y_a) \cdot \frac{N_{cr,B}}{EI} = \left(1 - \frac{y_a}{y_0}\right) \cdot \frac{N_{cr,B} \cdot y_0}{EI} = \frac{N_{cr,B} \cdot y_0}{EI} \left[1 - \left(\frac{x}{L}\right)^2\right] \quad (3.39)$$

leads to the establishment of the assumed deflection y_a .

$$\frac{y_a}{y_0} = \left(\frac{x}{L}\right)^2 \Rightarrow y_a = \left(\frac{x}{L}\right)^2 \cdot y_0$$

Observe that the table represents the element member in that the top row is the top of the member. Note also that the values displayed under y_a are factors of y_0 .

Ex: where $x/L = 0.5$:

$$y_a = 0.25 \cdot y_0; \quad \text{that is 25\% of the maximum deflection } y_0.$$

Table 3.2: Second step

$\frac{x}{L}$	y_a	y''	y'	y_b	$\frac{y_a}{y_b}$
1	1	0			
0.9	0.81	0.19			
0.8	0.64	0.36			
0.7	0.49	0.51			
0.6	0.36	0.64			
0.5	0.25	0.75			
0.4	0.16	0.84			
0.3	0.09	0.91			
0.2	0.04	0.96			
0.1	0.01	0.99			
	0	1			
	y_0	$\frac{N_{cr,B} \cdot y_0}{EI}$	$\frac{N_{cr,B} \cdot y_0}{EI} \cdot \Delta x$	$\frac{N_{cr,B} \cdot y_0}{EI} \cdot \Delta x^2$	

The second step is the calculation of y'' which is the curvature. Here again the differential equation is used.

$$y'' = \frac{-M}{EI} = (y_0 - y_a) \cdot \frac{N_{cr,B}}{EI} = \left(1 - \frac{y_a}{y_0}\right) \cdot \frac{N_{cr,B} \cdot y_0}{EI} = \frac{N_{cr,B} \cdot y_0}{EI} \left[1 - \left(\frac{x}{L}\right)^2\right] \quad (3.39)$$

The numbers that appear in the column y'' are factors of $\frac{N_{cr,B} \cdot y_0}{EI}$ which leads to the

$$\text{values being } y'' = \frac{-M}{EI} = \frac{N_{cr,B} \cdot y_0}{EI} \left[1 - \left(\frac{x}{L} \right)^2 \right] \Rightarrow y'' = \frac{N_{cr,B} \cdot y_0}{EI} \cdot (1 - y_a)$$

$$\Rightarrow y'' = 1 - y_a; \text{ for the iteration table.}$$

Table 3.3: Third step

$\frac{x}{L}$	y_a	y''	y'	y_b	$\frac{y_a}{y_b}$
1	1	0	6.65		
0.9	0.81	0.19	6.46		
0.8	0.64	0.36	6.10		
0.7	0.49	0.51	5.59		
0.6	0.36	0.64	4.95		
0.5	0.25	0.75	4.20		
0.4	0.16	0.84	3.36		
0.3	0.09	0.91	2.45		
0.2	0.04	0.96	1.49		
0.1	0.01	0.99	0.50		
	0	1	0		
	y_0	$\frac{N_{cr,B} \cdot y_0}{EI}$	$\frac{N_{cr,B} \cdot y_0}{EI} \cdot \Delta x$	$\frac{N_{cr,B} \cdot y_0}{EI} \cdot \Delta x^2$	

The third stage involves the calculation of the angle y' . The calculation starts here at the bottom of the column where the angle is zero. This represents the assumption that the column is fully fixed to the ground. At the next levels the value for y' is derived through $y'_n = y'_{n-1} + y''_{n-1} \cdot \Delta x$. At the first level near the base, the curvature is referring to half the length of Δx . See Figure 3.12.

Example: for $x/L=0.1$ is obtained $y'_{x/l=0.1} = 0 + 1 \cdot \frac{\Delta x}{2} = 0.5 \cdot \Delta x$

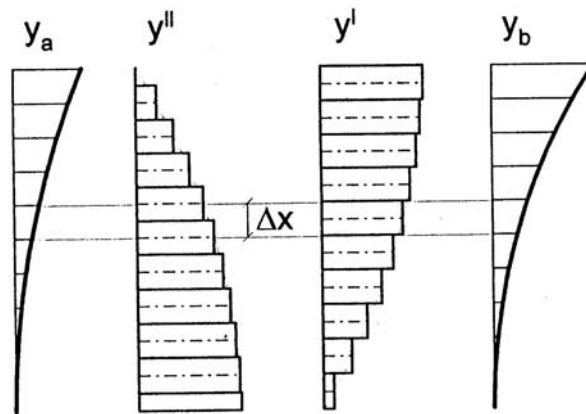


Figure 3.12: Curvatures relating to Δx .

Table 3.4: Forth step

$\frac{x}{L}$	y_a	y''	y'	y_b	$\frac{y_a}{y_b}$
1	1	0	6.65	41.75	
0.9	0.81	0.19	6.46	35.10	
0.8	0.64	0.36	6.10	28.64	
0.7	0.49	0.51	5.59	22.54	
0.6	0.36	0.64	4.95	16.95	
0.5	0.25	0.75	4.20	12.00	
0.4	0.16	0.84	3.36	7.80	
0.3	0.09	0.91	2.45	4.44	
0.2	0.04	0.96	1.49	1.99	
0.1	0.01	0.99	0.50	0.50	
0	0	1	0	0	
	y_0	$\frac{N_{cr,B} \cdot y_0}{EI}$	$\frac{N_{cr,B} \cdot y_0}{EI} \cdot \Delta x$	$\frac{N_{cr,B} \cdot y_0}{EI} \cdot \Delta x^2$	

The value y_b , the first calculation of a new updated deflection, is derived in the forth stage, Table 3.4. Again the deflection on ground level is zero, due to the element

being fully fixed. The following values are derived from the equation $y_{b,n} = y_{b,n-1} + y'_n \cdot \Delta x$.

For example: where $\frac{x}{L} = 0.5$ the deflection $y_b = 7.8 + 4.2 = 12$ is obtained.

This shows how each successive change in angle is added to the previous deflection in order to obtain the subsequent deflection.

Table 3.5: Fifth step

$\frac{x}{L}$	y_a	y''	y'	y_b	$\frac{y_a}{y_b}$
1	1	0	6.65	41.75	0.024
0.9	0.81	0.19	6.46	35.10	0.023
0.8	0.64	0.36	6.10	28.64	0.022
0.7	0.49	0.51	5.59	22.54	0.022
0.6	0.36	0.64	4.95	16.95	0.021
0.5	0.25	0.75	4.20	12.00	0.021
0.4	0.16	0.84	3.36	7.80	0.021
0.3	0.09	0.91	2.45	4.44	0.020
0.2	0.04	0.96	1.49	1.99	0.020
0.1	0.01	0.99	0.50	0.50	0.020
0	0	1	0	0	0.000
	y_0	$\frac{N_{cr,B} \cdot y_0}{EI}$	$\frac{N_{cr,B} \cdot y_0}{EI} \cdot \Delta x$	$\frac{N_{cr,B} \cdot y_0}{EI} \cdot \Delta x^2$	

The fifth step, Table 3.5, involves the division of y_a/y_b . This value should converge on a common value in order for the results to be correct; that is that the relationship between the assumed and the derived values of deflection is constant through the structure. If the values do not converge, a new iteration is required.

Table 3.6: Sixth step

$\frac{x}{L}$	y_a	y''	y'	y_b	$\frac{y_a}{y_b}$
1	1	0	6.39	40.75	0.025
0.9	0.84	0.16	6.23	34.36	0.024
0.8	0.69	0.31	5.91	28.14	0.024
0.7	0.54	0.46	5.45	22.22	0.024
0.6	0.41	0.59	4.86	16.77	0.024
0.5	0.29	0.71	4.15	11.91	0.024
0.4	0.19	0.81	3.33	7.76	0.024
0.3	0.11	0.89	2.44	4.43	0.024
0.2	0.05	0.95	1.49	1.99	0.024
0.1	0.01	0.99	0.50	0.50	0.024
0	0	1	0	0	0.000
	y_0	$\frac{N_{cr,B} \cdot y_0}{EI}$	$\frac{N_{cr,B} \cdot y_0}{EI} \cdot \Delta x$	$\frac{N_{cr,B} \cdot y_0}{EI} \cdot \Delta x^2$	

The sixth step, Table 3.6, involves an iteration of the previous calculations. Now it is the estimated y_a which is altered through the use of the derived y_b .

For example: to obtain the new y_a value where $x/L = 0.5$, the relationship between the derived total deflection, 41.75 in this case, and for the deflection derived at the position $x/L = 0.5$, which is 12. (Note that these values are taken from Table 3.5; the fifth step)

$$\frac{12}{41.75} = 0.29$$

which becomes the new value for y_a used in Table 3.6.

This procedure is repeated for all levels and it is observed that the relationship between y_a and y_b becomes nearly constant through the structure. One more iteration can be carried out to improve the results.

Table 3.7: Seventh step

$\frac{x}{L}$	y_a	y''	y'	y_b	$\frac{y_a}{y_b}$
1	1	0	6.36	40.63	0.025
0.9	0.84	0.16	6.20	34.27	0.025
0.8	0.69	0.31	5.89	28.07	0.025
0.7	0.55	0.45	5.44	22.18	0.025
0.6	0.41	0.59	4.85	16.74	0.025
0.5	0.29	0.71	4.14	11.90	0.025
0.4	0.19	0.81	3.33	7.76	0.025
0.3	0.11	0.89	2.44	4.43	0.025
0.2	0.05	0.95	1.49	1.99	0.025
0.1	0.01	0.99	0.50	0.50	0.025
0	0	1	0	0	0.000
	y_0	$\frac{N_{cr,B} \cdot y_0}{EI}$	$\frac{N_{cr,B} \cdot y_0}{EI} \cdot \Delta x$	$\frac{N_{cr,B} \cdot y_0}{EI} \cdot \Delta x^2$	
Total	4.14			168.46	
Δx	0.1				
$N_{cr,B}$	2.46 (k)	$\frac{EI}{L^2}$			

Now the value for y_a/y_b has converged. It is now possible to establish the critical load $N_{cr,B}$. The value $N_{cr,B}$ is derived from:

$$N_{cr,B} = \left(\frac{\sum y_a}{\sum y_b} \right) \cdot \left(\frac{EI}{(\Delta x \cdot L)^2} \right) = k_V \cdot \frac{EI}{L^2} \quad (3.38)$$

and can also be compared with the value derived from using Euler buckling:

$$N_{cr,B} = \frac{\pi^2 \cdot EI}{(k_E \cdot L)^2} \quad (3.5)$$

The final value of $2.46 \cdot \frac{EI}{L^2}$ is very close to $\frac{\pi^2}{2^2}$; where 2 is the Euler constant k_E for a cantilever column. Be very aware of the difference between the Vianello k_V and the Euler buckling k_E -value. See case 1 in Section 3.1.2.

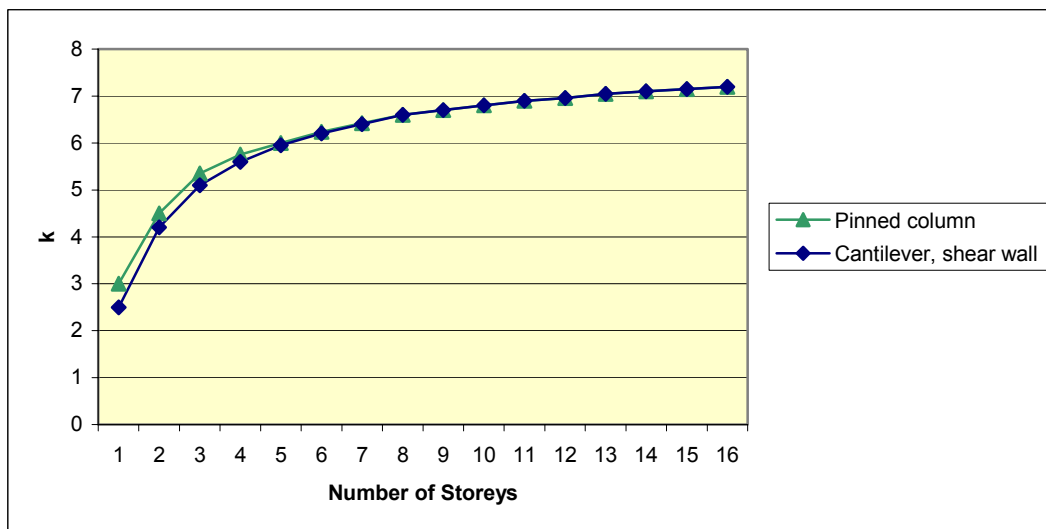


Figure 3.13: Diagram of k_V , depending on boundary conditions, graphed against the number of storeys in a building with evenly distributed load and constant EI .

The k_V taken from Figure 3.13 can be used for rough estimates if it is assumed that the structure is evenly loaded and has a constant EI value. The k_V value for such a structure is obtained from the figure above, as will be seen later in the thesis, by using this k_V the calculations will be, to a great extent, on the safe side. Observe that the maximum k_V , with the above assumptions, will gradually reach but not exceed 7.8.

Later in the thesis it will be seen how effective a tool the Vianello Method is. It is very important to get a more accurate value for k_V when dealing with structures with different stiffnesses and different loads per floor where an erroneous critical buckling load concerning bending will be reached if Table 3.13 is used.

3.4 Elastic restraint

The purpose of this section is to establish the equations which describe the relationship between the structure and the soil upon which the structure is situated. A final N_{cr} value shall be obtained and an explanation of how it is further used in calculating stability shall be explained.

Structures that are not founded directly in the bedrock have an interaction between their foundations and the ground. The assumption that the foundations are fully fixed i.e. that the soil is infinitely firm, can not always be satisfactorily applied. In reality the buildings foundations will undergo a certain amount of movement depending on the deformations from the soil properties.

A structure, situated on soil with assumed elastic properties, alters from being a fully fixed connection to becoming a pinned joint. This assumption about elasticity can only be taken as a liberal approximation because in reality the connection is based on a united action between the structure and the ground which is actually seldom completely elastic. Even though there is not a linear relationship between the connection and the deformation of the building it is assumed that there is because to try to follow the exact relationship will lead to nonlinear irregularities. It may not be a perfect model of reality but this assumption of elasticity does give a calculation that is on the safe side. [Lorentsen *et al.* (2000)]

In elastic restraint calculations one has to deal with four buckling load parameters of N .

$(\Sigma N)_{cr,tot}$ = Total critical buckling load.

$(\Sigma N)_{cr,elrest}$ = Total critical buckling load regarding elastic restraint.

$(\Sigma N)_{cr,B}$ = Total critical buckling load regarding bending.

$(\Sigma N)_{cr,S}$ = Total critical buckling load regarding shear.

The angle γ_{er} describes the elastic restraint. The angle is reached as the restrained cross section is acted upon by a moment that equals one, or the moment which is needed is influenced by an angle γ_{er} which equals one. [Lorentsen *et al.* (2000)]

The previously described Vianello method for calculating the buckling load while considering bending can be implemented. The one alteration is that the previous boundary condition of $y'=0$ is now, because of elastic restraint, taken as $y'=M\gamma_{er}$. Through the iteration is acquired the critical load $N_{cr,B}$. Figure 3.14 below describes the model used for an elastically restrained Vianello iteration with a three storey building with three loads applied.

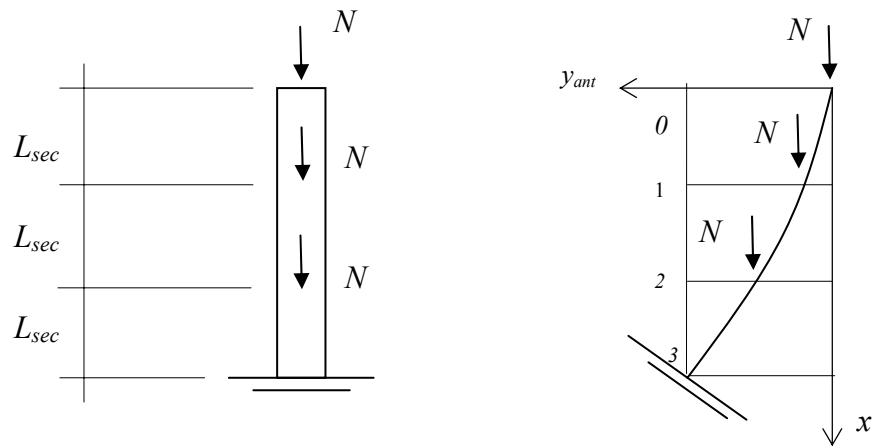


Figure 3.14: Model used for an elastically restrained Vianello iteration.

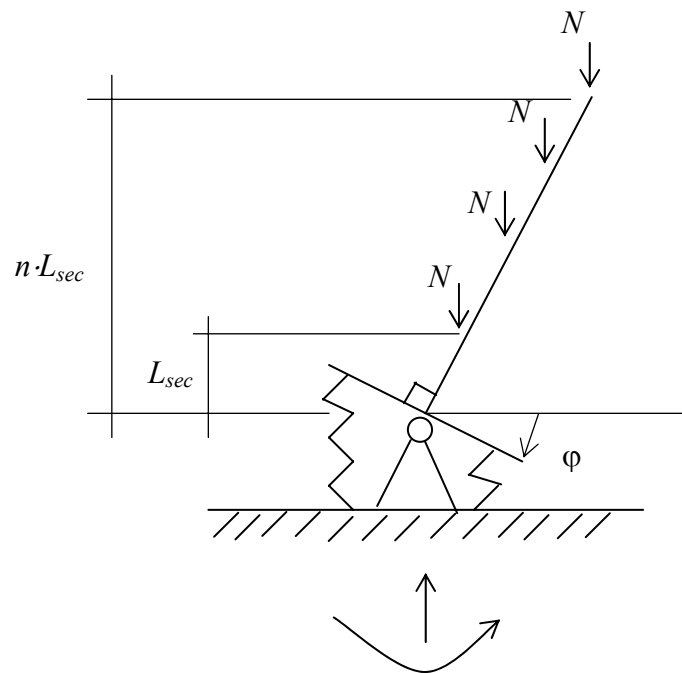


Figure 3.15: An elastic connection between the structure and the ground.

For calculating $N_{cr,elrest}$, the model in Figure 3.15 is used. Here it is assumed that the structure has infinite bending stiffness and hence the shape of the column will remain a straight line. The column is tilting because of the elastic restraint between the structure and the ground. The restraint moment, M_{er} , is calculated through assuming first the deflection, by multiplying the angle at the base by the vertical distance to the force, and then multiplying that deflection by the appropriate force. The equation can be written in a series form to describe the number of floors and forces applied. [Lorentsen (2000)]

$$M_{er} = \varphi \cdot L_{sec} \cdot (1N + 2N + 3N + \dots + nN)$$

This equation can be summarized as:

$$M_{er} = \varphi \cdot L_{sec} \cdot N \cdot \frac{n+1}{2} \cdot n \quad (3.40)$$

When the structure barely reaches buckling it is realized that $\Sigma N = \Sigma N_{cr,elrest}$. For this to be true, the angle change φ must be equal to the previously described γ_{er} , describing elastic restraint, times the restraint moment M_{er} .

$$\varphi = M_{er} \cdot \gamma_{er} \quad (3.41)$$

Combined with $N = N_{cr,elrest}$ is obtained:

$$M_{er} = M_{er} \cdot \gamma_{er} \cdot L_{sec} \cdot N_{cr,elrest} \cdot \frac{n+1}{2} \cdot n \Rightarrow N_{cr,elrest} = \frac{2}{n \cdot (n+1) \cdot L_{sec} \cdot \gamma_{er}}$$

It is known that $(\Sigma N)_{cr,elrest} = n \cdot N_{cr,elrest}$. So therefore the summation term for all total critical buckling loads, with regards to elastic restraint, can be written as:

$$(\Sigma N)_{cr,elrest} = \frac{2}{(n+1) \cdot L_{sec} \cdot \gamma_{er}} \quad (3.42)$$

To then obtain the $(\Sigma N)_{cr,tot}$ value, the formula below is used:

$$\frac{1}{(\Sigma N)_{cr,tot}} = \frac{1}{(\Sigma N)_{cr,B}} + \frac{1}{(\Sigma N)_{cr,elrest}} \quad (3.43)$$

The value $(\Sigma N)_{cr,B}$ is here the bending defined for instance through the Vianello method; where k_V is obtained from Figure 3.13, depending on the number of storeys.

Using this method it should be observed that the value $(\Sigma N)_{cr,tot}$ derived through a Vianello iteration for an elastically restrained structure is the theoretically correct result and the value for $(\Sigma N)_{cr,tot}$ derived through combining the values for $(\Sigma N)_{cr,elrest}$ and $(\Sigma N)_{cr,B}$ is a value which lands on the safe side.

If shear is also taken into consideration then the solution becomes:

$$\frac{1}{(\Sigma N)_{cr,tot}} = \frac{1}{(\Sigma N)_{cr,B}} + \frac{1}{(\Sigma N)_{cr,S}} + \frac{1}{(\Sigma N)_{cr,elrest}} \quad (3.44)$$

[Lorentsen *et al.* (2000)]

4 Calculation methods for stabilising systems

This chapter considers first the one storey systems where the buildings symmetry provides the engineer with the option of only calculating in one plane due to the columns of each wall being isolated. Rotation is not relevant to this type of calculation. The concept of stiffness is introduced to the calculations and the method describes how columns which are stabilising or non-stabilising are integrated into the calculations. It is explained how the design forces and moments are acquired and a numerical example is presented in order to facilitate understanding.

Secondly, the phenomenon buckling in space is investigated. Here rotation is included in the calculations. A method is described of how one first establishes the critical buckling load, due to bending and shear, and thereafter a new stiffness value is derived. The calculating of the location of the rotational centre is explained and the concept of the *polar moment of inertia* is introduced. It is then explained how this method is used for single storey structures and how the Vianello k_V is used in the calculations on multi-storey buildings. One numerical example is presented for a single storey structure and a second for a multi-storey building.

4.1 Single storey system acting in a plane

Buildings, which consist of many different stabilising components of different stiffness, can be quite complicated to solve through hand calculations. As the components have different stiffness values they will also behave differently, and the force distributions through an entire building can be hard to establish. Stiffer units will attract greater moments and forces than weaker ones. The establishment of the force distribution is of vital importance, as without the knowledge of how a building reacts from the applied forces, wrong approximations could contribute to a faulty design of the structure. In Section 2.4.1, different stabilising components are described separately and in this section combined components and how they act together will be presented. During calculation, the rigidity is often represented by a *stiffness number*, j . It is important to understand how the stiffness number influences the stability of a system and it is therefore introduced by a simple single storey system acting in one plane.

4.1.1 Assumptions

Normally it may be assumed that all columns fixed at the base are fully fixed. These suppositions are sufficient in most cases but the behaviour of the foundation or the ground, under heavy loading, has to be ensured. Another assumption, concerning the load distribution, affects the calculation method. If the columns have the same stiffness and the loads are evenly distributed on them, they can be treated as isolated columns. Otherwise, the calculation method has to represent a system of columns. Assumption regarding deflections is normally based on that no slip or extension occurs between stabilizing units, i.e. the columns have the same deflection, see Figure 4.1.

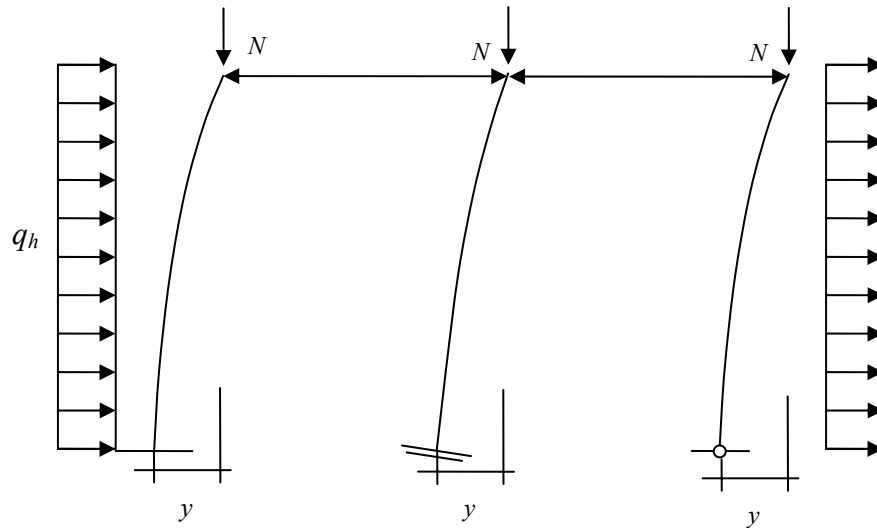


Figure 4.1: One storey system of columns showing equal deflections.

4.1.2 Stiffness number

Stiffness number, j , for a cantilever column is defined as the horizontal force applied at the top of the column which gives the deflection equal to 1, see Figure 4.2

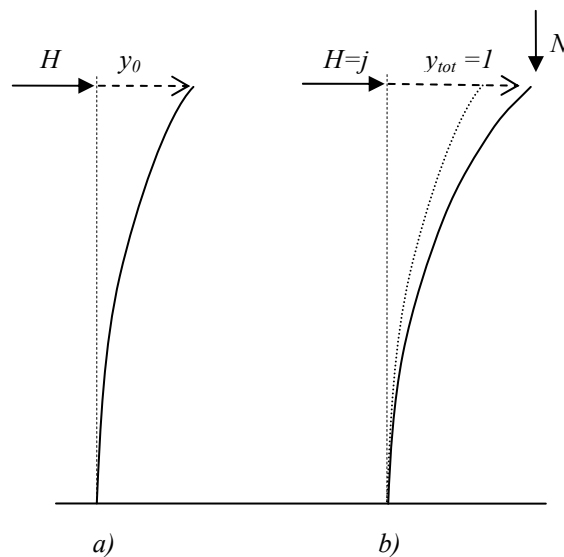


Figure 4.2: Establishment of stiffness number j .

The column is assumed to have constant stiffness along its length. y_0 is the top deflection that occurs from H only, Figure 4.2a. To include the 2nd order effects the total deflection is derived by multiplying with the magnification factor mentioned in Section 3.15.

$$y_{tot} = y_0 \cdot \frac{1}{1 - \frac{N}{N_{cr}}} \quad (\beta=1) \quad (4.1)$$

$$y_0 = H \cdot \frac{L^3}{3EI} \quad (4.2)$$

$$N_{cr,B} \text{ for a cantilever column with Euler } k_E=2, \text{ is } N_{cr,B} = \frac{\pi^2 EI}{4L^2}. \quad (3.5)$$

With $y_{tot} = 1$ the following expression gives the stiffness number j . Observe the definition of the stiffness number, $H = j$, see Figure 4.2b.

$$1 = \frac{j \cdot L^3}{3EI} \cdot \frac{1}{1 - \frac{N}{N_{cr}}} \Rightarrow j = \frac{3EI}{L^3} \left(1 - \frac{N}{N_{cr}} \right) \quad (4.3)$$

This expression is an approximation and is a very accurate one. The stiffness value, agrees very well with the exact values which are presented in Petersson and Sundquist (2002).

4.1.3 System of columns acting in one plane

The critical buckling load for a complete system, $N_{cr,sys}$ is to be derived. To determine the buckling load regarding a system of components, of equal or different stiffness, the buckling criterion is set so that the sum of all the components' stiffness values is equal to zero, i.e. $\Sigma j = 0$

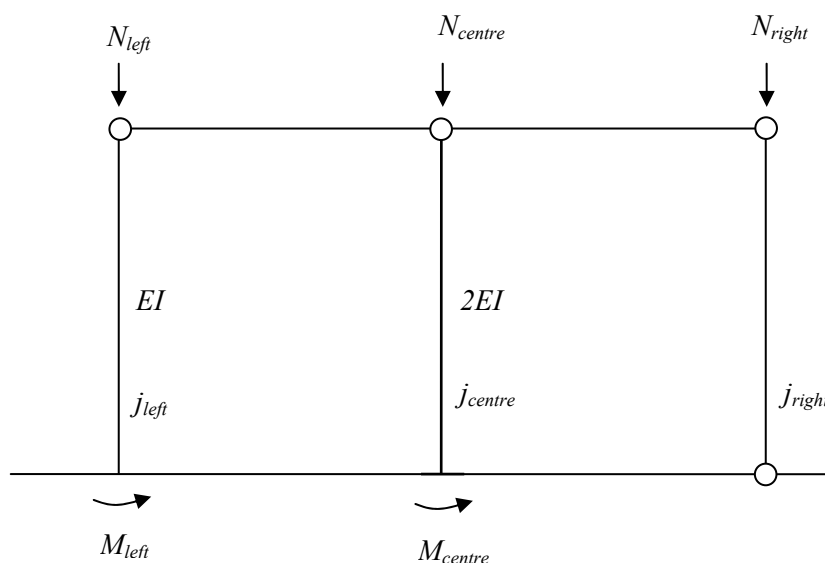


Figure 4.3: Columns acting in one plane.

Figure 4.3 illustrates a system of three columns where the left and the centre columns are fully fixed at the base, while the right one is pinned. This means that the left and the centre columns are the stabilising units of this system and they also have to brace the right column. In this example the centre column has twice the stiffness of the left one.

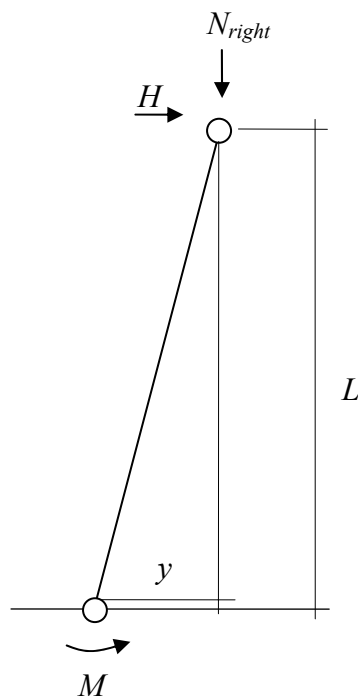
$$j_{left} = \frac{3 \cdot EI}{L^3} \left(1 - \frac{N_{left}}{N_{cr,left}} \right) \quad j_{centre} = \frac{3 \cdot 2EI}{L^3} \left(1 - \frac{N_{centre}}{N_{cr,centre}} \right) \quad (4.3)$$

$$j_{right} = ??? \Rightarrow \text{See Section 4.1.4}$$

$$N_{cr,left} = \frac{\pi^2 EI}{4L^2} \quad N_{cr,centre} = \frac{\pi^2 2EI}{4L^2} = 2 \cdot N_{cr,left} \quad (3.5)$$

4.1.4 Stiffness number for a non-stabilising unit

A non-stabilising unit can be identified with a pin ended column and will take vertical loads only. As a sway occurs in the system a horizontal load develops due to the vertical load.



Stiffness number for a non stabilising member:

$$M = H \cdot L + N \cdot y = 0 \Rightarrow H = -\frac{N \cdot y}{L}$$

$$j = \frac{H}{y} \Rightarrow j \cdot y = -\frac{N \cdot y}{L} \Rightarrow$$

$$j = -\frac{N}{L} \quad (4.4)$$

Figure 4.4: Establishing j for a non-stabilising column.

The result for a non stabilising component is always a negative value and reveals that it has to be stabilized by other units.

The sum of the stiffness numbers of the vertical components in this example are;

$$\Sigma j = j_{left} + j_{centre} + j_{right} \Rightarrow \frac{3EI}{L^3} \left[\left(1 - \frac{N_{left}}{N_{cr, left}} \right) + 2 \cdot \left(1 - \frac{N_{centre}}{2 \cdot N_{cr, left}} \right) \right] - \frac{N_{right}}{L}$$

The final expression is only referring to the above described example and is not a general expression. The example shows that the method can be used for all cases whether there are plenty of columns with different stiffness, different loads or with different boundaries.

The expression, $\Sigma j = 0$, can also be described as a condition for critical buckling

As mentioned earlier the stiffness number is equal to the horizontal force which gives a deflection equal to 1. When the stiffness number is larger than zero i.e. $N < N_{cr, tot}$, the system is stable.

4.1.5 Horizontal load distribution among columns in a plane

In a stabilising system which consists of vertical elements of unequal stiffness, the horizontal load will not be equally divided among them. The stiffer members will attract more load than the weaker. Using the previous example, the centre column which has twice the stiffness of the left column, will in this case attract a larger part of the total horizontal load.

The system is now to be subjected with a horizontal force H , see Figure 4.5.

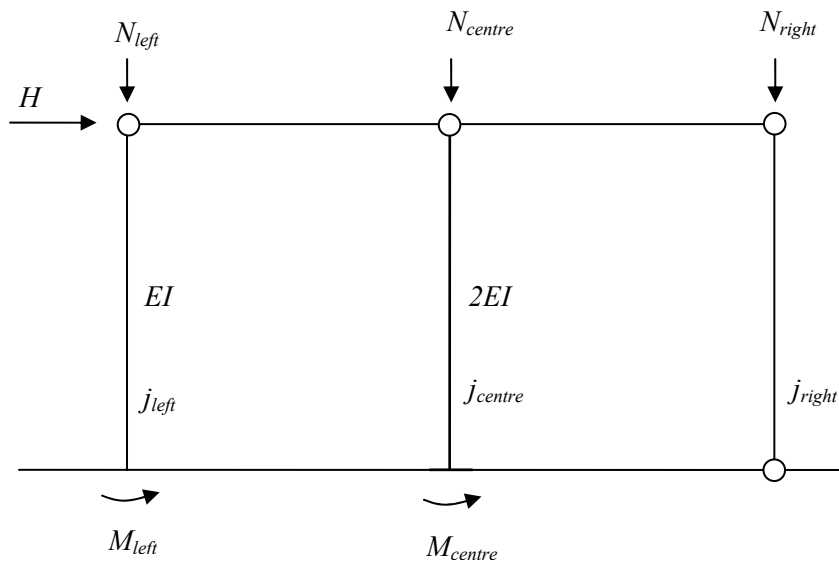


Figure 4.5: One Storey column system with applied force H .

The horizontal force which subjects each column can be derived by quotients of the total stiffness and the stiffness of the actual column.

$$H_{left} = \frac{j_{left}}{j_{system}} H = \frac{j_{left}}{\sum j} H \quad (4.5)$$

In Section 4.1.7, a numerical example shall be calculated to clarify this method.

4.1.6 Calculation method of moments on a single storey one plane system

In Section 4.1.5 above, horizontal forces on each column have been established from the stiffness distribution among the columns. These forces give a contribution to the maximum moment on the columns which is obviously highest at the base. The horizontal force is often coming from wind load on the façade and from unintended inclination. The arrangement of the facade, mentioned in Section 2.2.1, often means that the wind load on the facade is transferred to the slabs which further subject the columns with a concentrated load. In this example however, the columns are attached directly to the façade and are therefore subjected to a distributed load, see Figure 4.6. The moment, contributed from the distributed load, is here named *local moment* as it only affects the outer columns attached to the facades. To take into account both contributions the calculation method is divided into two parts. The total moment for a column is the sum of the moments.

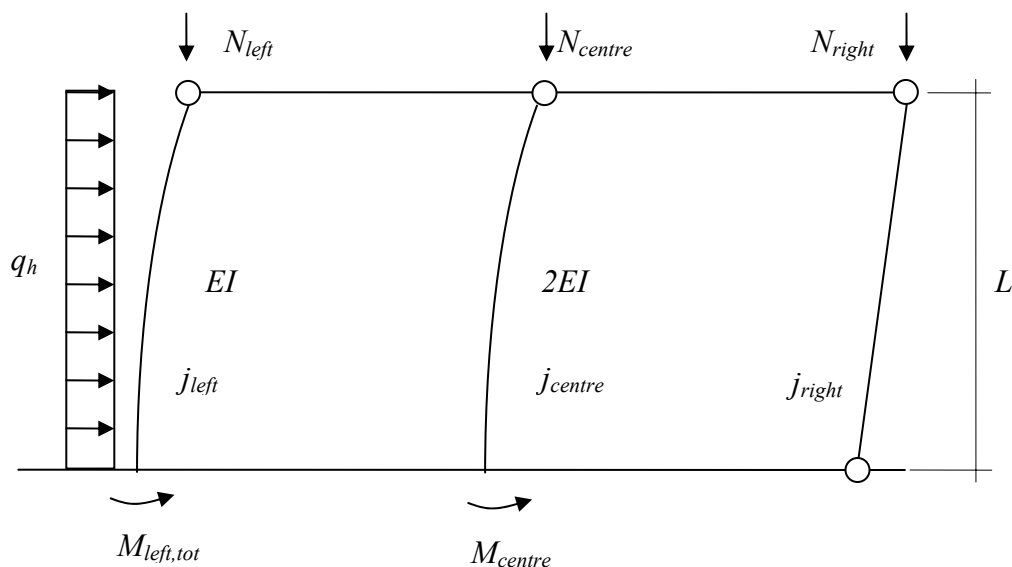


Figure 4.6: One storey column system.

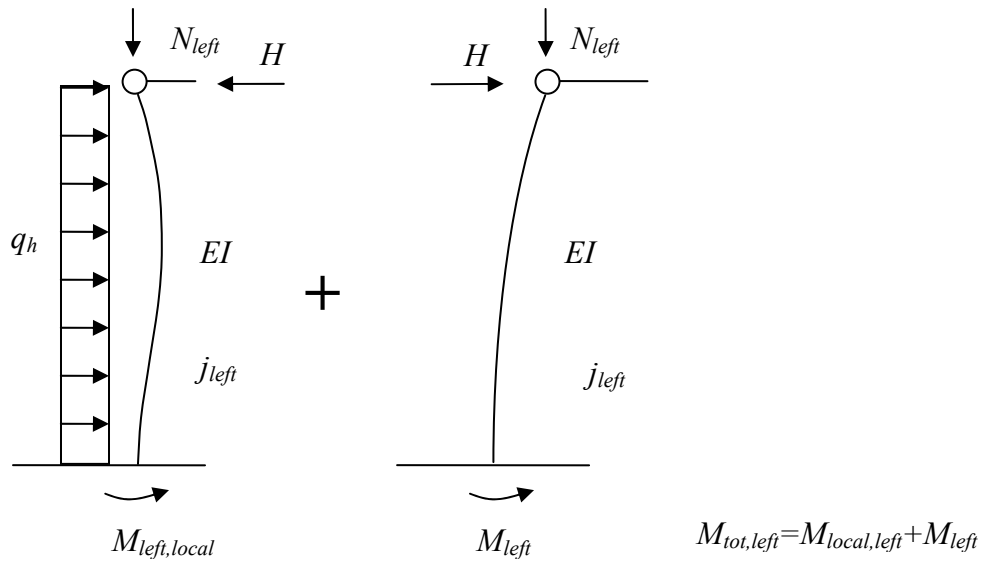


Figure 4.7: The two calculation parts.

1. This part concerns the establishment of the local moment.

To calculate the moment from the applied load the system is first imagined to be braced. The braced system will contribute with a horizontal reaction force which is a part of all the applied horizontal loads acting on the building. This includes the load contribution from unintended initial inclination. All vertical loads are here disregarded.

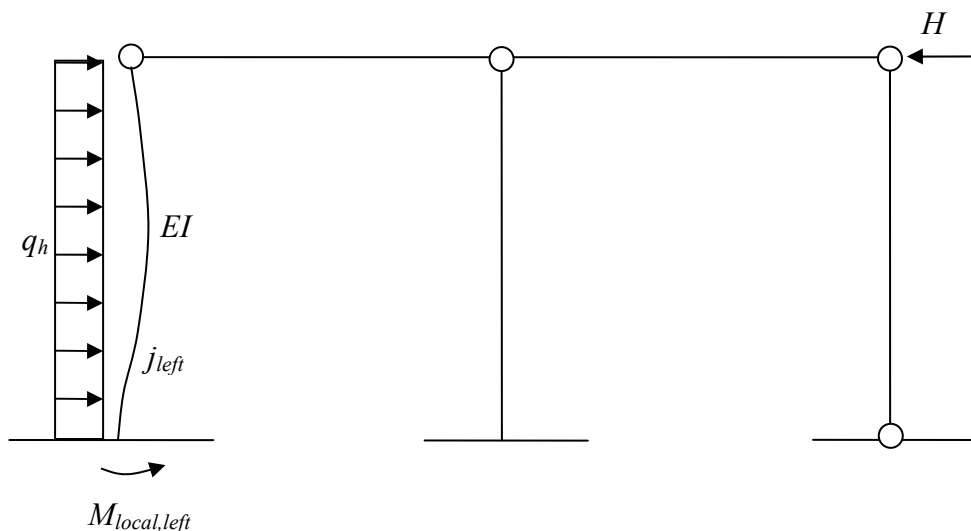


Figure 4.8: First part.

The bracing force, H , is in this case equal to a part of the distributed load and the horizontal force occurring from the unintended inclination.

$$H = \frac{3}{8} q_h L + \Sigma N \cdot \alpha_m \quad (4.6)$$

α_m : a factor regarding initial inclination. [Boverket (2002)]

Observe that the bracing force does not inflict the moment in this part, part 1. The bracing force is taken into account in part 2 but is established here.

Local moment:

In this case only the left column is affected by the distributed load.

$$\text{Left column: } M_{local, left} = q_h \frac{L^2}{8} \quad (\text{at the base}) \quad (4.7)$$

$$\text{Centre column: } M_{local, centre} = 0$$

- The second part concerns the moment occurring from the braced horizontal force established in part 1. The bracing force is a reaction force, and the moment is therefore now calculated with the same force but in the opposite direction.

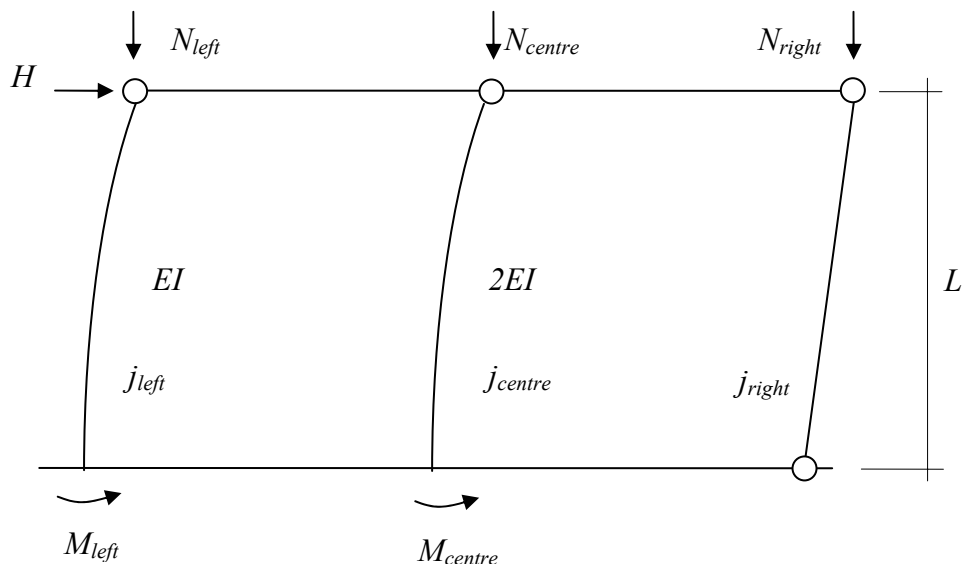


Figure 4.9: Second part.

The moment in this part consists of both the 1st and the 2nd order moments. The 2nd order moment is established from the vertical forces and the deflection. Observe that the horizontal force occurring from the *initial unintended inclination* is not a 2nd order effect. It is taken into account as a part of the 1st order contribution.

In this case the left and centre columns have unequal stiffness numbers and will not have the same contribution for stabilisation. The stiffness numbers are first established and are then used to calculate the total deflection of the system.

$$\Sigma j = \frac{3EI}{L^3} \left(1 - \frac{N}{N_{cr,left}} \right) + \frac{3 \cdot 2EI}{L^3} \left(1 - \frac{N}{N_{cr,col}} \right) - \frac{N}{L} \Rightarrow$$

$$y = \frac{H}{\Sigma j} \quad (4.8)$$

The deflection, y , is used to establish the second order moment.

$$M_{left} = M_{centre} = M_0 + \Delta M = \frac{1}{2} H \cdot L + N \cdot y$$

The total moment is established by summing both the contributions.

Left column: $M_{tot,left} = M_{local,left} + M_{left}$

Centre column: $M_{tot,centre} = M_{local,centre} + M_{centre}$

4.1.7 Numerical example - Columns in one plane

The same example used in Section 4.1.6 is utilised here. In this example the actual force and the moment in the left and centre columns are to be established. Thereafter the critical buckling load for the system shall be calculated. This example is an exercise and the parameter values do not represent a real structure.

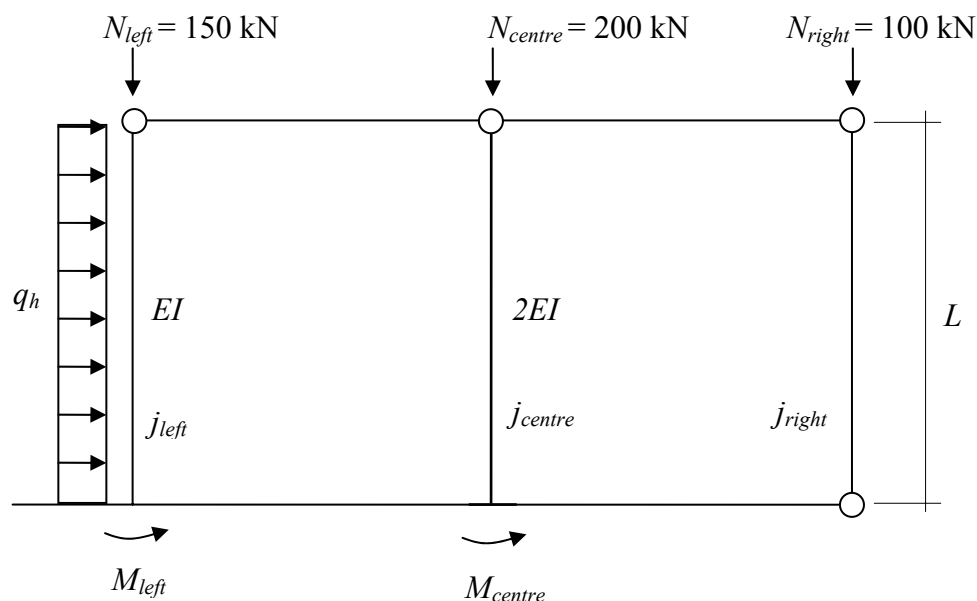


Figure 4.10: Numerical example.

Values: $q_h = 10 \text{ kN/m}$ $N_{left} = 150 \text{ kN}$,
 $EI = 9 \text{ MNm}^2$ $N_{centre} = 200 \text{ kN}$
 $L = 5 \text{ m}$ $N_{right} = 100 \text{ kN}$

Establishment of stiffness numbers:

From Equation (3.15) the critical buckling load due to bending is derived.

$$N_{cr,left} = \frac{\pi^2 EI}{4 \cdot L^2} = \frac{\pi^2 \cdot 9 \cdot 10^6}{4 \cdot 5^2} = 888 \text{ kN} \quad N_{cr,centre} = 2 \cdot N_{cr,left} = 1776 \text{ kN}$$

$$j_{left} = \frac{3 \cdot EI}{L^3} \left(1 - \frac{N_{left}}{N_{cr,left}} \right) \quad j_{left} = \frac{3 \cdot 9 \cdot 10^6}{5^3} \left(1 - \frac{150}{888} \right) = 179 \text{ kN/m}$$

$$j_{centre} = \frac{3 \cdot 2EI}{L^3} \left(1 - \frac{N_{centre}}{N_{cr,centre}} \right) \quad j_{centre} = \frac{3 \cdot 2 \cdot 9 \cdot 10^6}{5^3} \left(1 - \frac{250}{1776} \right) = 371 \text{ kN/m}$$

$$j_{right} = -\frac{N_{right}}{L} \quad j_{right} = -\frac{100 \cdot 10^3}{5} = -20 \text{ kN/m}$$

$$\Sigma j = 179 + 371 - 20 = 530 \text{ kN/m}$$

Horizontal force distribution on each column:

The bracing force, Equation (2.4), is to be established from the distributed load, q_h .

$$H = \frac{3}{8} q_h L + \Sigma N \cdot \alpha_m$$

$$\alpha_m = 0.003 + \frac{0,012}{\sqrt{n}} \quad n: \text{The number of columns above the floor.}$$

$$\alpha_m = 0.003 + \frac{0.012}{\sqrt{3}} = 0.0099 \approx 0.01$$

Bracing force: $H = \frac{3}{8} 10 \cdot 5 + (150 + 250 + 100) \cdot 0.01 = 23.75 \text{ kN}$

The horizontal force for the left and the centre columns can be directly established by quotients. The moments are thereafter established.

$$H_{left} = \frac{j_{left}}{\Sigma j} H = \frac{179}{530} \cdot 23.75 = 8.0 \text{ kN}$$

$$H_{centre} = \frac{j_{centre}}{\Sigma j} H = \frac{371}{530} \cdot 23.75 = 16.6 \text{ kN}$$

Observe that only 3/8 of the total horizontal load is applied on the top part.

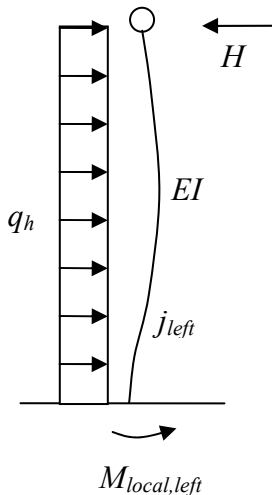
Moments: $M_{centre} = H_{centre} \cdot L + N_{centre} \cdot y$

y is the deflection derived from the applied horizontal force and the stiffness number.

$$y = \frac{H}{\Sigma j} \quad y = \frac{23.75 \cdot 10^3}{530 \cdot 10^3} = 0.045 \text{ m (deflection at the top of the columns)}$$

$$M_{centre} = 16.6 \cdot 5 + 200 \cdot 0.045 = 92 \text{ kNm}$$

The moment affecting the left column has an additional contribution, M_{local} , explained in part 1 Section 4.1.6.



$$M_{local,left} = \frac{q_h L^2}{8} = \frac{10 \cdot 5^2}{8} = 31.2 \text{ kNm}$$

$$M_{tot,left} = 8.0 \cdot 5 + 150 \cdot 0.045 + 31.2 = 78.1 \text{ kNm}$$

Figure 4.11: Part 1.

The establishment of the critical buckling load for the system:

To determine the buckling load for the whole system the same equations concerning the stiffness number are used. Observe in the equation below that N is here represented by a relative value obtained by quotients considering the vertical load distributions among the columns.

It is now decided that N_{centre} is set to N and the other two columns are quotients based upon the vertical load differences between the actual column and the centre column.

$$N_{centre} = N$$

$$N_{left} = \frac{N_{left}}{N_{centre}} = \frac{150}{200} = \frac{3}{4} \Rightarrow N_{left} = 0.75N$$

$$N_{right} = \frac{N_{right}}{N_{centre}} = \frac{100}{200} = 0.5 \Rightarrow N_{right} = 0.5N$$

$$\Sigma j = 0 \quad \Rightarrow \quad \Sigma j = j_{left} + j_{centre} + j_{right} = 0 \quad \Rightarrow$$

$$\frac{3EI}{L^3} \left(1 - \frac{0.75N}{N_{cr,left}} \right) + \frac{3 \cdot 2EI}{L^3} \left(1 - \frac{N}{N_{cr,centre}} \right) - \frac{0.5N}{L} = 0$$

$$\frac{3EI}{L^3} - \frac{0.75N}{N_{cr,left}} \frac{3EI}{L^3} + \frac{3 \cdot 2EI}{L^3} - \frac{N}{N_{cr,centre}} \frac{3 \cdot 2EI}{L^3} - \frac{0.5N}{L} = 0$$

$$\frac{3EI}{L^3} + \frac{6EI}{L^3} - \left(\frac{0.75}{N_{cr,left}} \frac{3EI}{L^3} + \frac{1}{2 \cdot N_{cr,left}} \frac{6EI}{L^3} + \frac{0.5}{L} \right) N = 0$$

$$\frac{9EI}{L^3} - \left(\frac{0.75}{N_{cr,left}} \frac{3EI}{L^3} + \frac{1}{N_{cr,left}} \frac{3EI}{L^3} + \frac{0.5}{L} \right) N = 0$$

$$\frac{9EI}{L^3} - \left(\frac{5.25EI}{N_{cr,left} \cdot L^3} + \frac{0.5}{L} \right) N = 0$$

$$N = \frac{\frac{9EI}{L^3}}{\left(\frac{5.25EI}{N_{cr,left} \cdot L^3} + 0.5 \right)} = \frac{\frac{9 \cdot 9 \cdot 10^6}{5^2}}{\left(\frac{5.25 \cdot 9 \cdot 10^6}{888 \cdot 10^3 \cdot 5^2} + 0.5 \right)} = 1.23 \text{ MN}$$

To establish the critical buckling load for the system a summation of the loads is made.

$$N_{cr,sys} = N + 0.75N + 0.5N = 1.23(1 + 0.75 + 0.5) = 2.77 \text{ MN}$$

The critical buckling load is compared with the sum of all vertical loads.

$$\Sigma N = 150 + 250 + 100 = 500 \text{ kN} \quad \Rightarrow \quad \Sigma N < N_{cr,sys}$$

In this example the method for establishing the moment at the base of the columns is to directly use the stiffness numbers. The second order effect is then included in the expression for the stabilising columns. In Section 3.1.5 the derivation of the magnification factor is shown which is used for more complex systems. This factor is

calculated by using the total vertical load in relation to the critical buckling load for the whole structure. This approach can also be used in the example above to establish the total moment by multiplying the first order moment with the magnification factor. The local moment at the left column is then not included. When using the above method it is not necessary to calculate $N_{cr,sys}$, but it can be done in order to compare with the total vertical load.

4.2 Stabilisation systems – Buckling in space

In Section 4.1.6, the buckling load has been derived for simple structures in one plane (buckling in x -direction for example). In this section *buckling in space* will be introduced for both single and multi storey structures. This section involves buckling in both x and y , i.e. translation, but also buckling through rotation. The method used for single storey structures differs from the one used in multi-storey structures but the basic theory is the same. [Lorentsen *et al.* (2000)] The expressions used for multi storey structures are a simplified method based upon the more accurate equations used for single storey structures. The theory is first derived and then explained through two examples concerning both single and multi-storey structures. Thereafter a summation of the equations for a single storey structure, i.e. the more accurate method, is presented and is followed by the expressions for a multi-storey structure. Two numerical examples will thereafter be presented, one concerning single storey structure and one for a multi storey building.

4.2.1 General expression of translation and rotation

Vianello's method is first used to establish the k_V -value which is used to calculate the buckling load, concerning bending, for the structure. The value can also be taken directly from Figure 3.13 in Section 3.3 if the storeys have equal stiffness and if the loads are evenly distributed through the building.

$$N_{cr,B} = k_V \cdot \frac{EI}{L_h^2} \quad (3.38)$$

Before the critical buckling load can be calculated the stiffness of the whole structure has to be established first. The stiffness is divided into x -, y -translation and rotation. The buckling criterion for each direction is:

Translation:

$$\sum_1^n J_{i,x} = 0 \quad \text{buckling in } x\text{-direction} \quad (4.9)$$

$$\sum_1^n J_{i,y} = 0 \quad \text{buckling in } y\text{-direction} \quad (4.10)$$

Rotation:

$$\sum_1^n (j_{i,x} y_i^2 + j_{i,y} x_i^2) = 0 \quad \text{buckling through rotation.} \quad (4.11)$$

The last expression describes the summation of all components, both stabilising and non-stabilising. Each stabilising component has a stiffness value which contributes, through rotation, to stabilisation. The stiffness of the unit, and its distance to the rotation centre of the building, reveals the rotation capacity of the stabilising unit. x_i and y_i are the distances from the units rotation centre to the rotation centre of the whole structure. Observe that the units stabilising in the x -direction are multiplied with the distance in y -direction and vice versa, see the derivation of Equation 4.11 in Section 4.2.2.

A complete structure consists not only of stabilising units but also of non-stabilising units. As described in Section 4.1.4, non-stabilising components, which are only loaded through vertical forces, have a negative contribution in the summation of the stiffness numbers.

$$j_{i,x} = \frac{3EI_x}{L^3} \left(1 - \frac{N}{N_{cr}} \right) \quad \text{Stabilising components (fixed and cantilever)} \quad (4.3)$$

$$j = -\frac{N}{L} \quad \text{Non-stabilising component, eg. a hinged column.} \quad (4.4)$$

4.2.2 Derivation of critical buckling load through rotation

In this section the critical buckling load through rotation will be derived for stabilising units. Non stabilising units, such as pin ended columns, are described in Section 4.2.3.4 using the polar moment of inertia as a simplified expression. This example is using *stabilising columns*, i.e. fixed at the base but hinged at the top. The column is stabilising in both main directions and therefore derives an expression regarding both x - and y -directions. It is then easy to understand how the expression is used for shear walls which are assumed to stabilise in one direction only.

Figure 4.12 below describes a stabilising column at a certain distance from the rotation centre, RC.

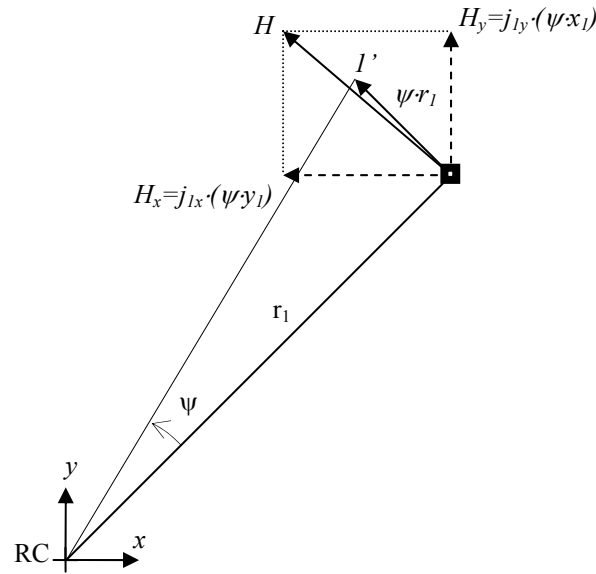


Figure 4.12: Stabilising column with a certain distance from a rotation centre.

A twisting moment is applied on the structure causing a rotation around the rotation centre. The stabilising components in a complete building are subjected to forces which are depending on the stiffness and the distance of the components from the RC. The stiffness number, j , earlier described in Section 4.1.2, is the force subjected to a unit which gives a deflection (at the top) equal to one. The rotation occurring from the moment applied gives a deflection of the column in tangential direction. The deflection is divided into x - and y -direction and the force subjected at the column follows analogous, see Figure 4.12. The force in x direction which gives a deflection equal to 1, is the stiffness number in x direction, j_x . The same follows for the y -direction. ψ is the rotation angle.

$$H_{i,x} = j_{i,x} \psi \cdot y_i \quad (4.12)$$

$$H_{i,y} = j_{i,y} \psi \cdot x_i \quad (4.13)$$

The sum of moments from all stabilising units is equal to the twisting moment applied.

$$M_{twist} = H_{1,x} y_1 + H_{1,y} x_1 + \dots + H_{n,x} y_n + H_{n,y} x_n = \sum_1^n (j_{i,x} \psi \cdot y_i^2 + j_{i,y} \psi \cdot x_i^2)$$

As the stabilising components are subjected to an increasing vertical load, the deflection increases until the load has reached the critical buckling load of rotation. In this stage the complete building has a rotation which gives rise to a deflection of all units without an external moment having been applied. The expression above is then equal to zero as the applied moment is zero.

$$M_{twist} = 0 \quad \Rightarrow \quad \sum_1^n (j_{i,x} \psi \cdot y_i^2 + j_{i,y} \psi \cdot x_i^2) = 0 \quad (4.14)$$

The angle, ψ , is then reduced and the final expression for the critical buckling load through rotation takes the form;

$$\sum_1^n (j_{i,x}y_i^2 + j_{i,y}x_i^2) = 0 \quad (4.11)$$

The expression is now general for all stabilising units that stabilise in both x - and y -directions. When, for example, shear walls are used the walls are assumed to stabilise in one direction only and one part is then equal to zero.

4.2.3 Calculation methods for establishing critical buckling load

This example derives the expressions for stabilising through translation and rotation. The complete structure consists of stabilising walls and vertical columns. The columns are assumed to take all vertical loads and do not contribute to the stabilisation, i.e. they are assumed to be hinged at both ends. The stabilising walls are subjected to horizontal loads only. The walls are fully fixed at the base and are assumed to be hinged at the top end. The columns are evenly distributed and are applied with equal vertical loads. See Figure 4.13. These assumptions are made to simplify the calculation for establishing a method applicable for common structures.

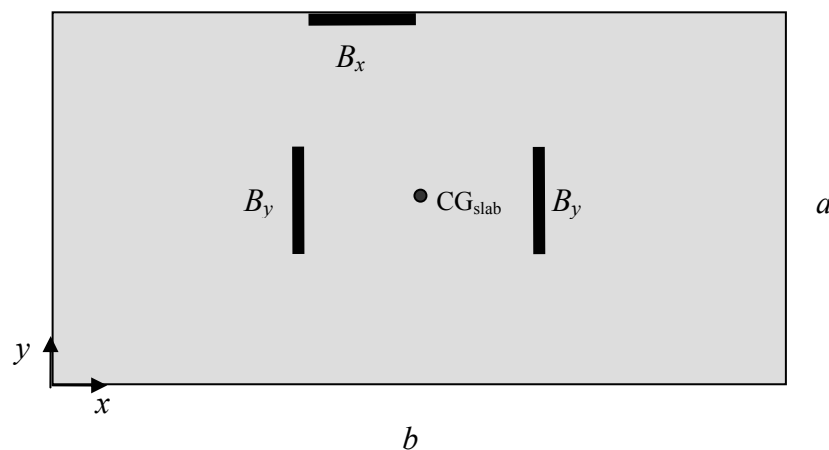


Figure 4.13: Floor plan; 3 shear wall.

4.2.3.1 Stiffness due to influence from shear

In most structures both bending and shear have to be taken into account. The stiffness is changed to B_x and B_y , for x - and y -directions respectively. The stiffness B is based on interaction from both bending and shear.

$$N_{cr,tot} \text{ from bending and shear: } N_{cr,tot} = \frac{1}{\frac{1}{N_{cr,B}} + \frac{1}{N_{cr,S}}} \quad (3.19)$$

$$\text{Establishment of the new stiffness value: } B = \frac{N_{cr,tot}}{N_{cr,B}} \cdot EI \quad (4.15)$$

The same derivation is used for y -direction. Observe that the stiffness B has to be established first before the location of the rotation centre is calculated.

4.2.3.2 Location of the rotation centre

If the building is supported by units placed with symmetrical distances from the centre of gravity of the slab, CG_{slab} , and with equal stiffness, the RC is then located at the CG_{slab} . This can be expressed as the stiffness times the distance; $(B_y \cdot x_{RC})$ is equal to $(B_y \cdot x_{RT})$ on the other side of CG_{slab} . The capacity of taking forces is the same on both sides of the CG_{slab} . If the building is supported by several stabilising units, it is not always obvious where the RC occurs. It is therefore necessary to establish the RC by calculation.

The location of the rotation centre is determined in x - and y -directions respectively.

$$x_{RT} = \frac{\sum (B_y \cdot x_{RT})_{unit}}{\sum B_y} \quad y_{RT} = \frac{\sum (B_x \cdot y_{RT})_{unit}}{\sum B_x} \quad (4.16)$$

Notice that the index on the stiffness B is related to the *direction* the unit stabilises. This index is not to be confused with the index on moment of inertia $I_{x,y}$ which is, in some literature, related to the rotating axis concerned. For this thesis the index on EI_x is therefore concerning the direction.

4.2.3.3 Simplification of stiffness numbers

In the simplified method, used for multi storey structures, no vertical loads are assumed to act on the stabilising walls and the expression concerning the stabilising components is therefore simplified. The expression for the stabilising components will then take the following form:

$$\sum j_x = \frac{3EI_x}{L^3} \left(1 - \frac{N}{N_{cr}} \right) \quad (4.3)$$

$$\Rightarrow \sum j_x \approx \frac{3EI_x}{L^3} \quad B_x \equiv EI_x \quad \Rightarrow \sum j_x = \frac{3B_x}{L^3} \quad (4.17)$$

The same derivation is applied for stiffness in y -direction, two walls.

$$\sum j_y = 2 \cdot \frac{3EI_y}{L^3} \left(1 - \frac{N}{N_{cr}} \right) \Rightarrow \sum j_y = 2 \cdot \frac{3B_y}{L^3}$$

Observe that it is assumed that the walls only stabilise in one direction. The thickness of the walls is minimal and the low contribution of stability in transverse direction is disregarded.

4.2.3.4 Non stabilising units

Translation:

The derivation for non-stabilising units is shown in Section 4.1.4.

$$j_{x,col} = j_{y,col} = -\frac{N_{col}}{L} = -\frac{q_v \cdot \Delta A_i}{L} \quad (\text{Translation}) \quad (4.4)$$

Rotation:

The columns are evenly distributed within the floor slabs and are acting together. The calculation is therefore referring to a whole system of columns and not a single one. The derivation below introduces the concept of the *polar moment of inertia*, I_p , which is related to the size of the slab supported by the distributed columns. The polar moment of inertia is an expression used in the simplified method used for multi storey structures and concerns the non stabilising components only. To use the polar moment of inertia it is assumed that the structure has an endless amount of columns placed with minimal spacing.

$$\sum_1^n (j_{i,x} y_i^2 + j_{i,y} x_i^2) = -\frac{q_v}{L} (y_i^2 + x_i^2) \Delta A = -\frac{q_v}{L} \int_A (y^2 + x^2) dA = -\frac{q_v}{L} I_p \quad (4.18)$$

$$I_p = I_{p,x} + I_{p,y} \quad (4.19)$$

(For rectangular sections, like slabs.)

$$I_p = \frac{ba^3}{12} + \frac{ab^3}{12} = \frac{ab(a^2 + b^2)}{12} \quad (4.20)$$

The Equation 4.20 is simplified from the general calculation of moment of inertia. When the rotation centre is not located at the centre of gravity of the slab, the general expression has to be used.

For y -direction, when RC is dislocated in y -direction from CG_{slab} .

$$I_{p,y} = \frac{b \cdot a^3}{12} + A_{slab} \cdot y_T^2 \quad (4.21)$$

For x -direction, when RC is dislocated in x -direction from CG_{slab} .

$$I_{p,x} = \frac{a \cdot b^3}{12} + A_{slab} \cdot x_T^2 \quad (4.22)$$

4.2.3.5 Buckling load for single storey building – summation

$$\text{Translation in } x\text{-direction: } \sum_1^n j_{i,x} = 0 \Rightarrow \frac{3B_x}{L^3} - \frac{q_v A}{L} = 0$$

$$\text{Translation in } y\text{-direction: } \sum_1^n j_{i,y} = 0 \Rightarrow 2 \cdot \frac{3B_y}{L^3} - \frac{q_v A}{L} = 0$$

Rotation:

$$\sum_1^n (j_{i,x} y_i^2 + j_{i,y} x_i^2) = 0 \Rightarrow \frac{3B_x}{L^3} \cdot y^2 + 2 \cdot \frac{3B_y}{L^3} \cdot x^2 - \frac{q}{L} \cdot \frac{ab(a^2 + b^2)}{12} = 0$$

Observe that the equations above are referring to the more accurate method used in single storey structures. The multiplication factor, 3, is derived from the equation of linear elasticity and refers to a single column subjected to a single point load at the top of the member, see Figure 3.13. This factor is the same as the value k_V established from Vianello's method which can be used for multi storey structures. The expression below shows the relationship concerning one stabilising column.

$$\text{Vianello formulation: } N_{cr,B} = k_V \cdot \frac{EI}{L_h^2} \quad (3.38)$$

For one storey the k_V is valued to 2.5, see Figure 3.13.

$$\text{Euler formulation: } N_{cr,B} = \frac{\pi^2}{4} \cdot \frac{EI}{L^2} = k_V \cdot \frac{EI}{L^2} \quad k_V \text{ is here valued to } \approx 2.5$$

The expression below shows the relation concerning one stabilising member combined with a pin ended column. This model is frequently used as it resembles a real structure, which uses columns supporting vertical load and bracing walls for the stabilisation.

$$\text{Single storey expression: } \frac{3B_x}{L^3} - \frac{q_v A}{L} = 0 \Rightarrow \frac{3B_x}{L^3} - \frac{N_{cr}}{L} = 0 \Rightarrow$$

$$N_{cr,B} = 3 \cdot \frac{EI}{L^2}$$

k_V is here valued to 3 and can be compared with value from Figure 3.13 referring to a pin ended column.

Notice that the expressions for the stabilising units are assumed not to be subjected to vertical loads, only the columns. This assumption is probably close to the real case but

not fully because the walls may be subjected to some vertical load as they may be connected to the slabs, depending on the floor system. The assumption simplifies the calculation and is utilised, as it is shown, in both single and multi storey calculations.

4.2.3.6 Buckling load - Multi-storey expressions

Equations used to calculate stability on multi-storey structures are based on the same expression as for single-storey structures, i.e the more accurate method. To use the accurate method it is assumed that the rotations centre is positioned at the centre of gravity of the structure. In the expressions used for multi storey structures the dislocation of the rotation centre from the centre of gravity is taken into account. The same expression is used to calculate the final buckling load.

$$N_{cr,B} = k_V \cdot \frac{C}{L_h^2} \quad (4.23)$$

The overall stiffness, C , has to first be established for each direction. The stiffness, for example B_x in x -direction, is not always the governing one because it is not only translation that occurs. When the rotations centre is not located at the centre of gravity the overall stiffness, C , in each direction is influenced. In these cases the overall stiffness, C , is also influenced by the polar moment of inertia, see Equations (4.24), (4.29) and (4.30). The complete expression for establishing the overall stiffness is a third degree equation. [Loretsen *et al.* (2000)]

$$[\Sigma(B_x) - C] \cdot [\Sigma(B_y) - C] \cdot \left[\Sigma(B_x y^2 + B_y x^2) - C \frac{I_p}{A} \right] = C^2 x_T^2 \cdot [\Sigma(B_x) - C] + C^2 y_T^2 \cdot [\Sigma(B_y) - C] \quad (4.24)$$

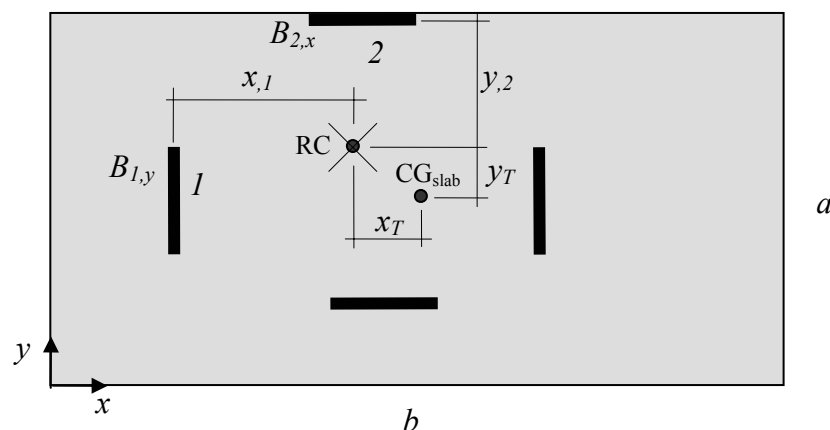


Figure 4.14: Illustration of x , y , x_T and y_T .

Notice that there are two symbols for distances in x and y direction.

The symbol x and y are the distances from the RC of the actual unit to the RC of the whole structure.

The symbols x_T and y_T are the distances describing the dislocation of the RC to the CG.

The left side of Equation (4.24) is a multiplication of the expressions for translation in x and y -direction and buckling in space. The approach here is to calculate the value of C , which is the same as the overall stiffness which will be used in the final expression for the buckling load.

The right side of Equation (4.24) is a contribution from asymmetrical structures, i.e. when the rotation centre is dislocated from the centre of gravity. With the special case, when both x_T and y_T are zero, the right side becomes equal to zero and the expression is simplified to

$$[\Sigma(B_x) - C] \cdot [\Sigma(B_y) - C] \cdot \left[\Sigma(B_x y^2 + B_y x^2) - C \frac{I_p}{A} \right] = 0 \quad (4.25)$$

To establish the overall stiffness C the three parts are set to zero separately and are compared.

$$[\Sigma(B_x) - C] = 0 \quad \text{Translation } x\text{-direction} \quad (4.26)$$

$$[\Sigma(B_y) - C] = 0 \quad \text{Translation } y\text{-direction} \quad (4.27)$$

$$\left[\Sigma(B_x y^2 + B_y x^2) - C \frac{I_p}{A} \right] = 0 \quad \text{Rotation} \quad (4.28)$$

Asymmetrical structures:

The general expression will be different depending on if only $x_T = 0$ and $y_T \neq 0$ or vice versa.

When $x_T = 0$ and $y_T \neq 0$, the Equation (4.25) can be written as

$$\begin{aligned} & [\Sigma(B_x) - C] \cdot [\Sigma(B_y) - C] \cdot \left[\Sigma(B_x y^2 + B_y x^2) - C \frac{I_p}{A} \right] = C^2 y_T^2 \cdot [\Sigma(B_y) - C] \Rightarrow \\ & [\Sigma(B_y) - C] \cdot \left([\Sigma(B_x) - C] \cdot \left[\Sigma(B_x y^2 + B_y x^2) - C \frac{I_p}{A} \right] - C^2 y_T^2 \right) = 0 \end{aligned} \quad (4.29)$$

When $x_T \neq 0$ and $y_T = 0$,

$$[\Sigma(B_x) - C] \cdot [\Sigma(B_y) - C] \cdot \left[\Sigma(B_x y^2 + B_y x^2) - C \frac{I_p}{A} \right] = C^2 x_T^2 \cdot [\Sigma(B_x) - C] \Rightarrow$$

$$[\Sigma(B_x) - C] \cdot \left([\Sigma(B_y) - C] \cdot \left[\Sigma(B_x y^2 + B_y x^2) - C \frac{I_p}{A} \right] - C^2 x_T^2 \right) = 0 \quad (4.30)$$

If both $x_T \neq 0$ and $y_T \neq 0$ the approach described above is not workable. Instead the general third degree Equation (4.24) is solved by a computer program. This general equation can of course be utilised for all cases. The equation provides three roots of which two roots refer to translation and one to rotation.

4.2.4 Numerical example - Single storey structure

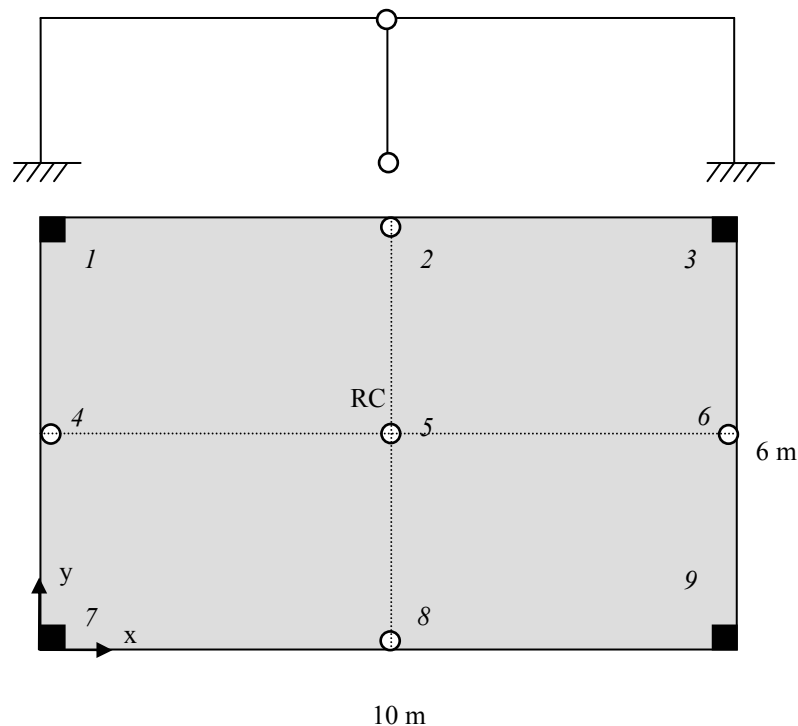


Figure 4.15: Plan of structure for calculation of buckling load for a one storey building.

Local buckling is assumed not to occur, i.e. buckling concerning Euler 2 cases.

$$L_h = 5 \text{ m} \quad q_v = 5 \text{ kPa} \quad E = 30 \text{ GPa}$$

4.2.4.1 Buckling load through translation

Stabilising columns: Columns 1,3,7,9

Stiffness number of each stabilising column:
$$j_x = j_y = \frac{3EI}{L_h^3} \left(1 - \frac{N}{N_{cr,col}} \right) \quad (4.3)$$

Dimensions: 0.2 m x 0.2 m

$$EI_x = EI_y = \frac{0.2 \cdot 0.2^3}{12} \cdot 30 \cdot 10^9 = 4 \cdot 10^6 \text{ Nm}^2$$

$$N_{cr,col,x} = N_{cr,col,y} = \frac{\pi^2 EI}{4L_h^2} = \frac{\pi^2 \cdot 4 \cdot 10^6}{4 \cdot 5^2} = 395 \text{ kN}$$

Non stabilising columns: Columns 2,4,5,6,8

$$j_x = j_y = -\frac{N}{L_h} \quad (4.4)$$

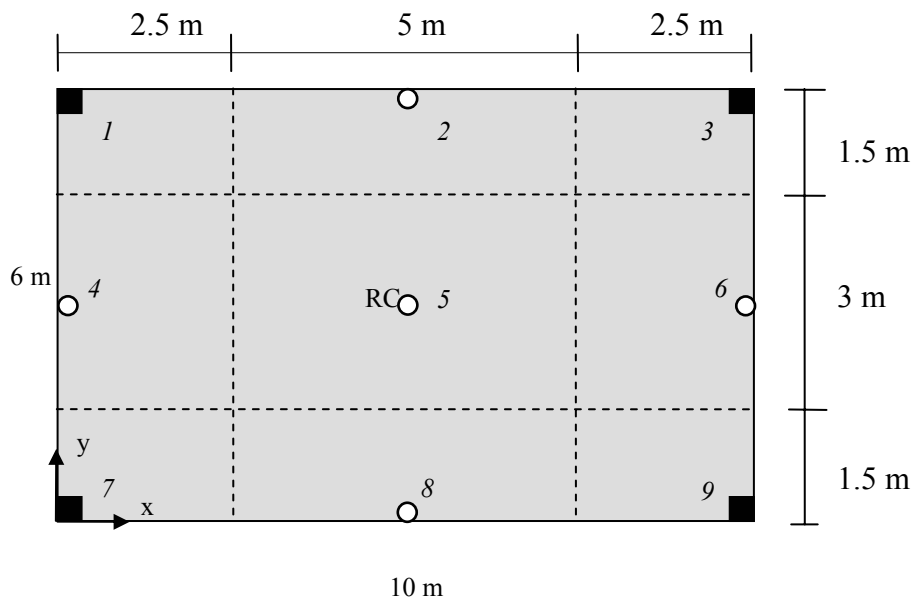


Figure 4.16: Load distribution

Load distribution:

Observe that the chosen load distribution is a rough estimate.

Total vertical load:

$$N_{tot} = 5 \cdot 10 \cdot 6 = 300 \text{ kN}$$

Stabilising columns in the corners:

$$\text{Applied load } N_{1,3,7,9} = A \cdot q_v = 2.5 \cdot 1.5 \cdot 5 = 18.75 \text{ kN}$$

For A is the area of load affecting that particular column.

Non stabilising columns:

$$\text{Applied load } N_{2,8} = A \cdot q_v = 5 \cdot 1.5 \cdot 5 = 37.5 \text{ kN}$$

$$N_{4,6} = A \cdot q_v = 2.5 \cdot 3 \cdot 5 = 37.5 \text{ kN}$$

$$N_5 = A \cdot q_v = 5 \cdot 3 \cdot 5 = 75 \text{ kN}$$

To establish the buckling load for the whole system the loads are normalised and are interpreted as loads with the amount of load related to each, depending on how much the actual column is taking.

The amount of the load which is applied on the stabilising columns is set to be equal to N . In this case all four corner columns are subjected to the same amount of the load. All other columns are then related to the load applied on the stabilising columns. In this case the structure is assumed to be subjected to an evenly distributed load, q_v , and quotations of the *load areas* between the different parts of the slab can therefore be used as well. For simple structures the load quotients can be made straight forward and the load areas, or the load part, for each column must not necessarily be establish first. This calculation example is referring to an easy structure and the load quotations are performed just to clarify the method for general cases.

Quotations from the load distribution:

$$N_{2,8} = \frac{37.5}{18.75} \cdot N = 2N$$

$$N_{4,6} = \frac{37.5}{18.75} \cdot N = 2N$$

$$N_5 = \frac{75}{18.75} \cdot N = 4N$$

The stiffness numbers for all units are then summarised in the expressions for establishing buckling load through translation and rotation.

$$\sum_1^n (j_{i,x}) = 0 \quad \sum_1^n (j_{i,y}) = 0 \quad \sum_1^n (j_{i,x}y_i^2 + j_{i,y}x_i^2) = 0$$

In this case the stabilising columns have the same stiffness in both x - and y -direction. The buckling load is therefore the same in both directions.

Buckling load through translation:

$$\sum_1^n (j_{i,x}) = \sum_1^n (j_{i,y}) = 0 \Rightarrow 4 \cdot \frac{3EI}{L_h^3} \left(1 - \frac{N}{N_{cr,col}}\right) - 2 \cdot \frac{2N}{L_h} - 2 \cdot \frac{2N}{L_h} - 1 \cdot \frac{4N}{L_h} = 0$$

$$4 \cdot \frac{3EI}{L_h^3} \left(1 - \frac{N}{N_{cr,col}}\right) - \frac{12N}{L_h} = 0 \Rightarrow \frac{12EI}{L_h^3} - \frac{12EI}{L_h^3} \cdot \frac{N}{N_{cr,col}} - \frac{12N}{L_h} = 0$$

$$\frac{12EI}{L_h^3} - \left(\frac{12EI}{L_h^3} \cdot \frac{1}{N_{cr,col}} + \frac{12}{L_h}\right)N = 0 \Rightarrow N = \frac{\frac{12EI}{L_h^2}}{\left(\frac{12EI}{L_h^3} \cdot \frac{1}{N_{cr,col}} + 12\right)} = 0$$

$$N = \frac{\frac{12 \cdot 4 \cdot 10^6}{5^2}}{\left(\frac{12 \cdot 4 \cdot 10^6}{5^2 \cdot 395 \cdot 10^3} + 12\right)} = 114 \text{ kN}$$

The loads from all units are then summarised and multiplied with the calculated load value.

$$N_{cr,x} = N_{cr,y} = 4 \cdot N + 2 \cdot 2N + 2 \cdot 2N + 1 \cdot 4N = 16N = 16 \cdot 114 = 1824 \text{ kN}$$

4.2.4.2 Buckling load through rotation

$$\sum_1^n (j_{i,x}y_i^2 + j_{i,y}x_i^2) = 0$$

The four stabilising columns at the corners of the building have the same contribution due to symmetry.

$$4 \cdot \left[\frac{3EI}{L_h^3} \left(1 - \frac{N}{N_{cr,col}}\right) \right] (y^2 + x^2) = \left[\frac{12EI}{L_h^3} \left(1 - \frac{N}{N_{cr,col}}\right) \right] (3^2 + 5^2) = \frac{408EI}{L_h^3} \left(1 - \frac{N}{N_{cr,col}}\right)$$

Non stabilising columns:

$$\text{Columns 2 and 8: } 2 \cdot \left[-\frac{2N}{L_h} \cdot (y^2 + x^2) \right] = 2 \cdot \left[-\frac{2N}{L_h} \cdot (3^2 + 0^2) \right] = -\frac{36N}{L_h}$$

$$\text{Columns 4 and 6: } 2 \cdot \left[-\frac{2N}{L_h} \cdot (y^2 + x^2) \right] = 2 \cdot \left[-\frac{2N}{L_h} \cdot (0 + 5^2) \right] = -\frac{100N}{L_h}$$

$$\text{Column 5 (at the RC)} \quad 1 \cdot \left[-\frac{4N}{L_h} \cdot (y^2 + x^2) \right] = 1 \cdot \left[-\frac{4N}{L_h} \cdot (0 + 0) \right] = 0$$

The contributions above are summarised and the buckling load is calculated.

$$\frac{408EI}{L_h^3} \left(1 - \frac{N}{N_{cr,col}} \right) - \frac{36N}{L_h} - \frac{100N}{L_h} = 0 \quad \Rightarrow \quad \frac{408EI}{L_h^3} - \frac{408EI}{L_h^3} \cdot \frac{N}{N_{cr,col}} - \frac{136N}{L_h} = 0$$

$$\Rightarrow$$

$$\frac{408EI}{L_h^3} - \left(\frac{408EI}{L_h^3} \cdot \frac{1}{N_{cr,col}} + \frac{136}{L_h} \right) N = 0$$

$$N = \frac{\frac{408EI}{L_h^2}}{\left(\frac{408EI}{L_h^2} \cdot \frac{1}{N_{cr,col}} + 136 \right)} = \frac{\frac{408 \cdot 4 \cdot 10^6}{5^2}}{\left(\frac{408 \cdot 5 \cdot 4 \cdot 10^6}{5^2 \cdot 395 \cdot 10^3} + 136 \right)} = 217 \text{ kN}$$

$$N_{cr,rot} = 4 \cdot N + 2 \cdot 2N + 2 \cdot 2N + 1 \cdot 4N = 16 \cdot N = 16 \cdot 217 = 3467 \text{ kN}$$

The structure is stable through rotation compared with translation.

$$N_{cr,x} = N_{cr,y} = 1824 \text{ kN}$$

$$N_{cr,rot} = 3467 \text{ kN}$$

The stabilising columns are placed far from the rotation centre and present an example of how the columns should be placed for obtaining a stable building. It should also be noticed that non stabilising columns, positioned far from the rotation centre, give a large negative contribution concerning stability through rotation of the structure, especially if they are subjected to high loads.

Comparison between the critical buckling loads and the total load applied on the structure:

$$\text{Total vertical load : } N_{tot} = 300 \text{ kN}$$

$$\text{Compared to buckling load through translation: } \frac{300}{1824} = 0.16 \quad (x\text{- and }y\text{-direction})$$

$$\text{Compared to buckling load through rotation: } \frac{300}{3467} = 0.09$$

The comparisons between the total vertical load and the critical buckling loads for the structure give an indication of how stable the structure is. The factors calculated above are different depending on which buckling load the total load is compared with. These quotients are also included in the expressions for the magnification factor, Equation (3.23), to calculate the contribution from the 2nd order effects.

4.2.5 Numerical example - Multi storey structure

This numerical example is based on the same assumption mentioned in the previous section i.e. no local buckling and the load is evenly distributed.

The case examined shows a building braced by one stabilising wall in x -direction, two stabilising walls in y -direction. The vertical loads are assumed to be borne down by evenly distributed columns and the stabilising walls are assumed to be subjected to horizontal loads only.

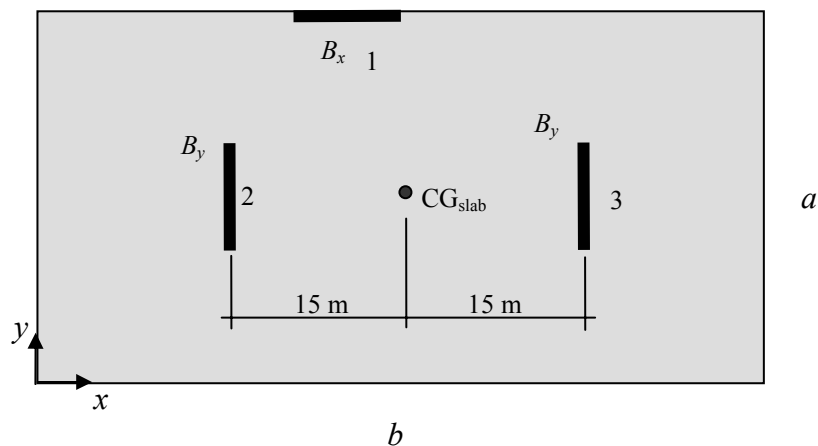


Figure 4.17: Plan of multi storey building.

Values: $a = 30 \text{ m}$ $b = 60 \text{ m}$ $E_{\text{wall}} = 25 \text{ GPa}$ $G_{\text{wall}} = 0.4 \cdot E_{\text{wall}}$

Storeys: 10 $L_h = 30 \text{ m}$ (total height of the building)

Wall dimensions: $t = 0.3 \text{ m}$ $b_{\text{wall}} = 10 \text{ m}$

All three walls have the same dimensions and material properties.

$L_{\text{sec}} = 3 \text{ m}$ (height of one storey)

Calculations:

Concerning stiffness for the walls: $EI_x = 25 \cdot 10^9 \cdot \frac{0.3 \cdot 10^3}{12} = 625 \text{ GNm}^2$

Wall 1:

$$N_{cr,B} = k_V \cdot \frac{EI_x}{L_h^2} = 6.8 \cdot \frac{625 \cdot 10^9}{30^2} = 4.72 \text{ GN}$$

Where $k_V = 6.8$ is taken from the Vianello method, see Figure 3.13.

$$N_{cr,S} = GA = 0.4 \cdot 25 \cdot 10^9 \cdot 0.3 \cdot 10 = 30 \text{ GN}$$

$$N_{cr,tot} = \frac{1}{\frac{1}{N_{cr,B}} + \frac{1}{N_{cr,S}}} = \frac{1}{\frac{1}{4.72} + \frac{1}{30}} = 4.08 \text{ GN}$$

Stiffness with regard to shear and bending:

$$B_x = \frac{N_{cr,tot}}{N_{cr,B}} \cdot EI_x = \frac{4.08}{4.72} \cdot 625 \cdot 10^9 = 540 \text{ GNm}^2 \quad B_{x,1} = B_{y,2} = B_{y,3}$$

As the walls have the same dimensions and material properties, the value of B_x is equal to B_y . In this case the bending is dominant as the shear buckling load is much greater than the bending buckling load. Still the stiffness of the wall is lowered with 85 GNm².

Position of the rotation centre RC is calculated with Equation (4.16):

$$x_{RT} = \frac{\sum (B_y \cdot x_{RT})_{unit}}{\sum B_y} = \frac{540 \cdot 20 + 540 \cdot 40}{540 + 540} = 30 \text{ m}$$

$$y_{RT} = \frac{\sum (B_x \cdot y_{RT})_{unit}}{\sum B_x} = \frac{540 \cdot 30}{540} = 30 \text{ m}$$

Observe that the origin of the coordinate system can be placed wherever one wishes during the calculation of the rotation centre. When the distances x_T and y_T are set, the origin of the coordinate system should be placed in the rotation centre and the distances describe the distances from RC to CG_{slab}.

The new origin is seen in Figure 4.18.

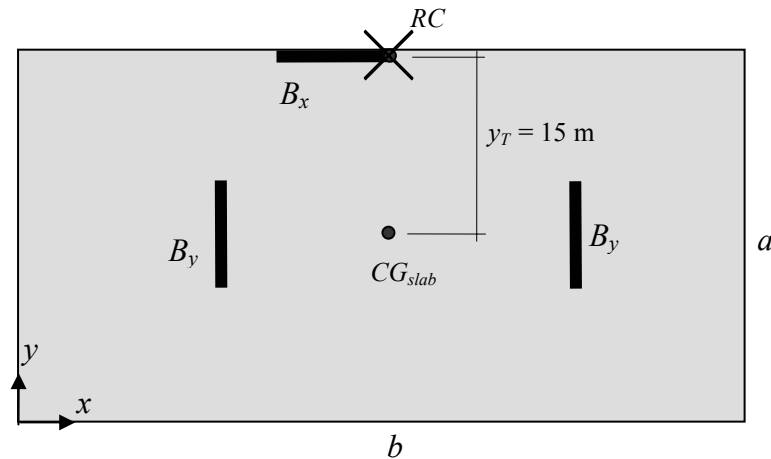


Figure 4.18: Situation of the new origin.

Polar moment of inertia:

$$I_p = I_{p,x} + I_{p,y} = \frac{30 \cdot 60^3}{12} + \frac{60 \cdot 30^3}{12} + 30 \cdot 60 \cdot 15^2 = 1.080 \text{ Mm}^4; \text{ see Section 4.2.3.4.}$$

Establishment of the overall stiffness C

From the general equation, Equation (4.24), the expression is rewritten due to the asymmetry in y -direction, see Section 4.2.3.6.

$$\left[\Sigma(B_y) - C \right] \cdot \left(\left[\Sigma(B_x) - C \right] \cdot \left[\Sigma(B_x y^2 + B_y x^2) - C \frac{I_p}{A} \right] - C^2 y_T^2 \right) = 0$$

$$\left[(2 \cdot 540) - C \right] \cdot \left(\left[540 - C \right] \cdot \left[(2 \cdot 540 \cdot 15^2) - C \frac{1.08 \cdot 10^6}{1800} \right] - C^2 \cdot 15^2 \right) = 0$$

The values are interpreted into the equation and the roots are solved by a calculator or a computer program.

The following roots were calculated:

$$C_1 = 275 \text{ GNm}^2$$

$$C_2 = 1080 \text{ GNm}^2$$

$$C_3 = 1200 \text{ GNm}^2$$

The critical buckling load is then calculated for each direction. As the second order contribution is derived through quotients between the critical buckling load and the applied vertical load the appropriate buckling load has to be used for each direction. Depending on how the walls are positioned in the building, whether they contribute to

stabilisation both in the translation and in the rotation or only translation, the choice of which critical buckling load that will be used is different.

It is recommended to first calculate all three buckling loads and thereafter apply the values for second order contribution. The reason is to reveal how the different values in each direction differ from each other and it is then clearer how the building is reacting.

$$N_{cr,building} = k_V \cdot \frac{C}{L_h^2} = 6.8 \cdot \frac{275 \cdot 10^9}{30^2} = 2.08 \text{ GN} \quad (3.38)$$

In this example, only one wall is stabilising in the x -direction. The rotation centre will therefore only depend on this single wall whose RC is positioned in its centre. This single wall only contributes to stabilising the building through translation, not rotation. Therefore, the second order effects, added to horizontal loads applied in the x -direction, will only be based upon the critical buckling load in x -direction and the rotation capacity is not considered.

$$\Sigma(B_x \cdot y) = 0 \quad \Rightarrow \quad N_{cr,x}$$

In y -direction, two walls are contributing to stabilise the building in the same direction. These walls are also stabilising through rotation. Therefore, the critical buckling load from both y -direction and rotation has to be considered and the lowest value is to be chosen.

$$\Sigma(B_x \cdot y) \neq 0 \quad \Rightarrow \quad N_{cr,y} \text{ or } N_{cr,rot}$$

4.3 Dimensioning forces and moments

When designing the stabilising components of a structure it is of vital importance to consider the force distribution through the building. The critical buckling load is first established in both horizontal directions, x and y , and also for rotation. These three values will be utilised in each mode to calculate the magnification factors which are later interpreted to establish the design moments for the stabilising units, i.e. adding the 2nd order affect to the first moment calculated. This approach is used for calculating on each component in each direction.

It is the force distribution through a structure which determines how the stabilising units are affected. The units are often spread out in a building and do not always have the same dimensions, which leads to varying stiffness throughout the building. In Section 4.1 it is explained, concerning the units in the same plane, how the force is applied on each component. In a real structure there is varying stiffness in both directions combined with horizontal forces in each direction. See Figure 4.19.

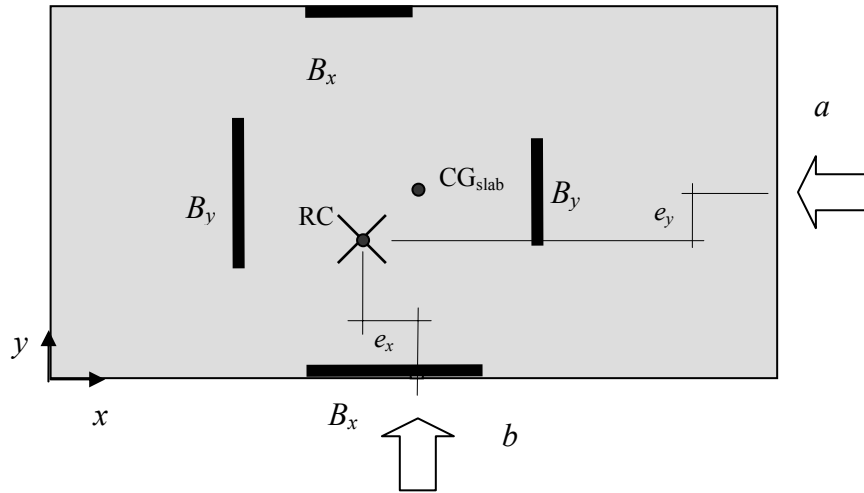


Figure 4.19: Building plan.

Figure 4.19 describes a system where the RC is dislocated in both x and y direction. The two force resultants, occurring from wind loads on each façade for example, pass to the side of the rotation centre. This leads to an eccentricity which, in this case, leads to a twisting moment of the structure caused by the resulting forces in each direction. The index, i , stands for the actual level (*storey*) calculated on, in the building.

Force contribution – Translation:

If the force resultants were passing through the RC only translation would occur.

$$H_{unit,tr,i,x} = H_{i,x} \cdot \frac{B_{unit,i,x}}{\Sigma(B_{unit,i,x})}; \quad H_{unit,tr,i,y} = H_{i,y} \cdot \frac{B_{unit,i,y}}{\Sigma(B_{unit,i,y})} \quad (4.31)$$

Force distribution – Twisting:

Figure 4.19 describes how the force resultants in each direction are passing the RC with an eccentricity e . The twisting moment from each force becomes

$$M_{twist,i,x} = H_{i,x} \cdot e_y \quad M_{twist,i,y} = H_{i,y} \cdot e_x \quad (4.32)$$

Total twisting moment:

$$M_{twist,i} = H_{i,x} \cdot e_y + H_{i,y} \cdot e_x \quad (4.33)$$

The force contribution on each stabilising unit is derived by a normalisation of the capacity of the actual unit and the rotation capacity of the whole system. In other words stiff units with large distances from the rotation centre will absorb greater forces than weak units closer to the rotation centre. It is important to observe that stabilising units in the transverse direction of the load will also be affected by twisting. The force contribution due to twisting becomes:

Contribution from horizontal forces in x -direction:

$$H_{unit,twist,i,x} = M_{twist,i} \frac{B_{unit,i,x} \cdot y_{unit}}{\Sigma(B_{unit,i,x} \cdot y_{unit}^2) + \Sigma(B_{unit,i,y} \cdot x_{unit}^2)} \quad (4.34)$$

The units, stabilising in the direction aligned with the actual force, will be a sum of the forces from both translation and twisting.

$$H_{unit,i,x} = H_{unit,tr,i,x} + H_{unit,twist,i,x}$$

$$H_{unit,i,x} = H_{i,x} \cdot \frac{B_{unit,i,x}}{\Sigma(B_{unit,i,x})} + M_{twist,i} \frac{B_{unit,i,x} \cdot y_{unit}}{\Sigma(B_{unit,i,x} \cdot y_{unit}^2) + \Sigma(B_{unit,i,y} \cdot x_{unit}^2)} \quad (4.35)$$

If loads are applied only in one direction with an eccentricity causing the building to both translate and twist, the stabilising units in the transverse direction compared to the load will contribute to resist the twisting moment. The units in the transversal direction will therefore be subjected to forces occurring from the twisting moment only. The expression below describes a unit stabilising in y -direction when the load is applied in the x -direction only.

$$H_{unit,i,y} = 0 + M_{twist,i,x} \cdot \frac{B_{unit,i,y} \cdot x_{unit}}{\Sigma(B_{unit,i,x} \cdot y_{unit}^2) + \Sigma(B_{unit,i,y} \cdot x_{unit}^2)} \quad (4.36)$$

Usually it is the bending moment at the base of the building that is of interest because it is there that the highest moment value is usually attained. If the stiffness is also varying through the height of the building, the force distribution has to be calculated for each floor. Thereafter the bending moment is established for each unit, for example at the base of the building. Observe not to confuse the *overall twisting moment*, M_{twist} , with the bending moment in the actual unit.

In some cases the building has a symmetry which places the RC at the centre of gravity. In cases where the CG is located at the same position as the RC, evenly distributed loads will have their force resultants passing through the RC. In these cases no twisting will occur, only translation acts on the stabilising units. But according to design codes, it is not only evenly distributed loads which have to be checked.

In addition to the load cases with uniform wind load on the facades, the case concerning uneven load has to be examined too. It is here important to understand where on the building the two unevenly distributed loads should be situated to develop the worst load case. An extreme load case, which gives a great twisting moment, will occur if the unevenly distributed load is positioned at that side of the building which places the force resultant at the greatest distance from the RC, see Figure 4.20.

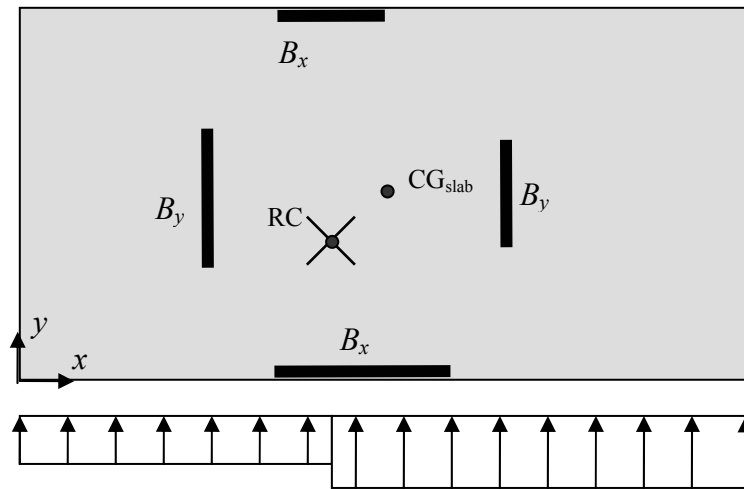


Figure 4.20: Uneven load case.

The specific case shown in Figure 4.20 shows a building with eccentricities in both x - and y -directions. This factor coupled with the unevenness of the wind load leads to an extreme situation which will lead to significant twisting. Figure 4.21 shows a most extreme situation where a wind load is assumed from the diagonal direction and its resultants unevenly inflict both x - and y -directions.

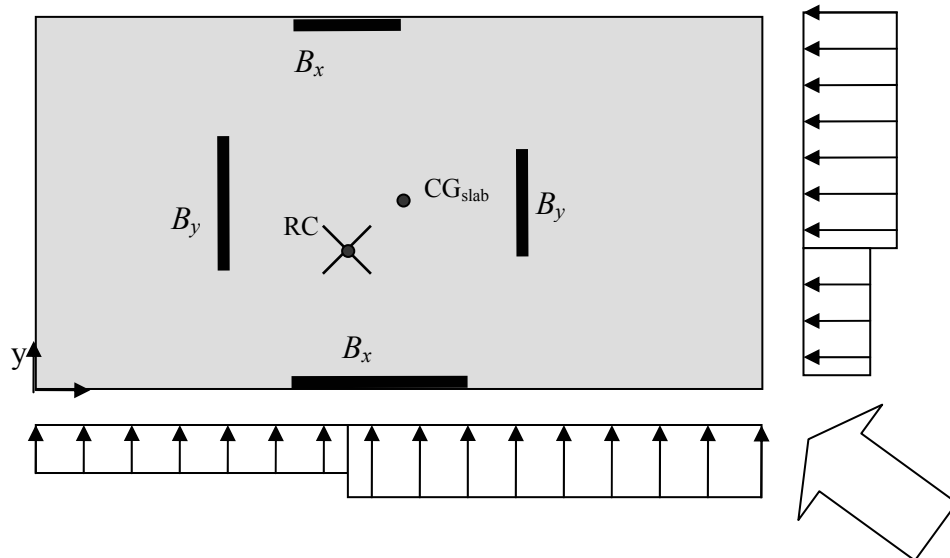


Figure 4.21: Extreme case where the effect of a diagonal wind load is investigated.

In Figure 4.21 the diagonal wind load is divided between the façades. Each inflicted façade has a further division of the resultant wind load in order to establish an extreme case. Observe that the larger components of the resultant wind loads are positioned so that the worst scenario occurs with regard to twisting. This is to consider the eccentricities that the building possesses in order to obtain the worst case of twisting.

The Swedish codes are not specific with how these extreme load cases are to be applied and dealt with and it seems to be differently interpreted in different engineering companies. It is also difficult to decide which critical loads should be used in which direction in order to estimate the 2nd order effects. It seems logical to assume the lowest critical load as the walls are affected in both directions due to the twisting effect. This approach would lead to each wall being investigated in its stabilising direction and that specific critical load being used to determine the 2nd order effects. The problem here is that using this approach there will be no utilisation of the critical twisting load for determining 2nd order effects which was what was of interest from the beginning. This is a conundrum which will hopefully be taken up by further studies.

Another problem with 2nd order effects is that the magnification factor gives a value in percent for increasing the sectional forces without paying attention to the distance from the RC. Observe in Figure 4.21, where twisting occurs, how the 2nd order effect should be different for each stabilising component depending on their distance from the RC. From Figure 4.21 is seen that more effect is experienced by wall B than by wall A. Wall B has more deformation than wall one and should therefore have a higher 2nd order effect. Should then the magnification factor be increased or decreased according to its effectiveness due to the distance from the RC?

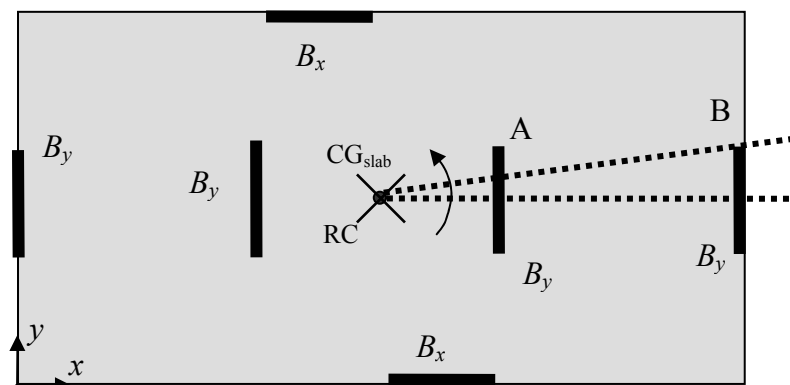


Figure 4.22: 2nd order effects due to distance from RC.

5 Investigations

Here is found the culmination of this project where the hand calculation methods are compared with the computer assisted FE-calculations in order to ascertain if the results from the hand calculations are relevant. A general description of finite element analysis is given and comparisons are given for solid shear wall calculations concerning buckling and deflection in order to ascertain the best usable mesh and node configurations for obtaining the best FE-analyses.

The Vianello method, described in Section 3.3, is to be studied for solid walls with non uniform stiffness and load application. The Vianello method is to be compared with the approximate Vianello method, i.e. k_V is taken from Figure 3.13, and the FE-method.

Thereafter follows comparisons between the FE-method and hand calculations on pierced shear walls. The hand calculation methods used for calculating critical buckling loads, see Section 3.2.1, and deflection, see Section 3.2.2, are to be investigated.

A study of the use of the polar moment of inertia, see Section 4.2.3.4, is undertaken. Whether or not its use is recommended will be decided after comparisons are made on calculated examples.

Force distributions in both single and multi storey structures are to be investigated. Three load cases, translation, rotation and combined translation and rotation, will be examined with or without vertical loads being included. The effectiveness of the calculation methods will be ascertained through making comparisons of the results with FE-results.

A study is made of the Equation (4.24), from Lorentsen *et al.* (2000), concerning the overall stiffness C , which refers to the stiffness values in translation and rotation. The coupled and uncoupled approaches concerning U-shaped core elements will be analysed and conclusions drawn.

Multi storey structures will be investigated concerning translation and rotation. The effect of introducing a core elements torsional resistance into the calculation method is examined. Calculation methods are also presented for taking into account warping effects.

5.1 FE-analyses of solid shear walls

The modern approach for solving complex problems, involving stresses, deflections and buckling loads, is to use computer programmes such as FE-program. Generally the finite element analysis, FE-analysis, produces quite good results and gives a good picture of how a real structure will react, depending on the assumptions, when subjected to different load cases. The FE-method is especially competent for checking complex structures which are extremely difficult or almost impossible to calculate by hand. In this thesis several hand calculations have been introduced and applied for

calculating buckling loads, design moments and deflection. As these methods are based upon different assumptions and approximations, it is not clear whether the results are accurate estimations or not. When considering pierced shear walls, these methods suppose several assumptions and it is suspected that these methods only produce rough estimates. It is also of great importance that the FE-model is properly set up and that, before examining complicated models, simple ones are first investigated. These preliminary investigations of less complicated models are done to evaluate how the program works and how, for example, different mesh intensities may affect the results. The FE-program used in this project is SOLVIA, SOLVIA (1999), and it does not have a graphic interface. Instead the coordinates are interpreted into a text file together with information that the program needs such as, element types, material data etc. The benefit of using SOLVIA is that the user has a good control of all the data that the program uses.

This chapter involves several models from straight solid shear walls to complete systems. The investigation starts with simple models to evaluate how SOLVIA works. Different mesh intensities combined with both 4-node and 9-node elements are interpreted to determine proper use of them for later use in the more advanced models.

5.1.1 Check of FE-model

This thesis contains evaluations of models of buildings and stabilising units. A fully fixed cantilever column or wall is frequently used for bracing and it is therefore important to start with models such as a straight solid wall with only one simple load case. Hand calculations of deflections and buckling loads for these structures are easy to solve and they use the same approximations used in the FE-model. The results from the two methods are expected to agree. All models are using a Young's modulus for concrete of 30 GPa and a shear modulus, G , set to 0.4 times the Young's modulus. In SOLVIA the shear modulus is set by using Poisson's constant, $\nu = 0.25$. A factor $\xi = 1.2$ is applied to decrease the shear stiffness, i.e. increasing the shear angle.

5.1.1.1 Modelling - Deflection of solid shear walls

This investigation begins with the study of three solid shear walls; a wide and low wall, a tall and slender wall followed by a wall lying in between these cases. The results will reveal if the SOLVIA deals with deflection caused by shear in a proper way. Figure 5.1 and 5.2 below describes the three walls investigated.

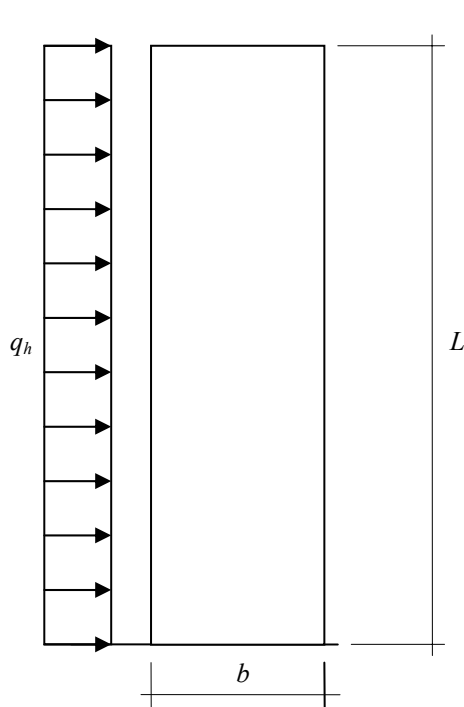


Figure 5.1: Distributed load case

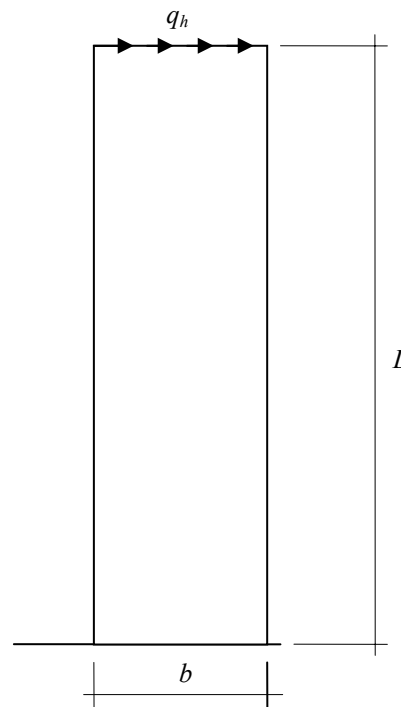


Figure 5.2: Concentrated load case

- | | | |
|----------------------------------|--------------------|--------------------|
| Wall 1- Low and wide; | $b = 10 \text{ m}$ | $L = 8 \text{ m}$ |
| Wall 2- High and slender; | $b = 4 \text{ m}$ | $L = 20 \text{ m}$ |
| Wall 3- Medium height and width; | $b = 5 \text{ m}$ | $L = 10 \text{ m}$ |

The walls have a thickness of 0.5 m.

The first three tests use a concentrated load at the top of the wall. In the FE-model this load has to be interpreted as a distributed load along the top edge. The reason for this is that in the FE-analyses other effects occur, such as local deformation where the load is applied, while in the hand calculation this effect is not taken into account. It has also been shown that in low and wide models the capacity of the wall is so high and the structure deflects like a sinus shape at the top producing results hard to compare with the hand calculation. Therefore the three walls have also been examined subjected to an evenly distributed load along the height of the wall. During these investigations the effect of mesh intensity combined with 4-node and 9-node elements has been examined for the slender wall and the broad wall. Figures 5.3 illustrate two different mesh intensities for the two walls subjected to a concentrated horizontal load. The results can be seen in Section 5.1.2.

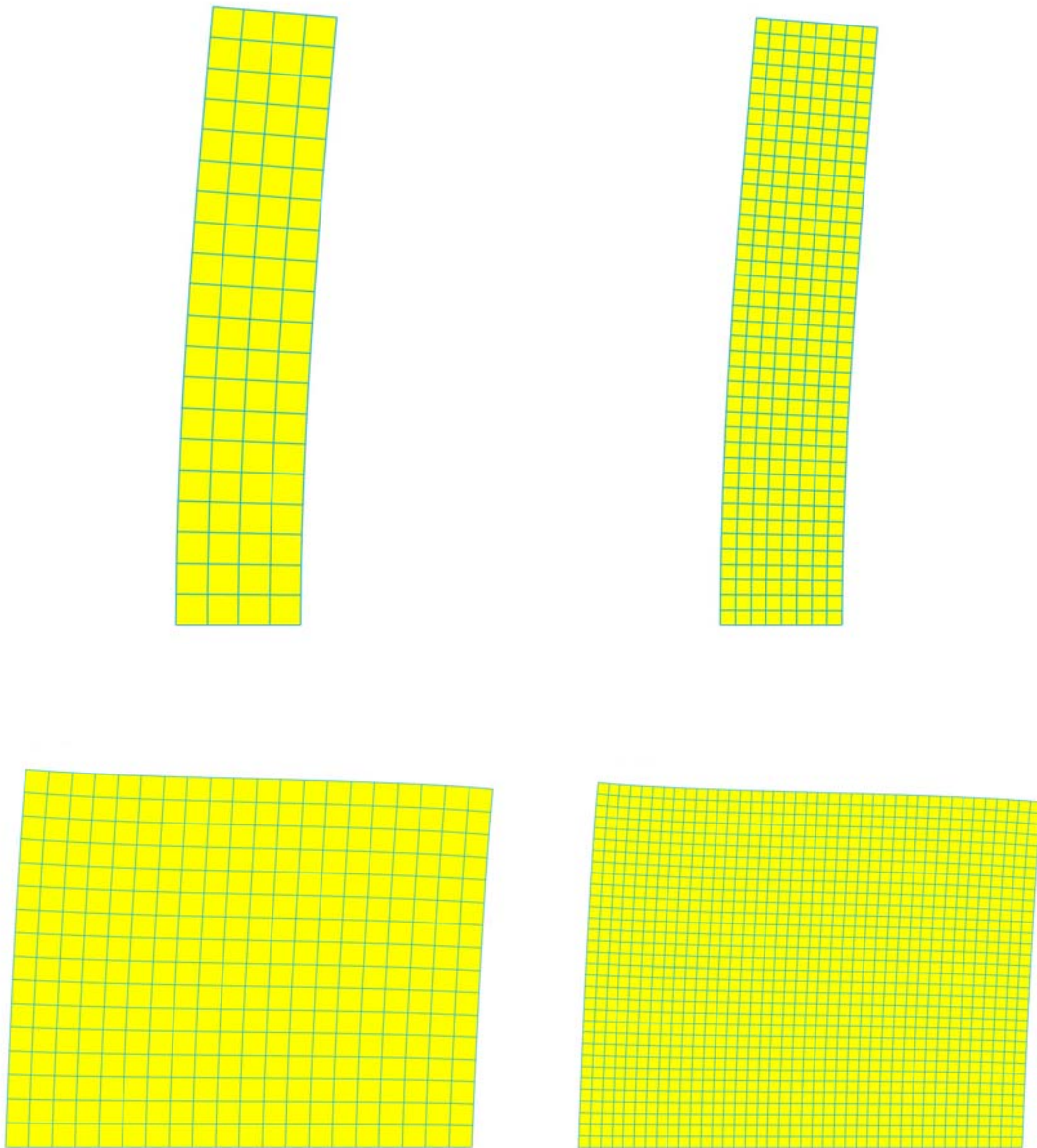


Figure 5.3: Mesh intensities of a slender wall and a wide wall

Hand calculation of deflection:

To establish the total deflection at the top of the wall the calculation is divided into two parts. Both bending and shear contribute to the deflection.

Equations for bending deformation;

Concentrated load at the top:
$$y_{B,c} = q_v \cdot \frac{L^3}{3EI} \quad (5.1)$$

Distributed load along the height:
$$y_{B,d} = q_h \cdot \frac{L^4}{8EI} \quad (5.2)$$

Equations for shear deformation:

Shear angle:
$$\gamma = \frac{\xi}{GA} \quad \equiv \quad y' = V \cdot \frac{\xi}{GA} \quad (V=q)$$

Concentrated load at the top:
$$y_{S,c} = y' \cdot L_h \quad (5.3)$$

The shear angle is defined for a shear force that is equal to 1, i.e. $y' = T \cdot \gamma$.

The distributed load, q_h , is set to 1 N/m. As can be seen in Figure 2.14 the shear angle alters along the height when a structure is subjected to a distributed load. A formula has been established during this thesis. This expression is suited for calculating shear deflections of a cantilever column/wall subjected to an evenly distributed horizontal load.

Distributed load along the height:
$$y_{S,d} = \xi \cdot 0.5 \cdot \frac{q_h L_h^2}{GA} \quad (5.4)$$

5.1.1.2 Modelling - Buckling of solid shear walls

The three shear walls in this investigation are subjected to vertical loads. These models represent stabilising walls in a 10 storey building. The walls are subjected to an evenly distributed vertical load on each floor, i.e. 10 loads applied on ten storeys. All three walls have the same height of 30 metres, see Figure 5.4. As the walls only stabilise in their stiff direction and are prohibited to move in the weak direction, because of the floor slabs in the building, the buckling mode in the weak direction must be prevented. In SOLVIA this is done by locking the degree of freedom in the weak direction. The first buckling mode will therefore only occur in the stabilising direction of the wall, see Figure 5.6.

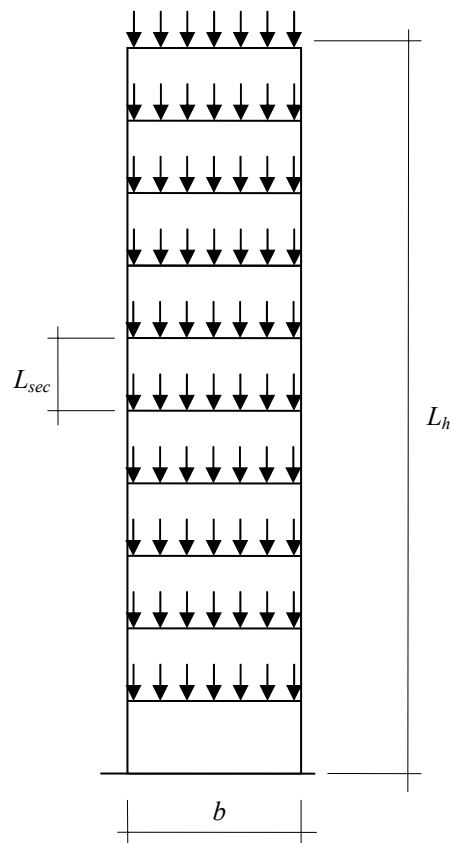


Figure 5.4: Load application for study of critical buckling loads

Wall 1- Wide wall;	$b = 16 \text{ m}$	$L_h = 30 \text{ m}$
Wall 2- Slender wall;	$b = 4 \text{ m}$	$L_h = 30 \text{ m}$
Wall 3- Medium wall;	$b = 8 \text{ m}$	$L_h = 30 \text{ m}$

The walls have a thickness of 0.5 m and each storey height is 3 meters.

The medium wide wall, 8 meters wide, has also been tested with two different mesh intensities combined with 4-node and 9-node elements. The sparse mesh uses an element size of 1.0 m x 0.75 m (width x height), while the dense mesh uses an element size of 0.5 m x 0.375 m. Figure 5.5 below illustrates the load case on the 8 m wide wall presented in the sparse mesh. Figure 5.6 presents the first buckling mode shown in the dense mesh.

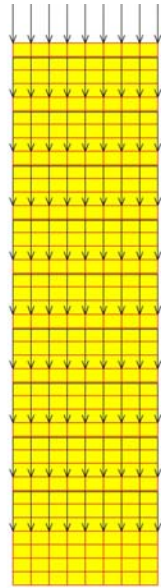


Figure 5.5: FEM - Load case.

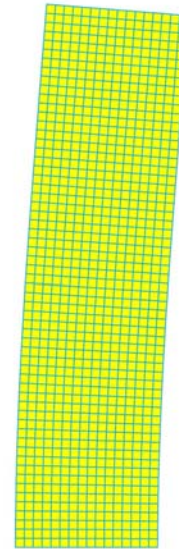


Figure 5.6: FEM - First buckling mode.

Hand calculation of buckling load for solid shear walls:

The critical buckling load is easy to calculate as the walls have the same load and the same stiffness on each floor. Using Figure 3.13 the k_V -value is taken as 6.8. The following equations are used to establish the buckling loads of the walls;

$$\text{Buckling load - bending part} \quad N_{cr,B} = k_V \frac{EI}{L_h^2} \quad (3.38)$$

$$\text{Buckling load - shear part} \quad N_{cr,S} = GA \quad (3.11)$$

$$\text{Buckling load - combined} \quad N_{cr,tot} = \frac{1}{\frac{1}{N_{cr,B}} + \frac{1}{N_{cr,S}}} \quad (3.19)$$

5.1.2 Results

5.1.2.1 Deflection

During these investigations the mesh intensities have been altered to achieve a proper balance between accurate results and the time it takes for SOLVIA to calculate. It can take a very long time to do a complex analysis. It is known that a 9-node element uses equations of higher order than a 4-node element which leads to the 9-node element giving a more accurate result. It is observed when using 4-node elements that the mesh has to be very dense compared to the 9-node elements which gives a good result without heavily meshing, see Table 5.1. The tests also reveal that a sparse mesh, combined with 4-node elements, produces results on the unsafe side, i.e. lesser values of deflection and higher values of buckling load. Table 5.2 presents some results from the tests of deflections from FE-analyses. Results of buckling are presented in Section 5.1.2.2. All values from the hand calculations are marked as HC in the tables. All results are nanometres (10^{-9} m).

Table 5.1: Mesh study in FE-program SOLVIA

Wall and load type	4N sparse [nm]	9N sparse [nm]	4N-dense [nm]	9N-dense [nm]
Wall 1 – Conc. load	-	-	2.24-2.45	2.25-2.53
Wall 2 – Conc. load	663.8	684.9	679	685

Table 5.2: Comparisons of deflections calculated by hand and FE-analyses.

Wall and load type	HC Deflection Bending [nm]	HC Deflection Shear [nm]	HC Deflection Total [nm]	FEA Deflection Total [nm]
Wall 1 – Conc. load	1.09	1.28	2.37	2.25-2.53
Wall 2 – Conc. load	667	200	687	685
Wall 3 – Conc. load	21.3	4	2.53	2.5-2.54
Wall 1 – Distr. load	0.41	0.64	1.05	0.97-1.32
Wall 2 – Distr. load	250	10	260	258
Wall 3 – Distr. load	8	2	10	10

In Table 5.2 the value from SOLVIA is taken from analyses with a dense mesh of 9-node elements. Results from walls 1 and 3 are given with an interval, from a low to a high value. It is presented this way to reveal that other effects occur in FE analyses which the hand calculations are not concerned with. The intervals show different deflections along the top edge of the wall i.e. some parts are more compressed than others. This effect is very small in slender structures, such as wall 2, but in general the hand calculations seem to agree well with the FE-analyses.

5.1.2.2 Buckling

Table 5.3 reveals that models, using 4-node elements, always produce results on the unsafe side. If 4-node elements are used it is important to have a very dense mesh. Comparing this with models using 9-node elements, it is evident that the results are very close for both a dense and a sparse mesh. Further investigation will therefore use 9-node elements and a mesh slightly denser than the one presented as the sparse mesh in Figure 5.3. If a dense mesh is used, the calculation time in SOLVIA will be much longer, especially in the advanced models which are later investigated.

Table 5.3: *Buckling load study of different node and mesh systems from FEA compared with hand calculations.*

Wall width	FEA 4N-sparse [MN]	FEA 9N-sparse [MN]	FEA 4N-dense [MN]	FEA 9N-dense [MN]	HC Total [MN]
Wall – 4 m	-	587	-	-	587
Wall – 8 m	4357	4332	4338	4331	4314
Wall – 16 m	26234	26167	-	-	26073

Table 5.4: *Buckling loads from FEA and hand calculations, with bending and shear contributions given.*

Wall – width	FEA 9N-Sparse [MN]	HC Bending [MN]	HC Shear [MN]	HC Total [MN]
Wall – 4 m	587	604	20000	587
Wall – 8 m	4332	4835	40000	4314
Wall – 16 m	26167	38700	80000	26073

Table 5.4 presents the buckling load calculated through FE-analysis and the hand calculated buckling load divided into its components due to bending and shear. It is obvious that the shear contribution in slender structures, barely affects the total buckling load, i.e. bending deformation is dominant. As the slenderness of a structure decreases, the contribution from shear deformation increases. According to the test results, the hand calculations are always on the safe side. As it has been mentioned earlier other effects occur in the FE-analyses. These effects are suspected to relate to shear effects as the more slender models agree better with the FE-results than the sturdy models.

5.2 Investigation of the Vianello method

An explanation of how the Vianello method works has now been presented in Section 3.3 and now the method shall be compared to results from FE-analyses. Four examples have been chosen where the walls are representing a stabilising wall in a ten storey building. The first is a solid shear wall with uneven stiffness distributions but with even load distribution. The second involves a solid shear wall with uneven loads and uneven stiffness distribution. The third involves a very slender solid shear wall with an unevenly distributed load and an uneven stiffness value. The fourth example is a very robust shear wall with an unevenly distributed load and an uneven stiffness value.

The critical buckling load from FE-analyses is calculated through the eigenvalue λ obtained through SOLVIA (1999).

$$N_{cr,FEM} = \lambda \cdot N \cdot n \cdot b \quad (5.5)$$

The result will be compared with the result obtained through using Equation (3.19):

$$N_{cr,tot} = \frac{1}{\frac{1}{N_{cr,B}} + \frac{1}{N_{cr,S}}} \quad (3.19)$$

$$N_{cr,tot,approx} = \frac{1}{\frac{1}{N_{cr,B,approx}} + \frac{1}{N_{cr,S}}}$$

The $N_{cr,B}$ value is obtained through using the Vianello iterations shown in Appendix A. The $N_{cr,B,approx}$ value is obtained through using the approximate k_V -value found in Figure 3.13. The $N_{cr,S}$ value through Equations (3.11) and (3.12):

$$N_{cr,S} = 0.4 \cdot E \cdot A \quad (3.11) \quad (3.12)$$

In those examples where the walls have two different stiffnesses the stiffness, which represents the part of the wall where shear failure will occur, is chosen. The section where the failure due to shear will occur depends on how the different stiffnesses are distributed in combination with the load distribution. In the four cases examined this

critical section is assumed to occur where the lowest Young's modulus is found. The influence from the buckling load due to shear is in the following cases very low due to a much higher shear buckling load.

5.2.1 Case 1: Even load, uneven stiffness

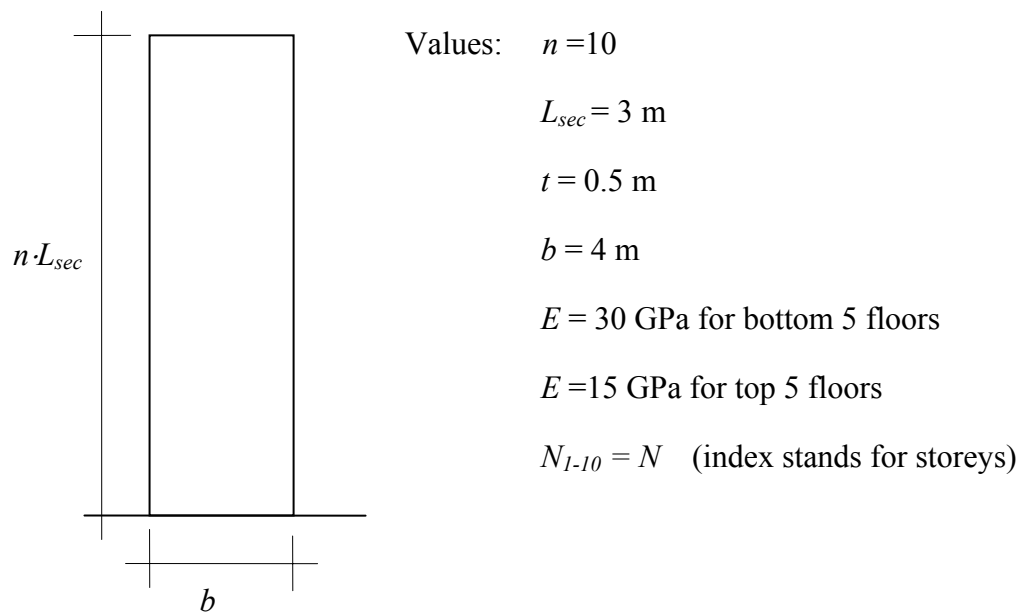


Figure 5.7: Case 1.

The shear contribution uses the lowest value of Young's modulus:

$$N_{cr,S} = 0.4 \cdot 15 \cdot 10^9 \cdot (0.5 \cdot 4) = 12 \text{ GN}$$

From the Vianello iteration shown in Appendix A is obtained: $N_{cr,B} = 565 \text{ MN}$

Which gives:
$$N_{cr,tot} = \frac{1}{\frac{1}{565 \cdot 10^6} + \frac{1}{12 \cdot 10^9}} = 540 \text{ MN}$$

Using the general Vianello $k_V = 6.8$, Figure 3.13, for a 10 storey building and lowest E value:

$$N_{cr,B,approx} = k_V \cdot \frac{EI}{(n \cdot L_{sec})^2} = 6.8 \cdot \frac{15 \cdot 10^9 \cdot \frac{0.5 \cdot 4^3}{12}}{30^2} = 302 \text{ MN}$$

The shear contribution uses the lowest value of Young's modulus:

$$N_{cr,S} = 0.4 \cdot 15 \cdot 10^9 \cdot (0.5 \cdot 4) = 12 \text{ GN}$$

$$N_{cr,tot,approx} = \frac{1}{\frac{1}{302 \cdot 10^6} + \frac{1}{12 \cdot 10^9}} = 295 \text{ MN}$$

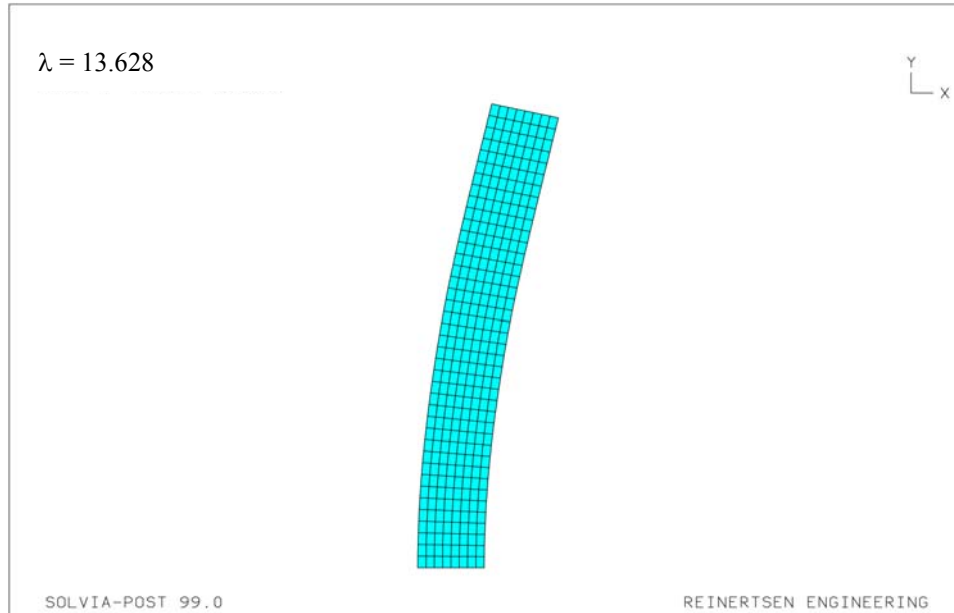


Figure 5.8: FEM first buckling mode case 1; with λ -value presented.

$$N_{cr,FEM} = 13.628 \cdot 1000 \cdot 10 \cdot 4 = 545 \text{ MN}$$

Results: $N_{cr,FEM} = 545 \text{ MN}$

$$N_{cr,tot} = 540 \text{ MN}$$

$$N_{cr,tot,appro} = 295 \text{ MN}$$

5.2.2 Case 2: Uneven load, uneven stiffness

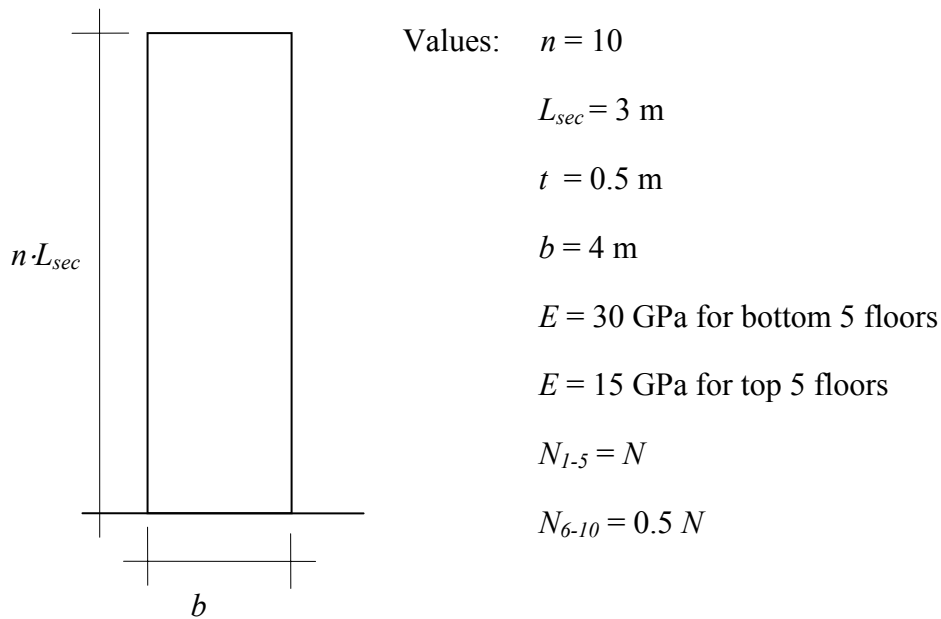


Figure 5.9: Case 2.

From the Vianello iteration shown in Appendix A is obtained: $N_{cr,B} = 769 \text{ MN}$

The shear contribution uses the lowest E value: $N_{cr,S} = 0.4 \cdot 15 \cdot 10^9 \cdot (0.5 \cdot 4) = 12 \text{ GN}$

$$\text{Which gives: } N_{cr,tot} = \frac{1}{\frac{1}{769 \cdot 10^6} + \frac{1}{12 \cdot 10^9}} = 723 \text{ MN}$$

Using the general Vianello $k_V = 6.8$, Figure 3.13, for a 10 storey building and lowest E value:

$$N_{cr,B,approx} = k_V \cdot \frac{EI}{(n \cdot L_{sec})^2} = 6.8 \cdot \frac{15 \cdot 10^9 \cdot \frac{0.5 \cdot 4^3}{12}}{30^2} = 302 \text{ MN}$$

The shear contribution uses the lowest E value:

$$N_{cr,S} = 0.4 \cdot 15 \cdot 10^9 \cdot (0.5 \cdot 4) = 12 \text{ GN}$$

$$N_{cr,tot,approx} = \frac{1}{\frac{1}{302 \cdot 10^6} + \frac{1}{12 \cdot 10^9}} = 295 \text{ MN}$$

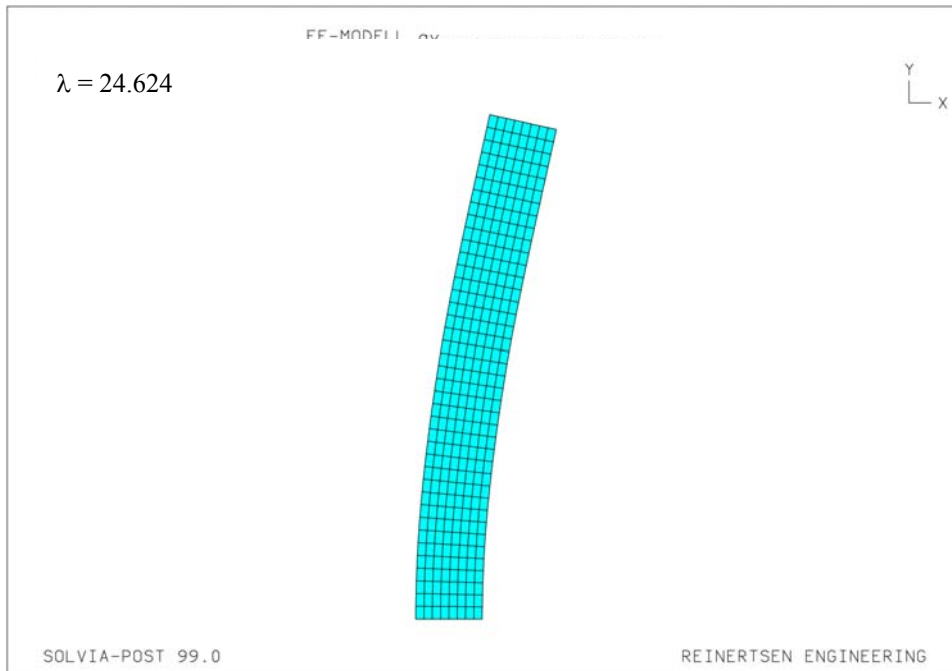


Figure 5.10: FEM first buckling mode case 2; with λ -value presented.

$$N_{cr,FEM} = 24.624 \cdot (5 \cdot (1000 + 500)) \cdot 4 = 739 \text{ MN}$$

Results: $N_{cr,FEM} = 739 \text{ MN}$

$$N_{cr,tot} = 723 \text{ MN}$$

$$N_{cr,tot,approx} = 295 \text{ MN}$$

5.2.3 Case 3: Slender wall - Uneven load, uneven stiffness

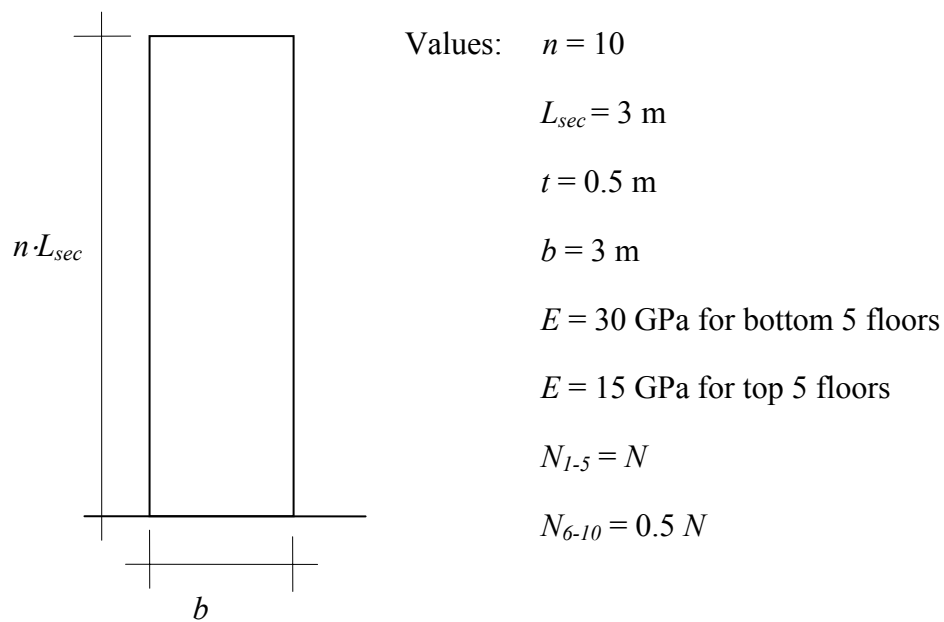


Figure 5.11: Case 3.

From the Vianello iteration shown in Appendix A is obtained: $N_{cr,B} = 324 \text{ MN}$

The shear contribution uses the lowest E value:

$$N_{cr,S} = 0.4 \cdot 15 \cdot 10^9 \cdot (0.5 \cdot 3) = 9 \text{ GN}$$

Which gives:
$$N_{cr,tot} = \frac{1}{\frac{1}{324 \cdot 10^6} + \frac{1}{9 \cdot 10^9}} = 312 \text{ GN}$$

Using the general Vianello $k_V = 6.8$, Figure 3.13, for a 10 storey building and the lowest E value:

$$N_{cr,B,approx} = k_V \cdot \frac{EI}{(n \cdot L_{sec})^2} = 6.8 \cdot \frac{15 \cdot 10^9 \cdot \frac{0.5 \cdot 3^3}{12}}{30^2} = 127.5 \text{ MN}$$

The shear contribution uses the lowest E value:

$$N_{cr,S} = 0.4 \cdot 15 \cdot 10^9 \cdot (0.5 \cdot 3) = 9 \text{ GN}$$

$$N_{cr,tot,approx} = \frac{1}{\frac{1}{127.5 \cdot 10^6} + \frac{1}{9 \cdot 10^9}} = 126 \text{ MN}$$

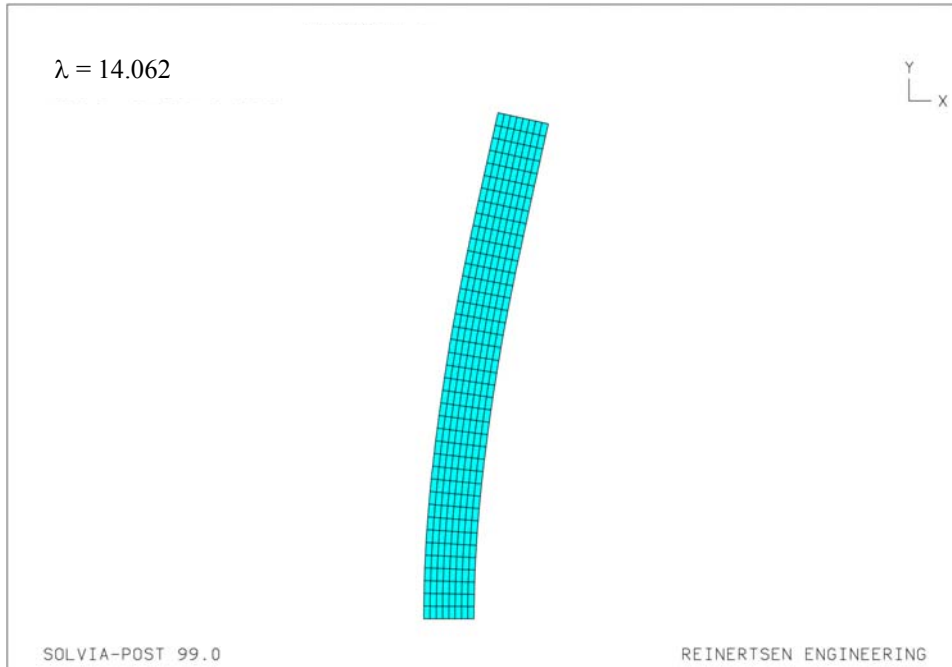


Figure 5.12: FEM first buckling mode; with λ -value presented.

$$N_{cr,FEM} = 14.062 \cdot (5 \cdot (1000 + 500)) \cdot 3 = 316 \text{ MN}$$

Results: $N_{cr,FEM} = 316 \text{ MN}$

$$N_{cr,tot} = 312 \text{ MN}$$

$$N_{cr,tot,approx} = 126 \text{ MN}$$

5.2.4 Case 4: Robust wall - Uneven load, uneven stiffness

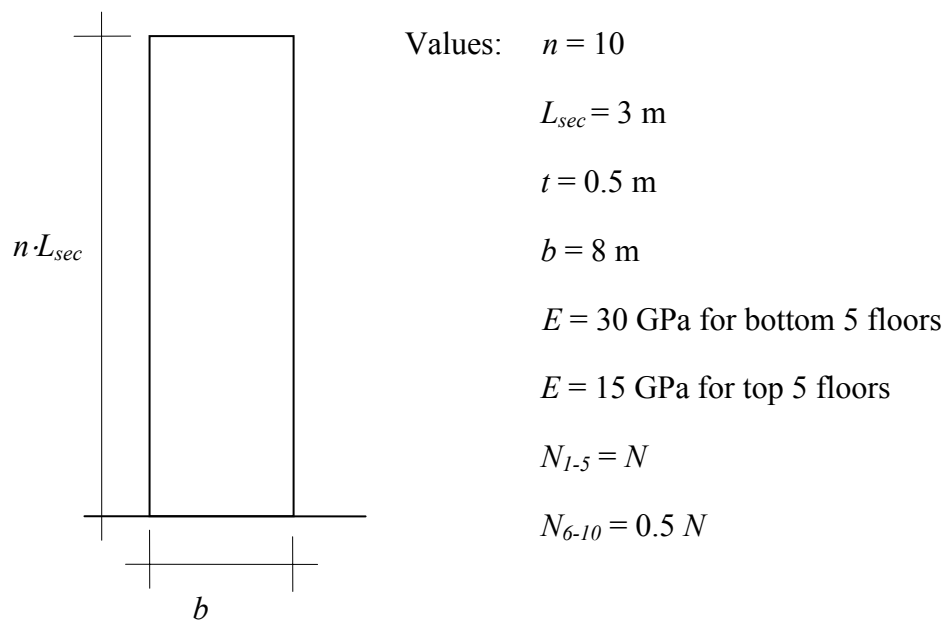


Figure 5.13: Case 4.

From the Vianello iteration shown in Appendix A is obtained: $N_{cr,B} = 6150 \text{ MN}$

The shear contribution uses the lowest E value:

$$N_{cr,S} = 0.4 \cdot 15 \cdot 10^9 \cdot (0.5 \cdot 8) = 24 \cdot 10^9 = 24 \text{ GN}$$

Which gives:
$$N_{cr,tot} = \frac{1}{\frac{1}{6150 \cdot 10^6} + \frac{1}{24 \cdot 10^9}} = 4895 \text{ MN}$$

Using the general Vianello $k_V = 6.8$, Figure 3.13, for a 10 storey building and the lowest E value:

$$N_{cr,B,approx} = k_V \cdot \frac{EI}{(n \cdot L_{sec})^2} = 6.8 \cdot \frac{15 \cdot 10^9 \cdot \frac{0.5 \cdot 8^3}{12}}{30^2} = 2418 \text{ MN}$$

The shear contribution uses the lowest E value:

$$N_{cr,S} = 0.4 \cdot 15 \cdot 10^9 \cdot (0.5 \cdot 8) = 24 \text{ GN}$$

$$N_{cr,tot,approx} = \frac{1}{\frac{1}{2418 \cdot 10^6} + \frac{1}{24 \cdot 10^9}} = 2197 \text{ MN}$$

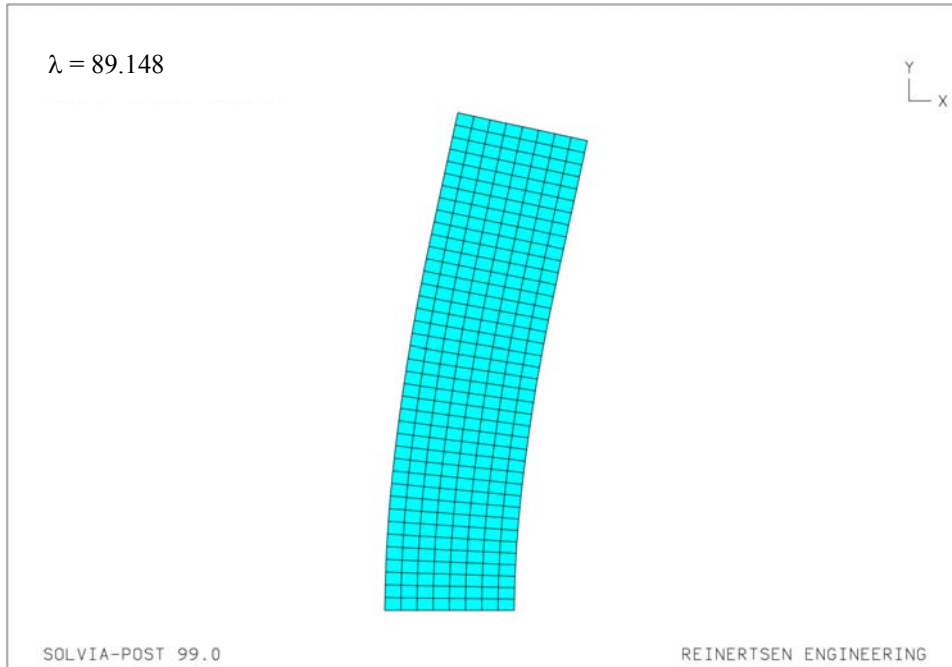


Figure 5.14: FEM first buckling mode for case 4; with λ -value presented.

$$N_{cr,FEM} = 89.148 \cdot (5 \cdot (1000 + 500)) \cdot 8 = 5349 \text{ MN}$$

Results: $N_{cr,FEM} = 5349 \text{ MN}$

$$N_{cr,tot} = 4895 \text{ MN}$$

$$N_{cr,tot,approx} = 2197 \text{ MN}$$

5.2.5 Results

The results in Table 5.5 show that using Vianello's method gives a critical load value close to the value obtained through FE-analyses. The value is not only close but also lands on the safe side of the FE-result in all the examples examined. The approximate Vianello results using k_{ν} -values from Figure 3.13, Section 3.3, are not nearly as accurate. Appendix A contains the Vianello iterations.

Table 5.5: Results of Vianello investigation.

Cases	$N_{cr,FEM}$ [MN]	$N_{cr,tot}$ [MN]	$N_{cr,tot,approx}$ [MN]	$N_{cr,tot}/$ $N_{cr,FEM}$	$N_{cr,tot,approx}/$ $N_{cr,FEM}$
1	545	540	295	0.99	0.54
2	739	723	295	0.98	0.40
3	316	312	126	0.99	0.40
4	5349	4895	2197	0.92	0.41

The advantage of using Vianello iterations for establishing critical buckling loads, instead of using k_V -values from Figure 3.13, has here been clarified. Observe that specifically for robust walls, case 4, there is a considerably stronger influence from $N_{cr,S}$. The accuracy is therefore reduced but is still very reasonable when compared with the results from using the k_V -values from Figure 3.13.

5.3 Investigation of pierced shear walls

In this section, pierced shear walls with different hole dimensions will be investigated. It is to be investigated if the rough estimates through hand calculation of pierced shear walls, described in Section 3.2, are realistic. The shear walls are modelled in SOLVIA through 9-node elements combined with a dense mesh, approximately 0.6 m x 0.6 m. It has been discovered that the FE-analyses include other effects which the hand calculations disregard, such as local deformations. It is expected that the results from the hand calculations and the FE-analyses will not concur as it is assumed in the hand calculations that plane cross-sections remain plane. The hand calculations include several assumptions, such as the deformable length of the transversal part, $c = c_0 + h_t$, and that the two vertical components have a united action, i.e. full cooperation.

The investigation entails comparisons of the deflections at the top of the wall when the wall is subjected to evenly distributed horizontal loads, and of the buckling loads when the wall is subjected to an evenly distributed vertical load. The critical buckling load is calculated assuming equal floor loads. The comparisons are made in three steps with the opening width, c_0 , is set to 1 m, 2 m and 3 m. In each step the transversal thickness, h_t , varies between 0.6 m to 2.2 m. The total breadth of the wall, b_0 and the height of each storey, L_{sec} are set equal to 8 m and 3 m respectively, see Figure 5.15.

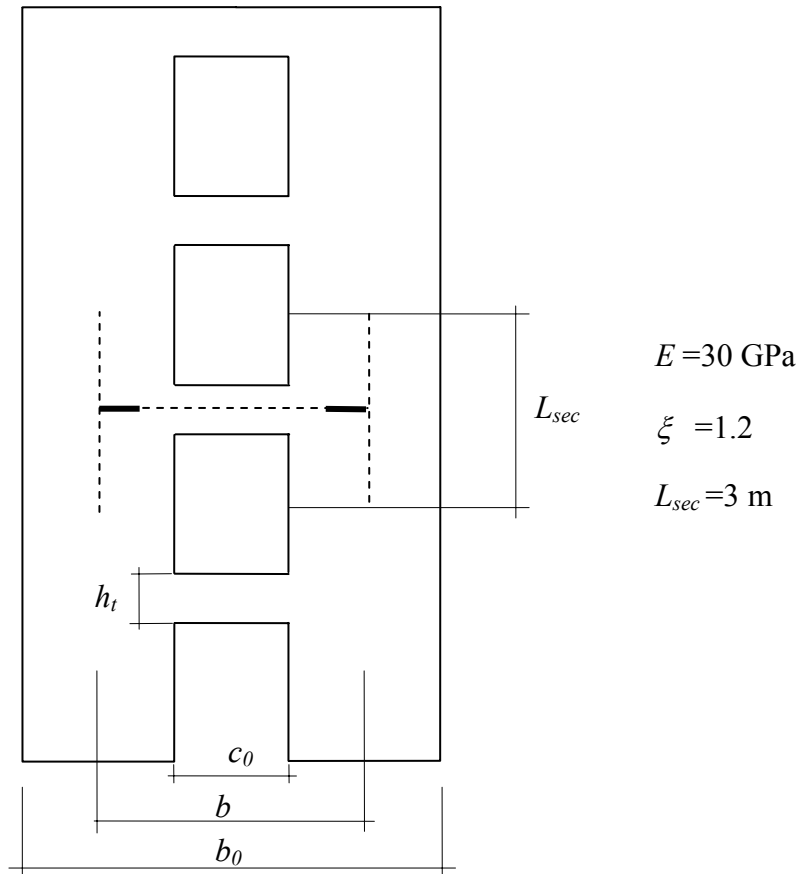


Figure 5.15: Picture of a pierced shear wall with values shown.

5.3.1 Results of deflection and buckling load

The tables below present the results from both the hand calculations and FE-analyses for deflection and buckling. HC stands for hand calculations.

Table 5.6: Results of deflection and buckling, $c_0 = 3$ m, and the h_t varies.

h_t [m]	Deflection FEA [nm]	Deflection HC [nm]	N_{cr} FEA [MN]	N_{cr} HC [MN]
0.6	165.8	174.0	1511	548
0.9	105.7	108.5	2330	1109
1.2	84.7	85.8	2914	1586
1.7	70.6	71.7	3461	2118
2.2	64.6	65.8	3736	2429

Table 5.7: Results of deflection and buckling, $c_0 = 2$ m, and the h_t varies.

h_t [m]	Deflection FEA [nm]	Deflection HC [nm]	N_{cr} FEA [MN]	N_{cr} HC [MN]
0.6	103.4	105.6	2392	991
0.9	78.4	78.2	3143	1668
1.2	69.4	68.4	3546	2127
1.7	62.9	62.1	3880	2569
2.2	60.0	59.5	4043	2809

Table 5.8: Results of deflection and buckling, $c_0 = 1$ m, and the h_t varies.

h_t [m]	Deflection FEA [nm]	Deflection HC [nm]	N_{cr} FEA [MN]	N_{cr} HC [MN]
0.6	69.8	67.7	3379	1964
0.9	63.4	60.8	3876	2511
1.2	60.8	58.3	4033	2794
1.7	58.7	56.5	4165	3036
2.0	57.9	55.9	4212	3120

Deflections:

The method for calculating deflections, see Section 3.2.2, gives a good approximation compared to the FE-analyses. The equations are complex and it is preferable to use programs like Excel, which has been used here, to establish the deflections.

Table 5.6 concerns the most slender models with a gap width of 3 m. The hand calculations show deflections slightly greater than the FE-analyses, i.e. on the safe side. The results with regard to increasing transversal thickness agree better with the FE-results.

Table 5.7 presents results of models with gap widths of 2 m and Table 5.8 with 1.0 m wide gaps. Both tables present results that reveal values slightly on the unsafe side from the hand calculations. The hand calculation underestimates the deflection for more solid structures but still the values are very close to the FE-results.

Buckling load:

The three tables above reveal that the hand calculation method, derived in Section 3.2.1, presents buckling loads that are not reasonable and are very much on the safe side, especially slender structures, walls with wide gap widths and thin transversal parts, which confer values that are almost one third of the results from FE-analyses. The comparison which agrees best is the least slender wall where $c_0 = 1.0$ m and $h_t = 2.0$ m.

5.3.2 Improvements for buckling load results

The results concerning the buckling loads in Section 5.3.1 demand further investigation in order to discover how the hand calculation method can be improved. The first step is to examine the hand calculation when the gap width decreases and the thickness of the transversal part increases to converge to being a solid shear wall. The

approximation of the deformable length of the transversal part is especially of interest. As it is described in the derivation, see Section 3.2.1, this length is estimated as the sum of the gap width and the transversal thickness, $c = c_0 + h_t$. It is suspected that this length becomes too long and therefore produces greater deflection of the transversal part which leads to a greater shear angle and finally a lower buckling load. The calculation method from Lorentsen (2000) is also used in Westerberg (1999). In Westerberg's publication the transversal length is set to $c = c_0$. It is not discussed why the deformable length in Lorentsen (2000) includes the transversal thickness. It is therefore this approximation which is investigated first.

5.3.2.1 Altering the deformable length of the transversal

The investigation starts with comparing results if the deformable length of the transversal part is set to the gap width, $c = c_0$. Tables 5.9 and 5.10 present results concerning shear walls which have such small gaps and therefore resemble solid walls. The walls have the same overall measurements as the ones previously examined.

Table 5.9: Comparison between two assumptions of the c -value and FEA results.

Wall- hole size	N_{cr} FEA [MN]	N_{cr} HC $c=c_0+h_t$ [MN]	N_{cr} HC $c=c_0$ [MN]
0.4 x 0.4 m	4317	3387	4100
Solid wall	4332	3491	4229

Table 5.10: Comparison between two assumptions of the c -value and FEA results.

Wall- hole size	N_{cr} FEA [MN]	N_{cr} HC $c=c_0+h_t$ [MN]	N_{cr} HC $c=c_0$ [MN]	Deformable length of transversal $c=c_0+h_t$. [m]	Deformable length of transversal $c=c_0$ [m]
1.0 x 1.0 m	4212	3120	3864	3	1
0.4 x 0.4 m	4317	3387	4100	3	0.4
Solid wall	4332	3491	4229	3	0

It is obvious from Table 5.10 that the assumed deformable length, $c = c_0 + h_t$, of the transversal part is too long. In the three cases shown above the deformable length always becomes 3 m, when it is assumed that $c = c_0 + h_t$ even though the sizes of the holes differ. When the deformable length is set to be equal to the gap width, $c = c_0$, all three examples present much better results compared to the FE-results. The best agreement is found for the case with the hole dimensions 0.4 x 0.4 m.

How the buckling loads varies depending on the thickness of the transversal, width of opening and assumed interaction is shown in Figures 5.16, 5.17 and 5.18.

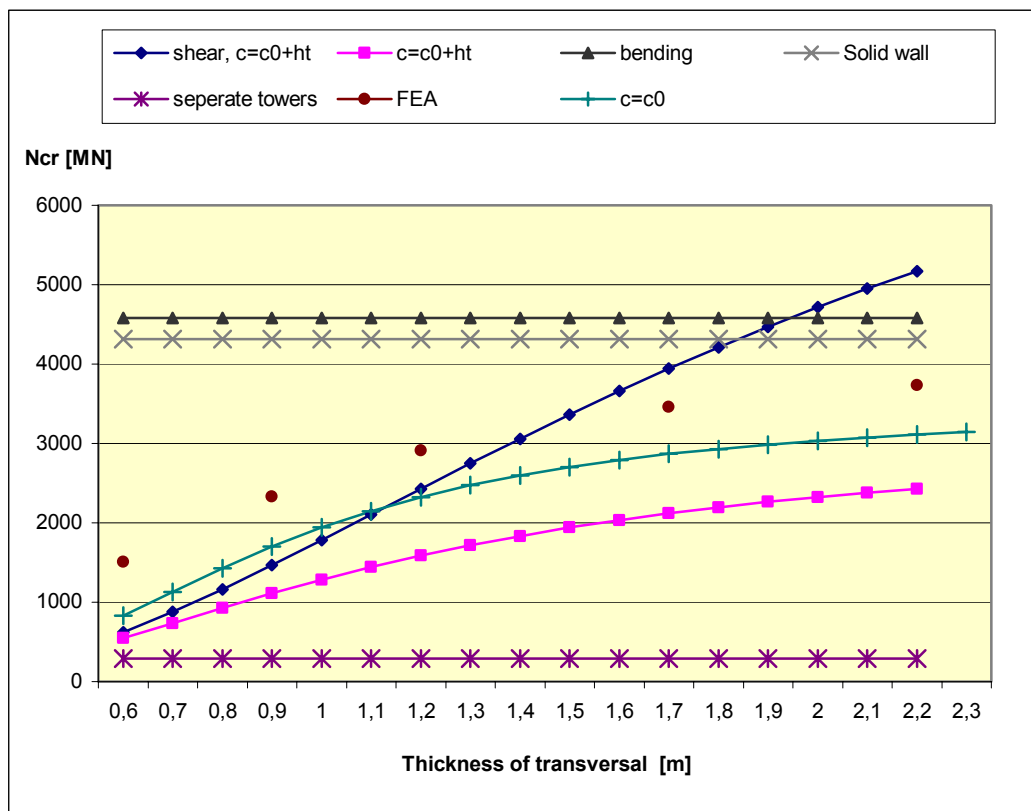


Figure 5.16: Comparison of critical buckling loads, 10 storeys, gap width $c_0 = 3$ m

Figure 5.16 shows seven different functions. Three functions show constant values, i.e. their values are not influenced by the thickness of the transversal. The straight line at the value of about 4600 MN, named *bending* in the graph, is the critical buckling load due to bending only. It is assumed that there is complete interaction between the two vertical parts and therefore the varying thickness of the transversal part has no effect. This approximation is on the unsafe side especially in slender walls where the connections between the vertical parts are weak. Still, when through combining the influence of shear with the contribution from bending the total critical buckling load is decidedly on the safe side. It is then obvious that the shear deformation is the overestimated part which must be improved.

The second straight horizontal line, *solid wall*, slightly below the results due to bending deformation, presents the buckling load for a solid wall with the same

breadth and height as the pierced ones. Both shear and bending deformations are considered.

The straight horizontal line at the lower area of the graph, *separate towers*, presents values of another hand calculation method. This method disregards the transversal parts completely and the wall is treated as two single walls without interaction. The stiffness of this structure is much smaller and the buckling load becomes considerably more on the safe side than the previous approaches.

The results from the hand calculation method that considers openings are plotted with two assumptions, $c_0 = c + h_t$ and $c_0 = c$. The results based on the assumption $c_0 = c$ reveal that the buckling load is on the safe side for all cases compared to the FE-results. Slender models, $h_t = 0.6\text{--}1\text{ m}$, have a great influence from the shear deformation. It is important here to observe that the so called *shear part* is not only shear effect when referring to calculation of *pierced* shear walls, see Section 3.2. If a quotation is made between the results from the hand calculations, $c_0 = c + h_t$ and $c_0 = c$, and the results from FE-analyses, then one can observe that for slender models the value decreases, see Table 5.13.

Two additional graphs are made for the models with gap widths of 1 m and 2 m, see Figures 5.17 and 5.18.

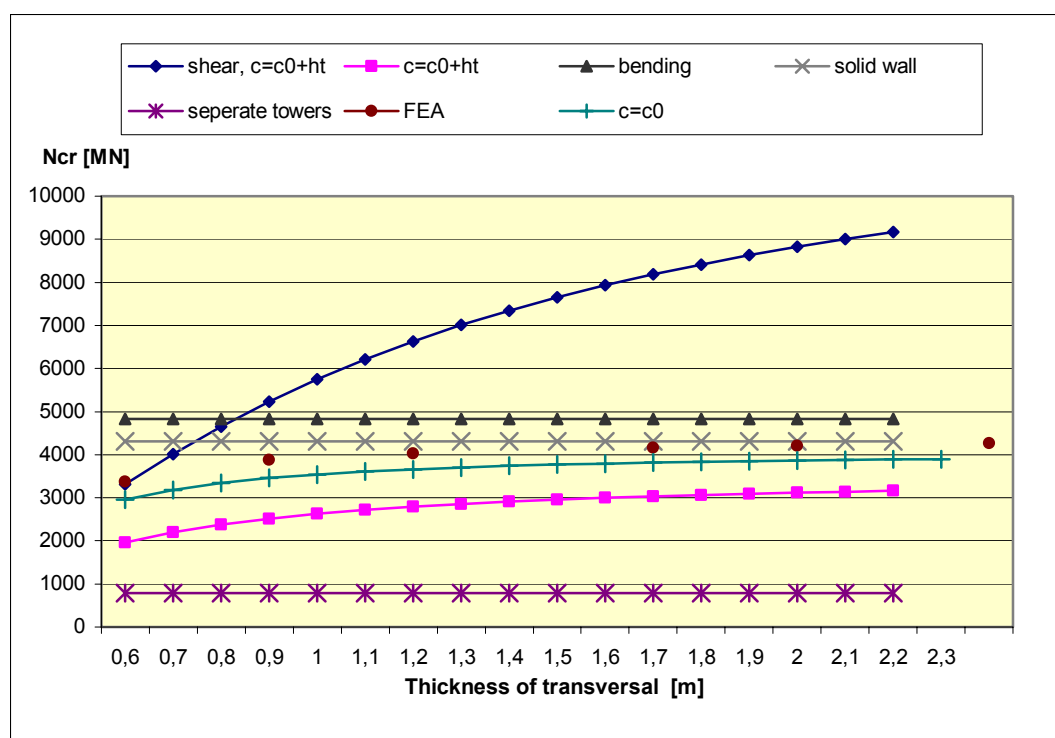


Figure 5.17: Comparison of critical buckling loads, 10 storeys, gap width $c_0 = 1\text{ m}$.

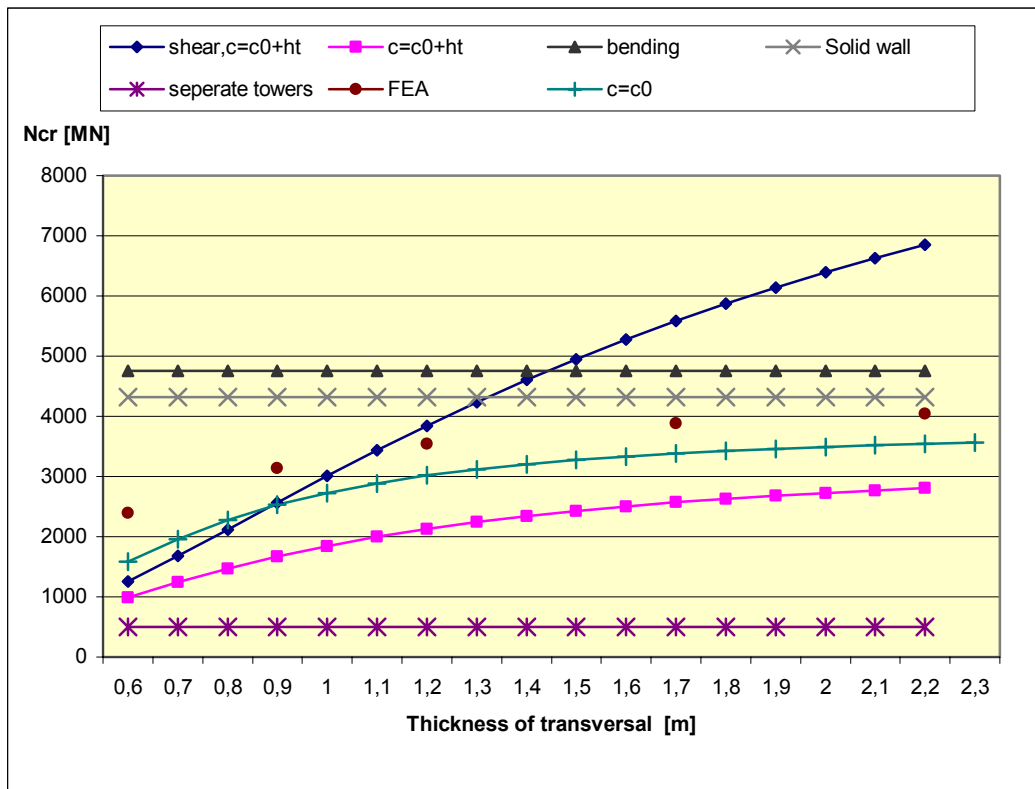


Figure 5.18: Comparison of critical buckling loads, 10 storeys, gap width $c_0 = 2$ m.

Table 5.11: Buckling analyses $c_0 = 1$ m; comparing hand calculations with $c = c_0 + h_t$ and $c = c_0$ and FE-results, and then presenting their accuracy compared to FE-results.

h_t [m]	N_{cr} FEA [MN]	N_{cr} HC $c = c_0 + h_t$ [MN]	N_{cr} HC $c = c_0$ [MN]	HC/FEA $c = c_0 + h_t$	HC/FEA $c = c_0$
0.6	3379	1964	2960	0.58	0.87
0.9	3876	2511	3457	0.65	0.89
1.2	4033	2794	3661	0.69	0.91
1.7	4165	3036	3814	0.73	0.92
2.0	4212	3120	3864	0.74	0.92

Table 5.12: Buckling analyses $c_0 = 2$ m; comparing hand calculations with $c = c_0 + h_t$ and $c = c_0$ and FE-results, and then presenting their accuracy compared to FE-results.

h_t [m]	N_{cr} FEA [MN]	N_{cr} HC $c = c_0 + h_t$ [MN]	N_{cr} HC $c = c_0$ [MN]	HC/FEA $c = c_0 + h_t$	HC/FEA $c = c_0$
0.6	2392	991	1585	0.41	0.66
0.9	3143	1668	2527	0.53	0.80
1.2	3546	2127	3016	0.60	0.85
1.7	3880	2569	3381	0.66	0.87
2.2	4043	2809	3542	0.69	0.88

Table 5.13: Buckling analyses $c_0 = 3$ m; comparing hand calculations with $c = c_0 + h_t$ and $c = c_0$ and FE-results, and then presenting their accuracy compared to FE-results.

h_t [m]	N_{cr} FEA [MN]	N_{cr} HC $c = c_0 + h_t$ [MN]	N_{cr} HC $c = c_0$ [MN]	HC/FEA $c = c_0 + h_t$	HC/FEA $c = c_0$
0.6	1511	548	831	0.36	0.55
0.9	2330	1109	1699	0.48	0.73
1.2	2914	1586	2323	0.54	0.80
1.7	3461	2118	2867	0.61	0.83
2.2	3736	2429	3112	0.65	0.83

In Table 5.13 the walls with the widest openings are presented, i.e. 3 m gap width. The case with $h_t = 0.6$ m shows a percentile of 36 % which means that the hand calculation based on $c = c_0 + h_t$ would lead to over dimensioning with $1/0.36$, i.e. the FE-results are 2.8 times greater than the hand calculation results. From analysing the quotients it can be observed that the shear contribution in the hand calculation method is misrepresentative. The quotations exemplify that the shear part of the hand

calculation method is faulty because pierced shear walls with greater openings have a greater influence from shear and therefore produce the less satisfying results obtained.

5.3.2.2 Shear factors

After shortening the length of the deformable part of the transversals to $c = c_0$, the hand calculated results are still not close to the FE-result especially not for structures with greater openings. A further investigation of how the shear contribution can be improved has been done through recalculating the same shear walls presented previously. In this investigation the results are first taken from the FE-analyses and are reduced by the bending part to obtain the shear part. The obtained value for the shear part is treated as the value that should have been obtained in the hand calculations for obtaining an exact buckling load, i.e. equal to the FE-results.

$$N_{cr,S,FEA} = \frac{1}{\frac{1}{N_{cr,FEA}} - \frac{1}{N_{cr,B}}} \quad (5.6)$$

A quotient is made once again between the new value obtained, $N_{cr,S,FEA}$, and the hand calculated shear value, $N_{cr,S}$. The quotients are made using the hand calculated $N_{cr,S}$ for $c = c_0 + h_t$ and for $c = c_0$. Tables 5.14, 5.15 and 5.16 present the results.

Table 5.14: Establishment of a shear factor for gaps where $c = 1$ m.

h_t [m]	$N_{cr,S,FEA}$ [MN]	$N_{cr,S}$ $c = c_0 + h_t$ [MN]	$N_{cr,S}$ $c = c_0$ [MN]	Shear Factor $c = c_0 + h_t$ $N_{cr,S,FEA} / N_{cr,S}$	Shear Factor $c = c_0$ $N_{cr,S,FEA} / N_{cr,S}$
0.6	11270	3313	7655	3.40	1.47
0.9	19690	5234	12187	3.76	1.62
1.2	24544	6634	15166	3.70	1.62
1.7	30409	8184	18188	3.72	1.67
2.0	33106	8823	19384	3.75	1.71

Table 5.15: Establishment of a shear factor for gaps where $c = 2$ m.

h_t [m]	$N_{cr,S,FEA}$ [MN]	$N_{cr,S}$ $c = c_0 + h_t$ [MN]	$N_{cr,S}$ $c = c_0$ [MN]	Shear Factor $c = c_0 + h_t$ $N_{cr,S,FEA} / N_{cr,S}$	Shear Factor $c = c_0$ $N_{cr,S,FEA} / N_{cr,S}$
0.6	4808	1251	2376	3.84	2.02
0.9	9252	2568	5387	3.60	1.72
1.2	13904	3844	8232	3.62	1.69
1.7	20987	5582	11670	3.76	1.80
2.2	26841	6853	13842	3.92	1.94

Table 5.16: Establishment of a shear factor for gaps where $c = 3$ m.

h_t [m]	$N_{cr,S,FEA}$ [MN]	$N_{cr,S}$ $c = c_0 + h_t$ [MN]	$N_{cr,S}$ $c = c_0$ [MN]	Shear Factor $c = c_0 + h_t$ $N_{cr,S,FEA} / N_{cr,S}$	Shear Factor $c = c_0$ $N_{cr,S,FEA} / N_{cr,S}$
0.6	2255	623	1015	3.62	2.22
0.9	4742	1464	2701	3.24	1.76
1.2	8008	2427	4713	3.30	1.70
1.7	14156	3941	7663	3.59	1.85
2.2	20254	5171	9705	3.92	2.09

The factors calculated in the tables above describe how much the original shear buckling load from the hand calculation should be magnified by in order to establish values that agree with FE-results. In the examples presented above, all *shear factors* when $N_{cr,S}$ is calculated for $c = c_0 + h_t$ are at least 3.2 which means that if all values, concerning the buckling load due to the shear, are multiplied with 3.2, the total buckling load will be closer to the FE-results and always on the safe side for the investigated walls. A shear factor is also produced for when $N_{cr,S}$ is calculated for $c = c_0$ and these results show a marked improvement. Three new graphs, Figures 5.19, 5.20 and 5.21, are established and present a new function of the total critical buckling load when the shear part has been multiplied with 3.2.

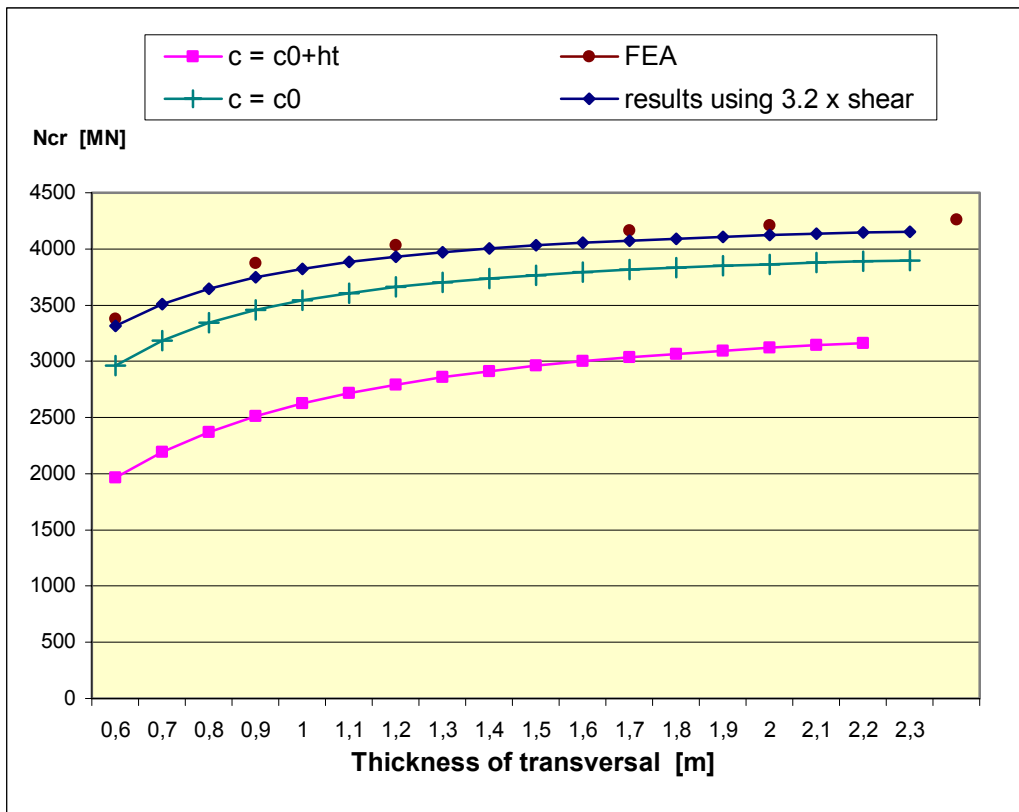


Figure 5.19: 10 storeys, variable transversal thickness, $c_0 = 1$ m

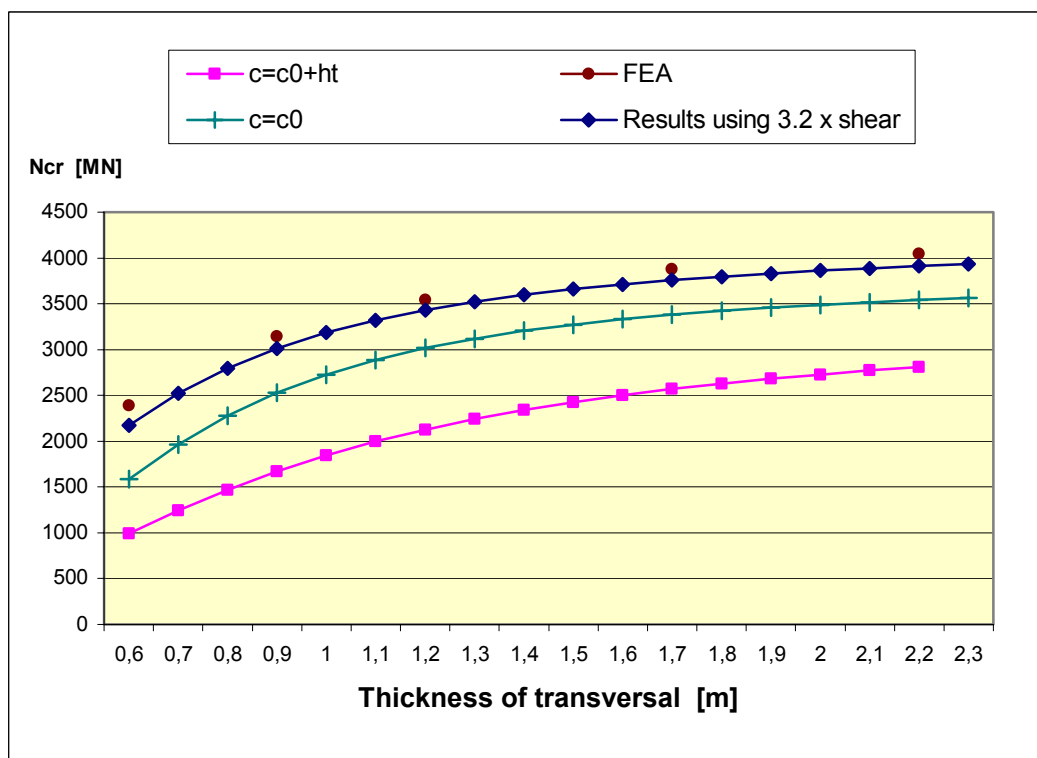


Figure 5.20: 10 storeys, variable transversal thickness, $c_0 = 2$ m

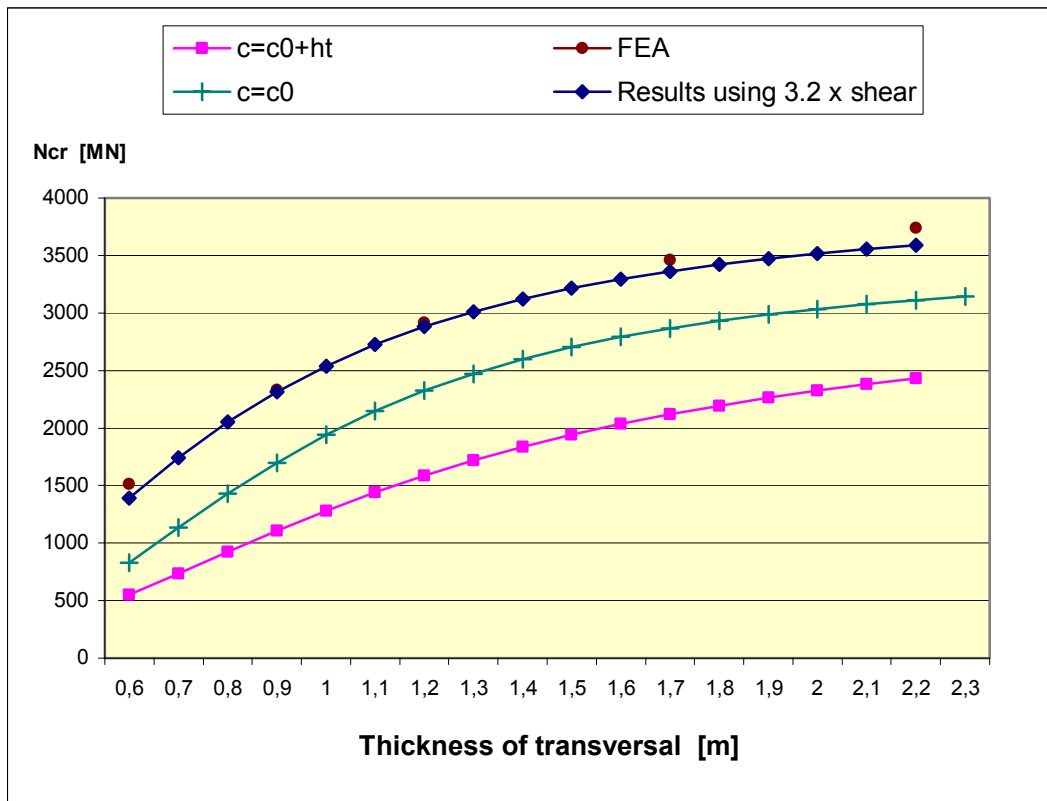


Figure 5.21: 10 storeys, variable transversal thickness, $c_0 = 3$ m

The new proposed function has the same shape as the FE-analysis and the function assuming $c = c_0$. In the models presented in this section it is possible to use a shear factor of 3.2 in order to get values close to the FE-results. The approach of using a shear factor is also applicable independent of the height of the building or the number of stories. The reason why this is possible depends on the derivation of the buckling load due to shear which does not depend on the height of the structure, see Section 3.2.1. The approach of manipulating the shear part is therefore possible for all multi-storey shear walls.

The models treated in this section are based upon buildings where $L_{sec} = 3$ m and the same total breadth of the wall, $b_0 = 8$ m, see Figure 5.14. As the shear angle is affected by these relations the models which have been examined in this section, are not representatives of all types of pierced shear walls. Further investigations of structures with different relations between the storey height and the total breadth, have to be examined to find out whether it is possible to use a general shear factor for improving the critical buckling load or not.

The investigation of how the shear factor is affected if the height of the storey and the breadth of the wall are changed. The length of the transversal part is first set to be equal to the gap width, i.e. $c = c_0$.

One series of models which has been examined are walls that are slender, i.e. higher and reduced breadth. The investigated walls have all a breadth of only 4.0 m and have a storey height of 4.0 m giving a total height of 40 m. What is different with these walls from the previously described is that the bending part dominates, i.e. the

buckling load due to the shear deformations is much higher than the buckling load obtained through global bending. Table 5.17 presents the results for 4 slender walls.

Table 5.17: Buckling loads and shear factors, $c_0 = 2$ m.

h_t [m]	$N_{cr,FEA}$ [MN]	$N_{cr,tot,HC}$ [MN]	$N_{cr,B,HC}$ [MN]	$N_{cr,S,HC}$ [MN]	$N_{cr,tot,HC}$ / $N_{cr,FEA}$	Shear factor $c = c_0$
0.6	219	186	298	493	0.85	1.68
1.2	268	234	298	1089	0.87	2.44
1.7	281	241	298	1272	0.86	3.87
2.2	289	244	298	1358	0.84	7.05

In models that concern slender walls, the critical buckling load in the hand calculations is closer to the buckling load through bending. The shear factor is based upon the difference between the buckling load from the FE-analysis and the buckling load due to bending. In walls where the buckling load due to bending is very close to the value from the FE-analysis, i.e. in slender walls, the shear deformation has to be increased dramatically in order to obtain a buckling load which agrees with the FE-analysis. Observe the great increase of the shear factor from the model at the top to the model at the end of Table 5.17. In the first model, $h_t = 0.6$ m, the shear buckling load still has a great influence on the total buckling load. The last two walls, $h_t = 1.7$ m and $h_t = 2.2$ m present a great difference despite the values from FE-analysis and the bending buckling load of the hand calculation being almost the same.

$$N_{cr,S,FEA} = \frac{1}{\frac{1}{N_{cr,FEA}} - \frac{1}{N_{cr,B}}} \quad (5.6)$$

In extremely slender walls the shear deformations can be neglected. This is observed also in the FE investigation of the solid walls in Section 5.1.1. In Equation (5.6) the buckling loads obtained from the FE-analyses will almost converge to the value obtained from the bending part in the hand calculation. This will lead to a very high shear factor to compensate for the difference. This investigation reveals that for very slender walls a correct shear factor for proper usage is probably impossible to establish. The walls examined above are slender in a global perspective and reveal that the buckling load from global bending is dominant with an increasing thickness of the transversal. It is here important to notice the difference between *global slenderness* and the *internal slenderness* regarding the vertical and transversal parts themselves.

The results from the hand calculations agree well with the FE-results. Since the shear factor is hard to establish and loses its purpose as a useful method, a closer look is

drawn to the four different contributions from the shear angle which are derived in Section 3.2.1.

5.3.2.3 Shear angles

From the derivation of the shear angle for pierced shear walls, the bending part of the transversal is much affected by the thickness of the transversal as the moment of inertia is increasing with the thickness, h_t , see Section 5.3.2.1. This part of the shear angle decreases rapidly with an increase in the transversal thickness when the gap width is constant. The *shear part* of the shear angle also decreases with an increase in the transversal thickness as the cross section area is influenced. The two remaining parts of the total shear angle are due to bending and shear deformation in the vertical parts. These are not affected by an increasing thickness of the transversal and are therefore constant for each gap width. With this knowledge, it is therefore suspected that the shear factors should be almost constant or at least follow a pattern for each table which, apparently, does not occur, see Tables 5.14, 5.15 and 5.16. Table 5.18 shows an example of how the four contributions to the shear angle vary with increasing thickness of the transversal for a gap width of $c_0 = 2$ m.

Table 5.18: All contributions to the total shear angle, $c_0 = 2$ m, $c = c_0$.

h_t [m]	Vert. Part Bending Eq. (3.27) [10^{-11} rad]	Vert. Part Shear Eq. (3.29) [10^{-11} rad]	Transv. Part Bending Eq. (3.26) [10^{-11} rad]	Transv. Part Shear Eq. (3.28) [10^{-11} rad]	Total shear angle Eq. (3.25) [10^{-11} rad]
0.6	1.11	3.33	29.60	8.00	42.10
0.9	1.11	3.33	8.78	5.33	18.56
1.2	1.11	3.33	3.70	4.00	12.10
1.7	1.11	3.33	1.30	2.82	8.57
2.2	1.11	3.33	0.60	2.18	7.23

Table 5.18 shows how the four parts of the angle vary with an increasing thickness of the transversal. The two columns concerning the deformation of the vertical parts have constant values. The equations are presented in Section 3.2.1.

In the hand calculation method it has been observed that if measurements for a solid wall are interpreted in the hand calculation, the parts concerning the shear angle from bending and shear in the vertical parts, still have a contribution. For a solid wall only the part concerning shear in the verticals should produce values. If the bending part is set equal to zero, only shear deformation of the verticals is left for determining the

total shear angle. When the deformable length of the transversal is set equal to the gap width, i.e. $c_0 = c$, combined with the vertical bending part being set to zero, the total shear angle becomes equal to the shear angle used for solid walls, see Equation (3.13)

$$c_0 = 0 \text{ (gap width)} \Rightarrow c = c_0 = 0$$

$$\text{Transversal part} \quad \gamma_{t,bend} = \frac{L_{sec} c^3}{12b^2 EI_t} = 0 \quad (3.26)$$

$$\gamma_{t,shear} = \xi \frac{L_{sec} c}{b^2 GA_t} = 0 \quad (3.28)$$

$$\text{Vertical parts} \quad \gamma_{v,bend} = \frac{L_{sec}^2}{24EI_v} = 0 \quad (3.27)$$

$$\gamma_{v,shear} = \frac{\xi}{2GA_v} = \gamma_{Tot} \quad (3.29)$$

Observe that $\gamma_{v,shear}$ is the same expression used for critical buckling load due to shear for solid walls.

$$N_{cr,S} = \frac{GA}{\xi} = \frac{G2A_v}{\xi} = \frac{\xi}{\gamma_{tot}} = \frac{\xi}{\gamma_{v,shear}} \quad (3.14)$$

A final study is made to investigate how the influence of bending deformations of the vertical parts affects the buckling load. All the walls in Table 5.19 have a thickness of 0.5 m. The contribution from bending deformations of the vertical parts, $\gamma_{v,bend}$, is set equal to zero.

Table 5.19: Comparisons of buckling loads when $c_0 = c$ and $\gamma_{v,bend} = 0$.

c_0 [m]	b_0 [m]	h_t [m]	L_{sec} [m]	$N_{cr,FEA}$ [MN]	$N_{cr,HC}$ [MN]	$N_{cr,HC}/N_{cr,FEA}$	SF $\gamma_{v,bend} = 0$
0.4	8.0	2.6	3.0	4317	4194	0.97	1.27
2.0	8.0	0.6	4.0	219	206	0.94	1.23
2.0	8.0	1.2	4.0	268	267	1.00	1.03
2.0	8.0	1.7	4.0	281	277	0.99	1.25
2.0	8.0	2.2	4.0	289	281	0.97	1.94
2.0	4.0	1.2	3.0	469	454	0.97	1.30
3.0	4.0	1.2	4.0	149	173	1.16	0.43

The study shows that the contribution from the bending deformations of the vertical parts is over estimated in the hand calculations for pierced walls that have substantial verticals. For frames and for walls that have slender vertical parts, the approach of setting $\gamma_{v,bend}$ equal to zero is not recommended as it can produce results on the unsafe side.

In Equation (3.27) the deformable length of the verticals is taken as the complete storey height, L_{sec} . This deformable length is suspected to be over estimated as with an increasing transversal thickness this length should decrease. It is assumed that bending will not occur at the centre of the verticals, i.e. the intersection between the verticals and the transversal, due to the section being robust. The length of the deformable part of the vertical is therefore reduced to obtain a new length influenced by the transversal thickness.

$$L_{sec,red} = L_{sec} - h_t \quad (5.7)$$

$$\gamma_{v,bend} = \frac{L_{sec}^2}{24EI_v} \quad \Rightarrow \quad \gamma_{v,bend} = \frac{(L_{sec} - h_t)^2}{24EI_v} \quad (5.8)$$

Table 5.20 presents the results when the vertical bending length has been altered to $L_{sec,red} = L_{sec} - h_t$.

Table 5.20: Comparisons of buckling loads when $c_0 = c$ and $L_{sec,red}$ is used.

c_0 [m]	b_0 [m]	h_t [m]	L_{sec} [m]	$N_{cr,FEA}$ [MN]	$N_{cr,HC}$ [MN],	$N_{cr,HC}/$ $N_{cr,FEA}$	SF
0.4	8.0	2.6	3.0	4317	4193	0.97	1.28
2.0	4.0	0.6	4.0	219	191	0.87	1.55
2.0	4.0	1.2	4.0	268	250	0.93	1.72
2.0	4.0	1.7	4.0	281	264	0.94	2.11
2.0	4.0	2.2	4.0	289	272	0.94	2.98
2.0	4.0	1.2	3.0	469	432	0.92	1.74
3.0	4.0	1.2	4.0	149	127	0.85	1.71

With the reduced deformable length of the vertical the hand calculation method gives reasonable values slightly on the safe side for all walls examined. Pierced walls with slender verticals are sensitive to an adjustment of the deformable length of the vertical. In contrast, models with robust verticals, for example the wall presented at the top in Tables 5.19 and Table 5.20, are hardly affected but still this modified approach seems to work for all walls investigated. The complete list of all walls examined during this study is presented in Appendix B.

5.3.3 Stress distribution

This investigation relating to pierced shear walls concerns the stress distribution at the base of the walls. The deformation figures from the FE-analyses show the behaviour of the walls and the interaction between the vertical parts. Here it shall be attempted to derive a fast and effective method for calculating stress distribution by hand. The stress distribution, through hand calculation, can be calculated in two different ways and each method shall assume a linear relationship for the stresses.

5.3.3.1 Hand calculation methods

First an analysis will be done on a shear wall that is solid, Figure 5.22, and the same wall but split in the middle, Figure 5.22b. This analysis is produced in order to acquire a picture of how the stresses will look depending on if the wall has complete cooperation between the two halves, Figure 5.22a, or if there is no cooperation, Figure 5.22b.

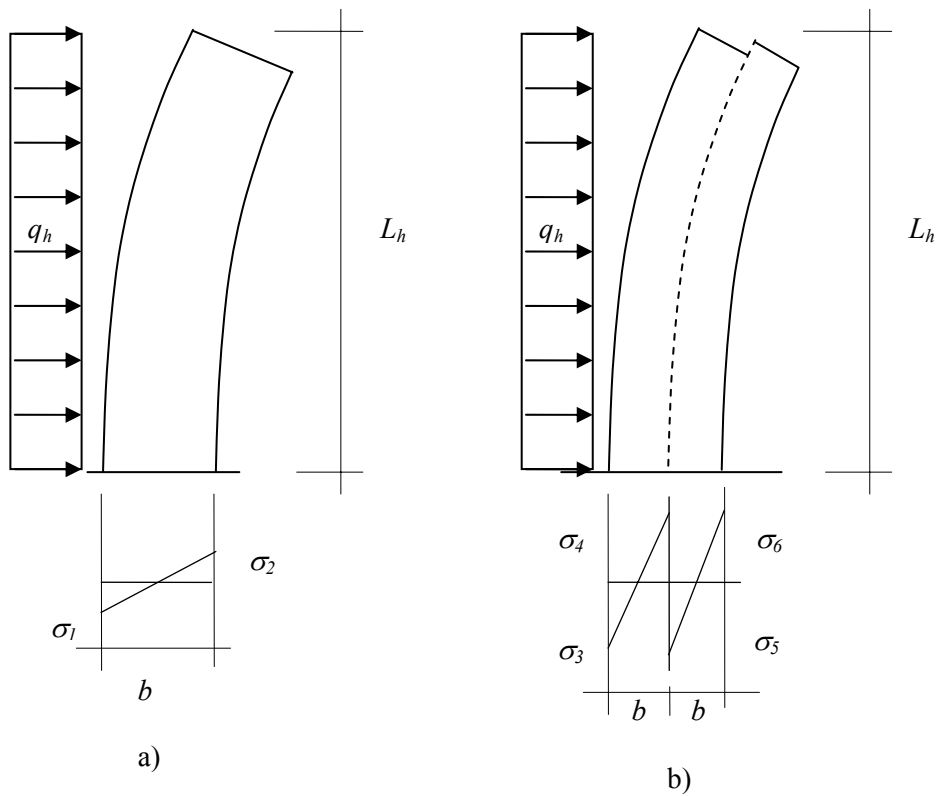


Figure 5.22:

Figure 5.22a: $t = 0.5 \text{ m}$, $b = 8 \text{ m}$, $L_h = 30 \text{ m}$, $q_h = 5 \text{ kNm}$, $E = 30 \text{ GPa}$.

Figure 5.22b: $t = 0.5 \text{ m}$, $b = 4 \text{ m}$, $L_h = 30 \text{ m}$, $q_h = 5 \text{ kNm}$, $E = 30 \text{ GPa}$.

Calculation of stresses, Figure 5.22a:

$$M = 5000 \cdot 30 \cdot \frac{30}{2} = 2250 \text{ kNm}$$

$$I = \frac{0.5 \cdot 8^3}{12} = 21.33 \text{ m}^4$$

$$\sigma_{\max} = \frac{M}{I} \cdot z \quad z = \frac{b}{2} \quad z = 4 \text{ m} \quad \Rightarrow \quad \sigma_{1,2} = \pm \frac{2250 \cdot 10^3}{21.33} \cdot 4 = \pm 422 \text{ kPa}$$

Calculations of stresses, Figure 5.22b:

$$M = 2250 \text{ kNm}$$

$$I_V = \frac{0.5 \cdot 4^3}{12} = 2.67 \text{ m}^4$$

$$\sigma_{\max} = \frac{M}{I} \cdot z \quad z = \frac{b}{2} \quad z=2 \text{ m} \quad \Rightarrow \quad \sigma_{3,4,5,6} = \pm \frac{2250 \cdot 10^3}{2.67} \cdot 2 = \pm 843 \text{ kPa}$$

Observe the difference in stress values when different assumptions are made. The stress values for Figure 5.22b are twice the values calculated for Figure 5.22a. Concerning pierced shear walls the stress distribution through the cross section is somewhere between the two examples shown in Figure 5.22a and 5.22b. Depending on the size of the holes in the walls the interaction between the two verticals will be influenced.

Three walls have been chosen for comparing hand calculations with FEA results. Example 1 has the smallest opening and example 3 has the largest, see Table 5.21.

Table 5.21: Pierced shear wall statistics. $c = c_0 + h_t$.

Ex.	t [m]	b_0 [m]	c_0 [m]	h_t [m]	W [kN/m]	E [GPa]	L_{sec} [m]	L_h [m]
1	0.5	8.0	1.0	2.0	5	30	3.0	30
2	0.5	8.0	1.0	0.6	5	30	3.0	30
3	0.5	8.0	2.0	1.2	5	30	3.0	30

Two hand calculation methods of calculating the highest stress values, occurring at the outer edges of the walls, are presented.

Method 1 directly uses the global moment of inertia, I_{global} . This approximation assumes the two vertical parts to fully interact. The calculation is therefore referring a wall which is stronger than the real wall and the results concerning the stresses are suspected to be on the unsafe side. Equation (5.9) shows how I_{global} is calculated.

$$I_{global} = \frac{t \cdot b^3}{12} - \frac{t \cdot c_0^3}{12} \quad (5.9)$$

Method 2 extracts a usable moment of inertia from Equation (5.10) through determining the y_{max} value from Equation (3.34). This new acquired moment of inertia should better represent the shear wall than the I_{global} used in Method 1. Through using Equation (3.34), the wall is treated in a more accurate way compared to Method 1. The properties from the transversal part are also taken into account and the moment of inertia for the transversal, I_t , is considered through the factor α .

$$y_{\max} = K \cdot \frac{W \cdot L_h^4}{8 \cdot E \cdot 2I_v} \Rightarrow \quad (3.34)$$

$$I = \frac{W \cdot L_h^4}{8 \cdot E \cdot y_{\max}} \quad (5.10)$$

$$K = \left[1 - \frac{1}{\mu} - \frac{8}{\mu} \left(\frac{\alpha L_h \sinh(\alpha L_h) - \cosh(\alpha L_h) + 1}{(\alpha L_h)^4 \cosh(\alpha L_h)} - \frac{1}{2(\alpha L_h)^2} \right) \right] \quad (3.35)$$

$$\alpha^2 = \frac{1}{\gamma 2EI_v} = \frac{12I_t}{\Sigma I_v} \left(\frac{b}{c} \right)^3 \frac{\mu}{bL_{\text{sec}}} \quad (3.36)$$

$$\mu = \frac{1}{1 - \frac{2EI_v}{EI}} = 1 + \frac{\Sigma A_v}{A_{v,1} A_{v,2}} \frac{\Sigma I_v}{b^2} \quad (3.37)$$

The c -value in the equation for α^2 is $c = c_0 + h_t$.

5.3.3.2 Results

Figures 5.23, 5.24 and 5.25 show the FE-results. The results from the FE-analyses present the force distribution through the cross section. The stresses are established by dividing the force values with the thickness of the wall, i.e. 0.5 meters. The hand calculations of the three examples which are to be compared are not shown. Method 2 is calculated through using an excel program.

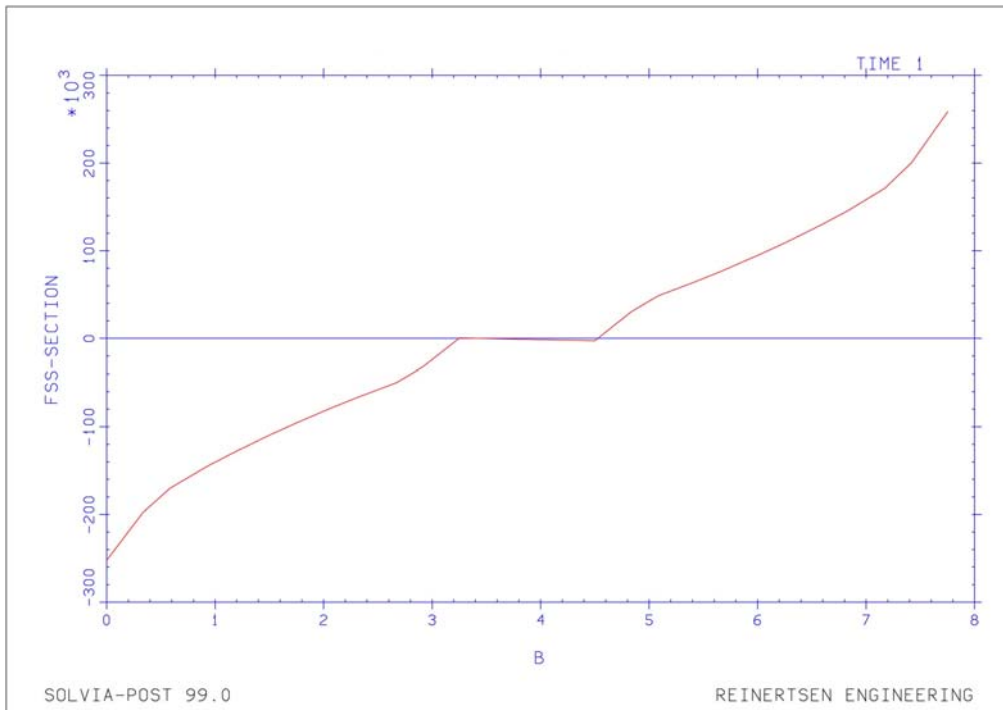
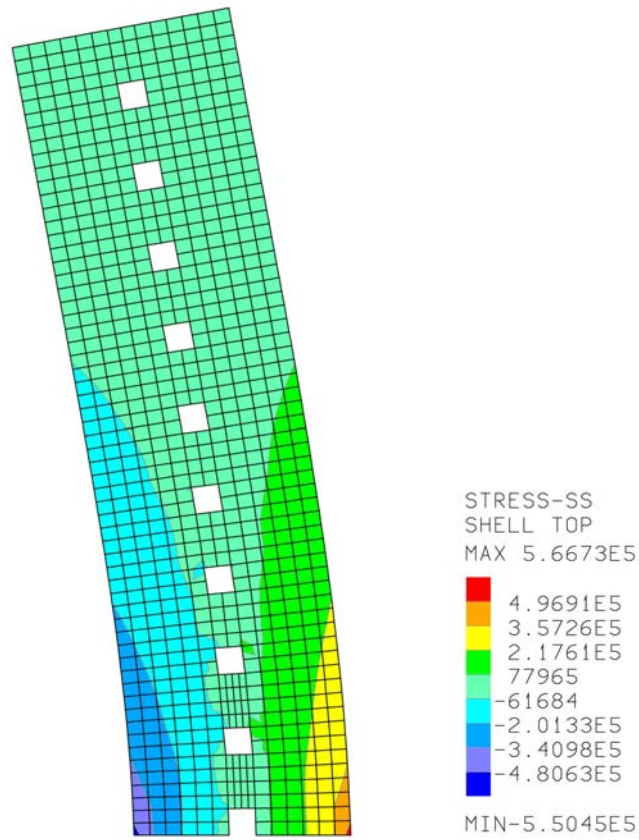


Figure 5.23: Stress and force distribution, Example 1: $c_0 = 1$ m, $h_t = 2$ m.

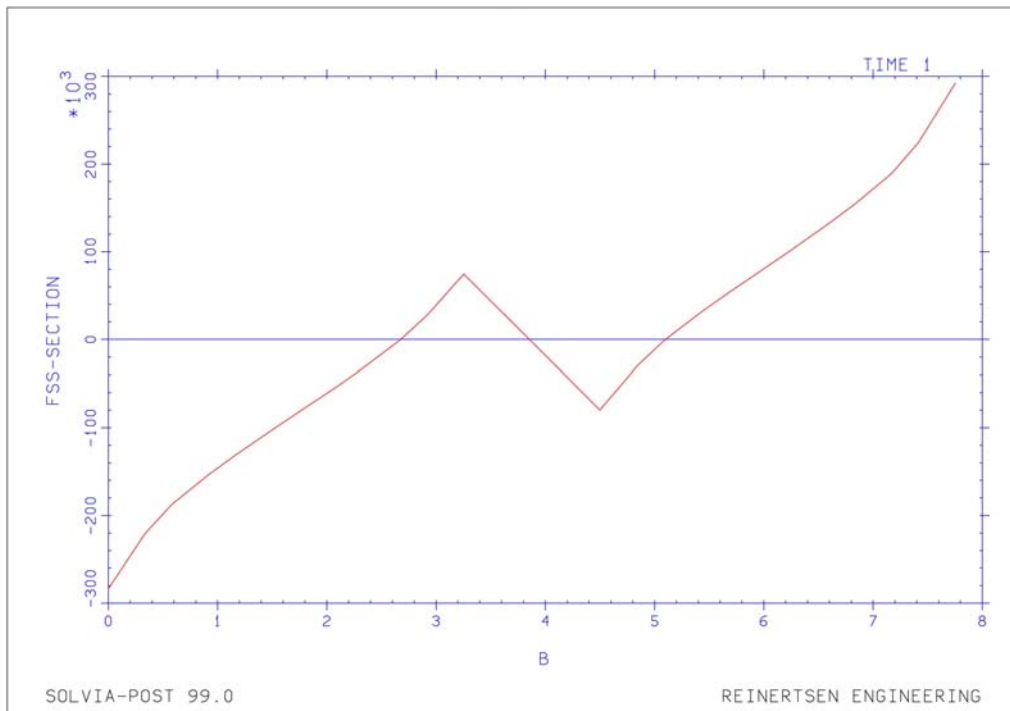


Figure 5.24: Stress and force distribution, Example 2: $c_0 = 1$ m, $h_t = 0.6$ m.

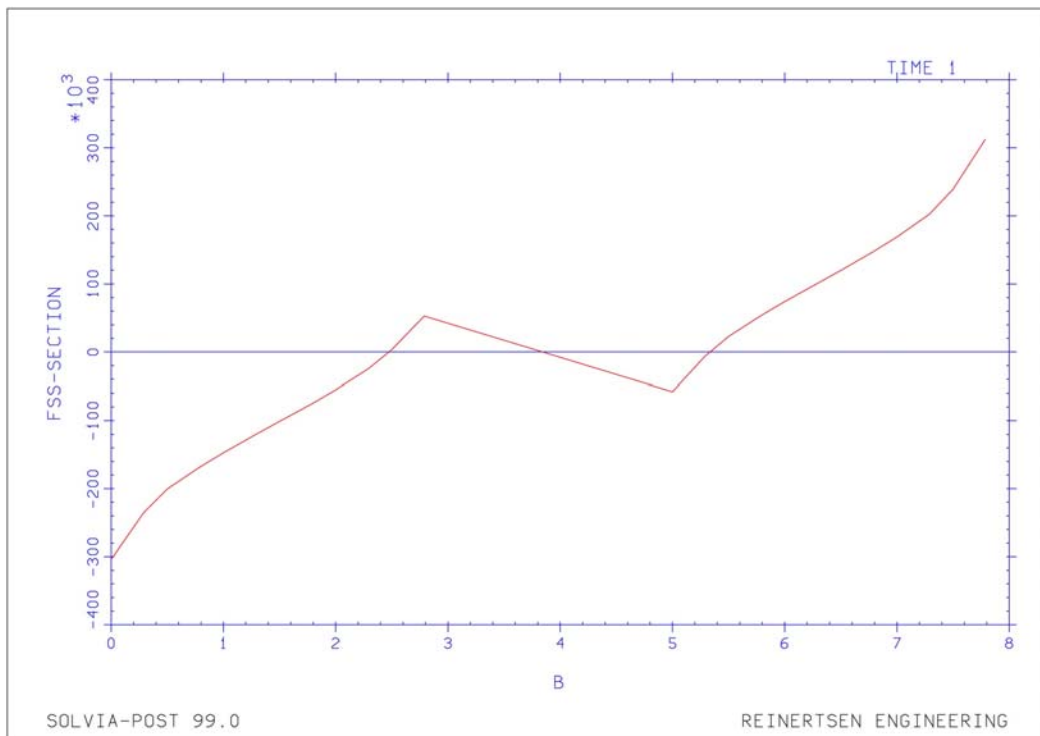
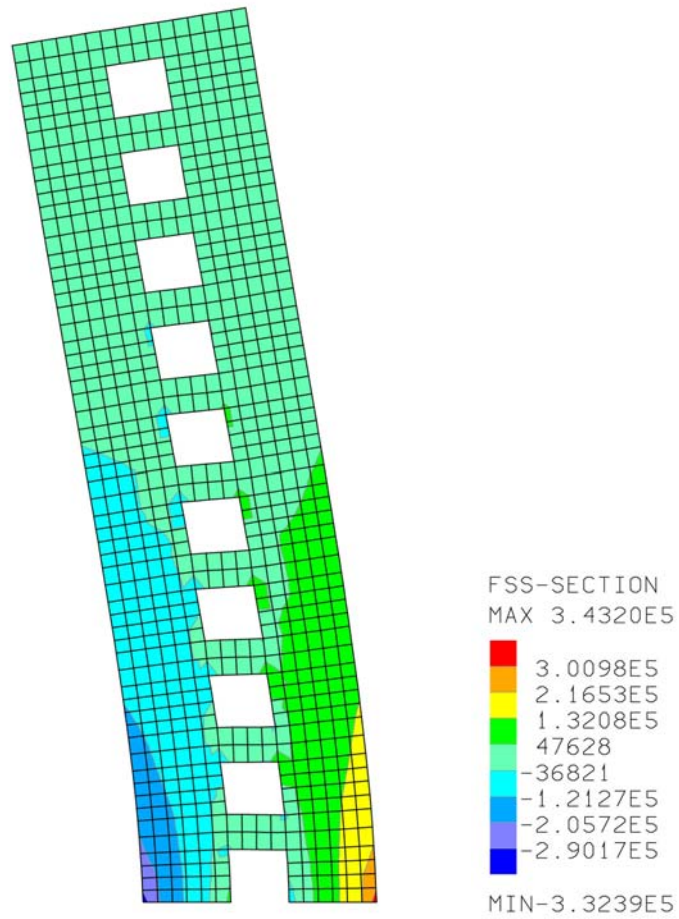


Figure 5.25: Stress and force distribution, Example 3: $c_0 = 2\text{ m}$, $h_t = 1.2\text{ m}$.

Table 5.22: Results of stress analyses.

	FEA [kPa]	Method 1 [kPa]	Method 2 [kPa]
Ex. 1	500	423	492
Ex. 2	560	423	596
Ex. 3	600	428	602

Table 5.22 displays the results of the stress analyses. Example 1 has the smallest holes and Example 3 the largest. Observe that method 1 results are inaccurate and land on the unsafe side of the FE-results. Determining a new moment of inertia, method 2, improves the value greatly. Observe that method 2 gives a result for example 1, which is not on the safe side but very close. Example 2 and 3, which have the larger holes, give a result very near to the FE-result and also on the safe side.

5.3.4 Conclusions and recommendations

Through this study, concerning the buckling loads, it has been learnt that the behaviour of pierced shear walls of different dimensions is not predictable. The hand calculation method that has been investigated and compared with FE-analyses, has shown a wide field of varying inaccuracy. It has been mentioned at the beginning of this section that other effects occur in the FE-analyses which are not taken into account in the hand calculations. It has, from an early stage of this investigation, been predicted that a *general* solution will not be found for obtaining exact values of the critical buckling load covering all different types of pierced walls. Still, this study consists of 30 pierced shear walls holding measurements in a wide field. These analyses are to be used as references when confronting evaluations of other shear walls. One is able to identify the authentic shear wall with some of those investigated, and draw conclusions on how a more accurate calculation of buckling loads can be achieved, see Appendix B.

The first approach for improving the accuracy in this study was through applying a modification factor to the shear buckling load, i.e. shear factors. These factors have served an important role for the after coming investigations, as an indication of how the next step for an improvement shall be approached. These factors, combined with the comparison values achieved through quotients between the FE-results and the hand calculation results, are important indicators for how the hand calculation is to be utilised for evaluating a pierced shear wall.

Through this study it has been decided that the deformable length of the transversal should be equal to the gap width, i.e. $c = c_0$. This improvement has shown buckling load results on the safe side for all walls investigated.

The next improvement concerns the adjustment of the deformable length of the vertical. All models can use a length reduced by the thickness of the transversal, i.e. $L_{sec,red}=L_{sec}-h_t$. This length is only to be interpreted into the equation of the shear angle due to bending deformations of the vertical only, Equation (3.27).

$$\gamma_{v,bend} = \frac{(L_{sec} - h_t)^2}{24EI_v} \quad (5.11)$$

When using the results of this study as a base, the equation above can, for obtaining a better result, be set equal to zero for walls with robust vertical parts.

Concerning the stress distribution in pierced shear walls, it may be concluded that Method 2 is effective when calculating on pierced shear walls. Observe that the method does not represent the real stress distribution in the wall but the method can be used to derive the maximum stresses at the edges of the wall. Method 1 is not recommended because it does not represent the behaviour of a real wall and produces results on the unsafe side.

5.4 Investigation of the polar moment of inertia

In this section an assumption is to be investigated concerning the usage of the *polar moment of inertia*, I_p . The derivation of how I_p replaces the non stabilising units negative contribution is explained in Section 4.2.3.4. The usage of I_p is based upon the assumption of a structure consisting of an infinite amount of evenly distributed non stabilising columns which are subjected to an evenly distributed vertical load from the floor slab. The stabilising units are then assumed to be subjected to horizontal loads only. The method of replacing the effect of hinged columns with I_p is therefore suspected do give accurate results for a surrealistic structure using an endless amount of columns placed with minimal distance between them. In a real building, columns are placed as sparse as possible so that a structure can benefit from its open spaces. It is therefore important for this investigation to ascertain if the method using I_p is suitable for common buildings or not.

The numerical example, from Section 4.2.4, is to be modified with an increasing amount of columns. The example is first modified by replacing the stabilising columns at the four corners with hinged columns, i.e. non stabilising columns. The stabilising columns are then imagined to be placed at the same position as the corner columns, connected to the non stabilising columns for stabilising the structure, but do not connect to the vertical loads from the slab. This is done to simplify the calculation by using the same load distribution among the columns but leaving the stabilising columns free from vertical loads. It will then be clearer how the buckling load will be affected for an almost identical structure. Figure 5.26 can be compared to Figure 5.27, which has 8 shear walls, 4 stabilising in each direction. The non stabilising columns are represented by a circle symbol and the stabilising columns are squared.

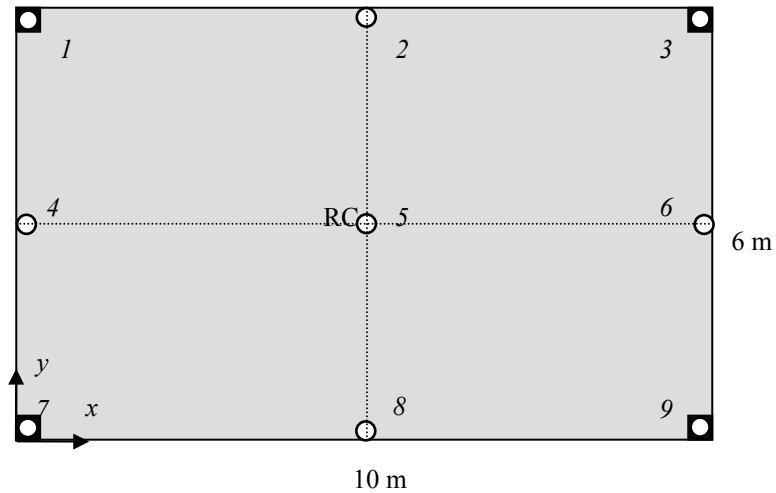


Figure 5.26

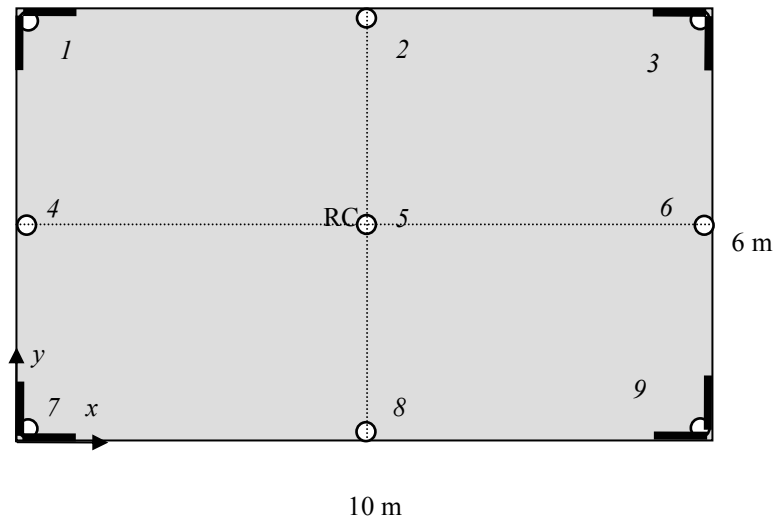


Figure 5.27

The expression for the stabilising columns takes now the same form as shown in Section 4.1.2, for applying the method suited for polar moment of inertia.

$$j_x = j_y = \frac{3EI}{L_h^3} \left(1 - \frac{N}{N_{cr,col}} \right) \Rightarrow j_x = j_y = \frac{3EI}{L_h^3}$$

From the example in Section 4.2.2 the load distribution is producing the stiffness summations shown below. The four added hinged columns at the corners are now taking the same vertical loads which were previously carried on the stabilising columns.

Buckling load through translation:

$$\sum_1^n (j_{i,x}) = \sum_1^n (j_{i,y}) = 0 \Rightarrow$$

$$4 \cdot \frac{3EI}{L_h^3} \left(1 - \frac{N}{N_{cr,col}} \right) - 2 \cdot \frac{2N}{L_h} - 2 \cdot \frac{2N}{L_h} - 1 \cdot \frac{4N}{L_h} = 0 \Rightarrow$$

$$4 \cdot \frac{3EI}{L_h^3} - 2 \cdot \frac{2N}{L_h} - 2 \cdot \frac{2N}{L_h} - 1 \cdot \frac{4N}{L_h} - 4 \cdot \frac{N}{L_h} = 0 \Rightarrow$$

$$\frac{12EI}{L_h^3} - \frac{16N}{L_h} = 0$$

$$N = \frac{12EI}{16L_h^2} = \frac{3EI}{4L_h^2} = \frac{3 \cdot 4 \cdot 10^6}{4 \cdot 5^2} = 120 \text{ kN}$$

$$N_{cr,x} = N_{cr,y} = 2 \cdot 2N + 2 \cdot 2N + 1 \cdot 4N + 4N = 16N = 16 \cdot 120 = 1920 \text{ kN}$$

The buckling load is compared with the value calculated in Section 4.2.4.

Buckling load – translation:

Buckling load from Section 4.2.4: $N_{cr,x,y} = 1824 \text{ kN}$

Buckling load, modified example: $N_{cr,x,y} = 1920 \text{ kN}$

It is suspected that the results should nearly agree because the two structures are almost the same. Still, the results show a slightly higher buckling load concerning translation when the stabilising columns are not subjected to the vertical load.

The buckling load through rotation is now to be compared between the example in Section 4.2.4 and the above modified example.

From the example in Section 4.2.4, the expression is now to be edited to suite the modified example.

$$4 \cdot \left[\frac{3EI}{L_h^3} \left(1 - \frac{N}{N_{cr,col}} \right) \right] (y^2 + x^2) \Rightarrow 4 \cdot \frac{3EI}{L_h^3} (3^2 + 5^2) = \frac{408EI}{L_h^3}$$

Non stabilising columns:

Columns 2 and 8: $2 \cdot \left[-\frac{2N}{L_h} \cdot (y^2 + x^2) \right] = 2 \cdot \left[-\frac{2N}{L_h} \cdot (3^2 + 0) \right] = -\frac{36N}{L_h}$

Columns 4 and 6: $2 \cdot \left[-\frac{2N}{L_h} \cdot (y^2 + x^2) \right] = 2 \cdot \left[-\frac{2N}{L_h} \cdot (0 + 5^2) \right] = -\frac{100N}{L_h}$

$$\text{Column 5 (at the RC)} \quad 1 \cdot \left[-\frac{4N}{L_h} \cdot (y^2 + x^2) \right] = 1 \cdot \left[-\frac{4N}{L_h} \cdot (0 + 0) \right] = 0$$

The hinged columns at the corner are now added.

$$4 \cdot \left[-\frac{N}{L_h} \cdot (y^2 + x^2) \right] = 4 \cdot \left[-\frac{N}{L_h} \cdot (3^2 + 5^2) \right] = -\frac{136N}{L_h}$$

The modified system is now summarised and the buckling load through rotation is calculated.

$$\frac{408EI}{L_h^3} - \frac{36N}{L_h} - \frac{100N}{L_h} - \frac{136N}{L_h} = 0 \quad \Rightarrow \quad \frac{408EI}{L_h^3} - \frac{272N}{L_h} = 0$$

$$N = \frac{408EI}{272 \cdot L_h^2} = \frac{408 \cdot 4 \cdot 10^6}{272 \cdot 5^2} = 240 \text{ kN}$$

$$N_{cr,rot} = 2 \cdot 2N + 2 \cdot 2N + 1 \cdot 4N + 4N = 16N = 16 \cdot 240 = 3840 \text{ kN}$$

The result from the modified example is compared with result from the example in Section 4.2.4.

Buckling load – rotation:

$$\text{Buckling load from Section 4.2.4:} \quad N_{cr,rot} = 3467 \text{ kN}$$

$$\text{Buckling load, modified example:} \quad N_{cr,rot} = 3840 \text{ kN}$$

The results show an increased buckling load for the modified system.

The result from this study reveal that an authentic building, where the stabilising components are subjected to vertical loads but are treated as components which are not subjected to vertical loads, delivers results on the unsafe side. It is then suspected further in this investigation that the method of using the *polar moment of inertia* will provide buckling loads, concerning rotation, with values higher than for a real structure. Residential buildings do not use columns as the dividing walls between apartments will bear all the vertical loads in combination with their stabilising function.

The Example from Section 4.2.4 is now to be approached with the calculation method using the polar moment of inertia. The stabilising components are taking the same expression used in the modified example, i.e. they are not subjected to vertical loads. The polar moment of inertia is only applied when establishing the buckling load through rotation. The calculation concerning translation is therefore not of interest.

Stabilising columns at the corners:

$$4 \cdot \frac{3EI}{L_h^3} (y^2 + x^2) = 4 \cdot \frac{3EI}{L_h^3} (3^2 + 5^2) = \frac{408EI}{L_h^3}$$

The non stabilising columns are now replaced by the expression of I_p . See Section 4.2.3.4 for the derivation.

$$\begin{aligned} \sum (j_{i,x}y^2 + j_{i,y}x^2) &\Rightarrow -\frac{q}{L_h} I_p \Rightarrow \\ -\frac{q}{L_h} \frac{ab(a^2 + b^2)}{12} &\Rightarrow -\frac{N}{L_h} \cdot \frac{(a^2 + b^2)}{12} \end{aligned}$$

The symbols a and b are the length and the breadth of the slab which the vertical load, N , is evenly distributed upon.

$$\sum (j_{i,x}y^2 + j_{i,y}x^2) = 0 \Rightarrow$$

$$\frac{408EI}{L_h^3} - \frac{N}{L_h} \cdot \frac{(a^2 + b^2)}{12} = 0 \Rightarrow$$

$$N_{cr,rot} = \frac{408EI \cdot 12}{L_h^2 \cdot (a^2 + b^2)} = \frac{408 \cdot 4 \cdot 10^6 \cdot 12}{5^2 \cdot (10^2 + 6^2)} = 5760 \text{ kN}$$

The result shows a value of the buckling load through rotation which is much higher than the buckling load calculated with the exact load distribution in the example in Section 4.2.4. If the method of using polar moment of inertia is used for this structure it will produce much smaller second order effects compared to the method used in Section 4.2.4. It follows that the design moment will be lower compared to the real structure and the columns will be under dimensioned, i.e. results on the unsafe side. Table 5.23 below presents a comparison between the critical buckling loads. I_p in the table refers to the method using the polar moment of inertia.

Table 5.23: Comparisons of the critical buckling loads between the methods.

N_{cr}	Exact method Section 4.2.4 [kN]	Modified example [kN]	Mod. / Exact [kN]	I_p [kN]	I_p / Exact [kN]
$N_{cr,y}$	1824	1920	1.05	-	-
$N_{cr,rot}$	3467	3840	1.11	5760	1.66

5.5 Force distribution in single storey structures.

To evaluate if the buckling loads from the hand calculations represent an actual structure, the force and the moment distribution among the stabilising columns are to be compared with FE-analysis. The example shown in Section 4.2.4 is used in three different horizontal load cases. The first load case considers an evenly distributed horizontal load applied at the long facades, with and without vertical loads. This case will cause the building to move only in translation, i.e. in this load case in y direction. The second load case will make the building twist without translation. The horizontal loads are here applied on both sides of the building but at half the length of the long facades, in opposite directions and one case with vertical load and one case without. The first two cases will ascertain if the hand calculation method gives values that agree with the FE-analysis concerning translation and rotation separately. The final load case, case 3, is to investigate how the results turn out when a combination of an uneven translation and rotation of the building occurs. The horizontal load is here applied on half the long façade, with and without vertical loading. The three load cases will also be studied with a combination of an evenly distributed vertical load applied on the slab. The vertical load will contribute to a second order moment on the columns due to the deflection caused by the horizontal loads.

5.5.1 FE-model

The analysis considers three load cases. Three different horizontal load cases combined with and without vertical loads. The three cases without vertical load will establish the first order force and the moment distribution among the four stabilising columns. The horizontal loads are applied as line loads at the long side of the slab which is positioned at the top of the columns. The vertical load is modelled as an evenly distributed pressure load on the slab. When the vertical load is combined with the horizontal load, the force and the moment distribution will have the second order contribution included. This is modelled through FE-analysis by interpreting *large deformation* in the command program in SOLVIA. All load cases can be examined in Appendix C. In the FE-model the four stabilising columns are interpreted as fully fixed at the base with all degrees of freedom locked, and the top ends are interpreted as hinged, i.e. free to rotate but locked in translation. The five non stabilising columns are prevented from moving in all translation directions and around their own axial axis, i.e. only the rotation around x and y direction (plane coordinates) are free to move.

5.5.2 Case 1 – Study of translation

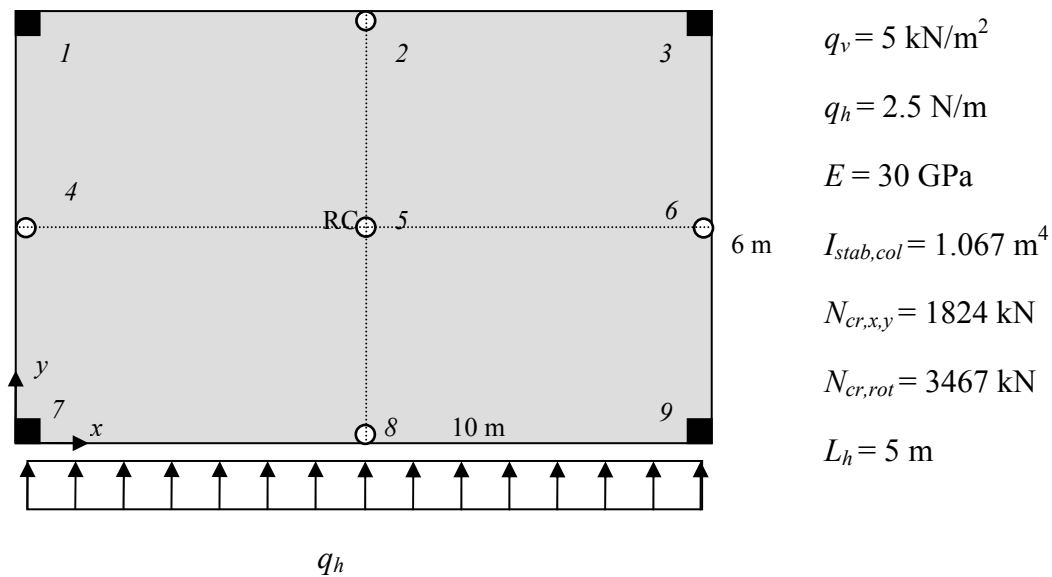


Figure 5.28: Case 1. Translation study

Calculation of the moment at the base of each stabilising column, 1, 3, 7 and 9.

1st order moment.

Horizontal force:

$$H_{tot,y} = 2.5 \cdot 10 = 25 \text{ kN}$$

All columns have equal stiffness and the force is therefore equal divided among them.

$$H_{col,tr,y} = \frac{25}{4} = 6.25 \text{ kN} \Rightarrow M_0 = 6.25 \cdot 5 = 31.25 \text{ kNm}$$

The index $_{col}$ stands for column, $_{tr}$ for translation and $_0$ indicates 1st order.

In this example there is no local moment on the external columns. This study is only for comparing hand calculation with FE-analysis and the horizontal load is therefore applied in the same way as it is in the FE-analysis, i.e. a line load at the top. Observe that indexes, x and y , stand for the *direction*.

2nd order moment.

Vertical force:

$$N = 10 \cdot 6 \cdot 5 = 300 \text{ kN}$$

$$\beta=1 \Rightarrow M_{d,y} = M_0 \cdot \left(\frac{1}{1 - \frac{N}{N_{cr}}} \right) = 31.25 \cdot \left(\frac{1}{1 - \frac{300}{1824}} \right) = 31.25 \cdot 1.197 = 37.41 \text{ kNm}$$

In Table 5.24 the results are compared with the FE analysis performed in SOLVIA.

Table 5.24: Results of case 1 investigation

Case 1	HC	FEA
1 st order moment	31.25	31.31
2 nd order moment included	37.41	37.04

5.5.3 Case 2 – Study of rotation

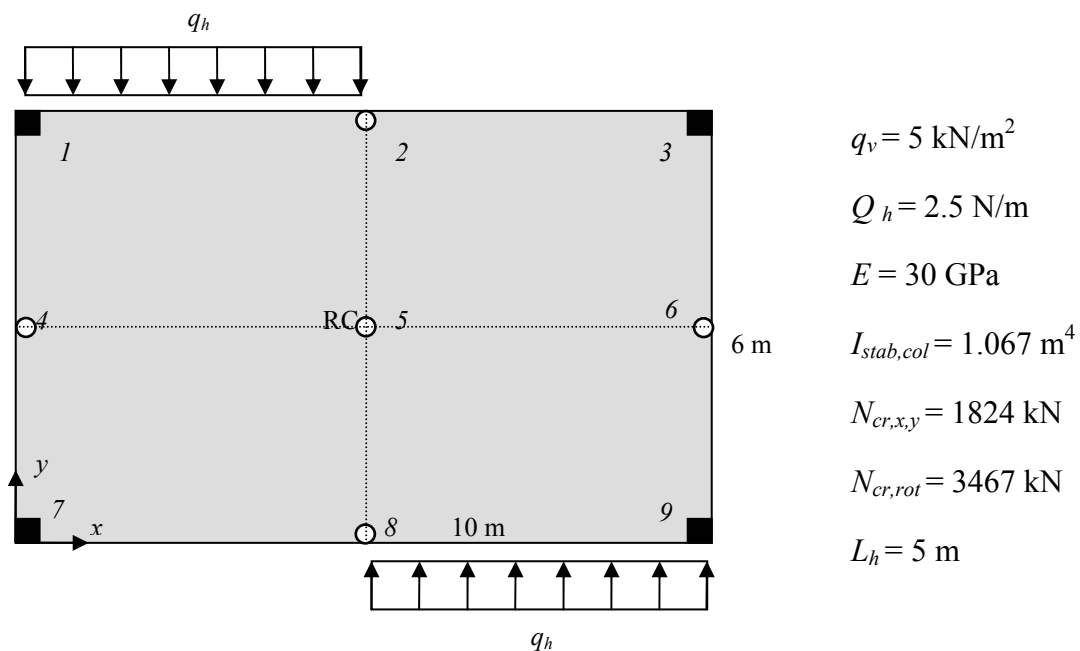


Figure 5.29: Case 2. Rotation study

Moment calculation at the base of each stabilising column; columns 1, 3, 7 and 9:

The system is first transformed by repositioning the force resultants so that they pass through the RC and from the eccentricity thereof, a twisting moment is acquired.

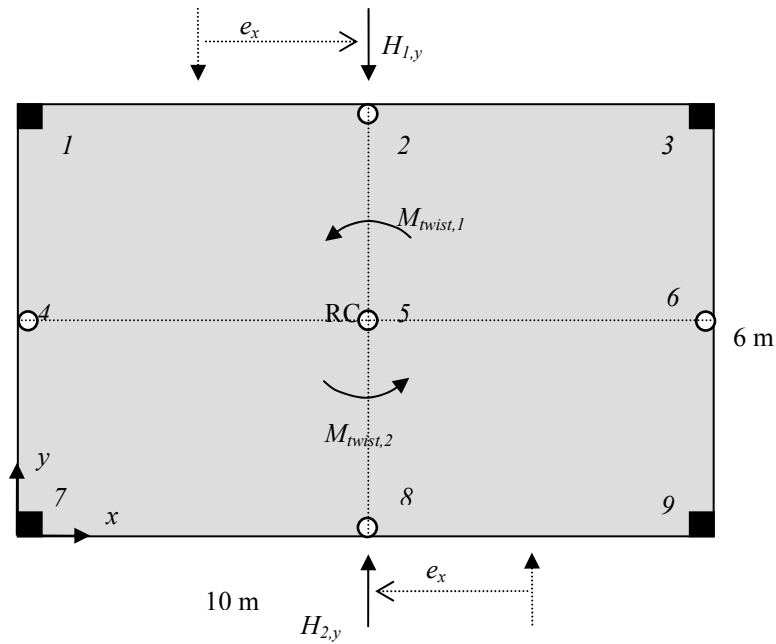


Figure 5.30: Case 2, transformed system.

1st order moment:

Horizontal force:

$$H_{tot,y} = 2.5 \cdot 5 - 2.5 \cdot 5 = 0 \text{ kN} \quad (\text{No translation occurs.})$$

Twisting moment:

$$M_{twist} = M_{twist,1} + M_{twist,2} = H_{1,y} \cdot e_x + H_{2,y} \cdot e_x = 2.5 \cdot 5 \cdot \frac{5}{2} + 2.5 \cdot 5 \cdot \frac{5}{2} = 62.5 \text{ kNm}$$

Force distribution on the stabilising columns due to twisting moment:

The columns are stabilising in both x - and y -directions. The twisting moment will create forces on each stabilising column in both directions. Bending moments will therefore occur in the x - and the y -direction. The columns are situated symmetrically with regards to the rotation centre and they are equally affected.

$$H_{col,twist,y} = M_{twist} \cdot \frac{EI_{col,y} \cdot x}{\sum (EI_{i,y} \cdot x^2 + EI_{i,x} \cdot y^2)} = 62.5 \cdot \frac{4 \cdot 10^6 \cdot 5}{4(4 \cdot 10^6 \cdot 5^2 + 4 \cdot 10^6 \cdot 3^2)} \Rightarrow$$

$$H_{col,twist,y} = 62.5 \cdot \frac{5}{4(5^2 + 3^2)} = 2.30 \text{ kN} \quad H_{col,twist,x} = 62.5 \cdot \frac{3}{4(5^2 + 3^2)} = 1.38 \text{ kN}$$

$$M_{0,y} = 2.30 \cdot 5 = 11.49 \text{ kNm} \quad M_{0,x} = 1.38 \cdot 5 = 6.89 \text{ kNm}$$

2nd order moment:

Vertical force:

$$N_{tot} = 10 \cdot 6 \cdot 5 = 300 \text{ kN}$$

When establishing the total moment there are three critical buckling loads which can be applied.

$$N_{cr,x} = N_{cr,y} = 1824 \text{ kN} \qquad N_{cr,rot} = 3467 \text{ kN}$$

Depending on which buckling mode is used, different values will be obtained for the second order contribution and different design moments will follow. It is preferable to use the lowest critical buckling value to achieve values on the safe side but to get values as close as possible to the real structure; the choice may not be so simple. In this case the building is only subjected to twisting, and translation does not occur. It is then preferable to choose the buckling load which refers to rotation as it reflects the same, or the closest, deflection mode as the horizontal load case generates.

2nd order moment using buckling load from translation:

$$M_{d,col,y} = 11.49 \cdot \left(\frac{1}{1 - \frac{300}{1824}} \right) = 11.49 \cdot 1.197 = 13.75 \text{ kNm}$$

$$M_{d,col,x} = 6.89 \cdot \left(\frac{1}{1 - \frac{300}{1824}} \right) = 6.89 \cdot 1.197 = 8.25 \text{ kNm}$$

2nd order moment using buckling load from rotation:

$$M_{d,col,y} = 11.49 \cdot \left(\frac{1}{1 - \frac{300}{3467}} \right) = 11.49 \cdot 1.095 = 12.58 \text{ kNm}$$

$$M_{d,col,x} = 6.89 \cdot \left(\frac{1}{1 - \frac{300}{3467}} \right) = 6.89 \cdot 1.095 = 7.55 \text{ kNm}$$

In this structure the choice of which buckling mode to use does not present great differences. In other cases the buckling loads may differ very much and the knowledge of the behaviour of the building from different load cases is important for calculating accurate values. Tables 5.25 and 5.26 below present Case 2 results in comparison with FE-analyses.

Table 5.25: Results of Case 2 concerning y-direction.

Case 2- y-direction	HC- $N_{cr,y}$ [kNm]	HC- $N_{cr,rot}$ [kNm]	FEA [kNm]
1 st order moment	11.49	11.49	11.47
2 nd order moment included	13.75	12.58	12.25

Table 5.26: Results of Case 2 concerning x-direction.

Case 2- x-direction	HC- $N_{cr,x}$ [kNm]	HC- $N_{cr,rot}$ [kNm]	FEA [kNm]
1 st order moment	6.89	6.89	6.86
2 nd order moment included	8.25	7.55	7.37

The results from the hand calculation using the buckling load through rotation agree well compared to the FE-analyses. A case where both translation and rotation are involved is considered in the next study, Case 3. It is here to reveal which buckling load that presents results closest to FE-results.

5.5.4 Case 3 – Study of combined translation and rotation

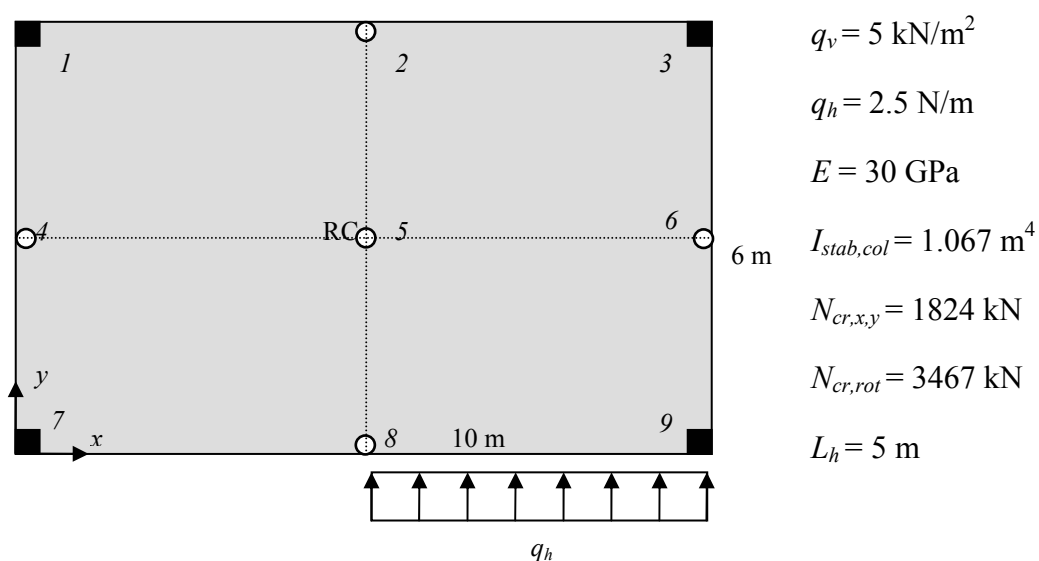


Figure 5.31. Case 3. Study of the combination of translation and rotation

1st order moment.

Horizontal force:

$$H_{tot,y} = 2.5 \cdot 5 = 12.5 \text{ kN}$$

Twisting moment:

$$M_{twist} = H_{tot,y} \cdot e_x = 2.5 \cdot 5 \cdot \frac{5}{2} = 31.25 \text{ kNm}$$

Force distribution on the stabilising columns due to translation:

$$H_{col,tr,y} = \frac{12.5}{4} = 3.125 \text{ kN} \quad (\text{Only in } y\text{-direction})$$

Force distribution on the stabilising columns due to twisting moment:

$$H_{col,twist,y} = M_{twist} \cdot \frac{EI_{col,y} \cdot x}{\sum(EI_{i,y} \cdot x^2 + EI_{i,x} \cdot y^2)} = 31.25 \cdot \frac{4 \cdot 10^6 \cdot 5}{4(4 \cdot 10^6 \cdot 5^2 + 4 \cdot 10^6 \cdot 3^2)} \Rightarrow$$

$$H_{col,twist,y} = 31.25 \cdot \frac{5}{4(5^2 + 3^2)} = 1.15 \text{ kN}$$

$$H_{col,twist,x} = 31.25 \cdot \frac{3}{4(5^2 + 3^2)} = 0.69 \text{ kN}$$

Total moment on each column:

Observe that columns 3 and 9 have forces from translation and rotation in the same direction. Columns 1 and 7 have a force occurring from rotation in the opposite direction than the translation.

$$\text{Column 3 and 9: } M_{0,y} = (3.125 + 1.15) \cdot 5 = 21.38 \text{ kNm}; \quad M_{0,x} = 0.69 \cdot 5 = 3.45 \text{ kNm}$$

$$\text{Column 1 and 7: } M_{0,y} = (3.125 - 1.15) \cdot 5 = 9.88 \text{ kNm}; \quad M_{0,x} = 0.69 \cdot 5 = 3.45 \text{ kNm}$$

2nd order moment:

The total moment will be calculated using critical buckling loads from translation and rotation, in order to make a comparison.

Total moment using buckling load from translation:

Columns 3 and 9.

Columns 1 and 7.

$$M_{d,col,y} = 21.38 \cdot 1.197 = 25.59 \text{ kNm}$$

$$M_{d,col,y} = 9.88 \cdot 1.197 = 11.83 \text{ kNm}$$

$$M_{d,col,x} = 3.45 \cdot 1.197 = 4.13 \text{ kNm}$$

$$M_{d,col,x} = 3.45 \cdot 1.197 = 4.13 \text{ kNm}$$

Total moment using buckling load from rotation:

Columns 3 and 9.

Columns 1 and 7.

$$M_{d,col,y} = 21.38 \cdot 1.095 = 23.41 \text{ kNm}$$

$$M_{d,col,y} = 9.88 \cdot 1.095 = 10.82 \text{ kNm}$$

$$M_{d,col,x} = 3.45 \cdot 1.095 = 3.78 \text{ kNm}$$

$$M_{d,col,x} = 3.45 \cdot 1.095 = 3.78 \text{ kNm}$$

A third alternative is introduced as this load case subjects the structure to both translation and twisting. This third approach is performed by dividing the two load contributions from translation and twisting and taking the 2nd order contribution into account by multiplying each contribution with the magnification factor related to the respectively deflection mode.

Total moment using buckling load from both translation and rotation:

$$\text{Column 3 and 9: } M_{d,col,y} = (3.125 \cdot 1.197 + 1.15 \cdot 1.095) \cdot 5 = 25 \text{ kNm}$$

$$M_{d,col,x} = 0.69 \cdot 1.095 \cdot 5 = 3.78 \text{ kNm}$$

$$\text{Column 1 and 7: } M_{d,col,y} = (3.125 \cdot 1.197 - 1.15 \cdot 1.095) \cdot 5 = 12.4 \text{ kNm};$$

$$M_{d,col,x} = 0.69 \cdot 1.095 \cdot 5 = 3.78 \text{ kNm}$$

Observe that the moment at the base of the columns in x -direction is only due to twisting. The magnification factor used is therefore taken from the buckling load through rotation.

The hand calculations are compared with the FE-analysis and *Table 5.27, 5.28 and 5.29* below presents the results.

Table 5.27: Results case 3, y-direction, columns 3 and 9.

Case 3 y-direction Column 3 and 9	HC- $N_{cr,y}$ [kNm]	HC- $N_{cr,rot}$ [kNm]	HC- $N_{cr,rot,y}$ [kNm]	FEA [kNm]
1 st order moment	21.38	21.38	21.38	21.40
2 nd order moment included	25.59	23.41	25	24.67

Table 5.28: Results of case 3, y-direction, columns 1 and 7.

Case 3 y-direction Column 1 and 7	HC- $N_{cr,y}$ [kNm]	HC- $N_{cr,rot}$ [kNm]	HC- $N_{cr,rot,y}$ [kNm]	FEA [kNm]
1 st order moment	9.88	9.88	9.88	10
2 nd order moment included	11.83	10.82	12.4	12.55

Table 5.29: Results of case 3, x-direction, columns 1, 3, 7 and 9.

Case 3 x-direction Column 1,3,7,9	HC- $N_{cr,y}$ [kNm]	HC- $N_{cr,rot}$ [kNm]	FEA [kNm]
1:st order moment	3.45	3.45	3.45
Total moment	4.13	3.78	3.69

In Appendix C the deformation pictures from the FE-analyses are presented. The last case, case 3, is of special interest as the results in the hand calculation present values on the unsafe side considering the usage of the buckling loads from translation and rotation. The third approach reveals that separating the loads due to translation and twisting and multiplying each contribution with their respective magnification factor, presents results which agree better compared to the FE-results.

Observe that if the assumption that the stabilising columns are not subjected to the vertical load and that the polar moment of inertia is used, then the design moments will be even more on the unsafe side as shown in section 5.4.

The results show small differences between the values, between the hand calculations and the FE-analyses. The study only reveals the problem concerning the different methods and the variations in the values may seem insignificant. It is here to be noticed that the values can differ greatly depending on the structure. In very tall buildings huge differences can arise, and the effects thereof can result in an under dimensioned building.

5.6 Study of the overall stiffness equation

It is not obvious which approach should be used for establishing the buckling load and the force distribution between stabilising components of a building. In Section 4.2.5, an example is presented to show a calculation method for a building stabilised with a combination of shear walls. The method is applicable for separated walls assumed to stabilise in their stiff direction only. Equation (4.24) is used for establishing the overall stiffness for the entire structure, C , which is used to determine the critical buckling load.

$$[\Sigma(B_x) - C] \cdot [\Sigma(B_y) - C] \cdot \left[\Sigma(B_x y^2 + B_y x^2) - C \frac{I_p}{A} \right] = C^2 x_T^2 \cdot [\Sigma(B_x) - C] + C^2 y_T^2 \cdot [\Sigma(B_y) - C] \quad (4.24)$$

Regarding the translation part of the calculation, the method is straight forward but the rotation part is questionable as it contains assumptions in polar moment of inertia. It is described in Section 4.2.3.6 how the variables y and x in Equation (4.24) represent the distance from the actual units rotation centre to the complete structures rotation centre in each direction. The equation is therefore suited for systems with several separate stabilising units.

The following example shows a system of only two stabilising walls. The two walls are each stabilising in different directions. This system is hard to imagine for a real building as it is a bad solution. The example is for educational purposes only, see Figure 5.32.

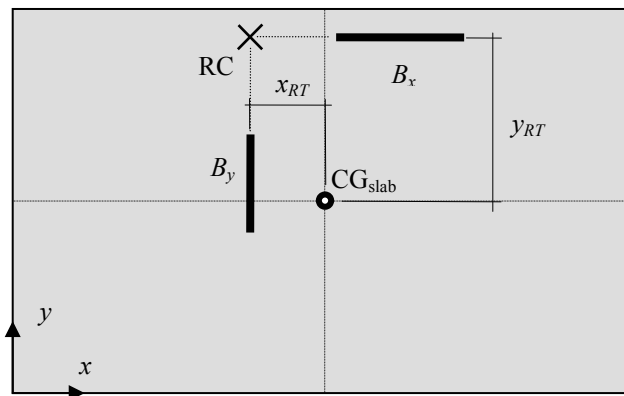


Figure 5.32: Building structure with two stabilising walls.

The rotation capacity is here investigated for explaining why Equation (4.24) is not recommended in all cases. When only *one* unit is stabilising in *each* direction, the rotation centre is located at the intersection of the two walls stiff directions, see Figure 5.32.

$$x_{RT} = \frac{\sum (B_y \cdot x_{RT,unit})}{\sum B_y} \quad y_{RT} = \frac{\sum (B_x \cdot y_{RT,unit})}{\sum B_x} \quad (4.16)$$

If the part concerning rotation in Equation (4.24) is studied for this specific case one can observe that the expression becomes zero and therefore the root concerning buckling through rotation also becomes zero.

$$\left[\Sigma(B_x y^2 + B_y x^2) - C \frac{I_p}{A} \right] \Rightarrow \left[(B_x \cdot 0^2 + B_y \cdot 0^2) - C \frac{I_p}{A} \right] \Rightarrow C = 0$$

For similar cases, when using the general formula, Equation (4.25), one of the three roots equals zero. In general terms, the answer tells us that no buckling will occur through rotation. The expression delivers values for buckling through translation only. It is obvious that this system has a very low rotation capacity and through the assumption that the walls only stabilise in their stiff direction, the rotation capacity becomes zero. Still, the walls do actually provide a rotation capacity. The problem becomes clearer if we let the two walls be connected as one coupled unit working together, i.e. an L-shaped unit. In this case the location of the rotation centre of the L-shaped unit also represents the RC of the whole structure and the coordinates for the RC are the same as in Figure 5.32, see Figure 5.33.

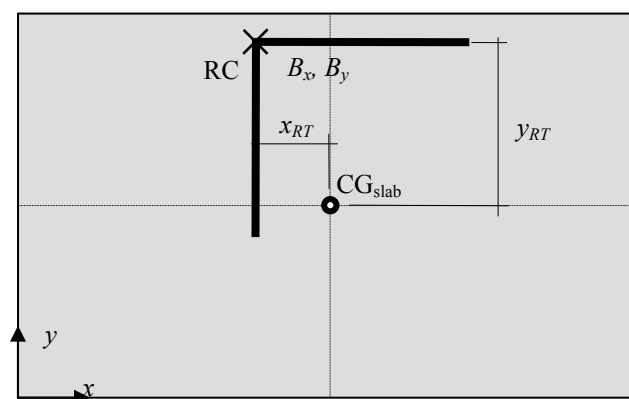


Figure 5.33: L-shaped stabilising component.

Due to interaction between the two stabilising parts, this coupled structure has a significantly higher stiffness for stabilising in x - and y -direction and the rotational stiffness is also greater. Still, the problem with the applied method remains.

$$\left[\Sigma(B_x y^2 + B_y x^2) - C \frac{I_p}{A} \right] \Rightarrow \left[(B_x \cdot 0^2 + B_y \cdot 0^2) - C \frac{I_p}{A} \right] \Rightarrow C = 0$$

This last case studied reveals that the usage of the method applied can deliver results that do not represent the real structure. It has been observed that the method does not take into account the components internal rotational stiffness. This approximation can in some cases lead to misjudgement of the structural behaviour and the predicted response of the structure may greatly disagree with the response of the real building.

5.6.1 Coupled and uncoupled approach

In the pretence of establishing buckling loads, and finally design moments, it is of vital importance to approach the structure in a suitable way. To clarify the effects of the choice made for approaching a structure at an early stage in the calculation process, a numerical example is presented.

The two cases described below are to be compared regarding the buckling load. Both models have the exact same measurements. In Case 1 the stabilising elements are considered as a coupled component, i.e. the three walls are unified and act together for stabilising the building. The U-shaped element is positioned so that its CG coincides with the floor slab's CG. Case 2 approaches the problem through assuming that the three walls are separate.

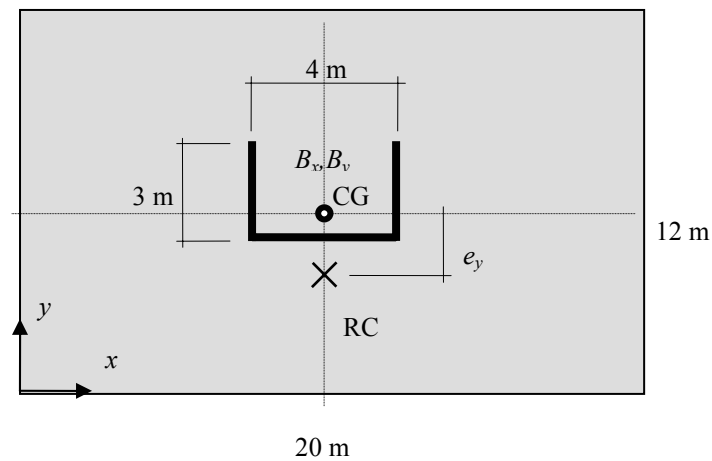


Figure 5.34: Case 1, coupled walls.

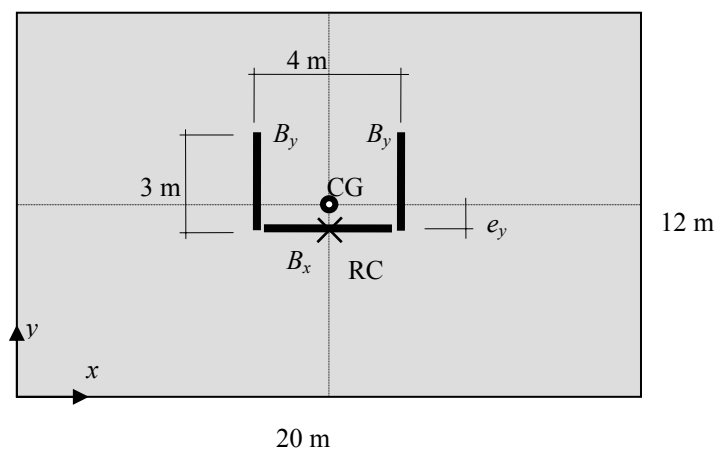


Figure 5.35: Case 2, uncoupled walls.

Both models assume that vertical forces are taken by non stabilising columns evenly distributed between the slabs (not visible in the figures). The stabilising component(s) take horizontal forces only. The models represent a 10 storey building which has the same stiffness at each storey and has an evenly distributed horizontal load applied through the building. All the walls are solid and have a thickness of 0.2 m and the total height of the building is 30 m.

This example will clarify the effect of the two different approaches. Case 1 is first calculated and the second case thereafter.

5.6.2 Case 1 - Coupled approach

Concerning the U-shaped cross section, the equations for calculating the moment of inertia, CG and RC for a U-shape are found in Appendix E. [Samuelsson and Wiberg (1993)].

Centre of gravity of u-section, c :

$$c = b \frac{ht_h + bt_b}{ht_h + 2bt_b} = 3 \frac{4 \cdot 0.2 + 3 \cdot 0.2}{4 \cdot 0.2 + 2 \cdot 3 \cdot 0.2} = 2.1 \text{ m}$$

Rotation centre:

$$RC = \frac{3b^2 \cdot t_b}{6bt_b + ht_h} = \frac{3 \cdot 3^2 \cdot 0.2}{6 \cdot 3 \cdot 0.2 + 4 \cdot 0.2} = 1.23 \text{ m} \Rightarrow y_T \approx 2.2 \text{ m} \quad (x_T = 0)$$

Moment of inertia:

$$I_y = \frac{t_b \cdot b^3}{6} 2t_b \cdot b \left(c - \frac{b}{2} \right)^2 + t_h \cdot h(b - c)^2$$

$$I_y = \frac{0.2 \cdot 3^3}{6} + 2 \cdot 0.2 \cdot 3 \left(2.1 - \frac{3}{2} \right)^2 + 0.2 \cdot 4(3 - 2.1)^2 = 1.98 \text{ m}^4 \quad (\text{weak direction})$$

$$I_x = \frac{t_h \cdot h^3}{12} + \frac{1}{2} t_b \cdot bh^2 = \frac{0.2 \cdot 4^3}{12} + \frac{1}{2} \cdot 0.2 \cdot 3 \cdot 4^2 = 5.87 \text{ m}^4 \quad (\text{strong direction})$$

Stiffness:

$$EI_y = 30 \cdot 10^9 \cdot 1.98 = 5.94 \cdot 10^{10} \text{ m}^2 \quad EI_x = 30 \cdot 10^9 \cdot 5.87 = 17.6 \cdot 10^{10} \text{ m}^2$$

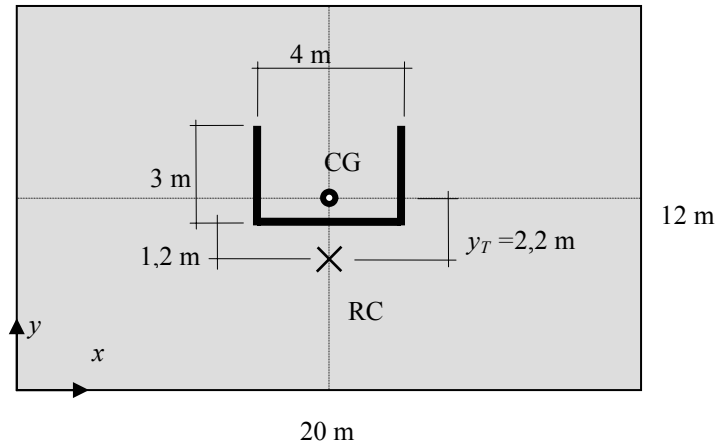


Figure 5.36: Case 1- Coupled walls.

Calculation of stiffness due to influence of shear:

Buckling load (*primary*): Equations (3.11) and (3.38)

Shear:

$$y\text{-direction} : N_{cr,S,y} = GA_y = 0.4 \cdot 30 \cdot 10^9 \cdot 2 \cdot 3 \cdot 0.2 = 14400 \text{ MN}$$

$$x\text{-direction} : N_{cr,S,x} = GA_x = 0.4 \cdot 30 \cdot 10^9 \cdot 4 \cdot 0.2 = 9600 \text{ MN}$$

Bending : 10 storeys $\Rightarrow k_V = 6.8$; from Figure 3.13.

$$y\text{-direction} : N_{cr,B,y} = k_V \frac{EI_y}{L_h^2} = 6.8 \frac{5.94 \cdot 10^{10}}{30^2} = 448.8 \text{ MN}$$

$$x\text{-direction} : N_{cr,B,x} = k_V \frac{EI_x}{L_h^2} = 6.8 \frac{1.76 \cdot 10^{11}}{30^2} = 1329.8 \text{ MN}$$

Observe that shear deformation has a greater influence in the x -direction due to a high buckling load in bending and a low buckling load in shear.

Total buckling load (*primary*): Equation (3.19)

$$N_{cr,tot} = \frac{1}{\frac{1}{N_{cr,B}} + \frac{1}{N_{cr,S}}}$$

$$\text{y-direction: } N_{cr,tot,y} = \frac{1}{\frac{1}{448.8} + \frac{1}{14400}} = 435.2 \text{ MN}$$

$$\text{x-direction: } N_{cr,tot,x} = \frac{1}{\frac{1}{1329.8} + \frac{1}{9600}} = 1168 \text{ MN}$$

Establishing of B_x and B_y : Equation (4.15)

$$\text{y-direction: } B_y = \frac{N_{cr,tot,y}}{N_{cr,B,y}} EI_y = \frac{435.2}{448.8} \cdot 5.94 \cdot 10^{10} = 5.76 \cdot 10^{10} \text{ m}^2$$

$$\text{x-direction: } B_x = \frac{N_{cr,tot,x}}{N_{cr,B,x}} EI_x = \frac{1168}{1329.8} \cdot 1.76 \cdot 10^{11} = 1.55 \cdot 10^{11} \text{ m}^2$$

Polar moment of inertia, I_p : Equations (4.20), (4.22) and (4.23)

$$I_p = I_x + I_y$$

$$I_y = \frac{L_x \cdot L_y^3}{12} + A_{slab} \cdot y_T^2 = \frac{20 \cdot 12^3}{12} + 240 \cdot 2.2^2 = 4074 \text{ m}^4$$

$$I_x = \frac{L_y \cdot L_x^3}{12} + A_{slab} \cdot x_T^2 = \frac{12 \cdot 20^3}{12} + 240 \cdot 0 = 8000 \text{ m}^4$$

$$I_p = 4074 + 8000 = 12074 \text{ m}^4$$

Area of floor slab: $A_{slab} = 12 \cdot 20 = 240 \text{ m}^2$

In this case the RC only dislocates in one direction from CG, $y_T \neq 0$, $x_T = 0$. Equation (4.30) can therefore be used, see Section 4.2.3.6.

$$\left[\Sigma(B_y) - C \right] \cdot \left(\left[\Sigma(B_x) - C \right] \cdot \left[\Sigma(B_x y^2 + B_y x^2) - C \frac{I_p}{A} \right] - C^2 y_T^2 \right) = 0$$

The stiffness values are inserted into the equation above and the overall stiffness, C , is solved by a calculator or a computer program. The expression will deliver three roots, i.e. three different overall stiffness values, two values for translation and one for rotation. In this case this method fails, as it will only present two roots representing translation capacities. The rotation stiffness is presented as a trivial root $C = 0$.

$$C_1 = 5.76 \cdot 10^{10} \text{ m}^2 \quad C_2 = 17.2 \cdot 10^{10} \text{ m}^2 \quad C_3 = 0 \text{ m}^2$$

It is possible to identify in which direction the three roots belong. The first root C_1 represents the y -direction, while C_2 represents the x -direction. Observe that the value C_2 for the x -direction is greater than the stiffness $\Sigma(B_x)$ is. This is an effect of the dislocation of the RC from the centre of gravity in the y -direction.

The result delivers only two critical buckling loads using Equation (4.24)

$$N_{cr,x} = 6.8 \frac{17.2 \cdot 10^{10}}{30^2} = 1300 \text{ MN} \quad N_{cr,y} = 6.8 \frac{5.76 \cdot 10^{10}}{30^2} = 435 \text{ MN}$$

5.6.3 Case 2 – Uncoupled approach

When the three walls are treated as uncoupled there is no interaction between the three walls. Instead the walls will now only stabilise in their stiff directions.

$$\text{Walls in } y\text{-direction: } I_y = \frac{0.2 \cdot 3^3}{12} = 0.45 \text{ m}^4 \quad \Rightarrow \quad \Sigma(EI)_y = 2.7 \cdot 10^{10} \text{ m}^2$$

$$\text{Wall in } x\text{-direction: } I_x = \frac{0.2 \cdot 4^3}{12} = 1.067 \text{ m}^4 \quad \Rightarrow \quad \Sigma(EI)_x = 3.2 \cdot 10^{10} \text{ m}^2$$

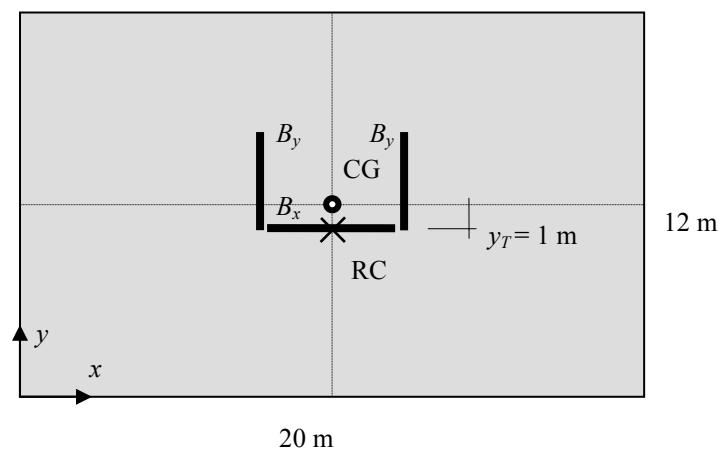


Figure 5.37: Case 2.

Due to symmetry, the RC only dislocates in y -direction affected only by the location of the wall stabilising in x -direction.

$$x_T = 0 \text{ m} \quad y_T = 1 \text{ m}$$

The following calculations of the stiffnesses with influence of shear, are not shown here as the method is an analogy of Case 1.

y -direction :

$$N_{cr,B,y} = 204 \text{ MN} \quad N_{cr,S,y} = 14400 \text{ MN} \quad \Rightarrow \quad N_{cr,tot,y} = 201 \text{ MN}$$

x -direction :

$$N_{cr,B,x} = 242 \text{ MN} \quad N_{cr,S,y} = 9600 \text{ MN} \quad \Rightarrow \quad N_{cr,tot,x} = 236 \text{ MN}$$

$$\Sigma B_y = 26.6 \cdot 10^9 \text{ m}^2 \quad \Sigma B_x = 31.2 \cdot 10^9 \text{ m}^2$$

Equation (4.24) is used with the newly acquired stiffness values. In this case three roots are calculated.

$$C_1 = 2.11 \cdot 10^9 \text{ m}^2 \quad C_2 = 26.6 \cdot 10^9 \text{ m}^2 \quad C_3 = 31.9 \cdot 10^9 \text{ m}^2$$

The three roots in this case have easily identifiable directions for each root. The experience gained through the previously calculated examples described in Section 5.5.1 reveals that the stiffness in y -direction is not influenced due to asymmetry in y -direction only. C_2 is therefore referring to the overall stiffness in y -direction. It is also obvious that C_3 is referring to the x -direction and the obtained value is in this case slightly higher than $\Sigma(B_x)$. The dislocation of the rotation centre in y -direction is actually a benefit for the capacity in x -direction. In this case the floor slab is not big enough for creating a great value of the polar moment of inertia and therefore the stiffness in the x -direction receives a slightly higher value. Due to the short distance to the RC, the two walls stabilising in y -direction derive a low resistance for rotation. Only one wall is stabilising in the x -direction and is not contributing to resist rotation. In Case 2, all three roots exist and the critical buckling loads can be established for both translation and rotation by using Equation (4.24).

$$N_{cr,y} = 6.8 \frac{26.6 \cdot 10^9}{30^2} = 201 \text{ MN}$$

$$N_{cr,x} = 6.8 \frac{31.9 \cdot 10^9}{30^2} = 241 \text{ MN}$$

$$N_{cr,rot} = 6.8 \frac{2.11 \cdot 10^9}{30^2} = 16 \text{ MN}$$

5.6.4 Conclusions

Comparing the two cases it is obvious that the two different approaches provide different critical buckling loads. If this example was an authentic building the cross section would probably be calculated as a coupled unit as in Case 1. This example reveals a great difference between the two different approaches. In a real building, consisting of several stabilising walls bonded together, it is not obvious which method should be chosen. Also, it has to be considered if it is possible to build the stabilising units according to the chosen approach. It is not always possible to achieve a full interaction between the components. Parts of the stabilising structure may have to be treated as uncoupled walls not acting together, while with other components it may be possible to design them assuming full interaction.

5.7 Force distribution in a multi storey structure

In Section 5.5 a study of the force distribution in a single storey structure is undertaken and the results from the FE-analyses and the hand calculation are compared. In this investigation the force distribution in a multi storey building is to be analysed. The differences between a single storey and a multi storey structure, concerning the hand calculations, are that the effects from all the assumptions made are greater due to there being more structural parts. The effects of the assumptions regarding the stiffness of the floor slabs are in this study influenced by ten floor slabs instead of one slab compared to the single store structure. It is suspected in this study that the stiffnesses of the slabs, in combination with the distances between the stabilising units, have a significant effect on the force distribution in the stabilising walls. The twisting effect from walls positioned close to the rotation centre is also suspected to influence the force distribution and the behaviour of the structure.

5.7.1 Modelling

This investigation consider two simple structures (indexed a and b) consisting of four stabilising walls. Each structure is to be investigated for two load cases (indexed 1 and 2), see Table 5.30 and Figure 5.38.

Table 5.30: Investigated cases.

Case	Wall situation	Load case
1a	Walls at the extremities	Translation
1b	Walls close to RC	Translation
2a	Walls at the extremities	Twisting
2b	Walls close to RC	Twisting

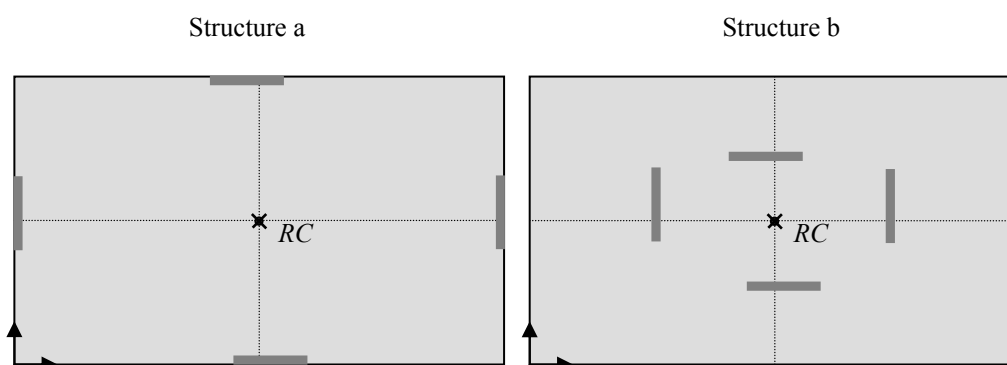


Figure 5.38: Structure a and b illustrated.

The four walls are all 3 m wide and have a thickness of 0.2 m. The Young's modulus is set to 15 GPa for the walls. The building is 40 meters high consisting of 10 storeys with a storey height of 4 m. Each storey is subjected to a distributed horizontal load, applied as a line load at the long side of the slabs, of 3 kN/m

Each case is to be studied by using two different stiffnesses of the floor slabs in the FE-analyses. The FE-model using stiff floor slabs refers to slabs with a Young's modulus of 30 GPa and they are 0.3 m thick. The second FE-model has a reduced thickness of 0.1 m and a lowered Young's modulus of 1 GPa. It is to be investigated here how the force distribution is affected by a reduced stiffness of the floor slabs. The interaction between the walls is suspected to be weaker in the case where the slabs are modelled with a lower stiffness. The study is done to reveal how the reduced stiffness of the slabs will affect the load distribution between the four walls. A hand calculation is also made to compare the stress results. Observe that in the hand calculation it is assumed that the slabs are not stiff *out of their plane* but stiff *in their plane*.

The complete results from the FE-analyses are presented in Appendix D.

The forces distributions in the four stabilising walls are presented by graphs describing the force distribution over the cross section. To calculate the stresses in each wall, the force values are divided with the thickness of the wall.

5.7.2 Study of translation

In the FE-analyses, concerning a translation load case, where stabilising walls are placed close to each other and the floor slabs are modelled as being rigid, the position of the walls, in the applied load direction, play a significant role for the load distribution. In the hand calculations the floor slabs are always considered to be stiff *in their plane* but not stiff *out of their plane*. With these assumptions it is possible to use the hand calculation method concerning force distribution explained in Section 4.3. The method seems to be a good approximation and the forces subjecting each stabilising wall are divided according to the walls specific stiffness. In the FE-models, used in this study, the slabs and the stabilising walls are assumed to be fully connected. If the floor slabs are interpreted to be rigid, a strong interaction between the stabilising walls will create a completely different structure compared to the envisaged hand calculation structure.

If the floor slabs are assumed to be rigid, the two cases shown in Figure 5.38 will have stress distributions that differ greatly. Concerning the case to the left in Figure 5.38, the stabilising units will have stress distributions that will agree well with the hand calculations as the centres of gravity of the walls are aligned. The case to the right, having the outer walls repositioned, is not comparable with the hand calculations. With a rigid floor slab, i.e. stiff out of plane, the three stabilising units will behave as one united cross section interacting together. The outer walls are in this case placed completely in the compression zone and the U-shaped cross section in the tensioned side (almost completely), see Figure 5.39. The interaction between the stabilising units, which occurs when the floor slabs are assumed to be rigid, is not taken into account in the hand calculation method and the results from the methods will not agree.

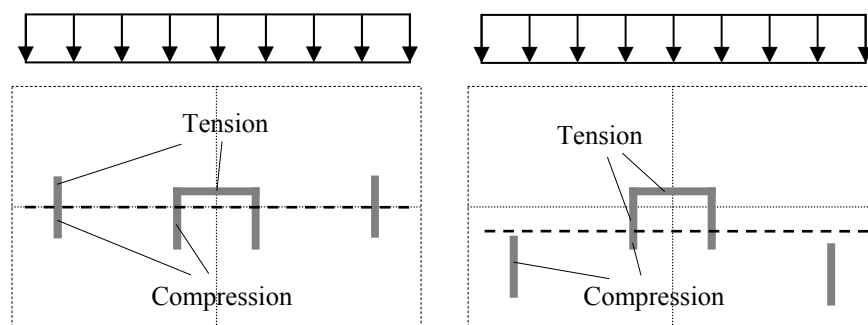


Figure 5.39: Illustration of different stress distributions in the stabilising units due to their positioning in a translation load case.

5.7.2.1 Case 1a - Walls at the extremities

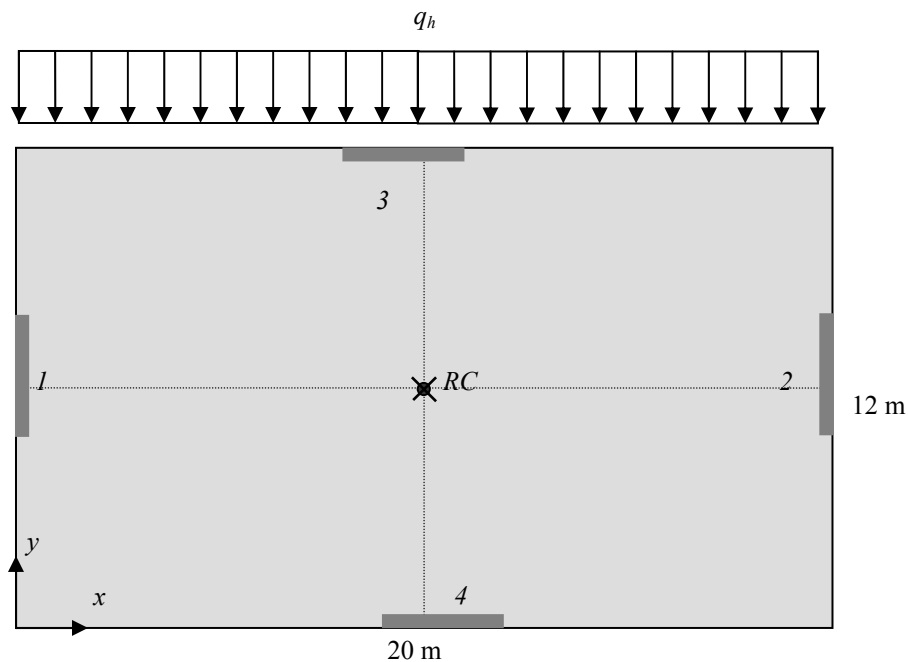


Figure 5.40: Translation load case, Case 1a.

Hand calculation:

Influence from shear deformation in the walls is here neglected as it hardly affects the stiffness due to the walls being slender.

The four walls have the same stiffness:

$$I_y = I_x = \frac{0.2 \cdot 3^3}{12} = 0.45 \text{ m}^4$$

$$B_x = B_y = 15 \cdot 10^9 \cdot 0.45 = 0.675 \cdot 10^{10} \text{ Nm}^2$$

Forces subjecting walls 1 and 2:

The distributed load, $q_h = 3 \text{ kN/m}$, is applied at the long side of the ten floor slabs.

$$H_{tot,y} = 3 \cdot 20 \cdot 10 = 600 \text{ kN}$$

It is here assumed that the forces are only taken by the walls stabilising in y direction.

$$H_{1,y} = H_{2,y} = 300 \text{ kN}$$

Bending moment at the base:

The distributed horizontal load applied at each storey has a load resultant at 22 m above the ground.

$$M_{0,1,y} = 300 \cdot 22 = 6600 \text{ kNm}$$

Maximum stresses at the edges of the wall:

Linear material response is assumed.

$$\sigma_{0,1,y} = \frac{6600 \cdot 10^3}{0.45} \cdot 1.5 = 22 \text{ MPa}$$

The stresses are compared with the results from the two models from the FE-analyses. Walls 3 and 4 do not have a linear stress distribution because the walls are acting like flanges. Wall 3 has tensile stresses while wall 4 has compressive stresses. The values presented for walls 1 and 2 are the highest stresses at the edges of the walls while the values for walls 3 and 4 represent the mean stresses in each wall. The deflection modes and the force distributions are presented in Appendix D.

Table 5.31: Case 1a – Translation load case. Maximum stresses compared between the models. The values from walls 3 and 4 in the FE-analyses refer to a mean value.

Wall	HC [MPa]	FEA $E = 30 \text{ GPa } t = 0.3 \text{ m}$ [MPa]	FEA $E = 1 \text{ GPa } t = 0.1 \text{ m}$ [MPa]
1	±22	±9.25	±21
2	±22	±9.25	±21
3	0	1.03	0.013
4	0	-1.01	-0.014

As the walls are positioned far from each other the interaction between the four walls is greatly influenced by the stiffness of the floor slabs (stiffness out of plane). Walls 3 and 4 can be seen as cross sections acting as flanges and their contribution for stabilisation is in this case depending on the stiffness of the slabs. Walls 1 and 2 in the FE-model, using weak slabs, obtain values that agree well with the hand calculations.

The same load case is now investigated with the walls positioned closer to each other. It is suspected that the interaction between the four walls is much stronger in this case due to the closeness of the walls. The force distribution established from the hand calculation is the same as presented in Case 1a.

5.7.2.2 Case 1b - Walls close to RC

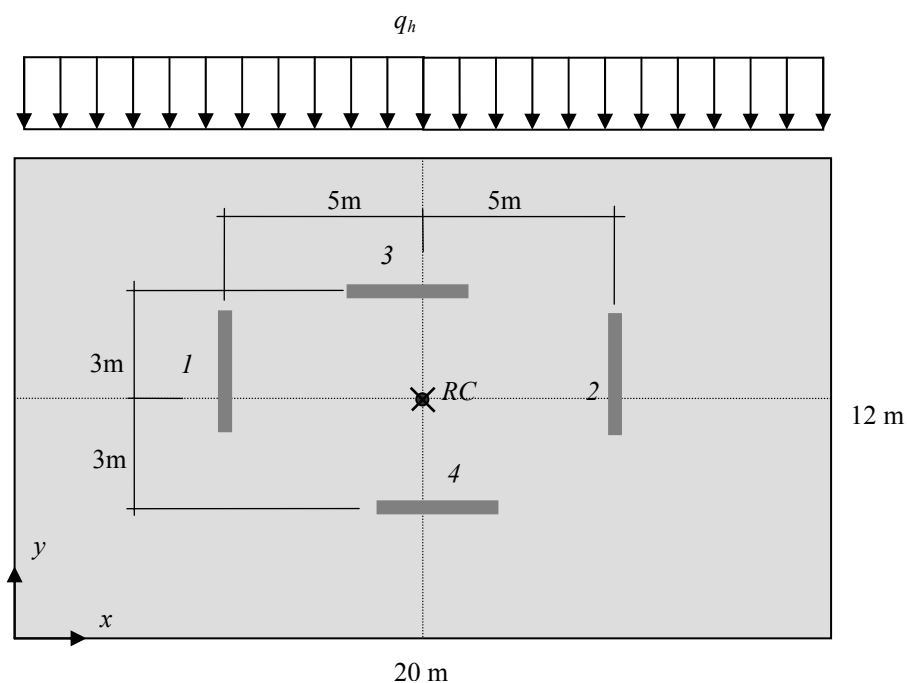


Figure 5.41: Translation load case with walls close to RC, Case 1b.

Table 5.31 presents the results concerning Case 1b.

Table 5.32: Case 1b – Translation load case. Maximum stresses compared between the models. The values from walls 3 and 4 in the FE-analyses refer to a mean value.

Wall	HC [MPa]	FEA $E = 30 \text{ GPa } t = 0.3 \text{ m}$ [MPa]	FEA $E = 1 \text{ GPa } t = 0.1 \text{ m}$ [MPa]
1	± 22	± 7	± 20
2	± 22	± 7	± 20
3	0	2.56	0.05
4	0	-2.36	-0.05

The results from FE-analyses show that a strong interaction occurs between the four stabilising walls. The FE model using the weaker slab presents a weaker cooperation between the walls. The stresses that occur in walls 3 and 4, concerning the FE-model using the stiffer floor slabs, seem to be small compared to walls 1 and 2, but the stabilising contribution is actually greater in walls 3 and 4 compared to walls 1 and 2.

To estimate the influence from walls 3 and 4, a mean value is taken from the two graphs presenting the force distribution of walls 3 and 4 in Appendix D.1.

The mean value is estimated at 500 kN/m acting along the breadth of the wall, i.e. 3 m. The walls 3 and 4 are placed 3 m from the CG of the four walls. The CG of the four walls is coinciding with the CG of the slab due to symmetry.

The total force in walls 3 and 4: $500 \cdot 3 = 1500$ kN.

Moment taken by walls 3 and 4: $2 \cdot 1500 \cdot 3 = 9000$ kNm

Total moment from the applied load: $M_{0,tot} = (3 \cdot 20 \cdot 10) \cdot 22 = 13200$ kNm

With this rough estimation it is obvious that walls 3 and 4, which are acting like flanges, contribute with over 2/3 of the total moment and significantly influence the force distribution. This effect is not assumed to occur for the hand calculation and the values are therefore hard to compare between the methods.

If the contribution from walls 3 and 4 is reduced from the total applied moment the remaining moment is taken by walls 1 and 2.

$$M_{0,1} = M_{0,2} = \frac{13200 - 9000}{2} = 2100 \text{ kNm}$$

Walls 1 and 2 are now subjected with the remaining moment and a new maximum stress value is calculated assuming linear stress distribution through the wall.

$$\sigma_{0,1} = \sigma_{0,2} = \frac{2100 \cdot 10^3}{0.45} \cdot 1.5 = \pm 7 \text{ MPa}$$

If this value is compared with the stresses from the FE-analysis in Table 5.31, it is seen that the results agree. Tables 5.33 and 5.34 below presents a comparison of the moments of each wall showing the contribution each wall gives to the total moment. The total applied moment is the same for the two cases, Case 1a and 1b, i.e. $M_0 = 13200$ kNm.

Table 5.33: Comparison of the moment contribution of the four walls, Case 1a.

Wall	HC [kNm]	HC M_{wall} / M_0	FEA $E = 30 \text{ GPa}$ $t = 0.3 \text{ m}$ [kNm]	FEA $E = 30 \text{ GPa}$ $t = 0.3 \text{ m}$ M_{wall} / M_0	FEA $E = 1 \text{ GPa}$ $t = 0.1 \text{ m}$ [kNm]	FEA $E = 1 \text{ GPa}$ $t = 0.1 \text{ m}$ M_{wall} / M_0
1	6600	0.5	2928	0.22	6551	0.496
2	6600	0.5	2928	0.22	6551	0.496
3	0	0	3708	0.28	47	0.0035
4	0	0	3636	0.28	50	0.004

Table 5.34: Comparison of the moment contribution of the four walls, Case 1b.

Wall	HC [kNm]	HC M_{wall} / M_0	FEA $E = 30 \text{ GPa}$ $t = 0.3 \text{ m}$ [kNm]	FEA $E = 30 \text{ GPa}$ $t = 0.3 \text{ m}$ M_{wall} / M_0	FEA $E = 1 \text{ GPa}$ $t = 0.1 \text{ m}$ [kNm]	FEA $E = 1 \text{ GPa}$ $t = 0.1 \text{ m}$ M_{wall} / M_0
1	6600	0.5	2172	0.165	6510	0.493
2	6600	0.5	2172	0.165	6510	0.493
3	0	0	4608	0.35	90	0.007
4	0	0	4248	0.32	90	0.007

5.7.3 Study of twisting

The cases studied in the previous section show great differences in the stress distributions in the building. The torsional stiffness is especially of interest as the components own torsional stiffness is not taken into account in the hand calculation methods presented in Section 4.5. It is here important to understand the basics of twisting phenomena, pure torsion and warping, which are explained in Section 2.3.2.

The method used in the hand calculation takes the structures resistance to torsion into account by combining the different stiffness of the stabilising walls, B_x and B_y , and their distance to the rotation centre. This approach is suitable for walls far from the rotation centre as they will almost only move in a lateral direction. Walls positioned close to the rotation centre will not only move in a lateral direction but also resist torsion by being subjected to twisting themselves. The total stabilising contribution of a unit, stabilising a building subjected to twisting, is actually depending on four contributions. The component will stabilise by bending stiffness in the stabilising direction and by shear stiffness in the stabilising direction. These two contributions in combination with the torsional and warping stiffness of the component give the total stabilising stiffness. In most cases of hand calculating, three of these four contributions are neglected and only stabilising through bending stiffness is taken into account. This approximation is on the safe side and is in most cases a good approximation. This investigation, Cases 2a and 2b, will present cases where these approximations do not interpret the actual behaviour of the structure.

The effect of twisting will first be explained through the example shown below in Figure 5.42. This example is presented to enlighten the fact that stabilising components close to the rotation centre have a different behaviour compared to stabilising components far from the rotation centre in a case where twisting occurs.

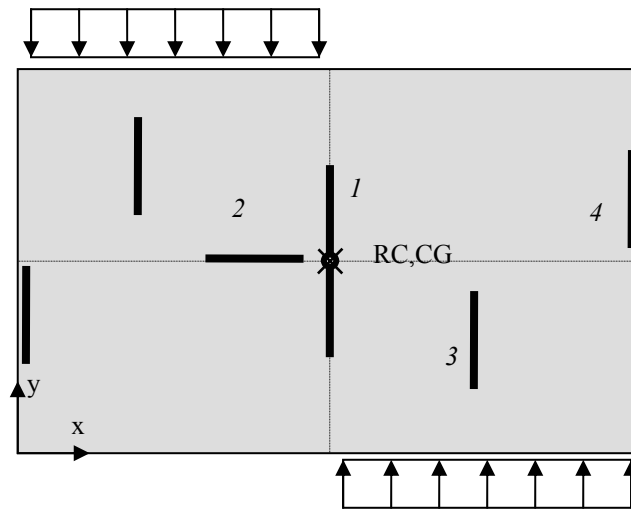


Figure 5.42: Illustration of wall positioning in a twisting load case.

Four walls are numbered in the figure above and their total torsional resistance is to be discussed. Wall 4 is positioned far from the rotation centre and when the building is subjected to rotation wall 4 will deflect almost only in y direction, see Figure 5.43. The stabilising contributions from this wall are due to bending and shear stiffness in the stabilising direction, i.e. y direction. If the wall is slender, shear stiffness can be neglected, but if the floor slabs are fully connected to the walls on each storey and are very stiff, bending may be resisted by the interaction between the floor slabs and the stabilising units. The shear stiffness is then of great importance and can not be neglected.

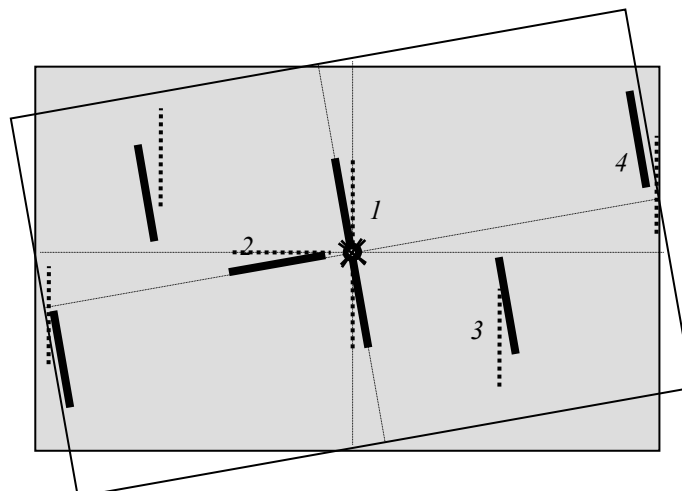


Figure 5.43: Illustration of the deflection of the walls when the structure is subjected to twisting.

Wall 1 is positioned with its rotation centre at the buildings rotation centre and is therefore subjected to pure twisting. This wall has no bending or shear contribution in its stabilising direction and warping is neglected due to it being a uniform solid section. The wall is therefore contributing with its own torsional stiffness which is a shear stiffness around its rotation axis, i.e. St Venant stiffness, see Section 2.3.2

$$M_{\text{twist,wall}_1} = GK_V \theta \quad (5.12)$$

K_V is the torsional stiffness factor of a unit and for walls, which are thin in relation to their breadths, K_V is estimated to $K_{V,\text{wall}} = \frac{bt^3}{3}$ where b is the breadth of the wall and t refers to the thickness.

Wall 3 is more difficult to treat. This wall is subjected to bending and shear in the stiff direction but also twisting in this wall, like the effect in wall 1, contributes for stabilising the building. Wall 3 is therefore referring a case of *lateral torsion*. It is difficult to establish the total contribution from this wall because the wall is not twisting around its own rotation centre and the expression used for wall 1 can not be used.

Wall 2 is a similar case to wall 3 but the bending and shear stiffness are not in its stiff direction and this contribution is therefore small. The twisting behaviour is therefore somewhere between wall 1 and wall 3.

The investigation of the force distribution is continued for twisting cases by using the same models used in Case 1a and Case 1b. In the translation study the stiffness of the slabs at each storey has shown a significant role for the force distribution. The following study reveals how the stiffness of the floor slabs, in combination with the positioning of the four stabilising walls, will influence the structure's behaviour when it's subjected to twisting.

5.7.3.1 Case 2a – Walls at the extremities

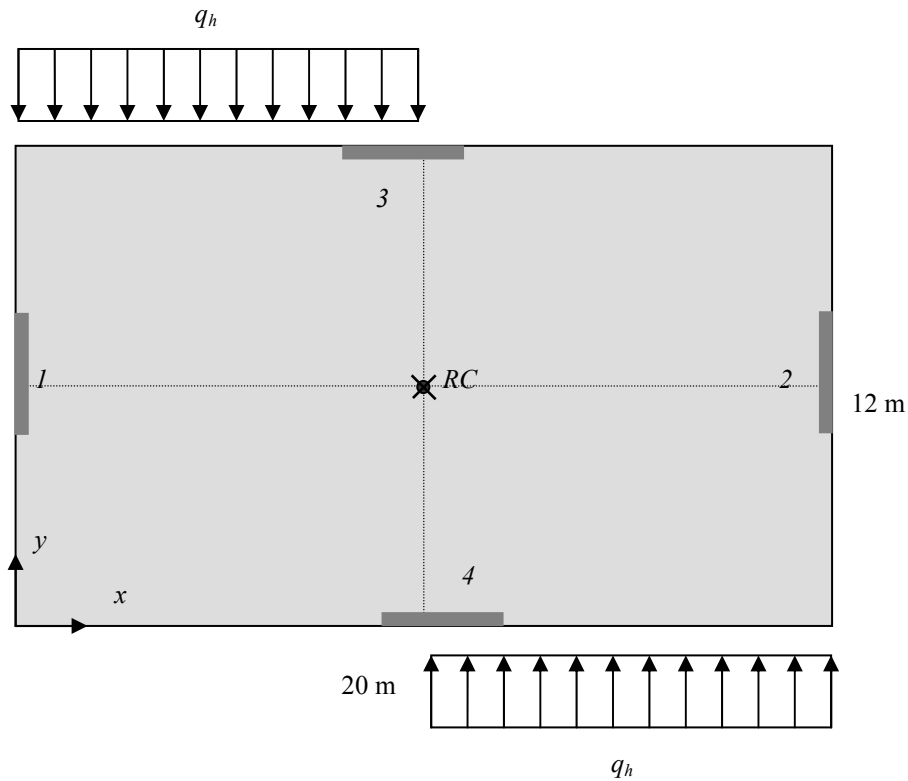


Figure 5.44: Twisting load case, Case 2a.

Hand calculation:

Twisting moment:

The distributed load, $q_h = 3 \text{ kN/m}$, is applied at half the long side of the ten floor slabs. The load resultants from each side have both an eccentricity of 5 m.

$$M_{twist} = (3 \cdot 10 \cdot 10 \cdot 5) + (3 \cdot 10 \cdot 10 \cdot 5) = 3000 \text{ kNm}$$

Force distribution between the four stabilising walls:

Walls 1 and 2: y-direction:

$$H_{1,twist} = H_{2,twist} = M_{twist} \cdot \frac{B_{1,y} \cdot x}{\Sigma(B_y \cdot x^2 + B_x \cdot y^2)}$$

$$H_{1,twist} = H_{2,twist} = 3000 \cdot \frac{0.675 \cdot 10^{10} \cdot 10}{2 \cdot 0.675 \cdot 10^{10} \cdot 10^2 + 2 \cdot 0.675 \cdot 10^{10} \cdot 6^2} \Rightarrow$$

$$H_{1,twist} = H_{2,twist} = 3000 \cdot \frac{\cdot 10}{2 \cdot 10^2 + 2 \cdot 6^2} = 110 \text{ kN}$$

$$M_{0,1,y} = 110 \cdot 22 = 2427 \text{ kNm}$$

Linear stress distribution is assumed.

$$\sigma_{0,1,y} = \frac{2427 \cdot 10^3}{0.45} \cdot 1.5 = 8.1 \text{ MPa}$$

Walls 3 and 4: x -direction:

$$H_{3,twist} = H_{4,twist} = 3000 \cdot \frac{\cdot 6}{2 \cdot 10^2 + 2 \cdot 6^2} = 66 \text{ kN}$$

$$M_{0,3,x} = 66 \cdot 22 = 1456 \text{ kNm}$$

Linear stress distribution is assumed.

$$\sigma_{0,1,x} = \frac{1456 \cdot 10^3}{0.45} \cdot 1.5 = 4.9 \text{ MPa}$$

The values from the hand calculation are compared with results from the two FE-models.

Table 5.35: Case 2a – Twisting load case. Maximum stresses compared between the models.

Wall	HC [MPa]	FEA $E = 30 \text{ GPa } t = 0.3 \text{ m}$ [MPa]	FEA $E = 1 \text{ GPa } t = 0.1 \text{ m}$ [MPa]
1	±8.1	±3.25	±7.5
2	±8.1	±3.25	±7.5
3	±4.9	±1.9	±4.5
4	±4.9	±1.9	±4.5

The results show that the stiffness of the floor slabs has a significant effect on the force distribution in cases where twisting occurs. The FE-model using the weaker floor slabs almost agrees with the hand calculation. The great distances between the walls, in combination with weak floor slabs, leads to the interaction between the four walls being significantly lower.

The next case, Case 2b, has the walls positioned in the same way as in Case 1b and compared to Case 2a the closer distances between the walls leads to the belief that a stronger interaction between the four walls will occur.

5.7.3.2 Case 2b – Walls close to the RC

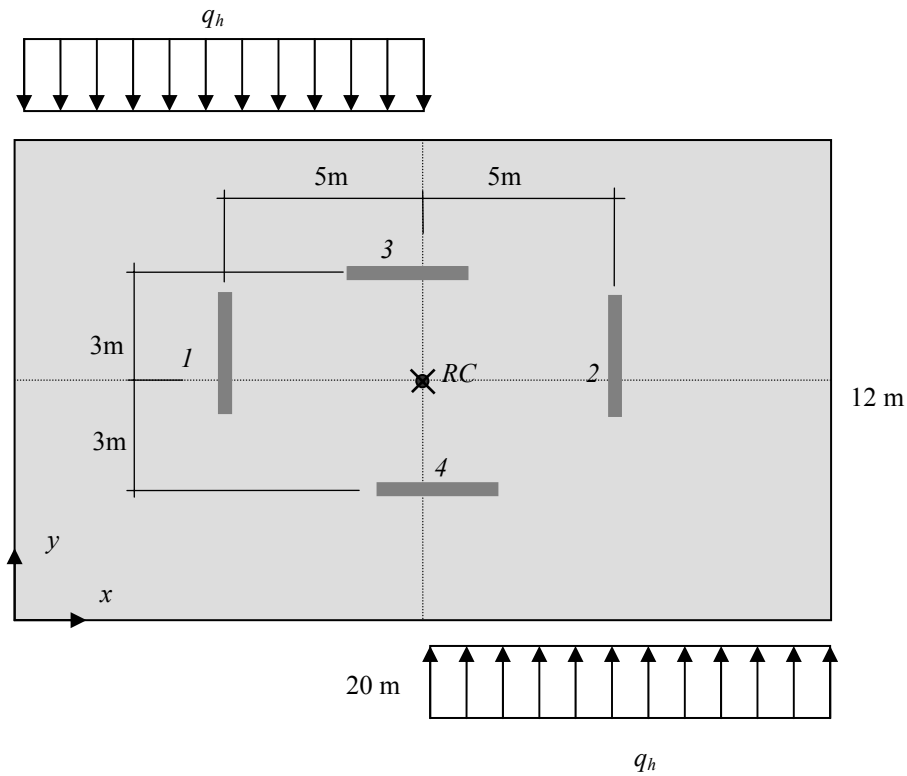


Figure 5.45: Twisting load case with walls close to RC, Case 2b.

Twisting moment:

$$q_h = 3 \text{ kN/m}$$

$$M_{twist} = (3 \cdot 10 \cdot 10 \cdot 5) + (3 \cdot 10 \cdot 10 \cdot 5) = 3000 \text{ kNm}$$

Force distribution between the four stabilising walls:

Walls 1 and 2: y-direction:

$$H_{1,twist} = H_{2,twist} = 3000 \cdot \frac{\cdot 5}{2 \cdot 5^2 + 2 \cdot 3^2} = 220 \text{ kN}$$

$$M_{0,1,y} = 220 \cdot 22 = 4852 \text{ kNm}$$

Linear stress distribution is assumed.

$$\sigma_{0,1,y} = \frac{4852 \cdot 10^3}{0.45} \cdot 1.5 = 16.2 \text{ MPa}$$

Walls 3 and 4: x-direction:

$$H_{3,twist} = H_{4,twist} = 3000 \cdot \frac{3}{2 \cdot 5^2 + 2 \cdot 3^2} = 132 \text{ kN}$$

$$M_{0,3,x} = 132 \cdot 22 = 2912 \text{ kNm}$$

Linear stress distribution is assumed.

$$\sigma_{0,1,x} = \frac{2912 \cdot 10^3}{0.45} \cdot 1.5 = 9.7 \text{ MPa}$$

The values from the hand calculation are compared with the results from the two FE-models.

Table 5.36: Case 2b – Twisting load case. Maximum stresses compared between the models.

Wall	HC [MPa]	FEA $E = 30 \text{ GPa}$ $t=0.3\text{m}$ [MPa]	FEA $E^* = 2 \text{ GPa}$ $t=0.1\text{m}$ [MPa]
1	±16.2	±3.75	±12.8
2	±16.2	±3.75	±12.8
3	±9.7	±2.1	±7.8
4	±9.7	±2.1	±7.8

* This load case, Case 2b, was not able to be run in the FE-program with such a low value of Young's modulus as 1 GPa. The value had to be increased to 2 GPa.

This last case, Case 2b, is a special case concerning the twisting of the structure. As it has been observed in the previous cases, the stiffness of the floor slabs plays a major role for force distributions. What differs between this case and the previous case, Case 2a, is the location of the four stabilising walls. From the table above, Table 2.35, it is observed that even with the weaker floor slabs the FE-model still does not agree with the hand calculation. The interaction between the walls is greater in the twisting case compared to the translation case. In the translation case the hand calculation agrees well with the FE-model using the weak slabs, but in the twisting case the values do not agree.

Earlier in this section, the four stabilising contributions of a wall were presented. In the hand calculations only the bending contribution is taken into account and by neglecting the other stabilising contributions, the stresses due to bending become very high. When the walls are placed far from the rotation centre the deflection of the walls in their stiff direction is much greater than all other deflections which are then neglected. In this case, the four walls are placed close to the rotation centre. The deflection due to twisting of the walls is then significant compared to the deflection of the walls in their stiff directions. The forces are therefore not taken only by bending but also through shear. Due to a strong interaction between the slabs and the walls, the

walls in each storey are resisted to bend and are forced by the slabs to be straight. The force distribution can therefore subjectively be compared with a St. Venant shear distribution in a closed cross section subjected to twisting. If only St. Venant stress distribution occurs, then no bending stresses would occur at all and only shear stresses in the walls would be observed. The last case studied, Case 2b, is a combination of, bending, shear in each walls stiff direction and shear occurring through twisting in each wall.

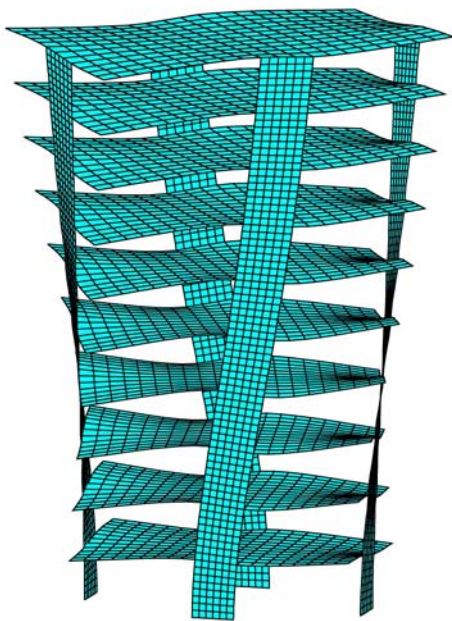


*Figure 5.46: Deflection Case 2a,
30 GPa $t=0.3$ m*

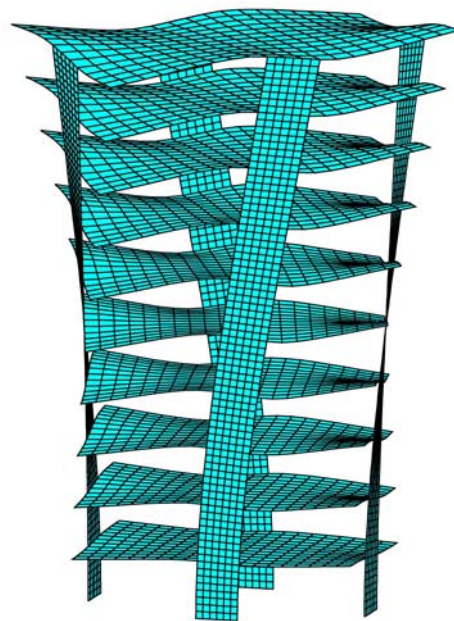


*Figure 5.47: Deflection Case 2a,
1 GPa $t=0.1$ m*

Figure 5.46 and Figure 5.47 illustrate the deflection modes of the twisting case for the model with the walls positioned at the edges of the building. In Figure 2.14 the deflection modes from bending and shear of a tall solid wall are presented. In Figure 5.47 the slab is weak and the deformations of the walls are considered as bending. The hand calculations agree well with this model as bending is only taken into account in the hand calculations. Figure 5.46 shows the effect when the stiff floor slabs are resisting the walls in each storey to bend and the deformation mode reveals a strong influence from shear.

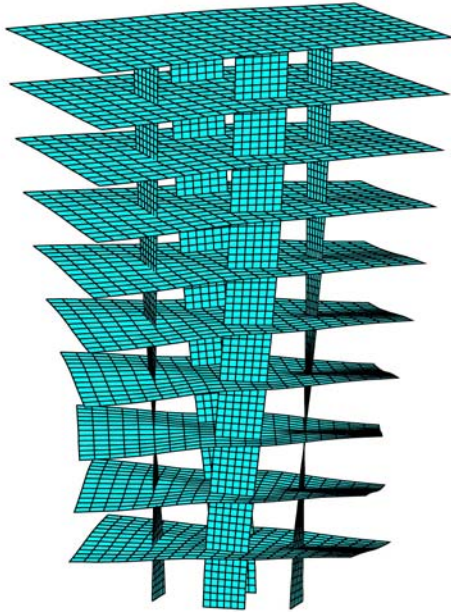


Figure 5.48: Deflection. Case 2b,
30 GPa, $t=0.3$ m

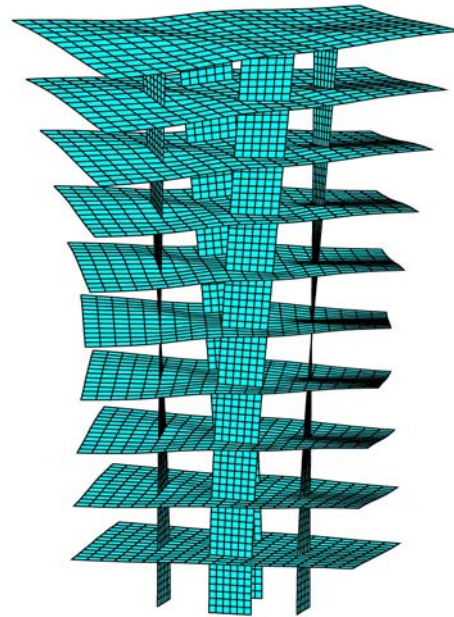


Figure 5.49: Deflection Case 2b,
2 GPa, $t=0.1$ m

The same comparison regarding Case 2a is made for Case 2b where the walls are closer to the rotation centre. The effect of twisting in each wall in combination with the *St. Venant effect*, contributes to stabilisation. The bending part is low which explains the great differences between the hand calculation and the FE-analyses. The deformation figure, Figure 5.48, reveals a low bending deformation in the walls and a great shear deformation. The stiff floor slabs are forcing the walls at each storey to be straight. Figure 5.49 is showing the case with the weaker slabs and the bending stiffness has in this case a greater influence for stabilisation. The walls are, due to the weaker floor slabs, able to bend and the shear deformations in the walls are smaller.

Figure 5.46 and 5.47, Case 2a, can be compared to Figure 5.48 and 5.49, Case 2b. The differences in the deflection modes reveal that bending deformation has a greater influence when the walls are far from each other and the shear stiffness is lower.

This thesis has been limited so that deeper investigations are not to be considered in to how to calculate the correct stress distribution in cases like Case 2b. It is obvious that it is very hard to establish a reasonable stress distribution by hand calculation but a deeper investigation with more detailed FE-models is suggested for further studies.

5.7.3.3 Discussion

For the cases investigated in sections 5.7.2 and 5.7.3 no interaction between the four walls is assumed in the hand calculations. The stresses are therefore much higher compared to the FE-analyses. This is because, in the FE-models the connections between the stabilising walls and the slabs are fully fixed. In the hand calculation method the connections between the stabilising walls and the slabs are assumed to be

hinged, i.e. not attracting moments. In the FE-models it is observed that the interaction between the walls decreases with a decreasing stiffness (in their plane) of the floor slabs and the stresses due to bending in the walls are increasing when the stiffness of the slabs is reduced. If the stiffness in the FE-model is further reduced and finally equals zero, the values in the FE-analyses will converge to the ones obtained in the hand calculation. Observe that here it is the stiffness *out of the plane* that is an issue. The problem occurs in the FE-model when Young's modulus is reduced to low values. The stiffness *in the plane* is also affected, and bending in the slabs plane will then occur and the force distribution is once again influenced. It is therefore hard to compare the hand calculation with values obtained from the FE-analyses. The real structure probably has friction joints between the slab parts and between the slabs and the walls. It is therefore suspected that the complete floor slab will not be able to transfer the stresses for obtaining a strong interaction between the stabilising components. Concerning concrete slabs cast in situ, the slabs are one unified element without joints and therefore it is possible that a stronger interaction occurs between the stabilising components. If the slabs, or the connections between the slabs and the stabilising units, are not designed for transferring the forces for obtaining a strong interaction, then there is a risk for cracking in the most critical parts. The stiffness of the slabs or the connections is then partly reduced and the interaction between the stabilising components is weakened.

If a hand calculation is not performed and only the FE-analysis is utilised in design, the interaction effect occurring in the FE-model may lead to lower design values, in some stabilising components, than are actually occurring in the components. If it is not secured that the slabs and the connection between the components are strong enough for keeping the interaction, the stabilising components become under dimensioned.

When using FE-analysis it has been observed from this study that the model built up in the FE-program has to be very detailed if the model is to resemble the real structure. Connections between the elements, for example the stabilising components and the slabs, are preferable to be interpreted as joints. If the joints are not considered in the FE-model, the slabs should be interpreted as not stiff out of the plane, in order to resemble the real structure and to make hand calculations comparable.

5.7.4 Torsional resistance in cores

In Section 2.3.2 torsional effects on opened and closed cross sections are presented. In this section the expressions for torsional stiffness of single cross sections is first taken up and is followed by a derivation of an expression for combining torsional stiffness of cores together with the contribution from the stabilising walls. The hand calculation method used in this thesis to establish the force distribution through a building subjected to twisting, does not take into account the torsional resistance of for example cores. It is a common solution in tall buildings to use a centrally positioned core, also utilised as an elevator shaft, in combination with stabilising walls or facades. To include the rotational stiffness of the cores into the expression used for establishing the force distribution through twisting, a new expression has to be derived.

The torsional resistance of a single component has the expression below describing the moment contribution from St. Venant and Vlasov.

$$M_{twist} = M_{twist,S} + M_{twist,V} = GK_V \theta - EK_W \theta'' \quad (2.5)$$

In this study the warping stiffness, i.e. the Vlasov part, is neglected. Instead only the stiffness related to pure torsion, i.e. St. Venant, is considered. The final expression derived has not been taken from any literature and has been established by the authors of this thesis. The expression was established in the final phase of this thesis and it has not been fully checked or investigated. The results from the hand calculations using this method are compared with the FE-analyses.

The derivation is based on finding the total deflection at the top of a chosen stabilising component. When the deflection is established for a chosen wall it can be utilised for deriving the deflection at the top of each stabilising component. When the top deflection of a stabilising unit is established the moment and the stress distribution along the unit can be derived.

This investigation starts with a derivation of the new expression by using a structure consisting of a U-shaped centred core and two outer stabilising walls, i.e. Case 1. The structure is first subjected to a distributed horizontal load, applied at the top of the structure on each side, for obtaining a case of twisting. To ensure that the FE-model and the hand calculations are compatible, the models are given a very stiff slab, between the three stabilising units, which acts like a stiff arm rotating about the structure, see Figures 5.50.

The derived expression is then used for two additional cases, Case 2 and 3, and the top deflections established through the new expression are compared with the results from the FE-analyses. Case 2 is similar to Case 1 except that the U-shaped core is replaced by a closed rectangular cross section. Case 3 uses the same structure as Case 2 but refers to a ten storey structure where the loads are applied at each storey, see Figure 5.51.

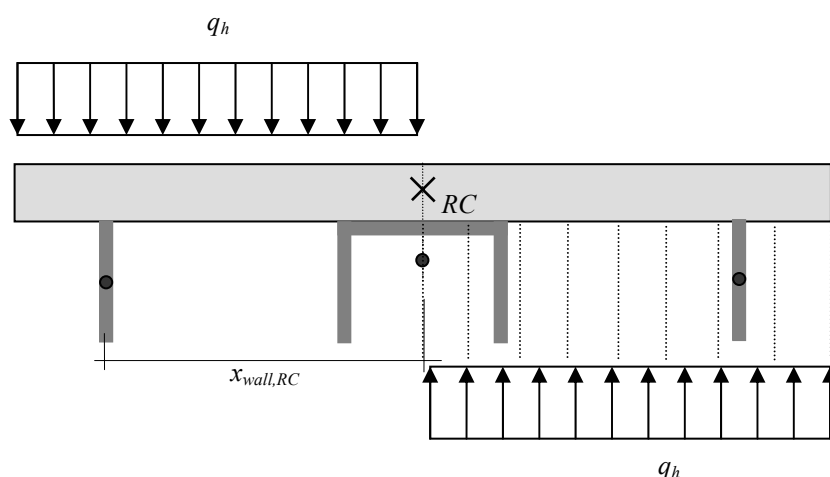


Figure 5.50: Case 1, U-shape model, distributed load at the top only.

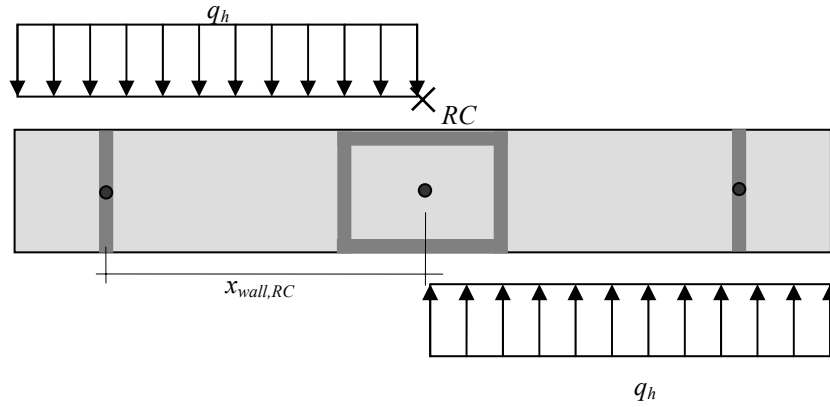


Figure 5.51: Case 2, Rectangular-shaped model, distributed load at the top only.
Case 3, Distributed load at all 10 storeys.

5.7.4.1 Expression for including torsional stiffness of cores

Through this derivation Case 1 is used and the load is applied on the top floor only. See Figure 5.50.

The slab is only 1.0 m wide and is acting as a stiff arm between the stabilising components. The slab is positioned to the sides of the components, not directly on them. This is done in order to keep the U-shaped cross section free without infringing on the behaviour of the flanges. The FE-model is then comparable with the model in the hand calculation.

Top deflection of a cantilever wall subjected to a point load at the top:

$$y_{top} = H_{top,wall} \cdot \frac{L^3}{3EI} \quad H_{top,wall} = \frac{M_{twist}}{x_{wall,RC}} \Rightarrow$$

$$y_{top} = \frac{M_{twist} \cdot L^3}{x_{wall,RC} \cdot 3EI} \quad (5.13)$$

$x_{wall,RC}$ is the distance from the wall to the rotation centre of the whole structure.

Top deflection angle of a twisted centre positioned core:

$$M_{twist} = GK_V \theta \quad \theta = \frac{dm}{dx} \Rightarrow \frac{dm}{dx} = \frac{M_{twist}}{GK_V} \Rightarrow$$

$$m_{top} = \frac{M_{twist}}{GK_V} \cdot L_h \quad (5.14)$$

(The equation can also be integrated and from the boundary condition at the base, $m_{x=0} = 0$, the same expression is derived.)

m_{top} is here the total angle that will occur from the base to the top of the twisted unit.

To combine Equation 5.13 with Equation 5.14, the deflection at the wall has to be established.

$$y_{top} = \frac{M_{twist} \cdot L^3}{x_{wall,RC} \cdot 3EI}; \quad y_{top} = m_{top} \cdot x_{wall,RC} \quad \Rightarrow \quad y_{top} = \frac{M_{twist}}{GK_V} \cdot L_h \cdot x_{wall,RC}$$

The two expressions are now treated as a sum of each capacity for resisting a twisting moment.

$$y_{top} = M_{twist} \cdot \frac{L^3}{x_{wall,RC} \cdot 3EI} \quad y_{top} = M_{twist} \cdot \frac{L_h \cdot x_{wall,RC}}{GK_V}$$

$$y_{top} = \frac{1}{\frac{1}{M_{twist} \cdot \frac{L_h^3}{x_{wall,RC} \cdot 3EI}} + \frac{1}{M_{twist} \cdot \frac{L_h \cdot x_{wall,RC}}{GK_V}}} \quad \Rightarrow$$

$$y_{top,wall} = \frac{M_{twist}}{\left(\frac{3EI \cdot x_{wall,RC}}{L_h^3} + \frac{GK_V}{L_h \cdot x_{wall,RC}} \right)} \quad (5.15)$$

In this study two stabilising walls are positioned with the same distances from the rotation centre and have the same stiffness values. The two walls will therefore contribute equally to provide torsional stiffness. The part concerning the stabilising wall can therefore be multiplied with 2.

$$y_{top,wall} = \frac{M_{twist}}{\left(\frac{3EI \cdot x_{wall,RC}}{L_h^3} \cdot 2 + \frac{GK_V}{L_h \cdot x_{wall,RC}} \right)}$$

In general cases where several walls are stabilising, the stiffness and the distance from the rotation centre from each wall, has to be interpreted through Equation (5.16).

$$y_{top,wall} = \frac{M_{twist}}{\left(\frac{3EI \cdot x_{wall,RC}}{L_h^3} + \sum_1^i \left(\frac{3EI_i \cdot x_{i,RC}}{L_h^3} \right) + \frac{GK_V}{L_h \cdot x_{wall,RC}} \right)} \quad (5.16)$$

The twisting angle can also be established by dividing with the distance of the chosen wall, i.e. $x_{wall,RC}$

$$\alpha_{twist} = \frac{y_{top,wall}}{x_{wall,RC}} = \frac{M_{twist}}{\left(\frac{3EI \cdot x_{wall,RC}^2}{L_h^3} + \sum_1^i \left(\frac{3EI_i \cdot x_{i,RC} \cdot x_{wall,RC}}{L_h^3} \right) + \frac{GK_V}{L_h} \right)} \quad (5.17)$$

It is recommended to use Equation (5.14) and first establish the top deflection of a chosen wall. The top deflection can easily be established for the other walls by quotients between the distance of the chosen wall, $x_{wall,RC}$, and the actual wall, as the deflection is varying linearly with the distance from the rotation centre.

$$\text{Walls stabilising in } y\text{-direction: } y_{top,i} = \frac{x_{i,RC}}{x_{wall,RC}} \cdot y_{top,wall}$$

$$\text{Walls stabilising in } x\text{-direction: } y_{top,i} = \frac{y_{i,RC}}{x_{wall,RC}} \cdot y_{top,wall}$$

In this example the chosen wall is stabilising in y -direction.

The calculations of the stiffnesses of the three stabilising units are not presented in the following three examples. For coupled cross sections, such as the U-shaped section and the rectangular-shaped, the data for calculating the stiffnesses can be found in Appendix E.

Horizontal distributed loads applied on each storey:

The derivation above is referring to a structure subjected to a horizontal distributed load at the top floor. An expression for the deflection at the top of the wall for a load case referring to a horizontal distributed load applied at each storey is now to be established. This derivation is based on the relationship between the top deflection on a cantilever component subjected to a concentrated load at the top and the top deflection when the cantilever component is subjected to a distributed horizontal load along the height.

Concerning the distributed load case, the load is summed up and applied at the top of the column subjecting the column with a concentrated load instead of a distributed load along the height.

$$\text{Distributed load : } y_{top,dist} = q_h \cdot \frac{L_h^4}{8EI}$$

$$\text{Concentrated load at the top: } y_{top,conc} = H_{top,wall} \cdot \frac{L_h^3}{3EI} \quad H_{top,wall} = q_h \cdot L_h$$

The two expressions are compared:

$$y_{top,conc} = q_h \cdot L_h \cdot \frac{L_h^3}{3EI} = q_h \cdot \frac{L_h^4}{3EI} \quad y_{top,dist} = q_h \cdot \frac{L_h^4}{8EI}$$

The expressions are identical except for the 3 and the 8. If the distributed load is summed up and placed at the top of the column the deflection will be 8/3 times the real deflection when the load is distributed along the column.

$$y_{top,dist} = \frac{3}{8} \cdot y_{top,point} \quad (5.18)$$

The same equation, Equation 5.14, is therefore used for establishing the deflection of a chosen wall subjected to a distributed load and is multiplied with 3/8.

$$y_{top,wall} = \frac{M_{twist}}{\left(\frac{3EI \cdot x_{wall,RC}}{L_h^3} \cdot 2 + \frac{GK_V}{L_h \cdot x_{wall,RC}} \right)} \cdot \frac{3}{8} \quad (5.19)$$

Observe that Equation (5.18) is an approximation of the real load case.

5.7.4.2 Case 1 – U-shaped core

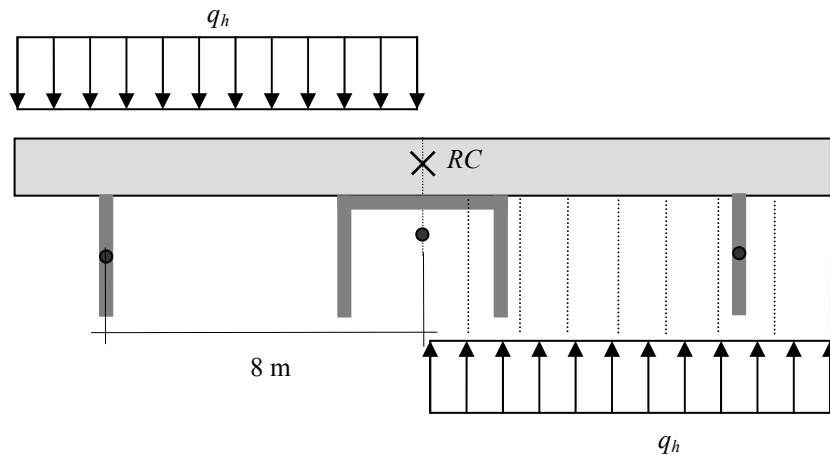


Figure 5.52: Case 1, U-shaped core.

$$t_{wall} = t_{U-shape} = 0.1 \text{ m}$$

$$q_h = 3 \text{ kN/m} \quad E_{wall} = E_{U-shape} = 30 \text{ GPa} \quad G = 0.4E = 12 \text{ GPa}$$

$$EI_{wall} = 0.67 \cdot 10^{10} \text{ Nm}^2 \quad K_{V,U-shape} = 0.00333 \text{ m}^4$$

$$M_{twist} = (3 \cdot 10 \cdot 1 \cdot 5) + (3 \cdot 10 \cdot 1 \cdot 5) = 300 \text{ kNm}$$

Both walls are placed with the same distance from the rotation centre.

$$y_{top,wall} = \frac{M_{twist}}{\left(\frac{3EI \cdot x_{wall,RC}}{L_h^3} \cdot 2 + \frac{GK_V}{L_h \cdot x_{wall,RC}} \right)} = \frac{300 \cdot 10^3}{\left(\frac{3 \cdot 0.67 \cdot 10^{10} \cdot 8}{40^3} \cdot 2 + \frac{12 \cdot 10^9 \cdot 0.00333}{40 \cdot 8} \right)}$$

$$y_{top,wall} = \frac{300 \cdot 10^3}{2512500 \cdot 2 + 124987} = 0.0582 \text{ m}$$

The calculated values, below the division line in the last expression, reveal the contributions from each stabilising component for resisting torsion. The second value, 124987 N, reveals that the U-shape contributes very little for stabilising compared to the walls positioned far from the rotation centre.

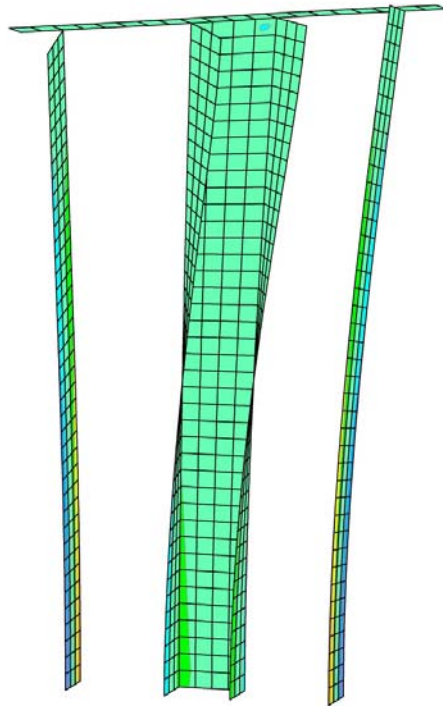


Figure 5.53: Deflection from FE-analysis, Case 1

The same calculation is now made for a similar building where the U-shaped core is replaced by a closed core.

5.7.4.3 Case 2 – Closed rectangular core, load on top floor

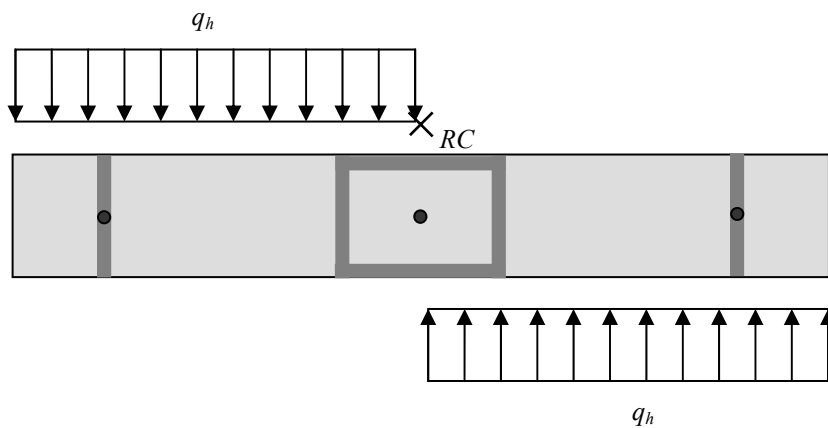


Figure 5.54: Case 2, closed rectangular core, load on top floor.

$$t_{\text{wall}} = t_{\text{closed}} = 0.1 \text{ m}$$

$$q_h = 3 \text{ kN/m} \quad E_{\text{wall}} = E_{U\text{-shape}} = 30 \text{ GPa} \quad G = 0.4E = 12 \text{ GPa}$$

$$EI_{wall} = 0.67 \cdot 10^{10} \text{ Nm}^2 \quad K_{V,U\text{-shape}} = 4.114 \text{ m}^4$$

Observe the great differences of the K_V -value compared to the U-shaped cross section. Closed cross sections are much stronger for resisting torsion.

$$M_{twist} = (3 \cdot 10 \cdot 1 \cdot 5) + (3 \cdot 10 \cdot 1 \cdot 5) = 300 \text{ kNm}$$

Both single walls are placed with equal distances from the rotation centre.

$$y_{top,wall} = \frac{M_{twist}}{\left(\frac{3EI \cdot x_{wall,RC}}{L_h^3} \cdot 2 + \frac{GK_V}{L_h \cdot x_{wall,RC}} \right)} = \frac{300 \cdot 10^3}{\left(\frac{3 \cdot 0.67 \cdot 10^{10} \cdot 8}{40^3} \cdot 2 + \frac{12 \cdot 10^9 \cdot 4.114}{40 \cdot 8} \right)}$$

$$y_{top,wall} = \frac{300 \cdot 10^3}{2512500 \cdot 2 + 154275000} = 0.00189 \text{ m}$$

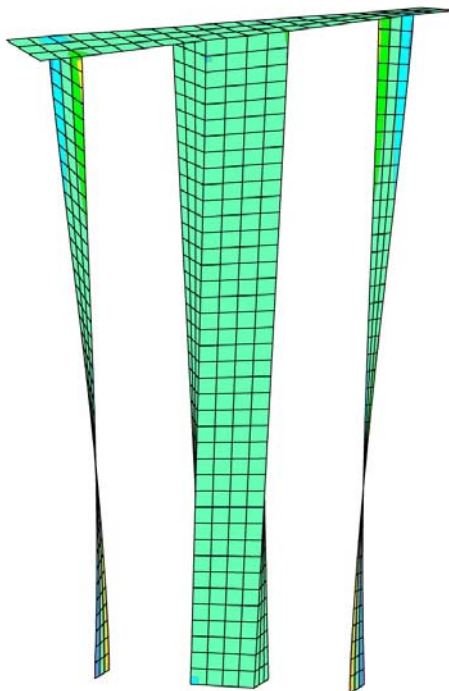


Figure 5.55: Deflection from FE-analysis, Case 2

For structures using closed cores, the torsional resistance of the core is important to include in the calculations. The last expression reveals that the closed core plays a significant role for resisting torsion in the structure.

The same structure used in Case 2 is now to be calculated for a distributed load case.

5.7.4.4 Case 3 – Closed rectangular core, load on all ten floors

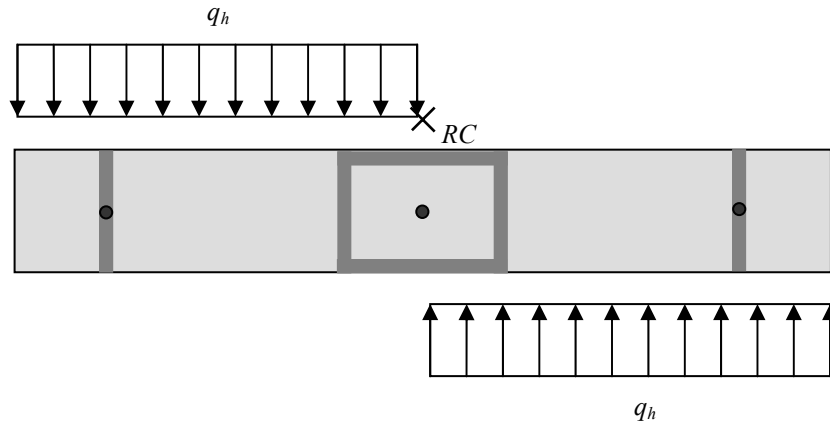


Figure 5.56: Case 3, closed rectangular core, load on all ten floors.

The loads are now applied on each storey.

$$M_{twist} = (3 \cdot 10 \cdot 10 \cdot 5) + (3 \cdot 10 \cdot 10 \cdot 5) = 3000 \text{ kNm}$$

The total twisting moment is now imagined to be reapplied at the top storey only.

$$y_{top,wall} = \frac{M_{twist}}{\left(\frac{3EI \cdot x_{wall,RC}}{L_h^3} \cdot 2 + \frac{GK_V}{L_h \cdot x_{wall,RC}} \right)} \cdot \frac{3}{8} = \frac{3000 \cdot 10^3}{\left(\frac{3 \cdot 0.67 \cdot 10^{10} \cdot 8}{40^3} \cdot 2 + \frac{12 \cdot 10^9 \cdot 4.114}{40 \cdot 8} \right)} \cdot \frac{3}{8}$$

$$y_{top,wall} = \frac{3000 \cdot 10^3}{2512500 \cdot 2 + 154275000} \cdot \frac{3}{8} = 0.007 \text{ m}$$

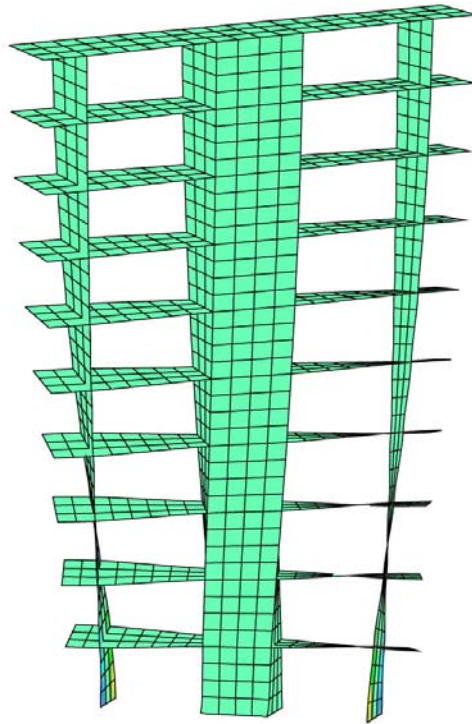


Figure 5.57: Deflection from FE-analysis, Case 3, loads on all floors.

5.7.4.5 Results

The three examples above have been calculated with two different load values and the results are compared with FE-analyses. O-shape means the closed rectangular core element.

Table 5.37: Results of deflection for torsional resistance investigations.

Structure/Load case	Load [kN/m]	HC Top deflection [mm]	FEA Top deflection [mm]	FEA/HC
U-shape – Top floor	3	58.2	52.5	0.90
U-shape – Top floor	1	19	17.3	0.91
O-shape – Top floor	3	1.89	1.83	0.97
O-shape – Top floor	1	0.63	0.61	0.97
O-shape – All floors	3	7.10	7.00	0.99
O-shape – All floors	1	2.35	2.33	0.99

The hand calculations agree well with the deflections obtained from the FE-analyses. The two cases concerning the U-shaped cross section present a slightly higher deflection than the FE-analyses produces. In the hand calculation the torsional resistance is slightly under estimated. The difference between a closed cross section and an open cross section subjected to torsion due to warping. Closed cross sections have almost no warping while open ones have. The torsional stiffness due to warping is not taken into account in the expressions derived in this section and is probably the reason why the U-shaped cross section presents slightly greater deflections.

5.7.5 Warping effects

Warping effects are considered when designing core elements. An introduction into torsional effects was given in chapter 2.3.2 and the application of these effects will be dealt with now. This is a theoretical section which does not provide analysis but does provide the tools for a possible future study of how to calculate with warping stresses included.

Vasilii Zakharovich Vlasov (1906-1958) was one of the leading developers of theory for warping torsion. The equations devised by him are used here and their derivations can be seen in Smith and Coull (1991). These equations are designed to be used for cores which are subjected to warping.

For determining rotation:

$$\theta(z) = \frac{m \cdot L^4}{E \cdot K_w} \left\{ \frac{1}{(\alpha L)^4} \left[\frac{\alpha L \cdot \sinh \alpha L + 1}{\cosh \alpha L} \cdot (\cosh \alpha z - 1) - \alpha L \sinh \alpha z + (\alpha L)^2 \left[\frac{z}{L} - \frac{1}{2} \left(\frac{z}{L} \right)^2 \right] \right] \right\} \quad (5.20)$$

Where: θ = rotation

m = torque per unit height

K_w = warping stiffness cross sectional factor

$$\alpha = \sqrt{\left(\frac{G \cdot k_v}{E \cdot k_w} \right)}$$

L = height of building

z = signifies where, along the height, the rotation shall be determined

In order to determine deformations the answer, in radians, must be multiplied with the distance from the façade, which is not horizontally loaded, to the rotation centre. In order to calculate the total deflection, this value must be then added to the deflection from bending and the deflection from shear.

For determining twist:

$$\frac{d\theta}{dz}(z) = \frac{m \cdot L^3}{E \cdot K_w} \left\{ \frac{1}{(\alpha L)^3} \left[\frac{\alpha L \cdot \sinh \alpha L + 1}{\cosh \alpha L} \cdot (\sinh \alpha z) - \alpha L \cosh \alpha z + \alpha L \cdot \left[1 - \frac{z}{L} \right] \right] \right\} \quad (5.21)$$

For determining axial deformations the following equation is used:

$$y(s, z) = -\omega(s) \frac{d\theta}{dz}(z) \quad (5.22)$$

Here s signifies the distance from the origin, z the height and ω is a principal sectorial coordinate which is another concept introduced by Vlasov into torsional theory. “A sectorial coordinate at a point on the profile of a warping core is the parameter that expresses the axial response (i.e., displacement, strain, and stress) at that point, relative to the response at other points around the section.” [Smith and Coull (1991)]

Consider now a core, see Figure 5.57, where the opening of the core is partially closed by beams i.e. transversals. The Vlasov effects will cause shears and moments in these transversals for which they will have to be designed for.

For shears in partially connecting beams:

$$\tau_b(z) = \frac{12I_b \Omega}{L_b^3} \cdot \frac{mL^3}{K_w} \left\{ \frac{1}{(\alpha L)^3} \left[\frac{(\alpha L \sinh \alpha L + 1)}{\cosh \alpha L} \cdot (\sinh \alpha z) - \alpha L \cosh \alpha z + \alpha L \cdot \left(1 - \frac{z}{L} \right) \right] \right\} \quad (5.23)$$

Where I_b = moment of inertia for beam

L_b = length of transversal

Ω = twice the area enclosed by the middle line of the core profile

The maximum bending moment in the beam is then:

$$M_b(z) = \tau_b(z) \cdot \frac{L_b}{2} \quad (5.24)$$

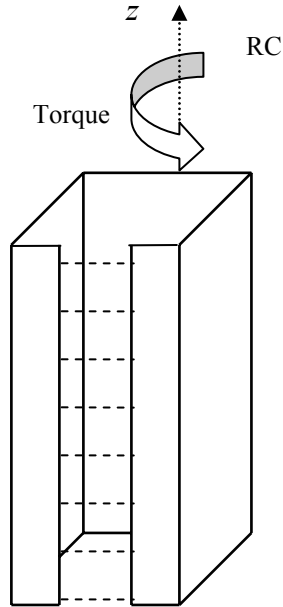


Figure 5.58: Core element partially closed with beams (transversals).

Vlasov introduced the concept of bimoment B ; which is a moment at a specific height times that height. Bimoments are then used for calculating the warping stresses.

$$B(z) = -mL^2 \cdot \left\{ \frac{1}{(\alpha L)^2} \cdot \left[\frac{\alpha L \sinh \alpha L + 1}{\cosh \alpha L} \cdot (\cosh \alpha z) - \alpha L \sinh \alpha z - 1 \right] \right\} \quad (5.25)$$

And warping stress is:

$$\sigma_w = \frac{B \cdot \omega}{K_w} \quad (5.26)$$

This warping stress must be combined with the bending stress, obtained through considering the tower to be a cantilever, in order to get the total axial stresses due to horizontal loading.

For determining rotation, twisting shear in the connecting beams and bending moments in the partially connecting beams it is possible to use K -values. This considerable hastens the calculation process.

$$\theta(z) = \frac{m \cdot L^4}{8 \cdot E \cdot k_w} \cdot K_1 \left(\alpha L, \frac{z}{L} \right) \quad (5.27)$$

This K_1 -value is taken from a diagram of curves depending on αL and α/L . See Figure 5.59 for clarification.

K_2 is used for twisting, see Figure 5.60

$$\frac{d\theta}{dz}(z) = \frac{m \cdot L^3}{6 \cdot E \cdot k_w} \cdot K_2\left(\alpha L, \frac{z}{H}\right) \quad (5.28)$$

For determining the bimoment B ; K_3 is used. See Figure 5.61.

$$B(z) = \frac{mL^2}{2} \cdot K_3\left(\alpha L, \frac{z}{L}\right) \quad (5.29)$$

For determining shear in the partially connecting beams; is used K_4 . See Figure 5.62.

$$\tau_b(z) = mL \cdot K_4\left(\alpha L, \frac{z}{H}\right) \quad (5.30)$$

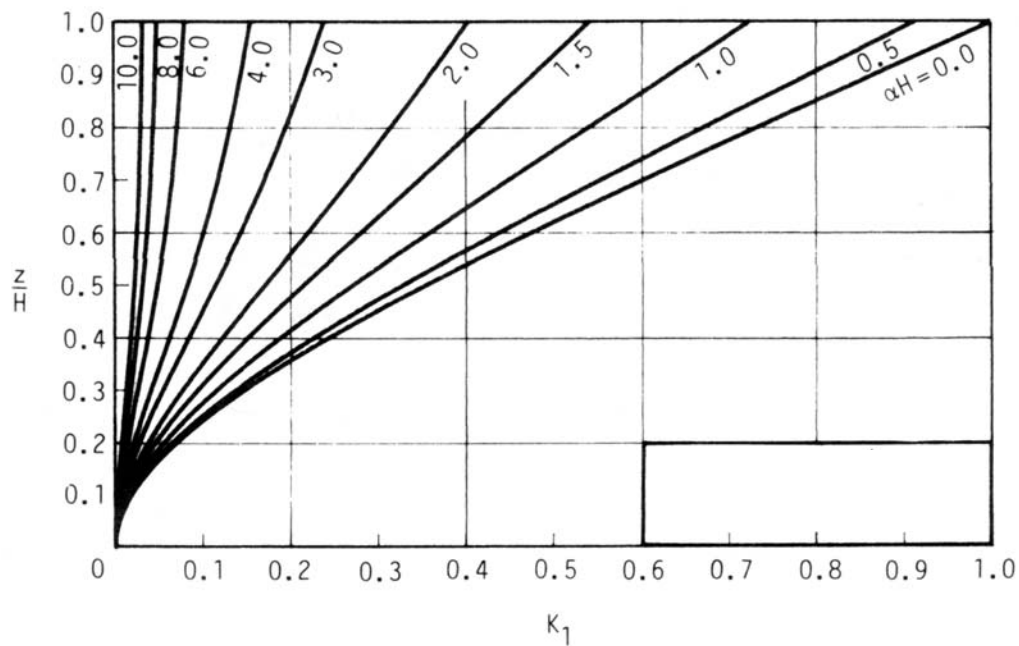


Figure 5.59: K_1 values. [Smith and Coull (1991)]

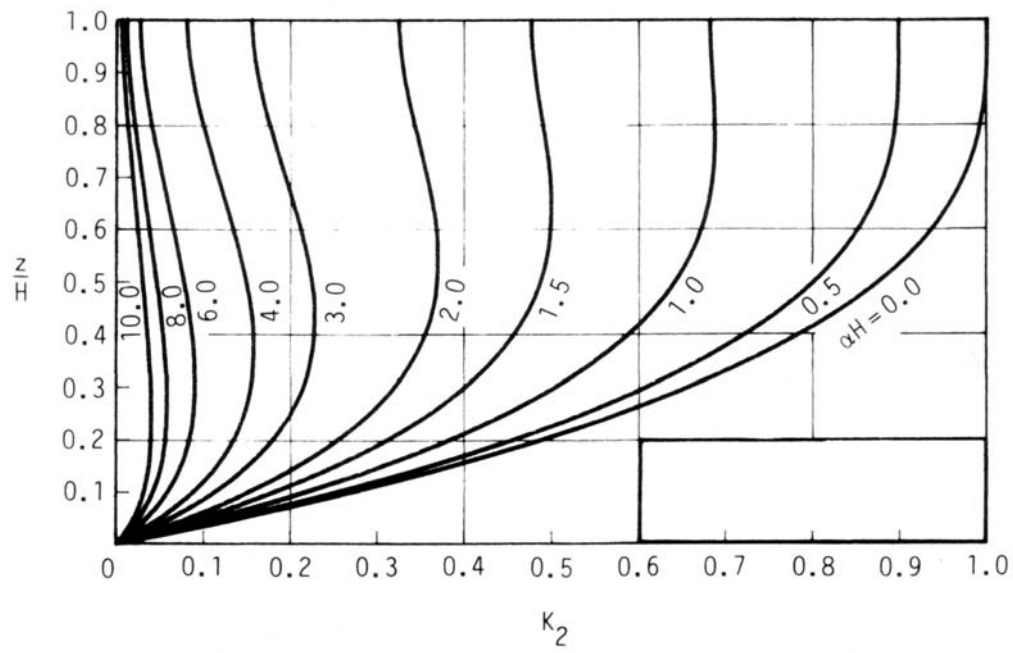


Figure 5.60: K_2 values. [Smith and Coull (1991)]

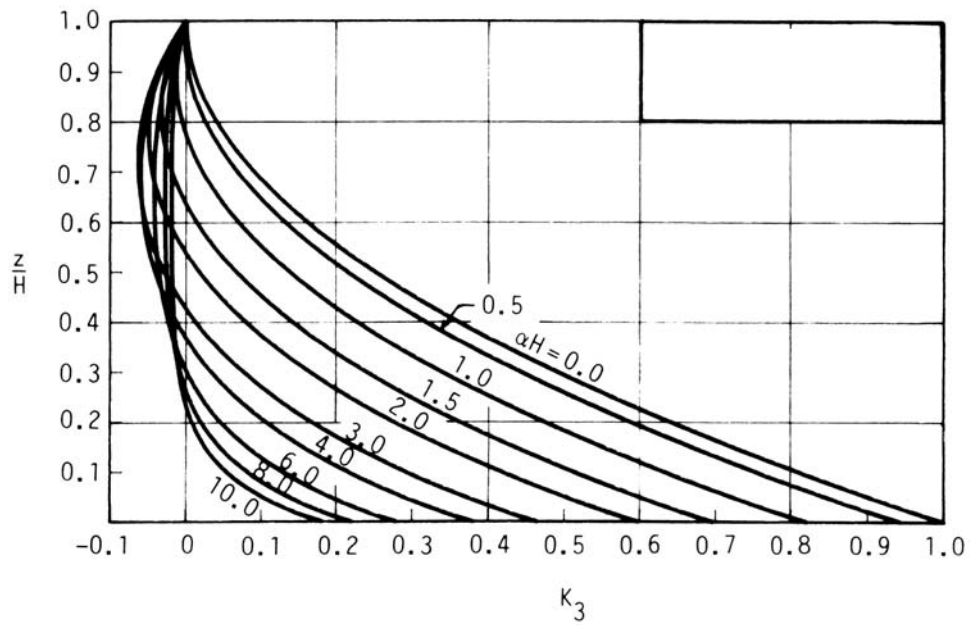


Figure 5.61: K_3 values. [Smith and Coull (1991)]

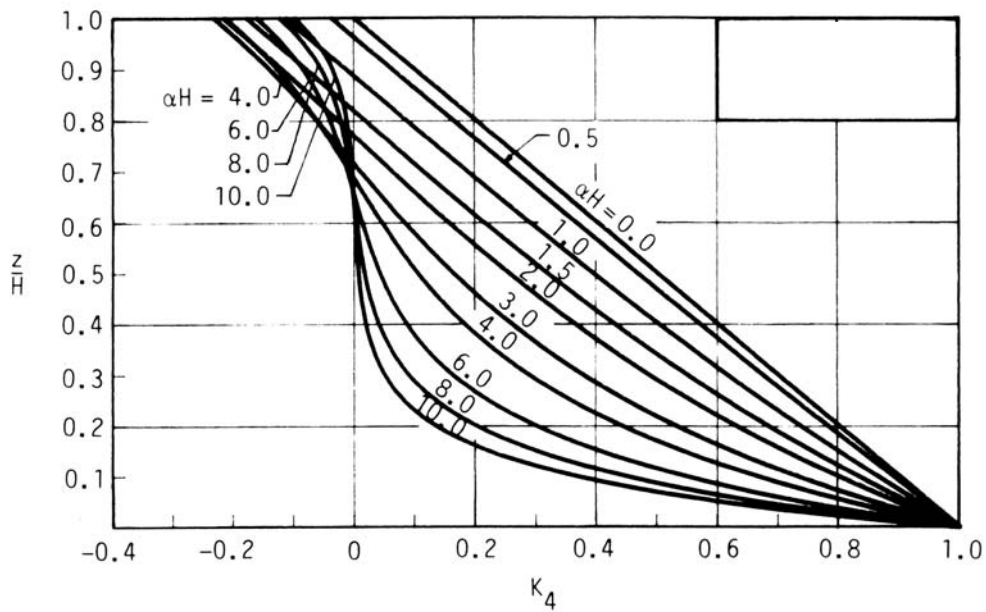


Figure 5.62: K_4 values. [Smith and Coull (1991)]

This method of reading K -values from diagrams is very fast and effective. Although the results from the design curves will not be exactly the same as those calculated through the complete equations they are accurate enough to use for preliminary designs. [Smith and Coull (1991)]

6 Conclusions and recommendations

6.1 Conclusions

This project has studied calculation methods for investigating stabilising components. Buckling due to bending, shear and torsion, deflections, 1st and 2nd order, and equations for determining the design forces and moments have been studied. Combinations of hand calculation methods and FE-analyses have been used.

The Vianello iterations, for determining critical buckling load due to bending, have proven themselves, against FE-analysis, to be very effective for calculating on columns and solid shear walls which have non-uniform stiffness and uneven load distributions.

An investigation has been done of pierced shear walls where the calculation method described in Lorentsen *et al.* (2000) has been compared with FE-analyses. The comparisons have shown a wide field of varying inaccuracy and some improvements to the equations used have been made. Comparing the pierced shear walls' critical buckling loads and deformations with FE-results shows that the equations used for calculating deformations give fairly accurate results and that the equations used for determining critical buckling load are very conservative and need improvements. Two improvements have been investigated. The first involves the bending transversal length c which should be set equal to the width of the gap in the wall and not the transversal height plus the width of the gap. This alteration led to much better results. Better results are achieved through also subtracting the transversal thickness h_t from the height L_{sec} while calculating the shear angle for the bending in the vertical. Both of these improvements combined, lead to better results that still land on the safe side of the FE-results. Considering pierced shear walls with robust verticals, the shear angle for the bending in the vertical can also be set equal to zero in order to achieve better results.

The method of using the polar moment of inertia will provide buckling loads with values higher than for a real structure. It follows that the design moment will be lower compared to the real structure and the columns will be under dimensioned, i.e. results will be obtained that are on the unsafe side.

Considering force distribution in single storey structures with 1st and 2nd order effects it has proved to be very important to be consequent when choosing whether to derive the final buckling load through either one of the critical translation buckling loads or the critical rotational buckling load. If the actual behaviour of a structure subjected to both rotation and translation is required then it is better to accurately apply each buckling load for each specific direction so that a more real interpretation can be completed

It has been discovered that the equations for global buckling, Equation (4.24), is inadequate for calculating rotational buckling loads. It has been concluded that this equation does not take into account a components torsional stiffness. Using this

equation may lead to rotation being misjudged and therefore the predicted behaviour of a structure may disagree with the structures real response.

Two approaches exist for calculating on cores. Their investigation concludes that different results will be obtained depending on which approach the engineer chooses. The uncoupled approach produces lower overall stiffness values than the coupled approach. Whether or not one approach is better than the other is debatable because either approach will work differently depending on the form of structure being investigated.

Considering multi storey structures it has been concluded that it is difficult to compare results because different assumptions are made in FE-analysis and the hand calculations. No interaction between the shear walls is assumed in the hand calculation which leads to the resulting stress values being considerably higher than the FE-results. FE-analyses show an interaction that strongly influences the stresses that occur in the stabilising walls. By using weaker plates in the FE-analyses the resulting stresses become more comparable with the hand calculations. Considering the results from FE-analyses it is observed that the interaction between the walls decreases and that the stresses due to bending in the walls increase, when less stiff floor slabs are successively tested. If the stiffness of the floor slabs is further reduced to zero, then the results will converge with the hand calculations.

Considering torsion, it has been concluded that it is vital to consider pure torsional resistance (St. Venant) and warping (Vlasov) while designing a structure. Better results are obtained through hand calculations that include torsional resistance. Warping effects in open cores will lead to axial deformations which in turn will lead to large stresses occurring in the connecting floor slabs. If the open core instead has beams positioned to partially close the core then these beams will have to be designed for shears and moments that will occur because of the warping effects.

6.2 Recommendations

It is recommended that the structural engineer takes an active roll in the preliminary design phase. It may be important for the engineer to discuss stabilising solutions with the architect early in the design phase and so hopefully save time and money through hindering foreseeable problems.

Vianello's iteration method is recommended for determining the critical buckling load due to bending. Through this method, can complicated shear walls and columns be quickly and effectively investigated and more accurate critical buckling loads achieved.

For calculating buckling loads on pierced shear walls it is recommended that the structural engineer develops an understanding, through study, of how the calculation method works for different forms of pierced shear wall. It is favourable to be familiar with how correct the method used will be, for walls of different degrees of slenderness.

The polar moment of inertia may produce design values which lead to under dimensioned structures. It is therefore recommended that this approach is implemented carefully.

It is highly recommended that an understanding of torsional buckling is properly applied. Attention to St. Venant and Vlasov effects is paramount when calculating on cores; specifically St. Venant for closed cross sections and Vlasov for open or partially closed cross sections.

6.3 Further studies

It would be very interesting to see if a relationship between variables concerning pierced shear walls could be established. This thesis did attempt such a study while searching for a *shear factor* and further studies may reach a significant conclusion that may further simplify calculation methods for pierced shear walls. An investigation of non linear behaviour of pierced shear walls is also of further interest.

A study of the interaction between stabilising components and floor slabs concerning how the interaction is interpreted in FE-analysis and hand calculations would be interesting. Results of a further investigation may lead to better calculation methods or at least to a better understanding of how the interaction is interpreted by FE-programmes.

7 References

Bangash M. Y. H. (1999): *Prototype building structures: analysis and design*. Thomas Telford Publishing, London, England.

Eurocode 1 *Basis of design and actions on structures* (1991)

Gambhir M. L. (2004): *Stability Analysis and Design of Structures*. Springer-Verlag Berlin, Heidelberg, Germany.

Lorentsen M. Petersson T. Sundquist H. (2000): *Stabilisering av byggnader (Stabilisation of Buildings)*. Royal Institute of Technology, Structural Engineering, Stockholm, Sweden.

Johansson M. (2005): Personal information

Petersson T. Sundquist H. (2002): *Envånings pelare och pelaresystem (One storey columns and column systems)* Royal Institute of Technology, Structural Engineering, Stockholm, Sweden.

Samuelsson A. and Wiberg N-E: *Byggnadsmekanik Hållfasthetslära (Mechanics of Materials)* (1993). Studentlitteratur, Lund, Sweden.

Smith B. S. and Coull A. (1991): *Tall Building Structures: Analysis and design*. John Wiley & Sons, Inc. New York, USA.

Timoshenko S. P. and Gere J. M. (1963): *Theory of Elastic Stability*. McGraw-Hill Book Co. Singapore.

Westerberg B. (1999): *Stabilisation of buildings*. Lectures notes from Bo Westerbergs lectures at Chalmers University of Technology, Gothenburg, Sweden.

Zalka K. A. and Armer G. S. T. (1992): *Stability of Large Structures*. Butterworth-Heinemann LTD, Oxford, England.

ONLINE

Ireland Mid West (2005):

<http://www.irelandmidwest.com/history/fieldmonuments.htm>

Interactive Interpretative Centre of the Burren (2005):

<http://www.burrenbeo.com/Kilmacduagh.html>

Global Security (2005):

<http://www.globalsecurity.org/military/world/iraq/babel.htm>

Museum of unnatural mystery (2005):

<http://www.unmuseum.org/babel.htm>

Service t-online (2005):

<http://home.t-online.de/home/m.dg.k/K.htm>

American Institute of steel construction (2005):

http://www.aisc.org/Content/NavigationMenu/Steel_Solutions_Center/Resources/Top_10_Lists/Louis_Geschwinder%E2%80%99s_Top_Ten_Significant_Steel_Buildings_You_Might_Not_Know/Rand_McNally.htm

The skyscraper museum (2005):

http://www.skyscraper.org/TALLEST_TOWERS/t_masonic.htm

Kent State University (2004):

<http://www.caed.kent.edu/History/Modern/Gilbert/woolworth1.jpg>

Emporis (2004):

<http://www.emporis.com>

Postgraduate medicine online (1999):

http://www.postgradmed.com/issues/1999/10_01_99/gahlinger.htm

Vibration data (2002):

http://www.vibrationdata.com/Newsletters/November2002_NL.pdf

University of Sydney (2004):

<http://www.civil.usyd.edu.au/publications/r804.pdf>

APPENDIX A: Vianello iterations

Four Vianello iterations made in excel are presented in this appendix. The four models represent solid stabilising walls in a 10 storey building. Each storey height is 3 m and the total height is 30 m. Each storey is divided into 4 increments. The results are compared in Section 5.2.

APPENDIX A: Vianello iterations

Case 1: Even load; $b = 4$ m; $E = 15$ GPa in top half; $E = 30$ GPa in bottom half.

dx	0.025
L	1
eI	40

N	1
EI	1

	x/L	N_{tower}	y	y_a	M_{tower}	EI	y''	y'	y_b	y_a/y_b	$New\ y$
0	1.00	1.00	1.00	0.00	0.00	0.50	0.00	2.42	0.00	0.00	0.00
1	0.98	0.00	0.95	0.05	0.05	0.50	0.10	2.41	0.06	1.22	0.04
2	0.95	0.00	0.90	0.10	0.10	0.50	0.20	2.41	0.12	1.24	0.08
3	0.93	0.00	0.86	0.14	0.14	0.50	0.29	2.40	0.18	1.25	0.12
4	0.90	1.00	0.81	0.19	0.19	0.50	0.38	2.39	0.24	1.27	0.16
5	0.88	0.00	0.77	0.23	0.28	0.50	0.56	2.38	0.30	1.28	0.20
6	0.85	0.00	0.72	0.28	0.37	0.50	0.73	2.36	0.36	1.30	0.24
7	0.83	0.00	0.68	0.32	0.45	0.50	0.90	2.34	0.42	1.31	0.28
8	0.80	1.00	0.64	0.36	0.53	0.50	1.06	2.31	0.48	1.33	0.31
9	0.78	0.00	0.60	0.40	0.65	0.50	1.30	2.28	0.54	1.34	0.35
10	0.75	0.00	0.56	0.44	0.76	0.50	1.53	2.24	0.59	1.35	0.39
11	0.73	0.00	0.53	0.47	0.87	0.50	1.75	2.20	0.65	1.37	0.43
12	0.70	1.00	0.49	0.51	0.98	0.50	1.96	2.15	0.70	1.38	0.46
13	0.68	0.00	0.46	0.54	1.12	0.50	2.24	2.09	0.76	1.39	0.50
14	0.65	0.00	0.42	0.58	1.25	0.50	2.50	2.03	0.81	1.40	0.53
15	0.63	0.00	0.39	0.61	1.38	0.50	2.76	1.96	0.86	1.41	0.57
16	0.60	1.00	0.36	0.64	1.50	0.50	3.00	1.88	0.91	1.42	0.60
17	0.58	0.00	0.33	0.67	1.65	0.50	3.29	1.80	0.96	1.43	0.63
18	0.55	0.00	0.30	0.70	1.79	0.50	3.58	1.71	1.00	1.44	0.66
19	0.53	0.00	0.28	0.72	1.92	0.50	3.84	1.62	1.04	1.44	0.69

	x/L	N tower	y	y_a	M tower	EI	y''	y'	y_b	y_a/y_b	New y
21	0.48	0.00	0.23	0.77	2.20	1.00	2.20	1.51	1.12	1.45	0.74
22	0.45	0.00	0.20	0.80	2.34	1.00	2.34	1.45	1.16	1.46	0.76
23	0.43	0.00	0.18	0.82	2.47	1.00	2.47	1.39	1.20	1.46	0.79
24	0.40	1.00	0.16	0.84	2.59	1.00	2.59	1.33	1.23	1.47	0.81
25	0.38	0.00	0.14	0.86	2.73	1.00	2.73	1.26	1.27	1.47	0.83
26	0.35	0.00	0.12	0.88	2.85	1.00	2.85	1.19	1.30	1.48	0.85
27	0.33	0.00	0.11	0.89	2.97	1.00	2.97	1.11	1.33	1.48	0.87
28	0.30	1.00	0.09	0.91	3.08	1.00	3.08	1.04	1.35	1.49	0.89
29	0.28	0.00	0.08	0.92	3.20	1.00	3.20	0.96	1.38	1.49	0.91
30	0.25	0.00	0.06	0.94	3.30	1.00	3.30	0.87	1.40	1.50	0.92
31	0.23	0.00	0.05	0.95	3.40	1.00	3.40	0.79	1.43	1.50	0.94
32	0.20	1.00	0.04	0.96	3.48	1.00	3.48	0.70	1.45	1.51	0.95
33	0.18	0.00	0.03	0.97	3.56	1.00	3.56	0.61	1.46	1.51	0.96
34	0.15	0.00	0.02	0.98	3.64	1.00	3.64	0.52	1.48	1.51	0.97
35	0.13	0.00	0.02	0.98	3.70	1.00	3.70	0.43	1.49	1.52	0.98
36	0.10	1.00	0.01	0.99	3.75	1.00	3.75	0.33	1.50	1.52	0.99
37	0.08	0.00	0.01	0.99	3.79	1.00	3.79	0.24	1.51	1.52	0.99
38	0.05	0.00	0.00	1.00	3.83	1.00	3.83	0.14	1.52	1.52	1.00
39	0.03	0.00	0.00	1.00	3.84	1.00	3.84	0.05	1.52	1.52	1.00
40	0.00	1.00	0.00	1.00	3.85	1.00	3.85	0.00	1.52	1.52	1.00
		10.00								1.42	

k 7.03

E	t	b	L	I	E	A
3.00E+10	0.50	4.00	30.0	2.67	3.00E+10	2.00

Final k 6.36

$N_{cr,B}$ 565 MN

Case 2: Uneven load; $b = 4$ m; $E = 15$ GPa in top half; $E = 30$ GPa in bottom half.

dx	0.025
L	1
el	40

N	1
EI	1

	x/L	N tower	y	y_a	M tower	EI	y''	y'	y_b	y_a/y_b	New y
0	1.00	0.50	1.00	0.00	0.00	0.50	0.00	1.28	0.00	0.00	0.00
1	0.98	0.00	0.95	0.05	0.02	0.50	0.05	1.28	0.03	0.65	0.04
2	0.95	0.00	0.90	0.10	0.05	0.50	0.10	1.28	0.06	0.66	0.08
3	0.93	0.00	0.86	0.14	0.07	0.50	0.14	1.28	0.10	0.67	0.12
4	0.90	0.50	0.81	0.19	0.10	0.50	0.19	1.27	0.13	0.67	0.16
5	0.88	0.00	0.77	0.23	0.14	0.50	0.28	1.26	0.16	0.68	0.19
6	0.85	0.00	0.72	0.28	0.18	0.50	0.37	1.25	0.19	0.69	0.23
7	0.83	0.00	0.68	0.32	0.22	0.50	0.45	1.24	0.22	0.70	0.27
8	0.80	0.50	0.64	0.36	0.27	0.50	0.53	1.23	0.25	0.70	0.31
9	0.78	0.00	0.60	0.40	0.32	0.50	0.65	1.21	0.28	0.71	0.35
10	0.75	0.00	0.56	0.44	0.38	0.50	0.76	1.19	0.31	0.72	0.38
11	0.73	0.00	0.53	0.47	0.44	0.50	0.87	1.17	0.34	0.73	0.42
12	0.70	0.50	0.49	0.51	0.49	0.50	0.98	1.15	0.37	0.73	0.45
13	0.68	0.00	0.46	0.54	0.56	0.50	1.12	1.12	0.40	0.74	0.49
14	0.65	0.00	0.42	0.58	0.63	0.50	1.25	1.09	0.43	0.75	0.52
15	0.63	0.00	0.39	0.61	0.69	0.50	1.38	1.05	0.46	0.75	0.56
16	0.60	0.50	0.36	0.64	0.75	0.50	1.50	1.02	0.48	0.76	0.59
17	0.58	0.00	0.33	0.67	0.82	0.50	1.65	0.98	0.51	0.76	0.62
18	0.55	0.00	0.30	0.70	0.89	0.50	1.79	0.93	0.53	0.77	0.65
19	0.53	0.00	0.28	0.72	0.96	0.50	1.92	0.88	0.56	0.77	0.68
20	0.50	1.00	0.25	0.75	1.03	1.00	1.03	0.86	0.58	0.77	0.70

	x/L	N tower	y	y_a	M tower	EI	y''	y'	y_b	y_a/y_b	New y
21	0.48	0.00	0.23	0.77	1.11	1.00	1.11	0.83	0.60	0.78	0.73
22	0.45	0.00	0.20	0.80	1.19	1.00	1.19	0.80	0.62	0.78	0.76
23	0.43	0.00	0.18	0.82	1.27	1.00	1.27	0.77	0.64	0.78	0.78
24	0.40	1.00	0.16	0.84	1.34	1.00	1.34	0.74	0.66	0.79	0.80
25	0.38	0.00	0.14	0.86	1.43	1.00	1.43	0.70	0.68	0.79	0.83
26	0.35	0.00	0.12	0.88	1.51	1.00	1.51	0.66	0.70	0.79	0.85
27	0.33	0.00	0.11	0.89	1.58	1.00	1.58	0.62	0.71	0.80	0.87
28	0.30	1.00	0.09	0.91	1.66	1.00	1.66	0.58	0.73	0.80	0.89
29	0.28	0.00	0.08	0.92	1.73	1.00	1.73	0.54	0.74	0.80	0.90
30	0.25	0.00	0.06	0.94	1.81	1.00	1.81	0.49	0.76	0.81	0.92
31	0.23	0.00	0.05	0.95	1.87	1.00	1.87	0.45	0.77	0.81	0.93
32	0.20	1.00	0.04	0.96	1.93	1.00	1.93	0.40	0.78	0.81	0.95
33	0.18	0.00	0.03	0.97	1.99	1.00	1.99	0.35	0.79	0.82	0.96
34	0.15	0.00	0.02	0.98	2.04	1.00	2.04	0.30	0.80	0.82	0.97
35	0.13	0.00	0.02	0.98	2.09	1.00	2.09	0.24	0.81	0.82	0.98
36	0.10	1.00	0.01	0.99	2.13	1.00	2.13	0.19	0.81	0.82	0.99
37	0.08	0.00	0.01	0.99	2.16	1.00	2.16	0.14	0.82	0.82	0.99
38	0.05	0.00	0.00	1.00	2.18	1.00	2.18	0.08	0.82	0.82	1.00
39	0.03	0.00	0.00	1.00	2.20	1.00	2.20	0.03	0.82	0.82	1.00
40	0.00	1.00	0.00	1.00	2.20	1.00	2.20	0.00	0.82	0.82	1.00
		7.50								0.76	

k 9.84

E	t	b	L	I	E	A
3.00E+10	0.50	4.00	30.00	2.67	3.00E+10	2.00

$final\ k$ 8.65 $N_{cr,B}$ 769 MN

Case 3: Uneven load; $b = 3$ m; $E = 15$ GPa in top half; $E = 30$ GPa in bottom half.

dx	0.025
L	1
eI	40

N	1
EI	1

	x/L	N tower	y	y_a	M tower	EI	y''	y'	y_b	y_a/y_b	New y
0	1.00	0.50	1.00	0.00	0.00	0.50	0.00	1.27	0.00	0.00	0.00
1	0.98	0.00	0.95	0.05	0.02	0.50	0.05	1.27	0.03	0.64	0.04
2	0.95	0.00	0.90	0.10	0.05	0.50	0.10	1.26	0.06	0.65	0.08
3	0.93	0.00	0.86	0.14	0.07	0.50	0.14	1.26	0.09	0.66	0.12
4	0.90	0.50	0.81	0.19	0.10	0.50	0.19	1.26	0.13	0.67	0.16
5	0.88	0.00	0.77	0.23	0.14	0.50	0.28	1.25	0.16	0.67	0.20
6	0.85	0.00	0.72	0.28	0.18	0.50	0.37	1.24	0.19	0.68	0.23
7	0.83	0.00	0.68	0.32	0.22	0.50	0.45	1.23	0.22	0.69	0.27
8	0.80	0.50	0.64	0.36	0.27	0.50	0.53	1.21	0.25	0.70	0.31
9	0.78	0.00	0.60	0.40	0.32	0.50	0.65	1.20	0.28	0.70	0.35
10	0.75	0.00	0.56	0.44	0.38	0.50	0.76	1.18	0.31	0.71	0.38
11	0.73	0.00	0.53	0.47	0.44	0.50	0.87	1.16	0.34	0.72	0.42
12	0.70	0.50	0.49	0.51	0.49	0.50	0.98	1.13	0.37	0.72	0.46
13	0.68	0.00	0.46	0.54	0.56	0.50	1.12	1.11	0.40	0.73	0.49
14	0.65	0.00	0.42	0.58	0.63	0.50	1.25	1.07	0.43	0.74	0.53
15	0.63	0.00	0.39	0.61	0.69	0.50	1.38	1.04	0.45	0.74	0.56
16	0.60	0.50	0.36	0.64	0.75	0.50	1.50	1.00	0.48	0.75	0.59
17	0.58	0.00	0.33	0.67	0.82	0.50	1.65	0.96	0.50	0.75	0.62
18	0.55	0.00	0.30	0.70	0.89	0.50	1.79	0.92	0.53	0.76	0.65
19	0.53	0.00	0.28	0.72	0.96	0.50	1.92	0.87	0.55	0.76	0.68

	x/L	N tower	y	y_a	M tower	EI	y''	y'	y_b	y_a/y_b	New y
20	0.50	1.00	0.25	0.75	1.03	1.00	1.03	0.84	0.57	0.76	0.71
21	0.48	0.00	0.23	0.77	1.11	1.00	1.11	0.81	0.59	0.77	0.73
22	0.45	0.00	0.20	0.80	1.19	1.00	1.19	0.79	0.61	0.77	0.76
23	0.43	0.00	0.18	0.82	1.27	1.00	1.27	0.75	0.63	0.77	0.78
24	0.40	1.00	0.16	0.84	1.34	1.00	1.34	0.72	0.65	0.78	0.81
25	0.38	0.00	0.14	0.86	1.43	1.00	1.43	0.68	0.67	0.78	0.83
26	0.35	0.00	0.12	0.88	1.51	1.00	1.51	0.65	0.69	0.78	0.85
27	0.33	0.00	0.11	0.89	1.58	1.00	1.58	0.61	0.70	0.79	0.87
28	0.30	1.00	0.09	0.91	1.66	1.00	1.66	0.57	0.72	0.79	0.89
29	0.28	0.00	0.08	0.92	1.73	1.00	1.73	0.52	0.73	0.79	0.91
30	0.25	0.00	0.06	0.94	1.81	1.00	1.81	0.48	0.75	0.80	0.92
31	0.23	0.00	0.05	0.95	1.87	1.000	1.87	0.43	0.76	0.80	0.94
32	0.20	1.00	0.04	0.96	1.93	1.000	1.93	0.38	0.77	0.80	0.95
33	0.18	0.00	0.03	0.97	1.99	1.000	1.99	0.33	0.78	0.80	0.96
34	0.15	0.00	0.02	0.98	2.04	1.000	2.04	0.28	0.79	0.80	0.97
35	0.13	0.00	0.02	0.98	2.09	1.000	2.09	0.23	0.79	0.81	0.98
36	0.10	1.00	0.01	0.99	2.13	1.000	2.13	0.18	0.80	0.81	0.99
37	0.08	0.00	0.01	0.99	2.16	1.000	2.16	0.12	0.80	0.81	0.99
38	0.05	0.00	0.00	1.00	2.18	1.000	2.18	0.07	0.81	0.81	1.00
39	0.03	0.00	0.00	1.00	2.20	1.000	2.20	0.01	0.81	0.81	1.00
40	0.00	1.00	0.00	1.00	1.00	1.000	1.00	0.00	0.81	0.81	1.00
		7.50								0.75	

k	9.98					
		E	t	b	L	I
		3.00E+10	0.50	3.00	30.00	1.13
						E
						3.00E+10
						A
						1.50
final k	8.65					
		$N_{cr,B}$	324	MN		

Case 4: Uneven load; $b = 8$ m; $E = 15$ GPa in top half; $E = 30$ GPa in bottom half.

dx	0.025
L	1
eI	40

N	1
EI	1

	x/L	N tower	y	y_a	M tower	EI	y''	y'	y_b	y_a/y_b	New y
0	1.00	0.50	1.00	0.00	0.00	0.50	0.00	1.27	0.00	0.00	0.00
1	0.98	0.00	0.95	0.05	0.02	0.50	0.05	1.27	0.03	0.64	0.04
2	0.95	0.00	0.90	0.10	0.05	0.50	0.10	1.26	0.06	0.65	0.08
3	0.93	0.00	0.86	0.14	0.07	0.50	0.14	1.26	0.09	0.66	0.12
4	0.90	0.50	0.81	0.19	0.10	0.50	0.19	1.26	0.13	0.67	0.16
5	0.88	0.00	0.77	0.23	0.14	0.50	0.28	1.25	0.16	0.67	0.20
6	0.85	0.00	0.72	0.28	0.18	0.50	0.37	1.24	0.19	0.68	0.23
7	0.83	0.00	0.68	0.32	0.22	0.50	0.45	1.23	0.22	0.69	0.27
8	0.80	0.50	0.64	0.36	0.27	0.50	0.53	1.21	0.25	0.70	0.31
9	0.78	0.00	0.60	0.40	0.32	0.50	0.65	1.20	0.28	0.70	0.35
10	0.75	0.00	0.56	0.44	0.38	0.50	0.76	1.18	0.31	0.71	0.38
11	0.73	0.00	0.53	0.47	0.44	0.50	0.87	1.16	0.34	0.72	0.42
12	0.70	0.50	0.49	0.51	0.49	0.50	0.98	1.13	0.37	0.72	0.46
13	0.68	0.00	0.46	0.54	0.56	0.50	1.12	1.11	0.40	0.73	0.49
14	0.65	0.00	0.42	0.58	0.63	0.50	1.25	1.07	0.43	0.74	0.53
15	0.63	0.00	0.39	0.61	0.69	0.50	1.38	1.04	0.45	0.74	0.56
16	0.60	0.50	0.36	0.64	0.75	0.50	1.50	1.00	0.48	0.75	0.59
17	0.58	0.00	0.33	0.67	0.82	0.50	1.65	0.96	0.50	0.75	0.62
18	0.55	0.00	0.30	0.70	0.89	0.50	1.79	0.92	0.53	0.76	0.65
19	0.53	0.00	0.28	0.72	0.96	0.50	1.92	0.87	0.55	0.76	0.68

	x/L	N_{tower}	y	y_a	M_{tower}	EI	y''	y'	y_b	y_a/y_b	$New\ y$
20	0.50	1.00	0.25	0.75	1.03	1.00	1.03	0.84	0.57	0.76	0.71
21	0.48	0.00	0.23	0.77	1.11	1.00	1.11	0.81	0.59	0.77	0.73
22	0.45	0.00	0.20	0.80	1.19	1.00	1.19	0.79	0.61	0.77	0.76
23	0.43	0.00	0.18	0.82	1.27	1.00	1.27	0.75	0.63	0.77	0.78
24	0.40	1.00	0.16	0.84	1.34	1.00	1.34	0.72	0.65	0.78	0.81
25	0.38	0.00	0.14	0.86	1.43	1.00	1.43	0.68	0.67	0.78	0.83
26	0.35	0.00	0.12	0.88	1.51	1.00	1.51	0.65	0.69	0.78	0.85
27	0.33	0.00	0.11	0.89	1.58	1.00	1.58	0.61	0.70	0.79	0.87
28	0.30	1.00	0.09	0.91	1.66	1.00	1.66	0.57	0.72	0.79	0.89
29	0.28	0.00	0.08	0.92	1.73	1.00	1.73	0.52	0.73	0.79	0.91
30	0.25	0.00	0.06	0.94	1.81	1.00	1.81	0.48	0.75	0.80	0.92
31	0.23	0.00	0.05	0.95	1.87	1.00	1.87	0.43	0.76	0.80	0.94
32	0.20	1.00	0.04	0.96	1.93	1.00	1.93	0.38	0.77	0.80	0.95
33	0.18	0.00	0.03	0.97	1.99	1.00	1.99	0.33	0.78	0.80	0.96
34	0.15	0.00	0.02	0.98	2.04	1.00	2.04	0.28	0.79	0.80	0.97
35	0.13	0.00	0.02	0.98	2.09	1.00	2.09	0.23	0.79	0.81	0.98
36	0.10	1.00	0.01	0.99	2.13	1.00	2.13	0.18	0.80	0.81	0.99
37	0.08	0.00	0.01	0.99	2.16	1.00	2.16	0.12	0.80	0.81	0.99
38	0.05	0.00	0.00	1.00	2.18	1.00	2.18	0.07	0.81	0.81	1.00
39	0.03	0.00	0.00	1.00	2.20	1.00	2.20	0.01	0.81	0.81	1.00
40	0.00	1.00	0.00	1.00	1.00	1.00	1.00	0.00	0.81	0.81	1.00
		7.50								0.75	

k	9.98					
		E	t	b	L	I
		3.00E+10	0.50	8.00	30.00	21.33
		E	A			
		3.00E+10	4.00			
$final\ k$	8.65					
		$N_{cr,B}$	6150	MN		

APPENDIX B. Results from all investigated pierced shear walls

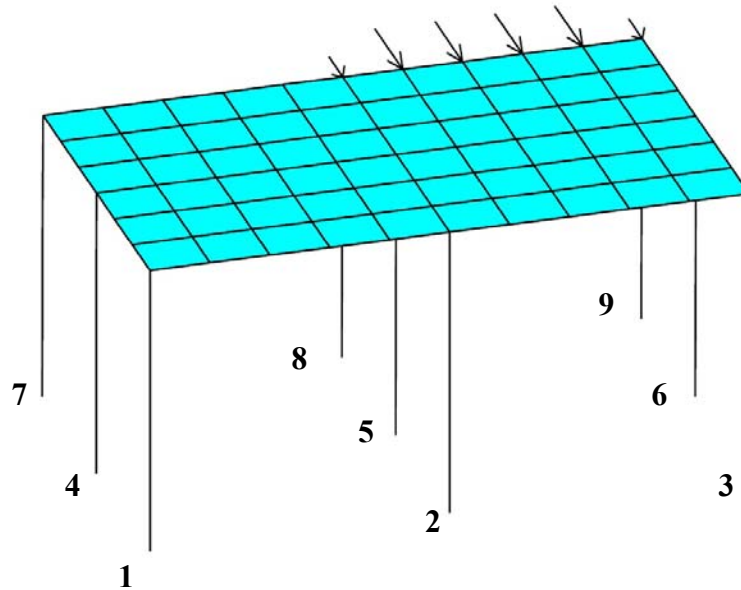
The walls are tabulated on two pages and each wall is given a number for simplicity. The numbers are only relative for this appendix and are not referred to in the text. The results are discussed in chapter 5.3.

This appendix is useful for comparing with real walls and to draw conclusions how the calculation method concerning the buckling loads is suitable for the real wall.

Wall number	Bending		FEM		Shear Factors				Comparison - Hand calculations & FEM			
	NcrB		Ncrsher-FEA		SF	SF	SF	SF	NcrHc/NcrFE	NcrHc/NcrFE	NcrHc/NcrFE	NcrHc/NcrFE
	[MN]	[MN]	[MN]	[MN]	c=c0	c=c0	c=c0	c=c0	c=c0+ht	c=c0	c=c0	c=c0
1	4835		40295		1,49	1,27	1,28		0,78	0,95	0,97	0,97
2	529		1147		1,66	1,31	1,53		0,63	0,83	0,91	0,86
3	786		3417		1,78	1,46	1,57		0,67	0,87	0,92	0,90
4	2796		86		2,87	2,87	2,87		0,31	0,36	0,36	0,36
5	298		826		1,68	1,23	1,55		0,67	0,85	0,94	0,87
6	298		2662		2,44	1,03	1,72		0,78	0,87	1,00	0,93
7	298		4926		3,87	1,25	2,11		0,79	0,86	0,99	0,94
8	298		9569		7,05	1,94	2,98		0,79	0,84	0,97	0,94
9	529		4135		2,54	1,30	1,74		0,74	0,85	0,97	0,92
10	335		6266		2,23	1,24	1,73		0,85	0,94	0,99	0,96
11	197		612		3,04	0,43	1,71		0,63	0,67	1,16	0,85
12	16240		27650		1,71	1,64	1,66		0,50	0,79	0,81	0,80
13	15720		11126		1,97	1,91	1,93		0,40	0,64	0,65	0,65
14	11480		2400		1,73	1,64	1,67		0,45	0,62	0,65	0,64
15	4581		2255		2,22	2,18	2,20		0,36	0,55	0,56	0,55
16	4581		4742		1,76	1,66	1,71		0,48	0,73	0,75	0,74
17	4581		8008		1,70	1,54	1,60		0,54	0,80	0,83	0,82
18	4581		14156		1,85	1,58	1,63		0,61	0,83	0,88	0,87
19	4581		20254		2,09	1,70	1,73		0,65	0,83	0,89	0,88
20	4760		4808		2,02	1,97	2,00		0,41	0,66	0,67	0,67
21	4760		9252		1,72	1,61	1,66		0,53	0,80	0,83	0,82
22	4760		13904		1,69	1,53	1,59		0,60	0,85	0,88	0,87
23	4760		20987		1,80	1,57	1,61		0,66	0,87	0,91	0,90
24	4760		26841		1,94	1,64	1,66		0,69	0,88	0,91	0,91
25	4826		11270		1,47	1,39	1,44		0,58	0,88	0,89	0,88
26	4826		19690		1,62	1,48	1,55		0,65	0,89	0,91	0,90
27	4826		24544		1,62	1,45	1,51		0,69	0,91	0,93	0,92
28	4826		30409		1,67	1,46	1,50		0,73	0,92	0,94	0,94
29	4826		33106		1,71	1,48	1,50		0,74	0,92	0,94	0,94

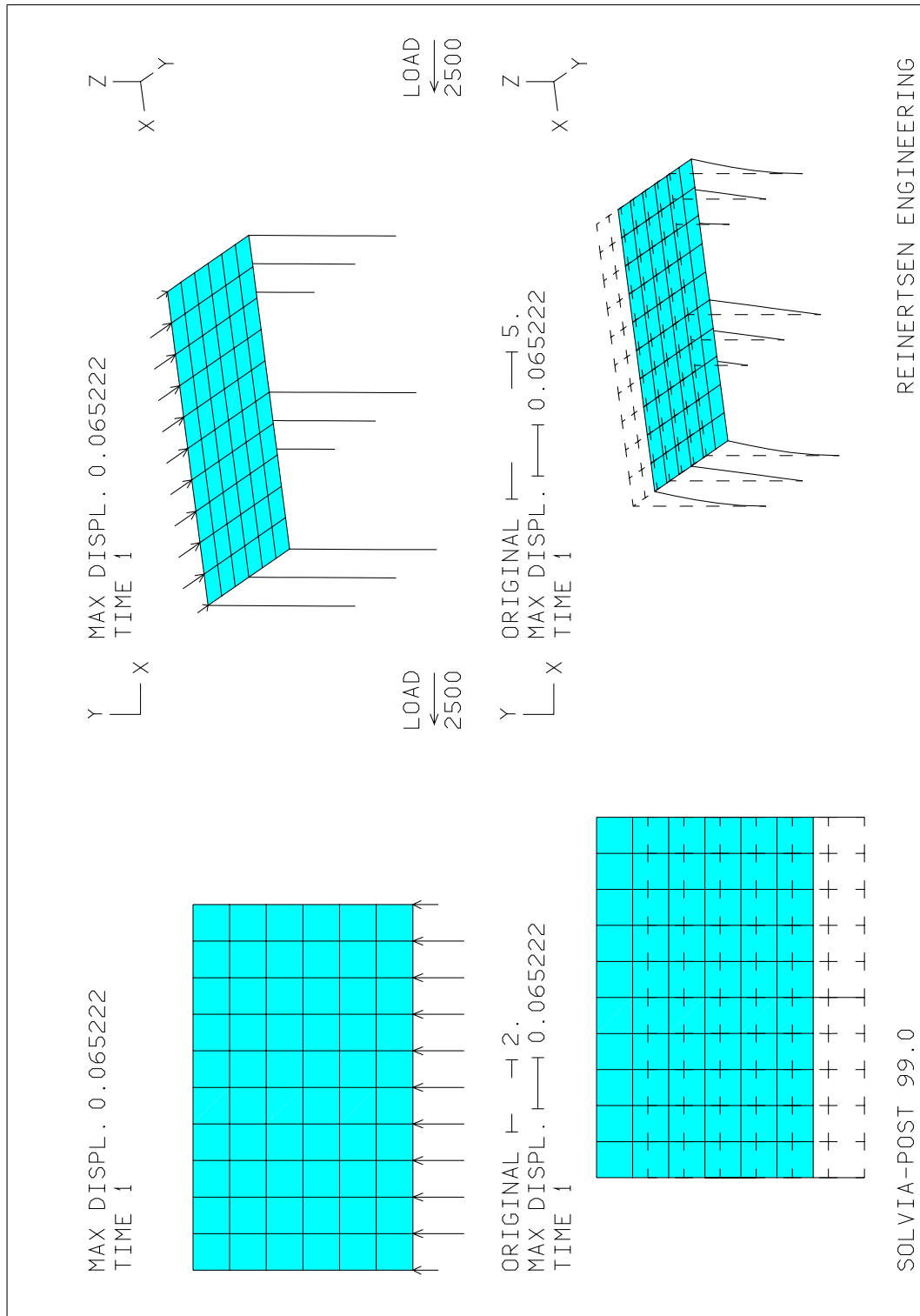
APPENDIX C. Force distribution in single storey structures

Appendix C presents the deformation figures and load application from the FE-analyses of a single storey structure. The figure below illustrates the identification numbers of the columns for comparing with the hand calculations in Section 5.5.2, 5.5.3 and 5.5.4.



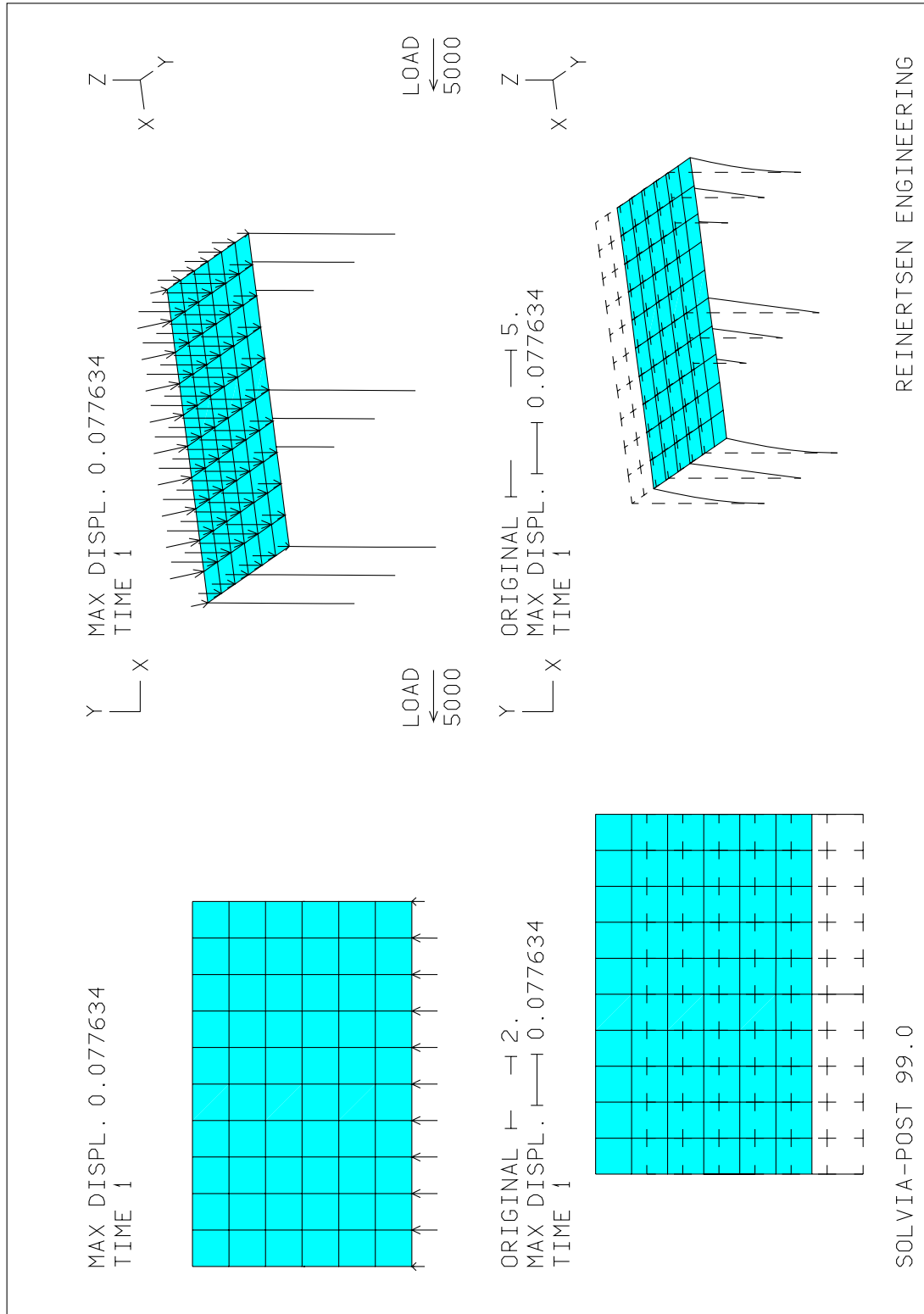
APPENDIX C. Force distribution in single storey structures

Load application and deformation. Case 1 – Translation



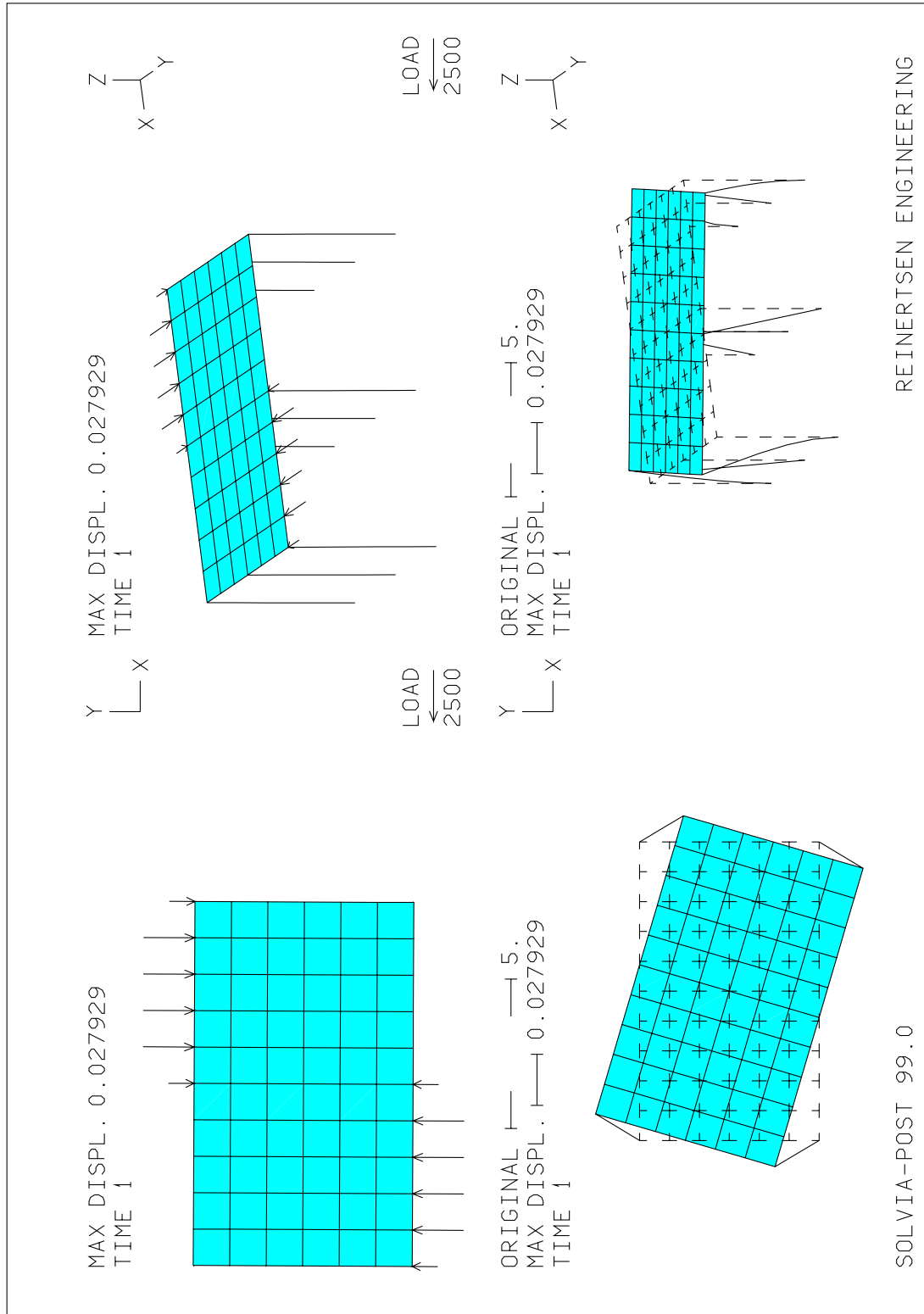
APPENDIX C. Force distribution in single storey structures

Load application and deformation. Case 1 – Translation with vertical load



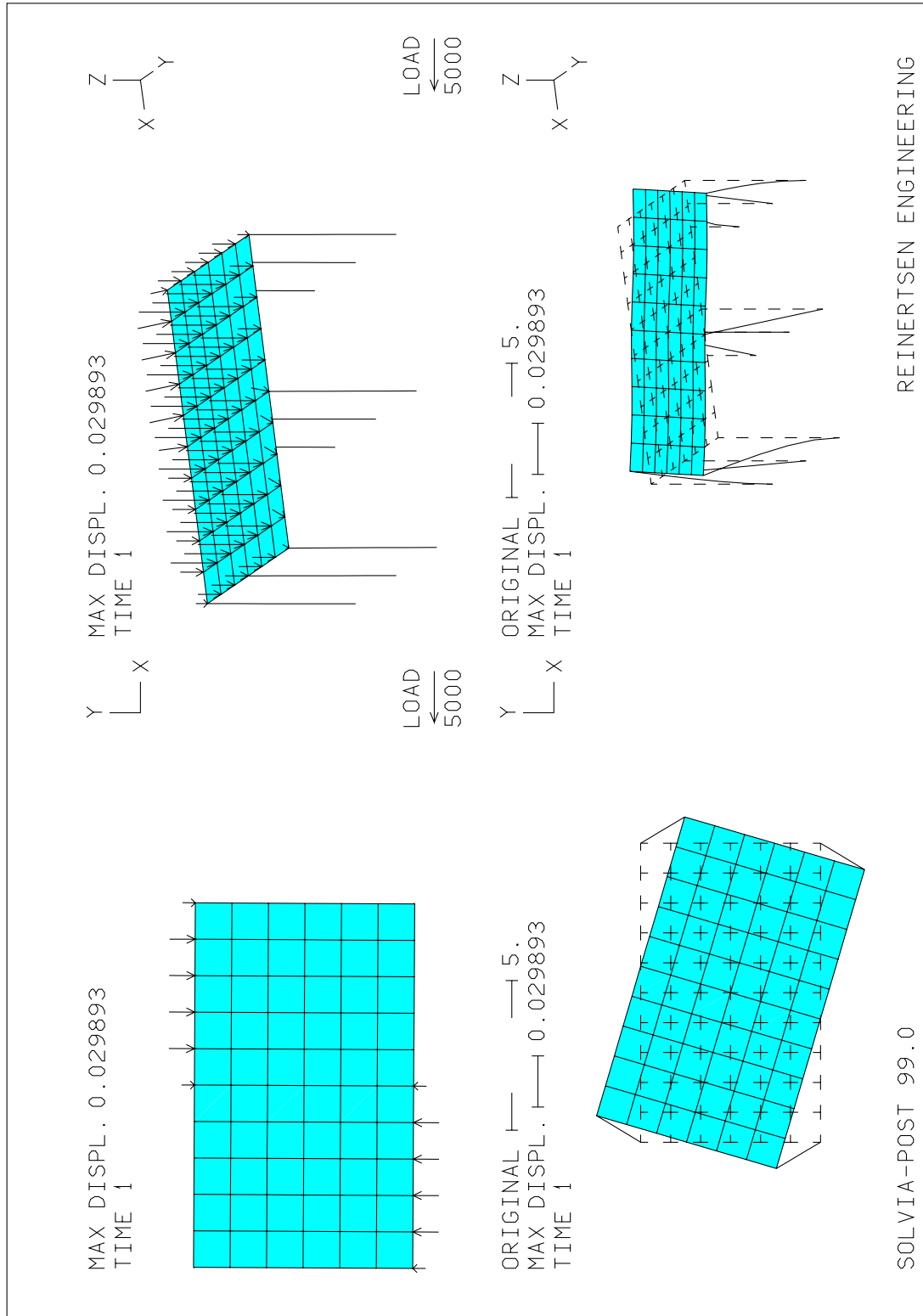
APPENDIX C. Force distribution in single storey structures

Load application and deformation. Case 2 – Twisting



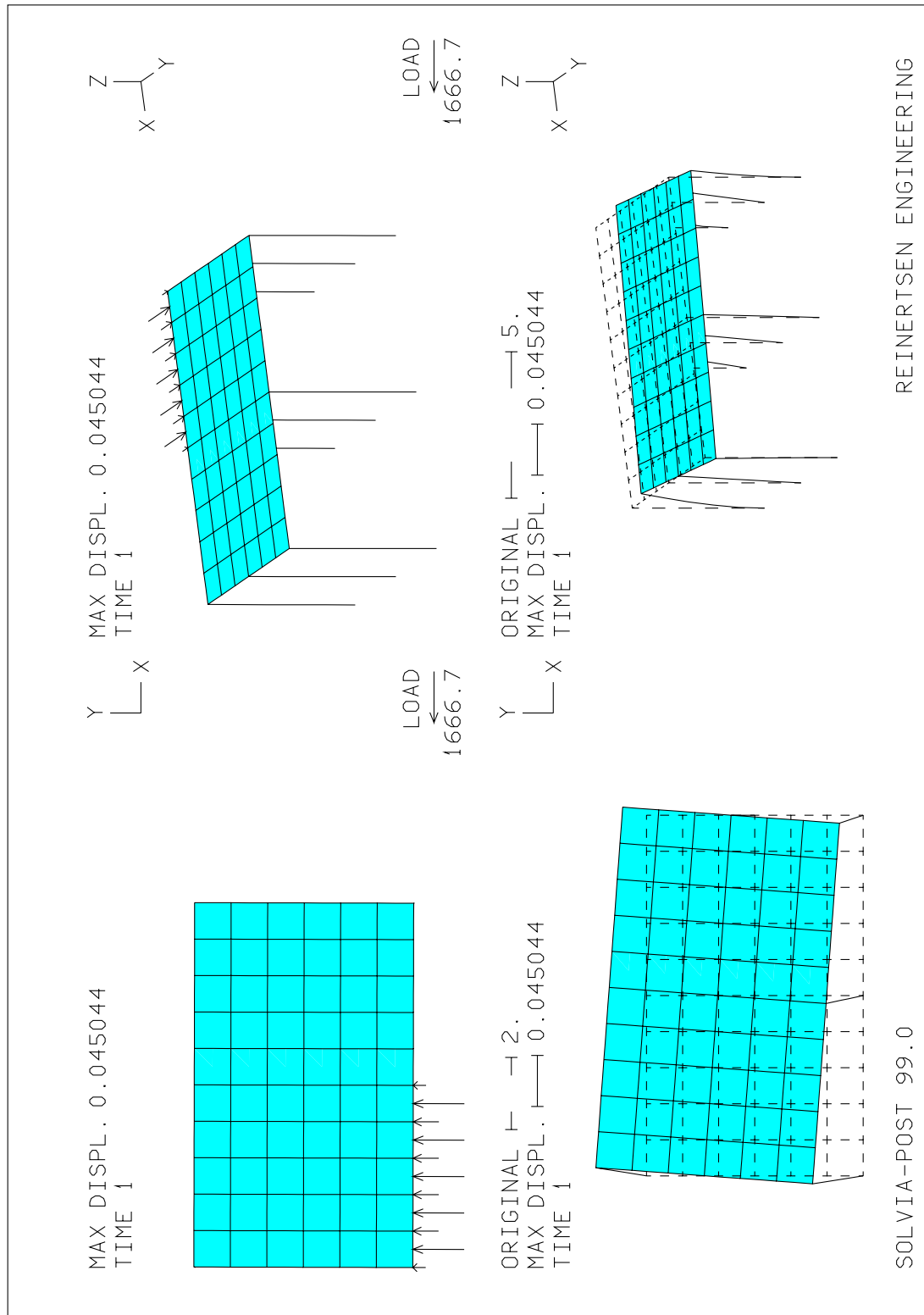
APPENDIX C. Force distribution in single storey structures

Load application and deformation. Case 2 – Twisting with vertical load.



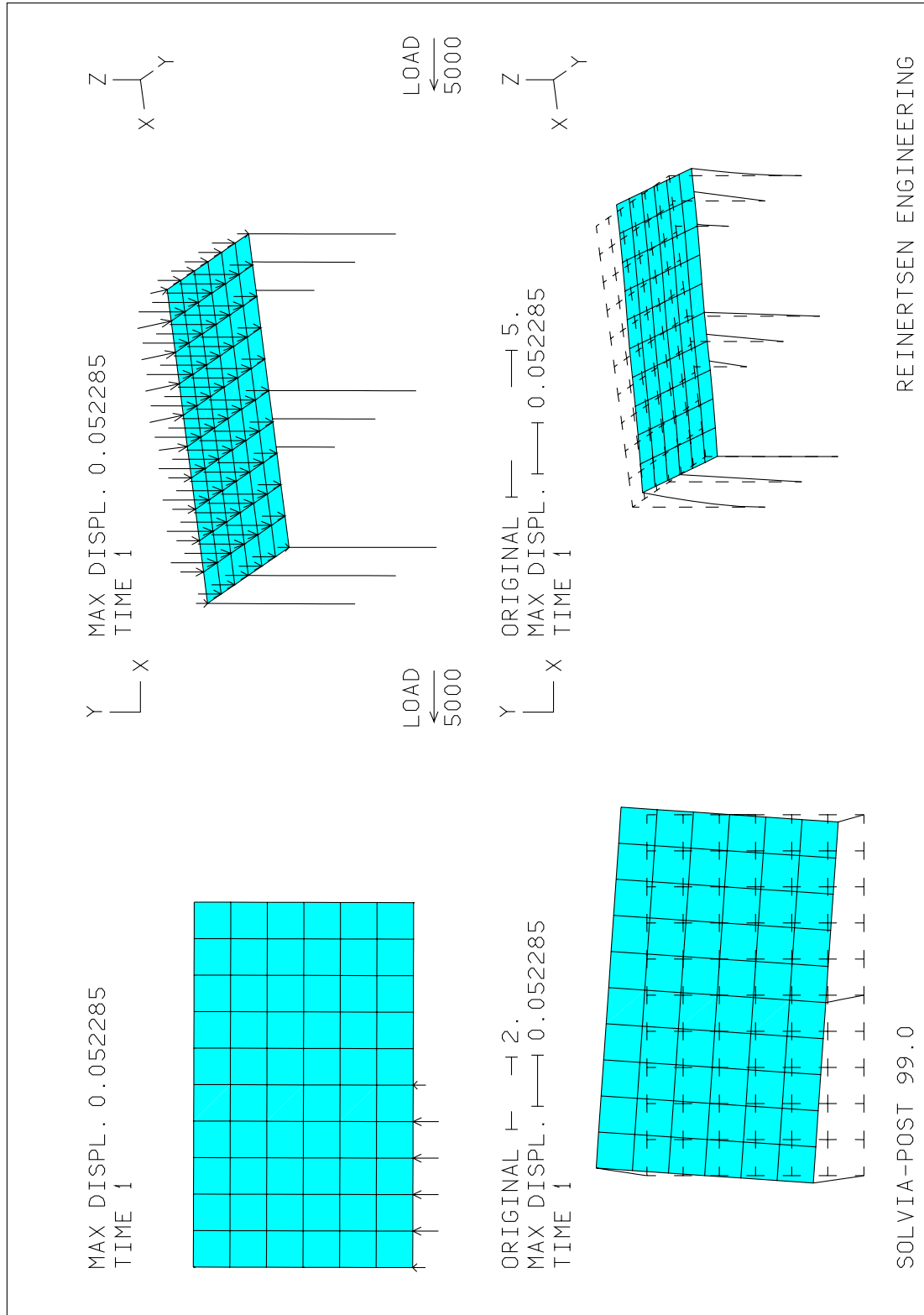
APPENDIX C. Force distribution in single storey structures

Load application and deformation. Case 3 – Combined translation and twisting.



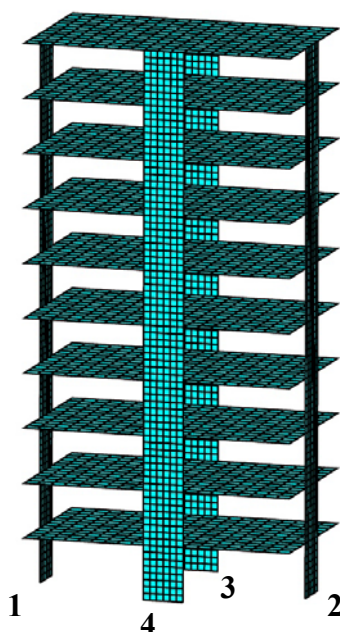
APPENDIX C. Force distribution in single storey structures

Load application and deformation. Case 3 – Combined translation and twisting with vertical load.

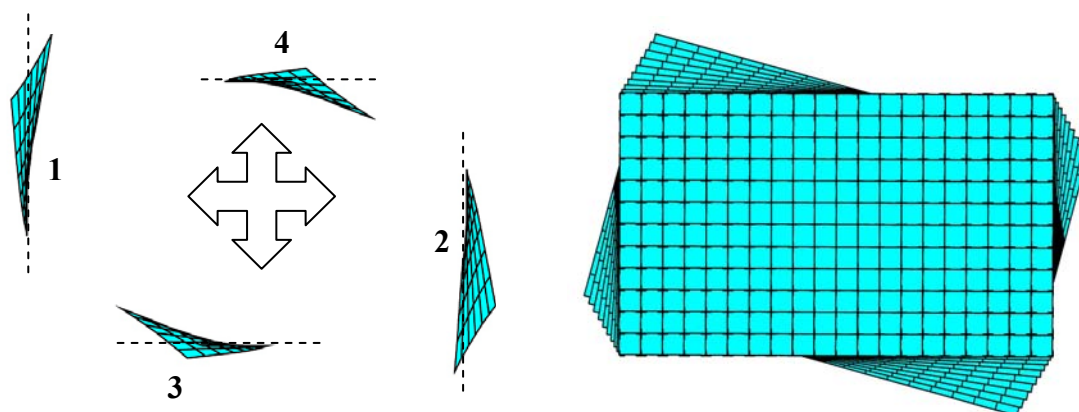


APPENDIX D Force distribution in a multi storey structure

The investigation of the force distribution in a multi storey structure considers two models. The numbering of the four walls, used in the hand calculation in Section 5.7.2 and 5.7.3, are explained by the figure below for comparing the FE-results with the hand calculation results. The force distribution in the four walls is presented in a graph for each wall. The graphs presents values of the force per meter and are plotted from the walls edge to the right edge when the wall is viewed from the inside, i.e. viewed from the centre of the four walls to the actual wall presented.



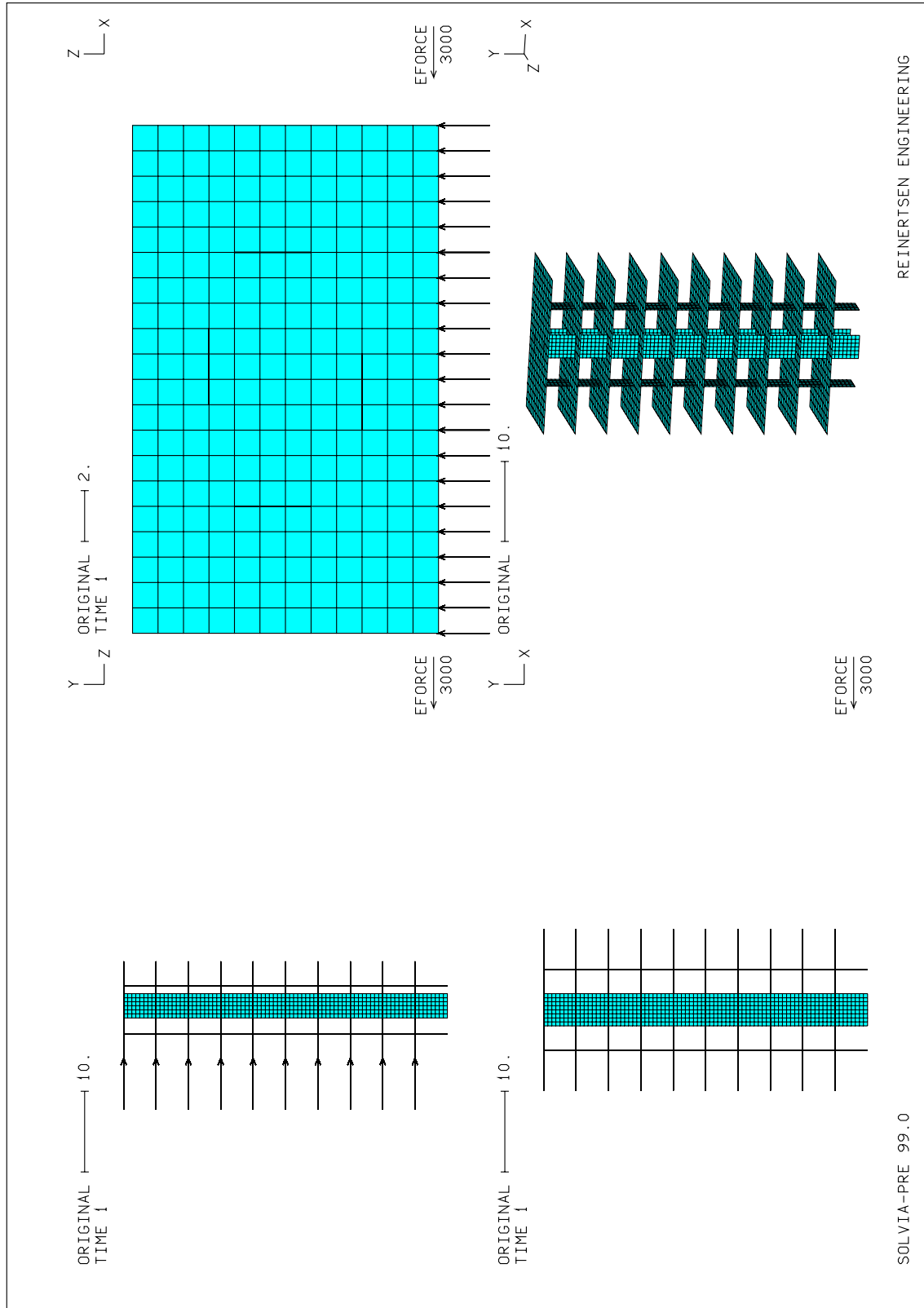
The figures concerning the deformation pictures of the four walls at the lowest storey and the floor slabs in this appendix, Appendix D, are viewed from the underneath.



APPENDIX D.1 Force distribution in a multi-storey structure

Load applications and figure illustrations. Case 1b – Translation

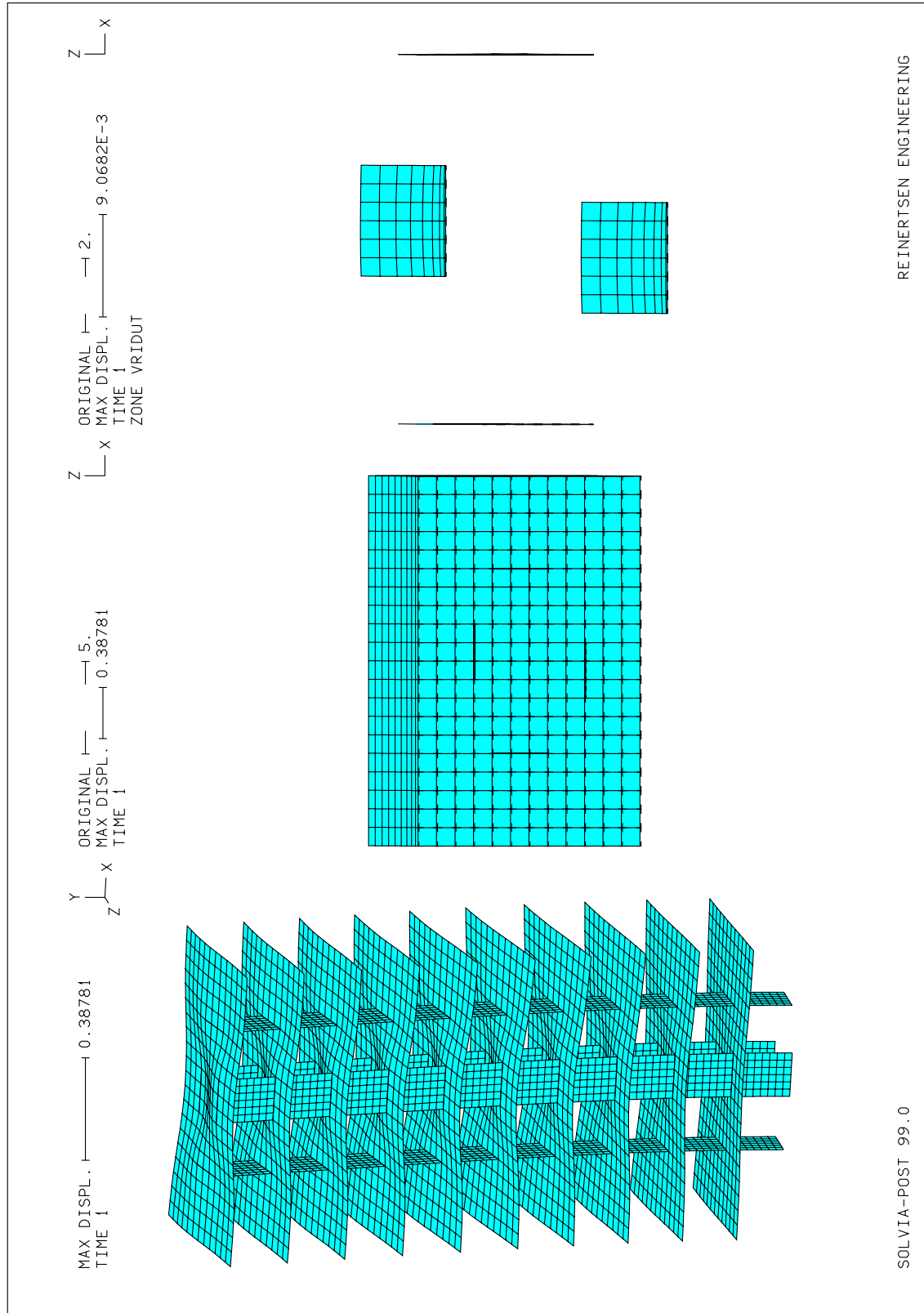
Floor slab: $E = 1\text{Gpa}$ $t = 0.1\text{ m}$



APPENDIX D.1 Force distribution in a multi-storey structure

Deformation figures. Case 1b – Translation

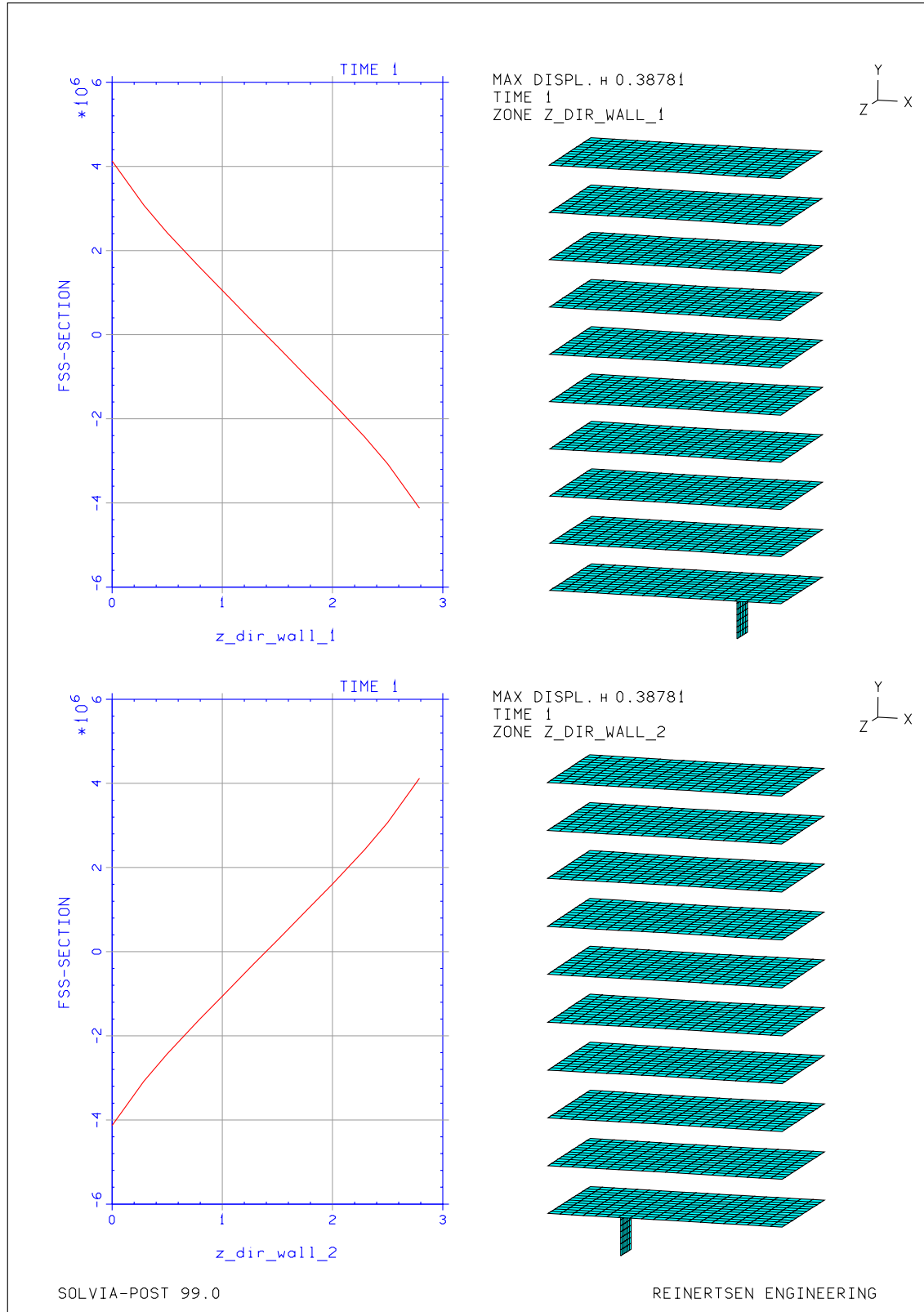
Floor slab: $E = 1\text{Gpa}$ $t = 0.1\text{ m}$



APPENDIX D.1 Force distribution in a multi-storey structure

Force distribution in wall 1 and 2. Case 1b – Translation

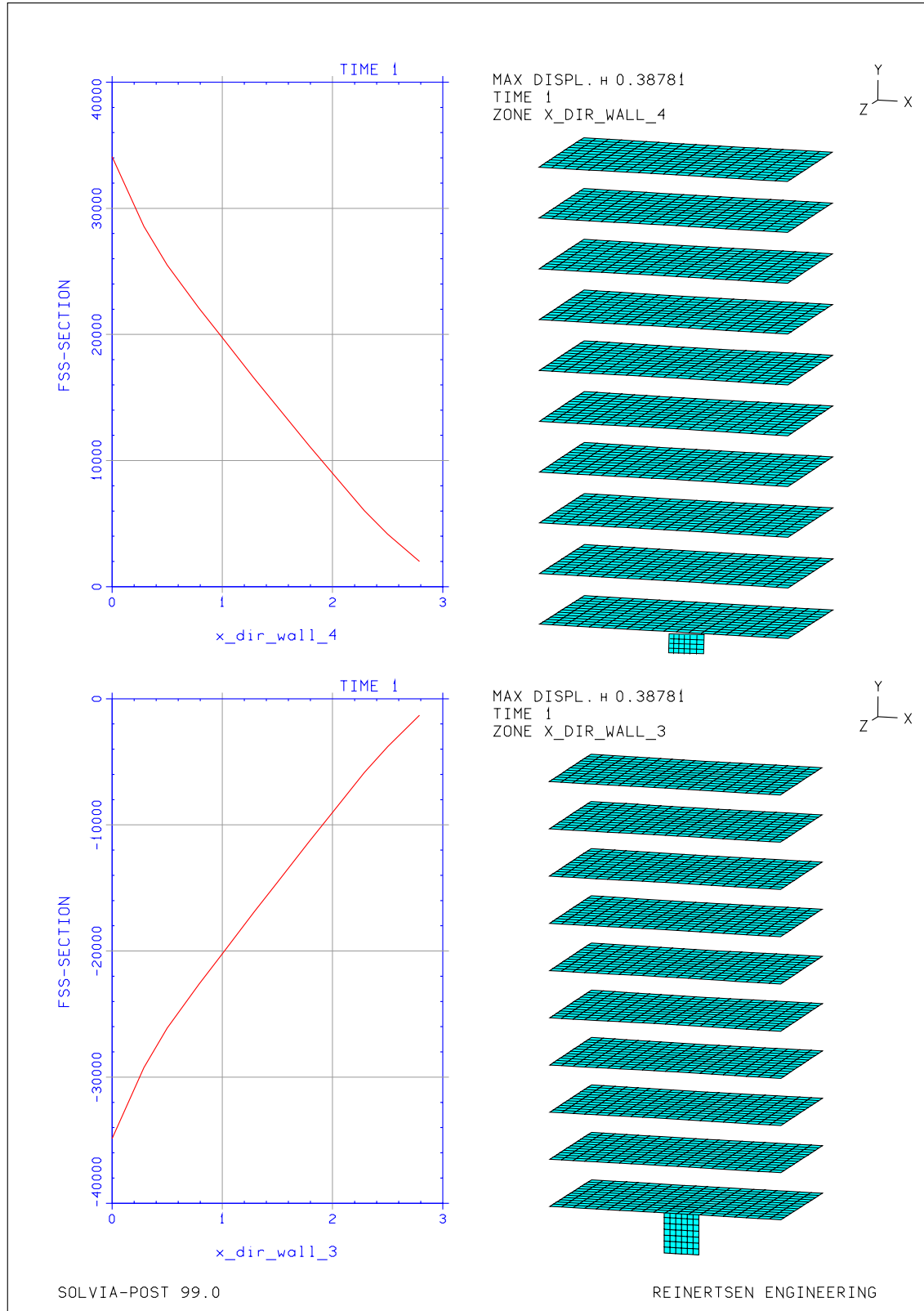
Floor slab: $E = 1\text{Gpa}$ $t = 0.1\text{ m}$



APPENDIX D.1 Force distribution in a multi-storey structure

Force distribution in wall 3 and 4. Case 1b – Translation

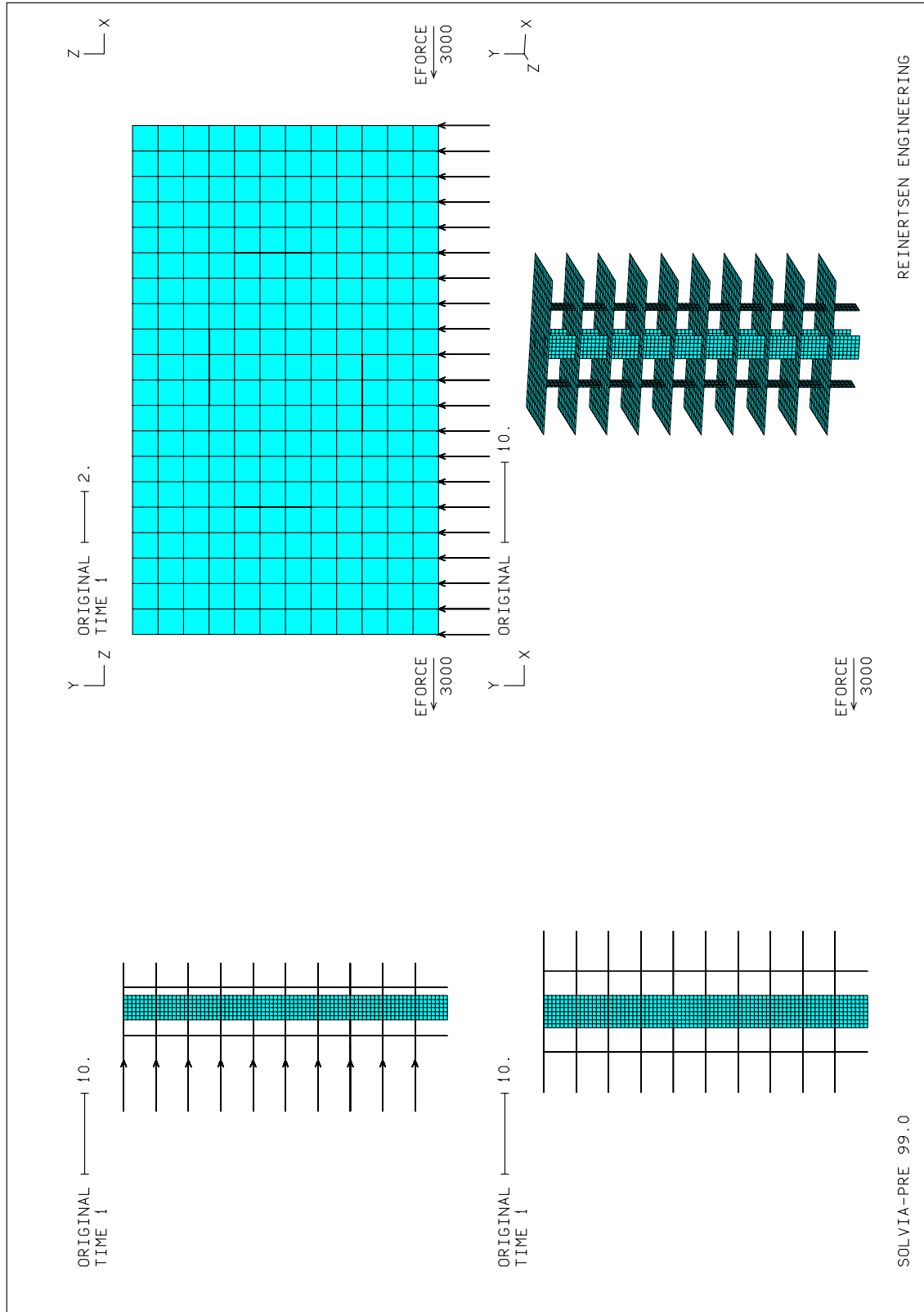
Floor slab: $E = 1\text{Gpa}$ $t = 0.1\text{ m}$



APPENDIX D.1 Force distribution in a multi-storey structure

Load applications and figure illustrations. Case 1b – Translation

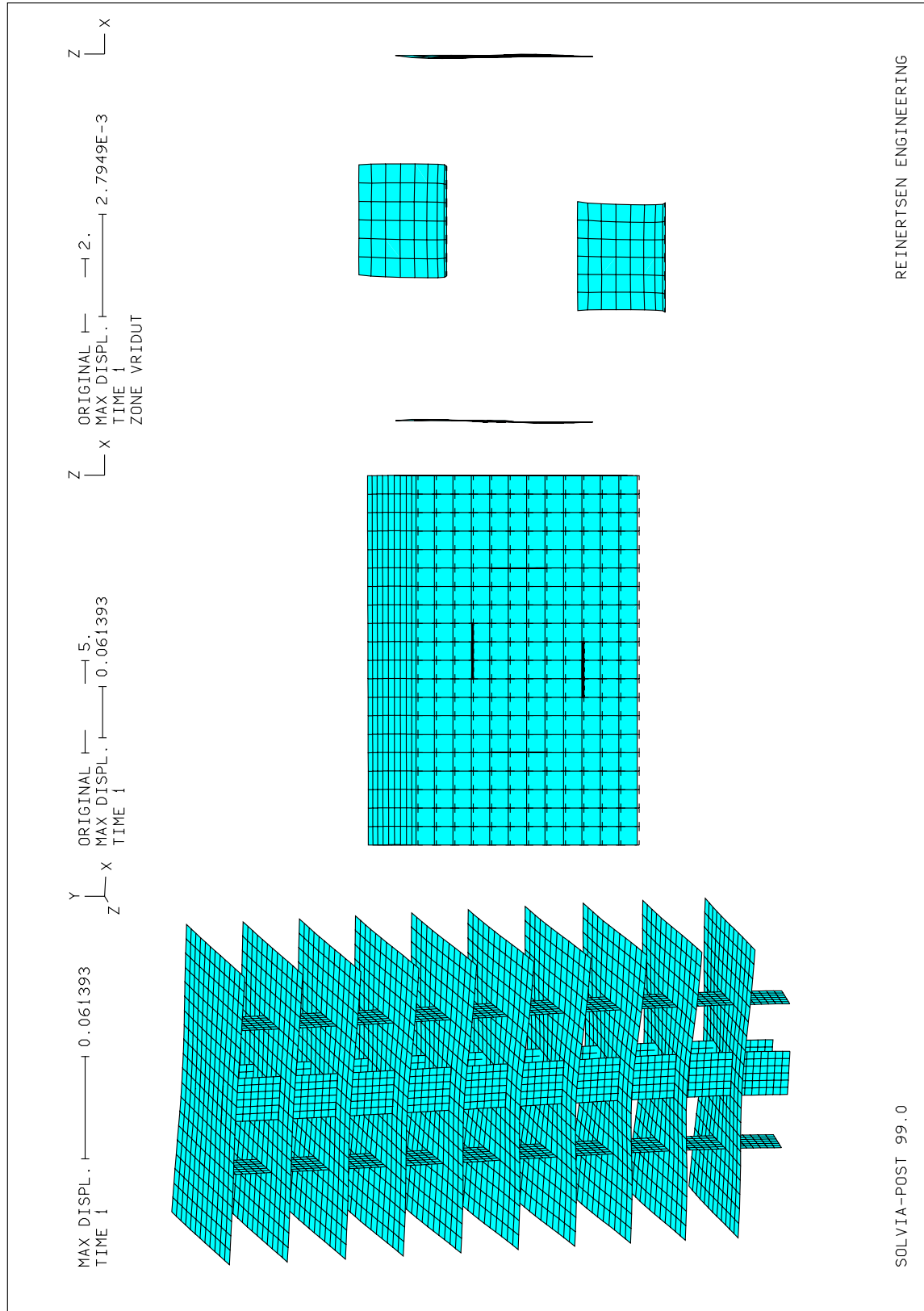
Floor slab: $E = 30 \text{ Gpa}$ $t = 0.3 \text{ m}$



APPENDIX D.1 Force distribution in a multi-storey structure

Deformation figures. Case 1b – Translation

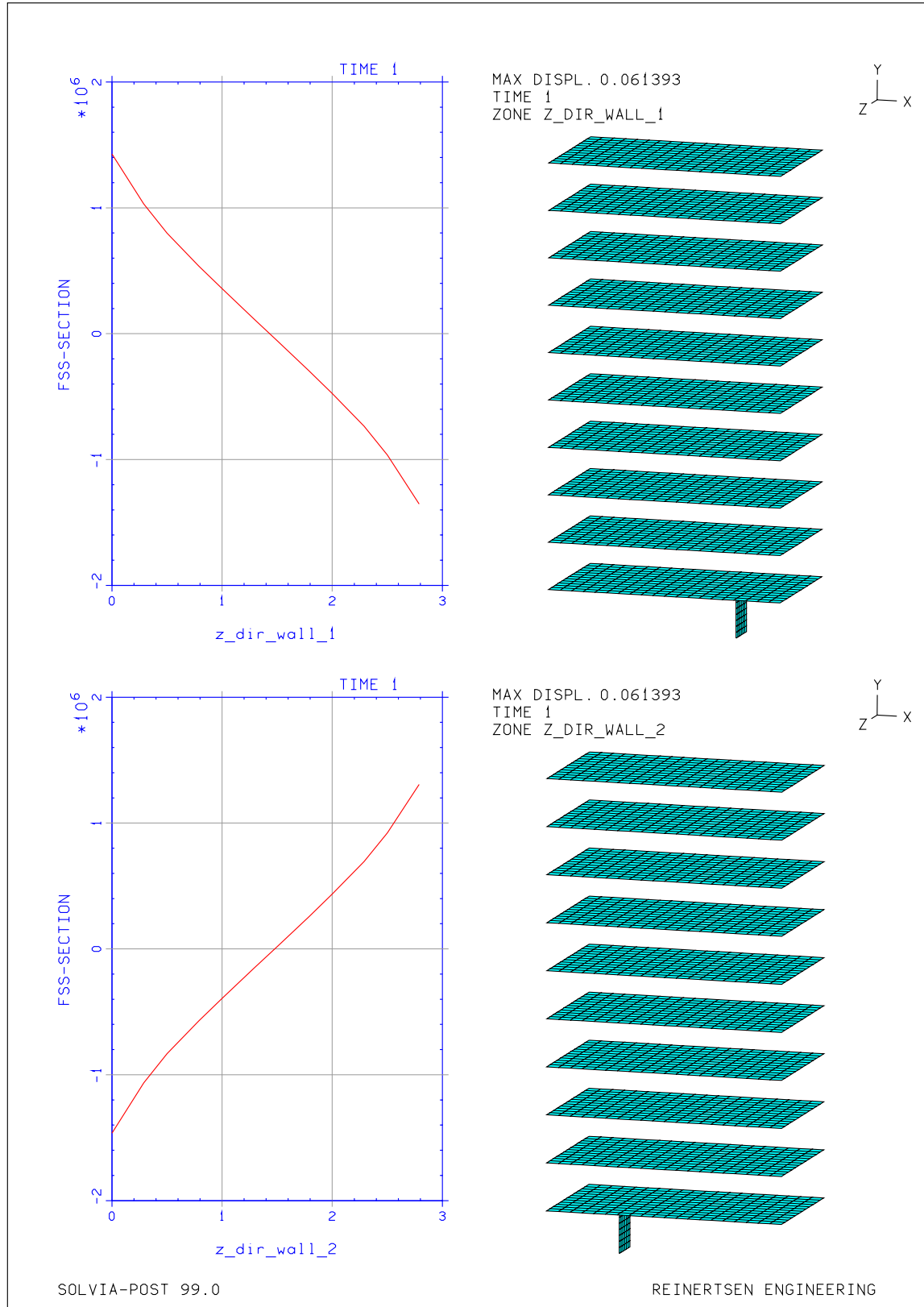
Floor slab: $E = 30 \text{ Gpa}$ $t = 0.3 \text{ m}$



APPENDIX D.1 Force distribution in a multi-storey structure

Force distribution in wall 1 and 2. Case 1b – Translation

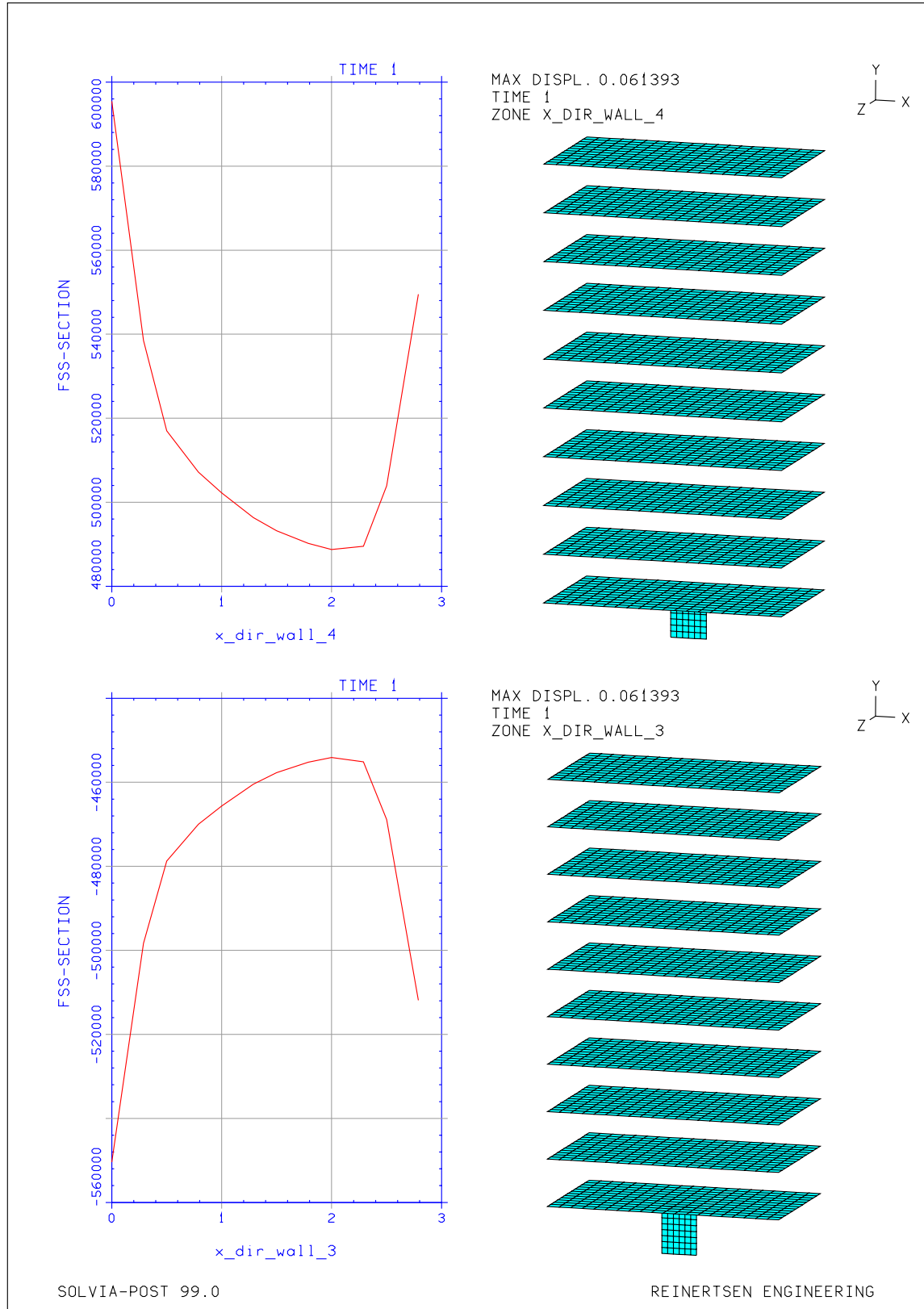
Floor slab: $E = 30 \text{ Gpa}$ $t = 0.3 \text{ m}$



APPENDIX D.1 Force distribution in a multi-storey structure

Force distribution in wall 3 and 4. Case 1b – Translation

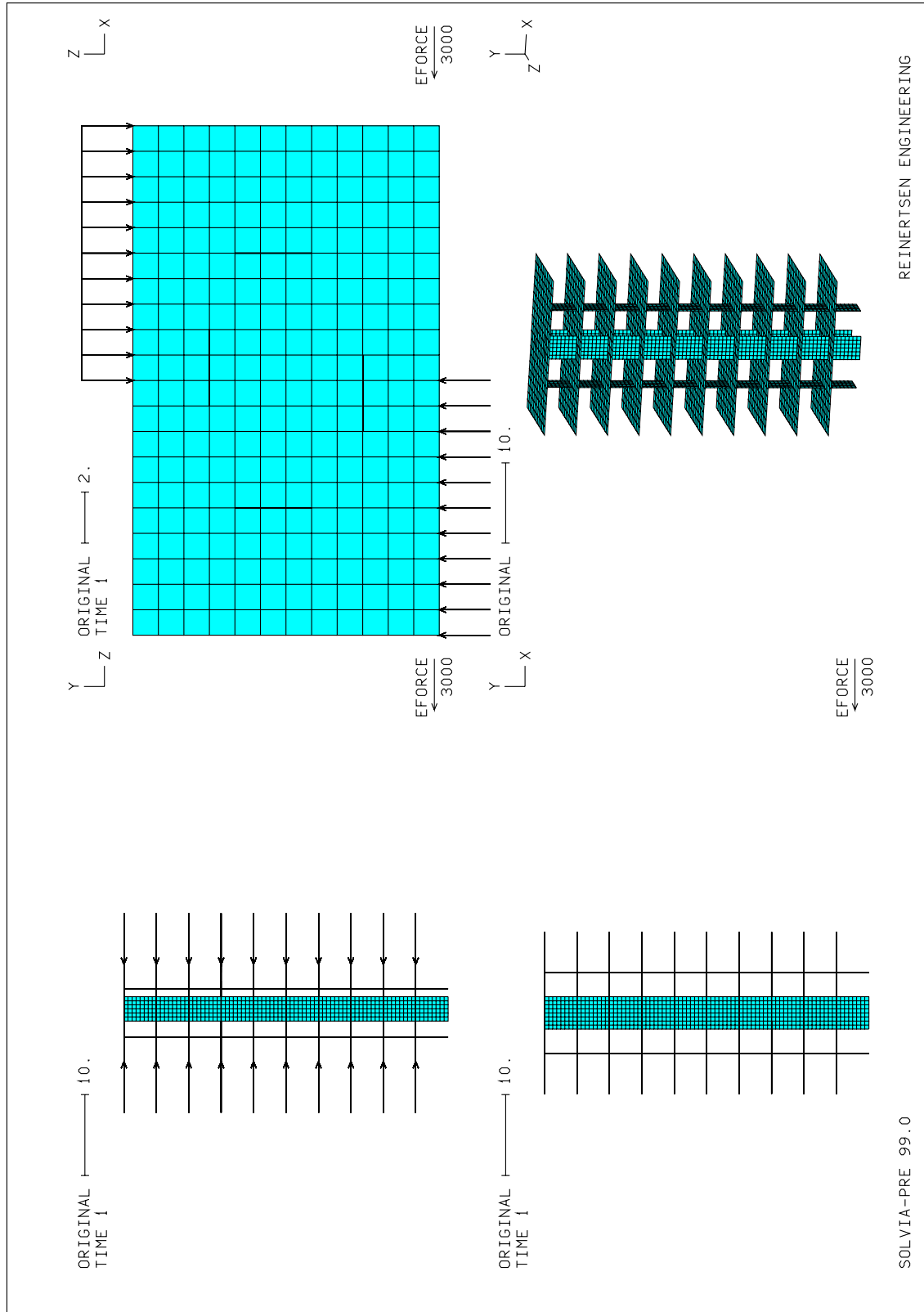
Floor slab: $E = 30 \text{ Gpa}$ $t = 0.3 \text{ m}$



APPENDIX D.2 Force distribution in a multi-storey structure

Load applications and figure illustrations. Case 2b – Twisting

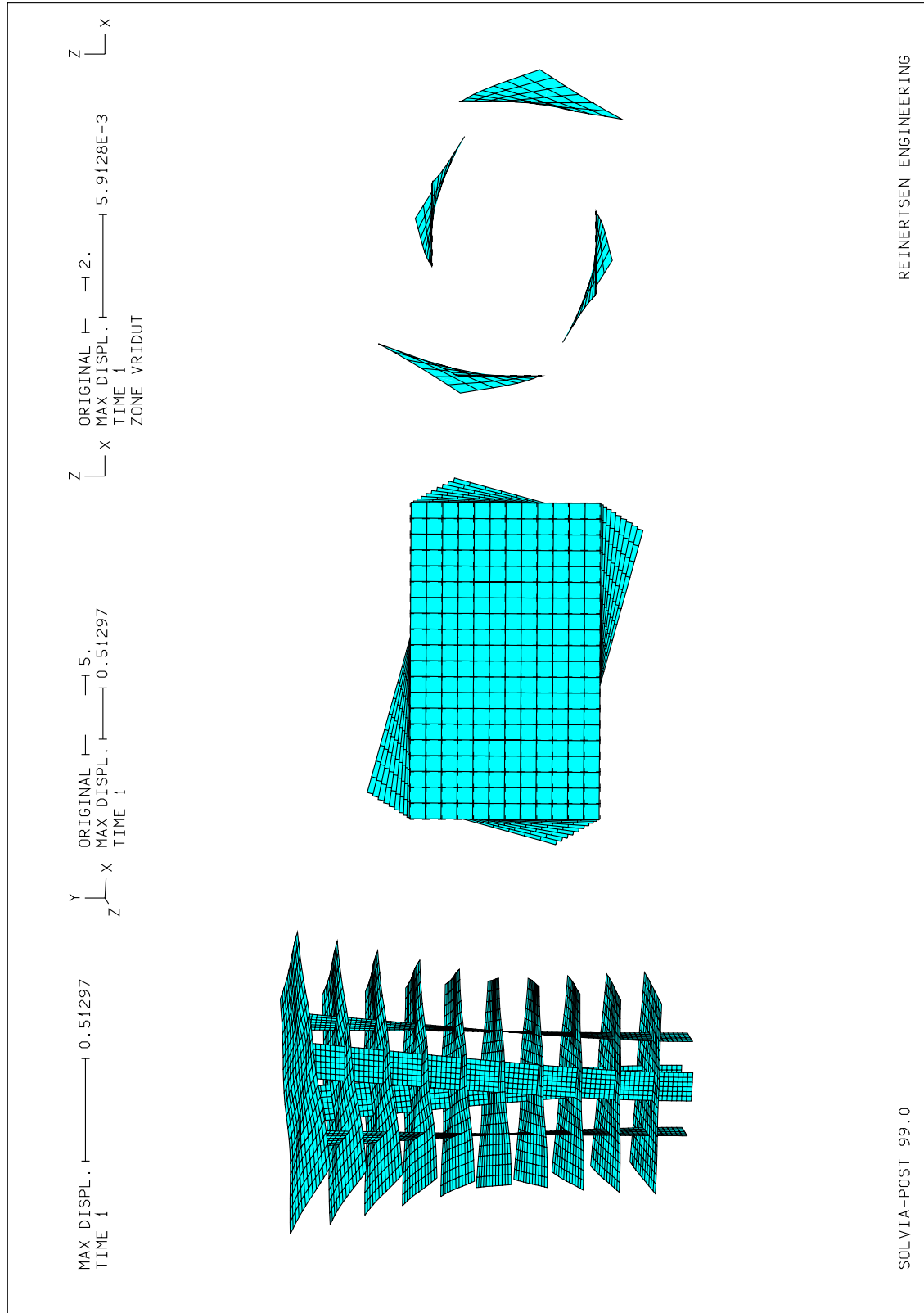
Floor slab: $E = 2\text{Gpa}$ $t = 0.1\text{ m}$



APPENDIX D.2 Force distribution in a multi-storey structure

Deformation figures Case 2b – Twisting

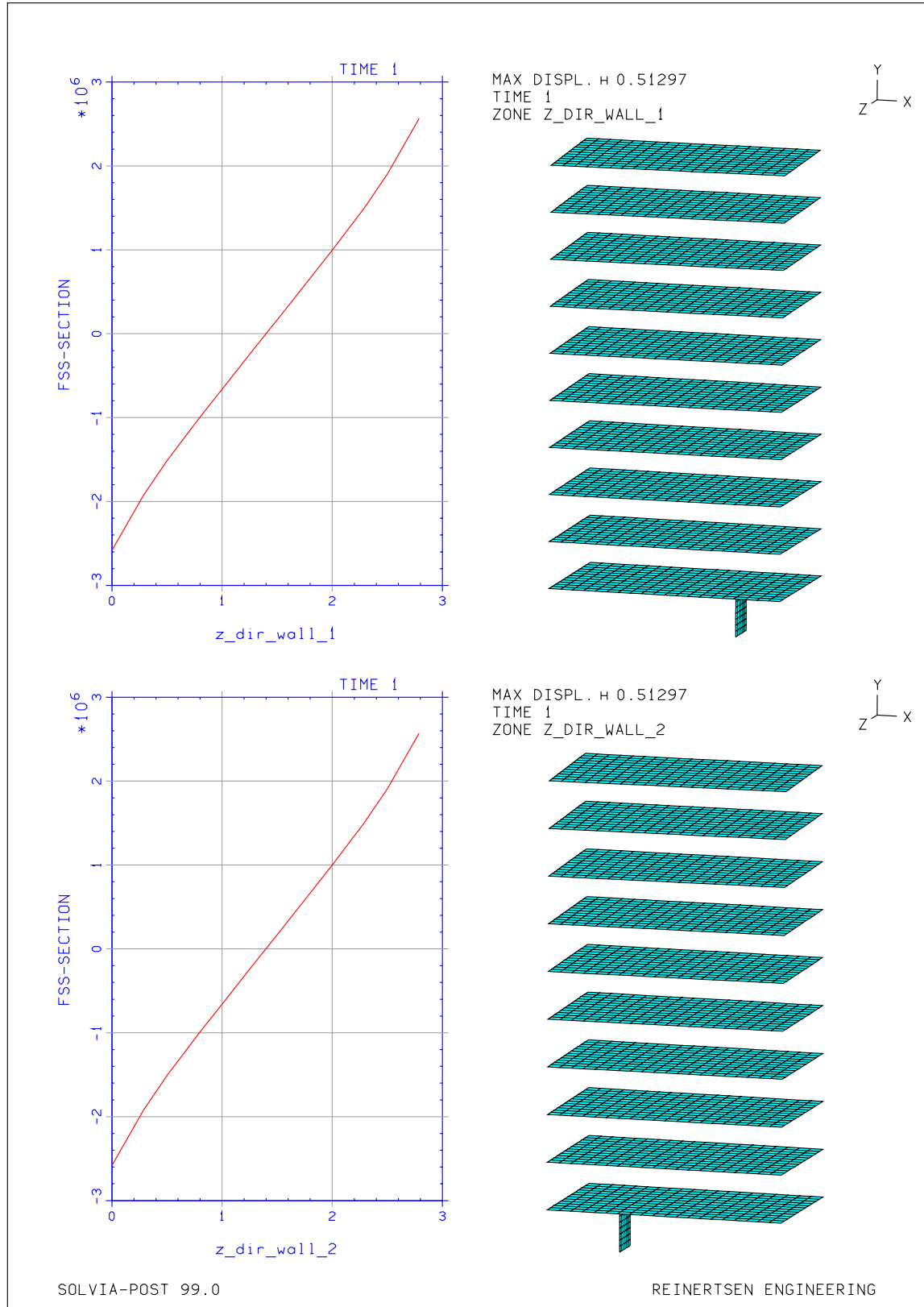
Floor slab: $E = 2\text{Gpa}$ $t = 0.1\text{ m}$



APPENDIX D.2 Force distribution in a multi-storey structure

Load distribution in wall 1 and 2. Case 2b – Twisting

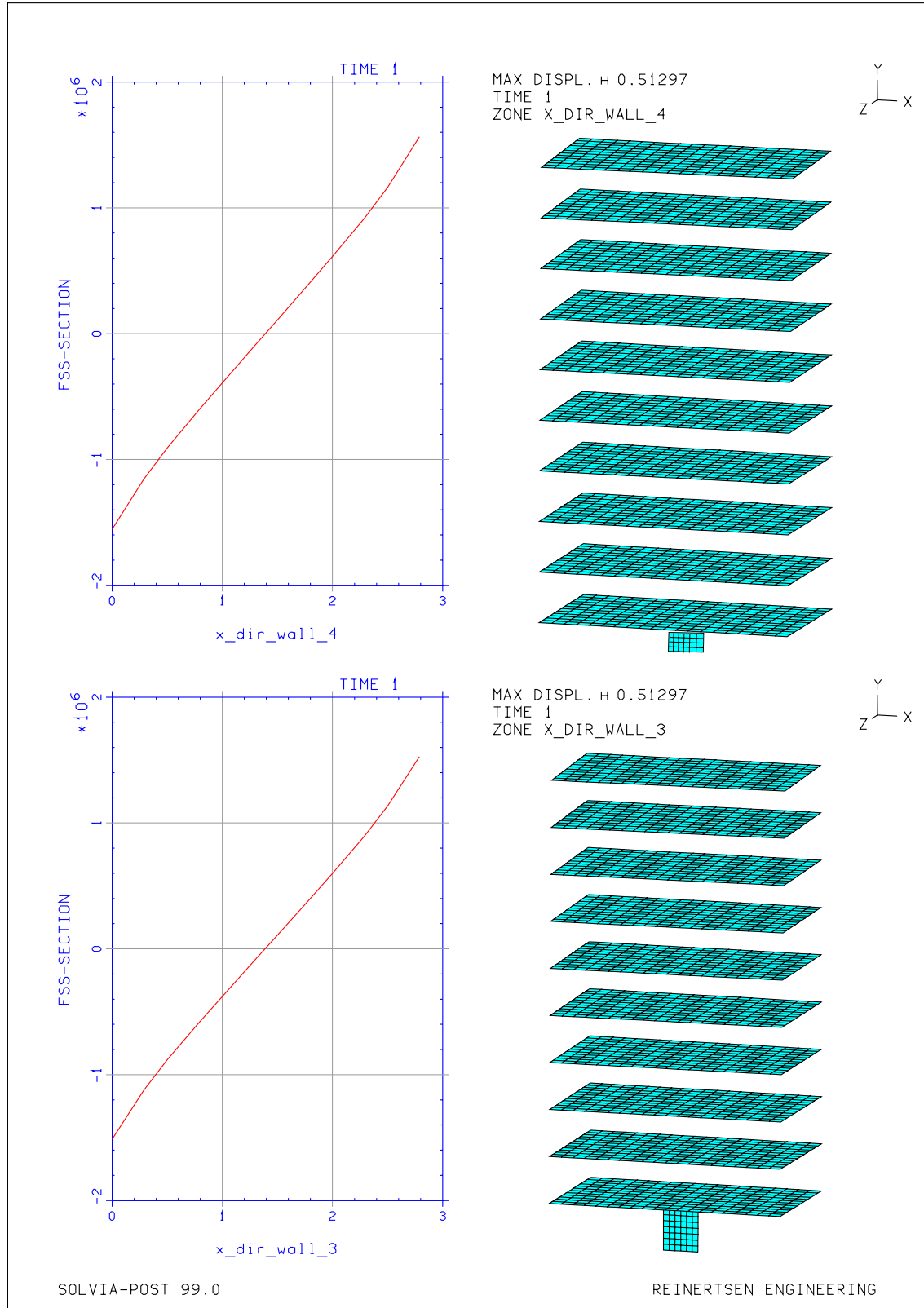
Floor slab: $E = 2\text{Gpa}$ $t = 0.1\text{ m}$



APPENDIX D.2 Force distribution in a multi-storey structure

Load distribution in wall 3 and 4. Case 2b – Twisting

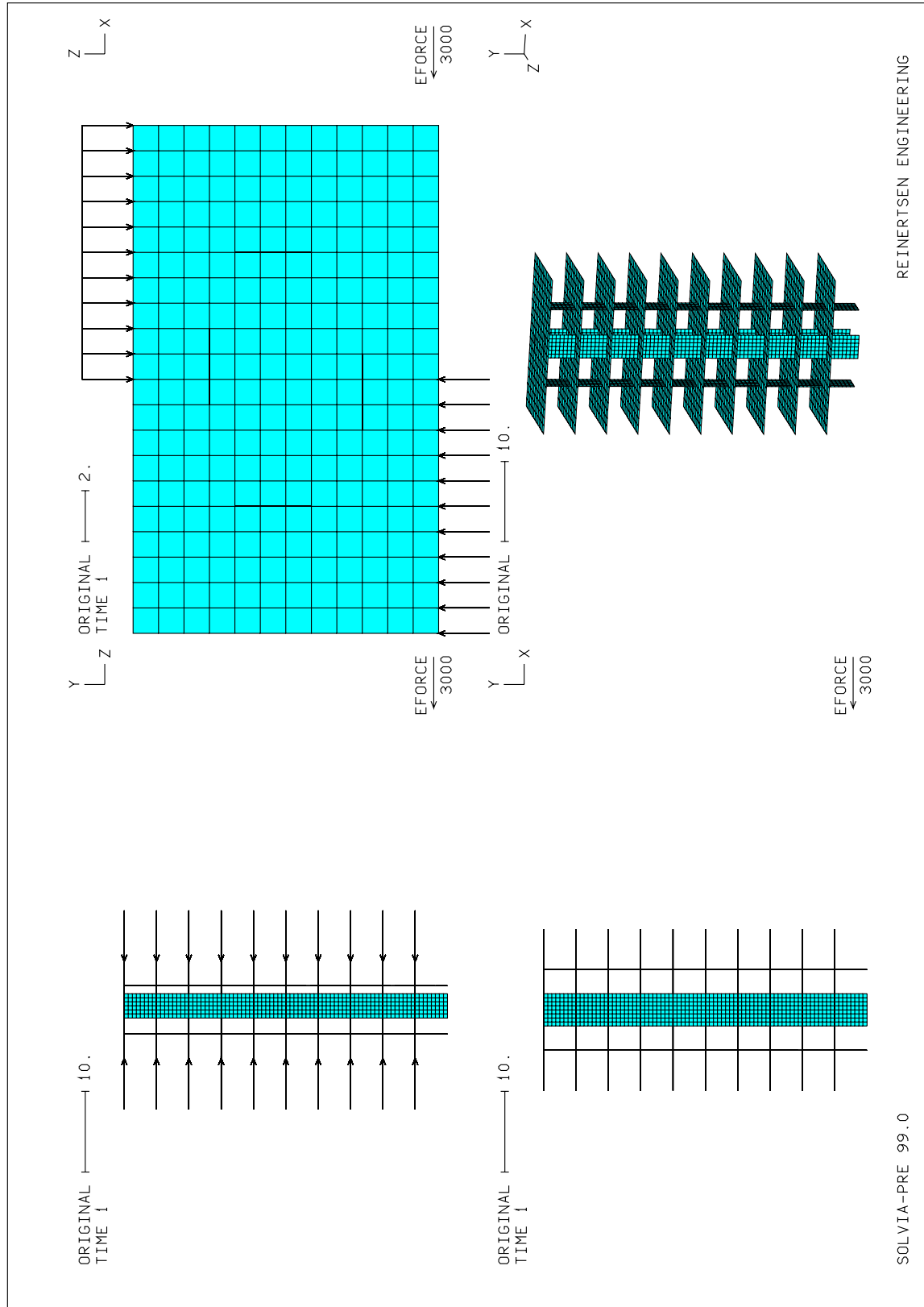
Floor slab: $E = 2\text{Gpa}$ $t = 0.1\text{ m}$



APPENDIX D.2 Force distribution in a multi-storey structure

Load applications and figure illustrations. Case 2b – Twisting

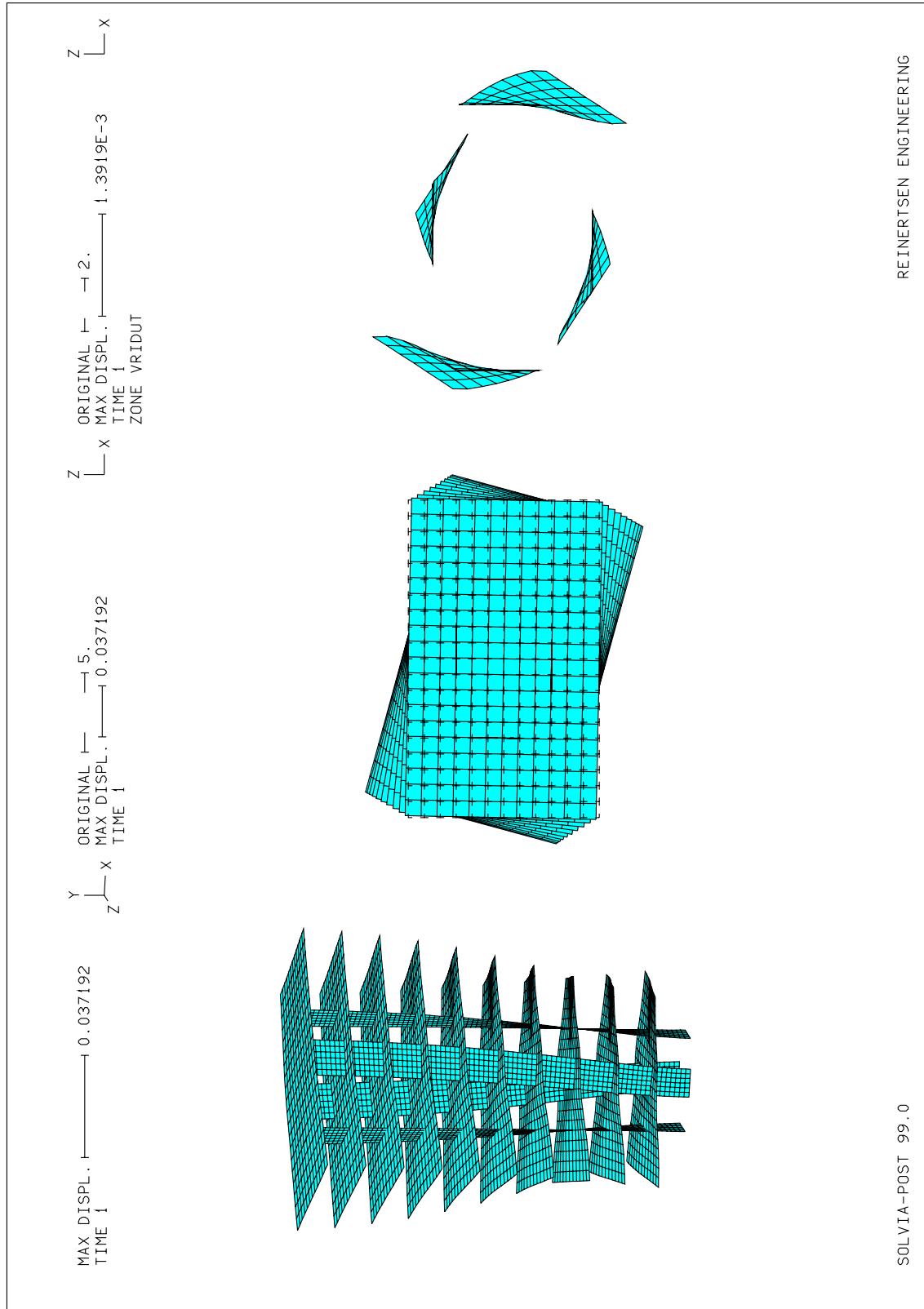
Floor slab: $E = 30 \text{ Gpa}$ $t = 0.3 \text{ m}$



APPENDIX D.2 Force distribution in a multi-storey structure

Deformation figures. Case 2b – Twisting

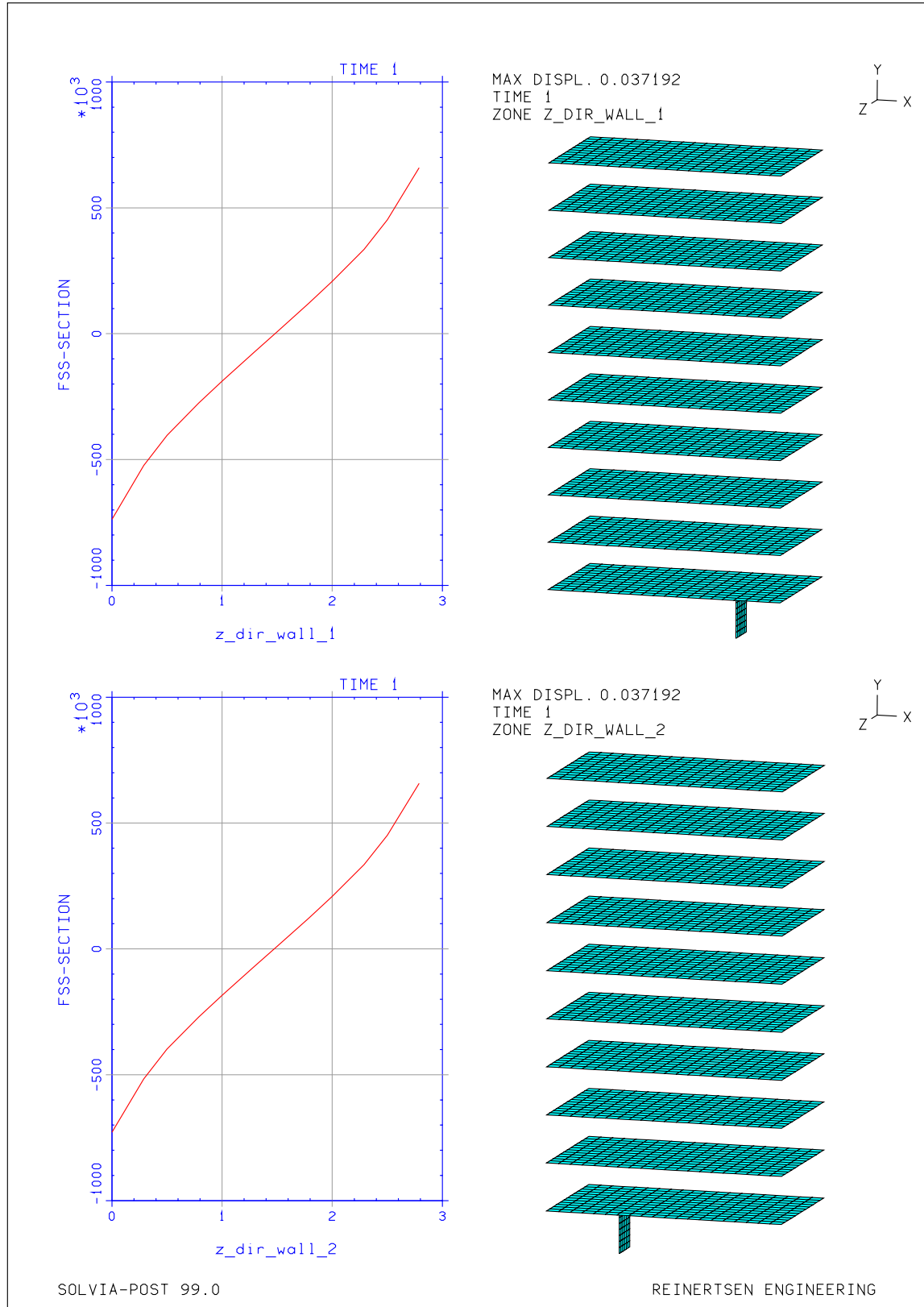
Floor slab: $E = 30 \text{ Gpa}$ $t = 0.3 \text{ m}$



APPENDIX D.2 Force distribution in a multi-storey structure

Load distribution in wall 1 and 2. Case 2b – Twisting

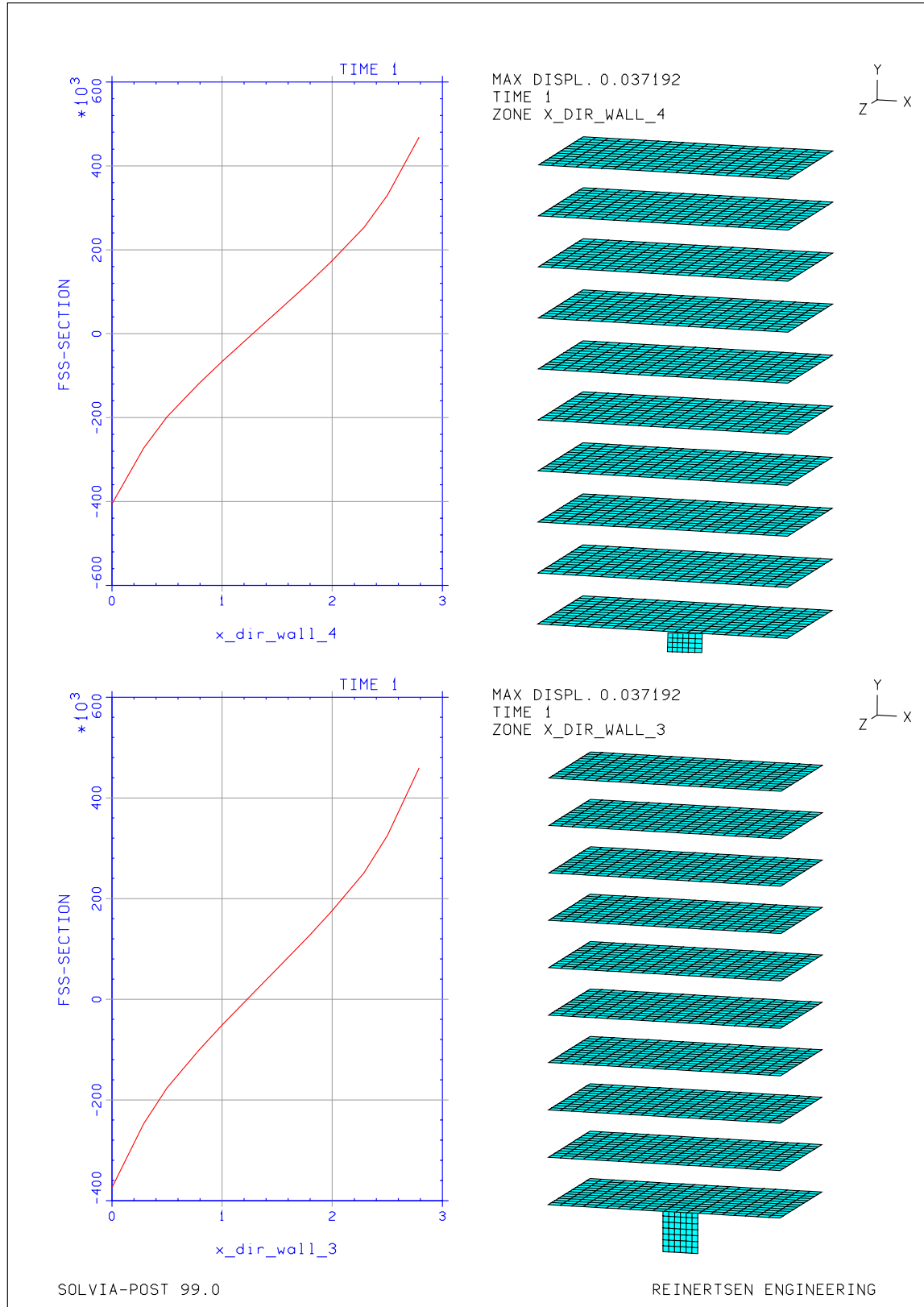
Floor slab: $E = 30 \text{ Gpa}$ $t = 0.3 \text{ m}$



APPENDIX D.2 Force distribution in a multi-storey structure

Load distribution in wall 3 and 4. Case 2b – Twisting

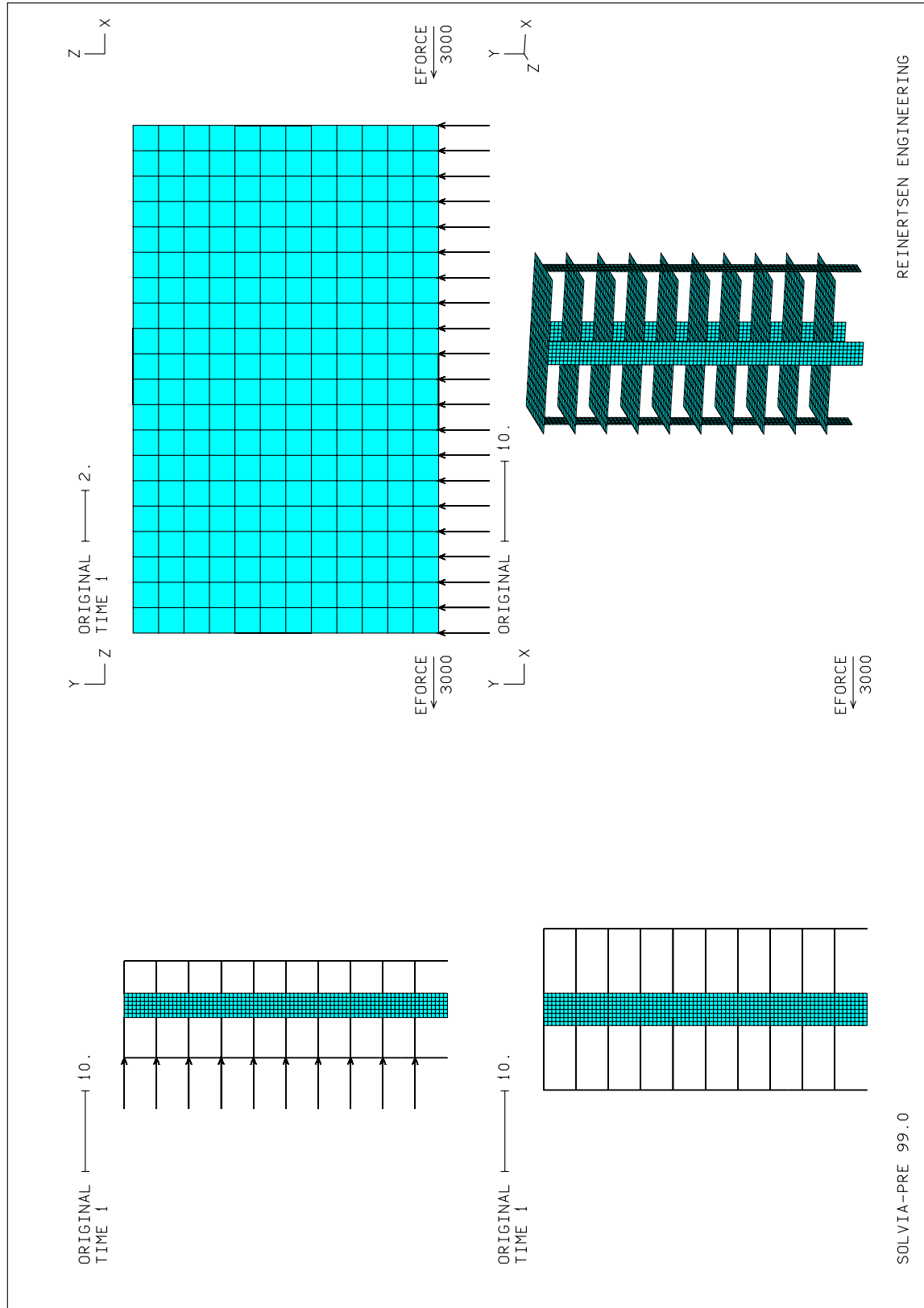
Floor slab: $E = 30 \text{ Gpa}$ $t = 0.3 \text{ m}$



APPENDIX D.3 Force distribution in a multi-storey structure

Load applications and figure illustrations. Case 1a – Translation

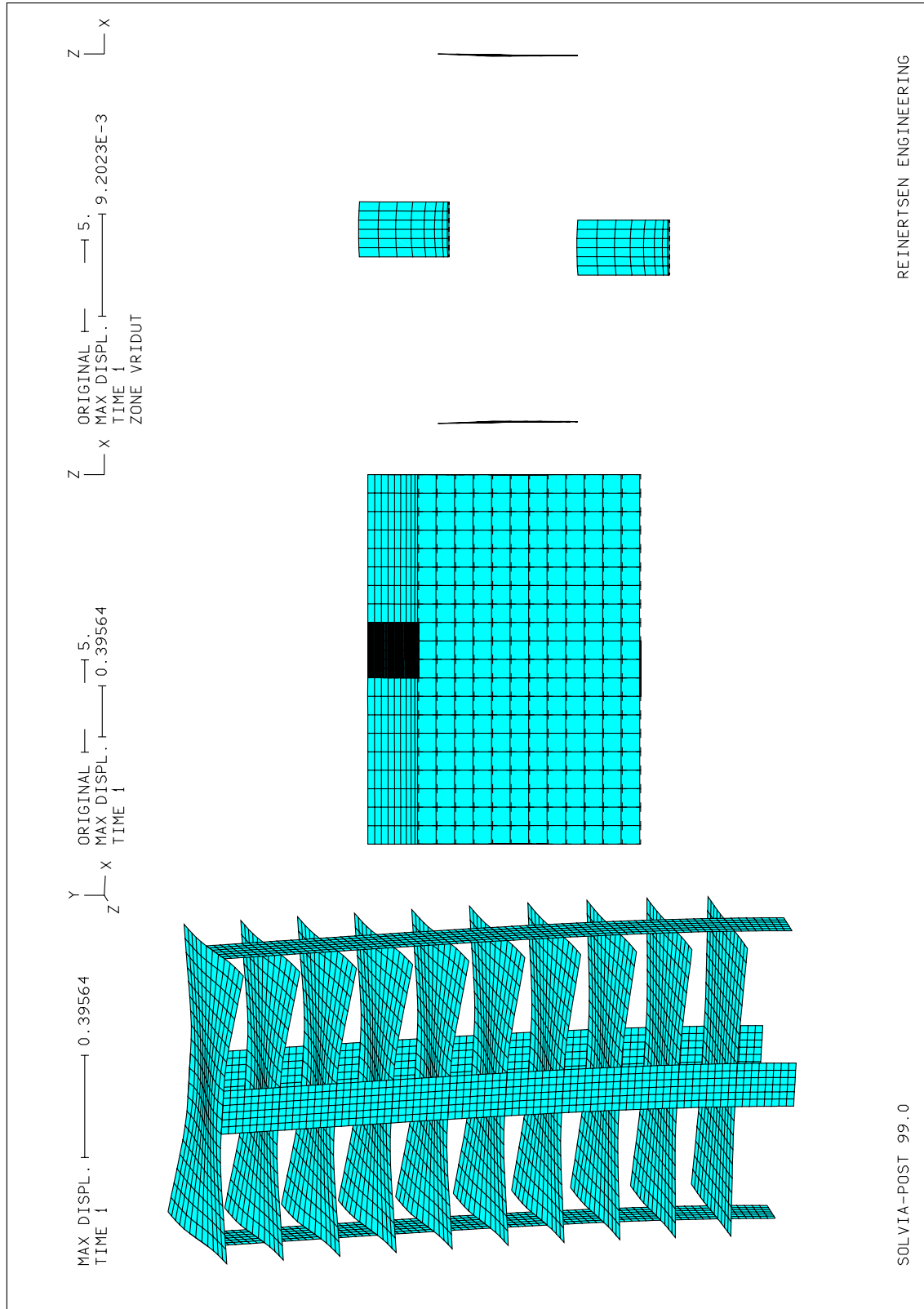
Floor slab: $E = 1 \text{ Gpa}$ $t = 0.1 \text{ m}$



APPENDIX D.3 Force distribution in a multi-storey structure

Deformation figures. Case 1a – Translation

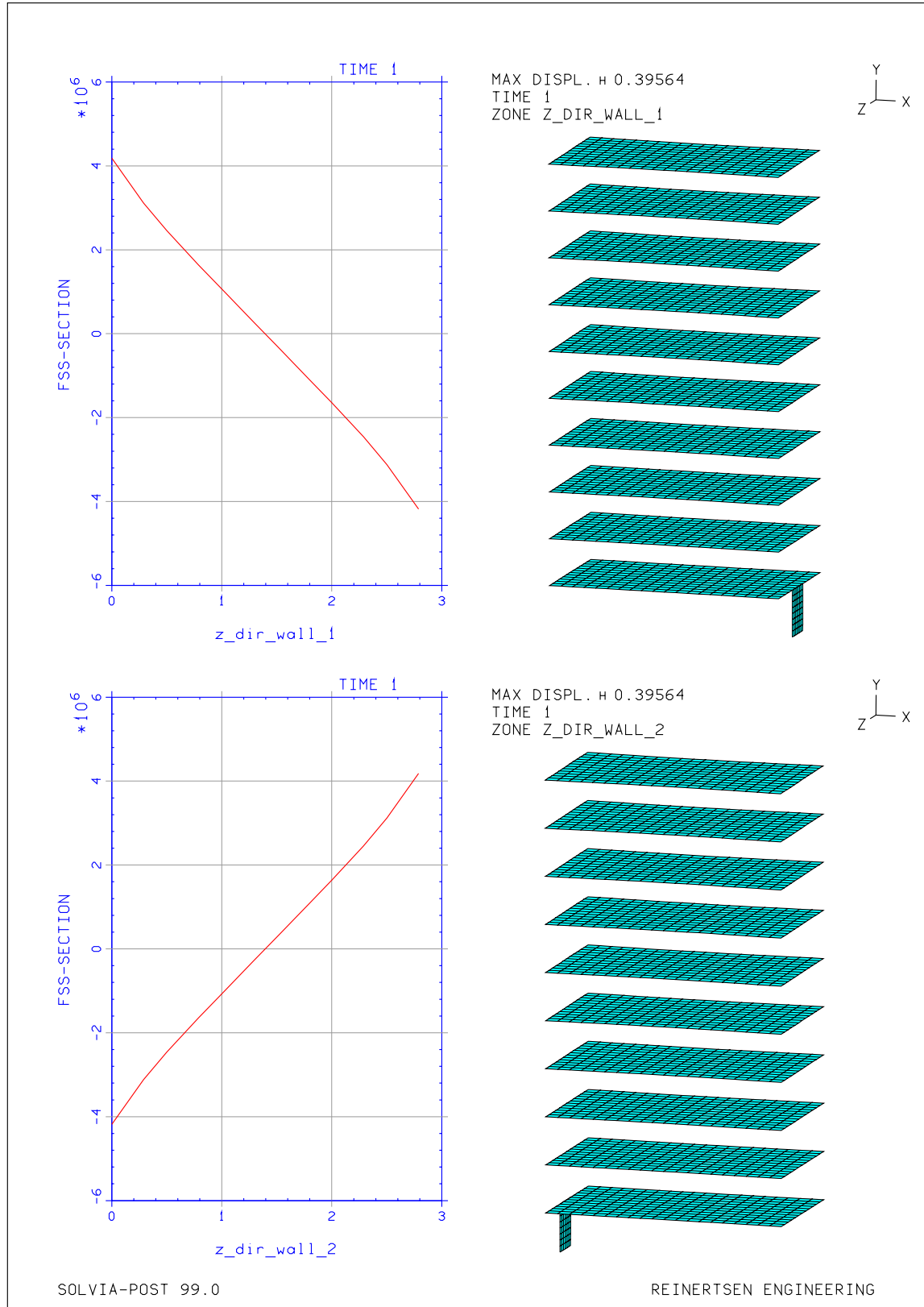
Floor slab: $E = 1 \text{ Gpa}$ $t = 0.1 \text{ m}$



APPENDIX D.3 Force distribution in a multi-storey structure

Force distribution in wall 1 and 2. Case 1a – Translation

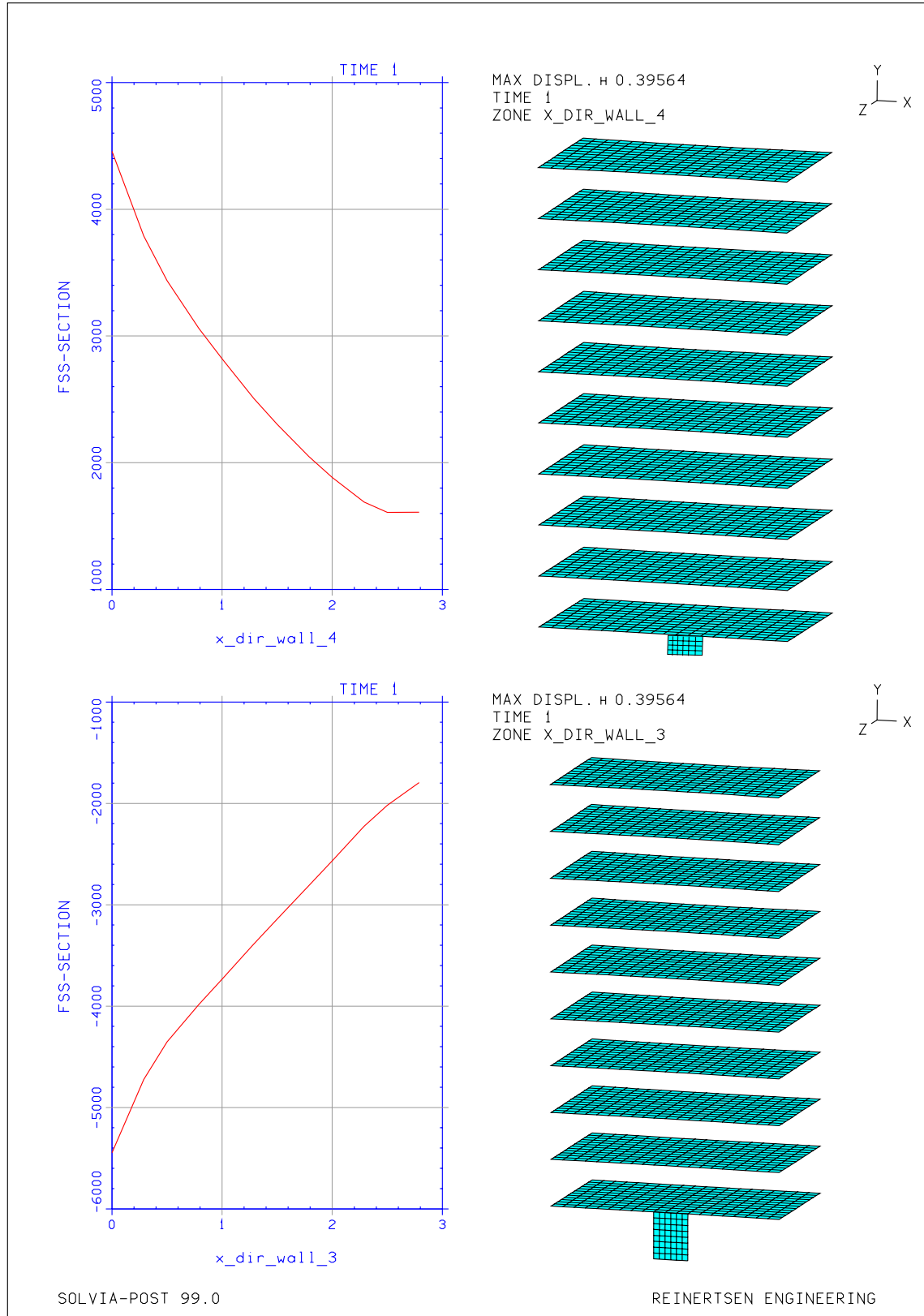
Floor slab: $E = 1 \text{ Gpa}$ $t = 0.1 \text{ m}$



APPENDIX D.3 Force distribution in a multi-storey structure

Force distribution in wall 3 and 4. Case 1a – Translation

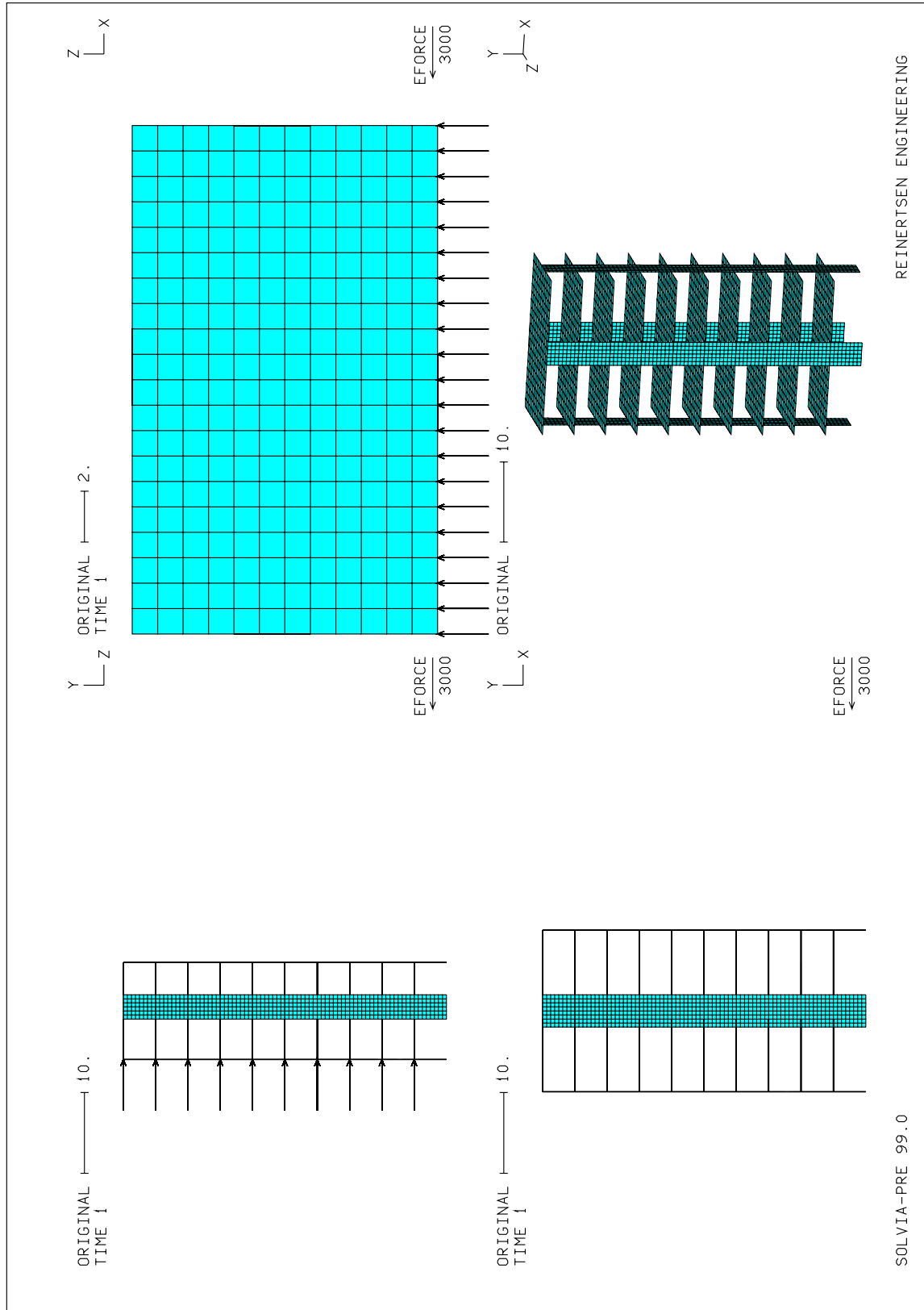
Floor slab: $E = 1 \text{ Gpa}$ $t = 0.1 \text{ m}$



APPENDIX D.3 Force distribution in a multi-storey structure

Load applications and figure illustrations. Case 1a – Translation

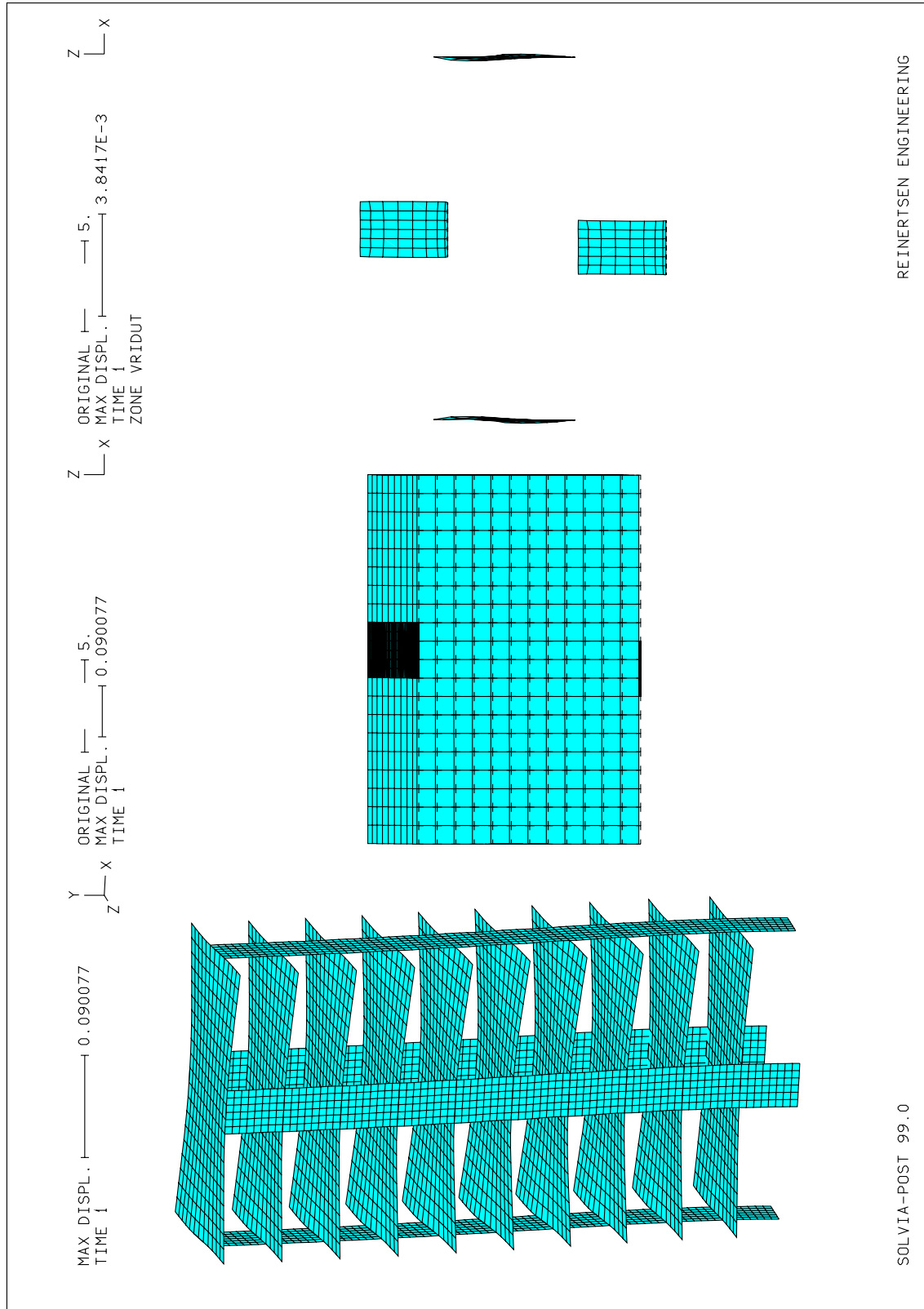
Floor slab: $E = 30 \text{ Gpa}$ $t = 0.3 \text{ m}$



APPENDIX D.3 Force distribution in a multi-storey structure

Deformation figures. Case 1a – Translation

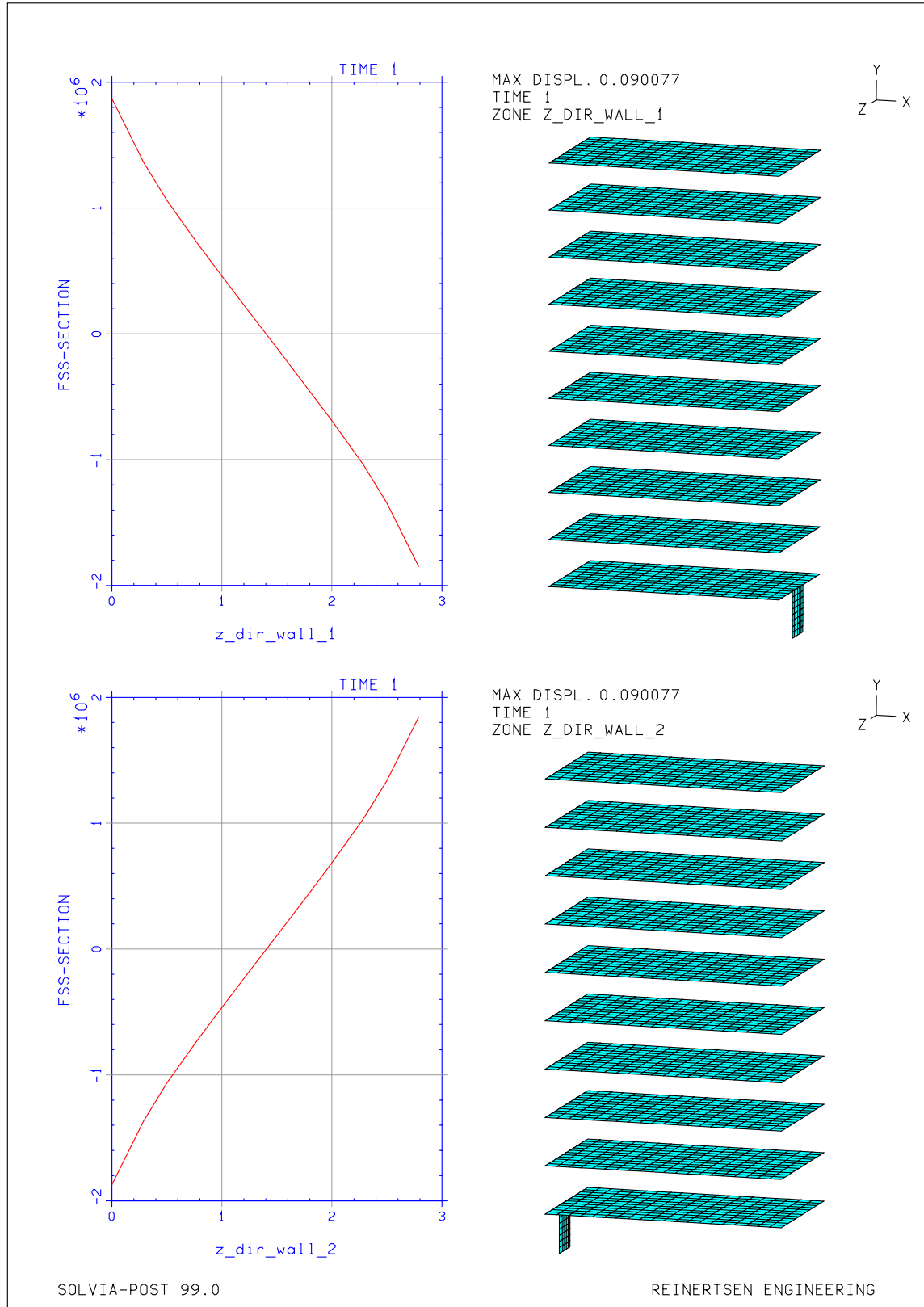
Floor slab: $E = 30 \text{ Gpa}$ $t = 0.3 \text{ m}$



APPENDIX D.3 Force distribution in a multi-storey structure

Force distribution in wall 1 and 2. Case 1a – Translation

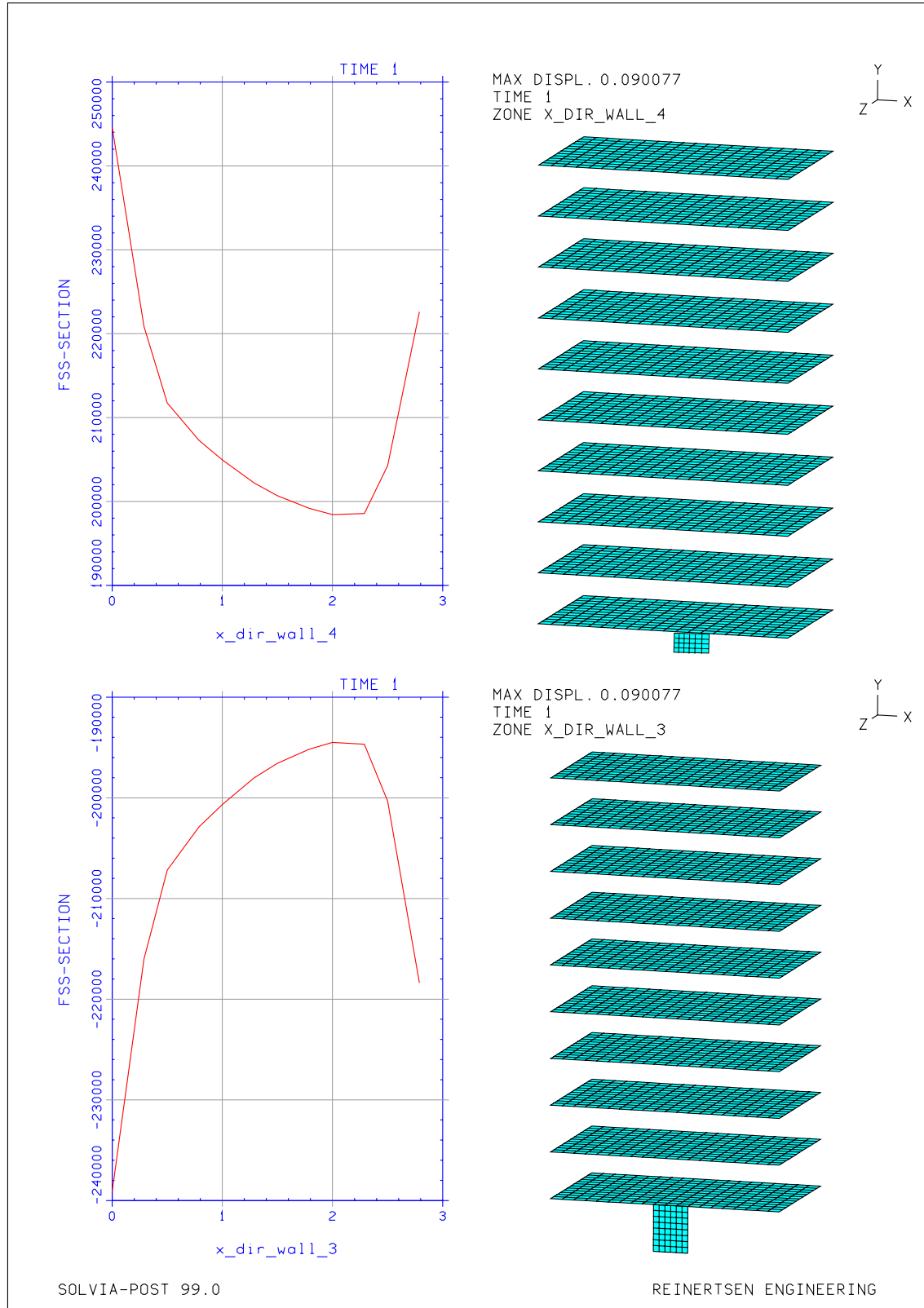
Floor slab: $E = 30 \text{ Gpa}$ $t = 0.3 \text{ m}$



APPENDIX D.3 Force distribution in a multi-storey structure

Force distribution in wall 3 and 4. Case 1a – Translation

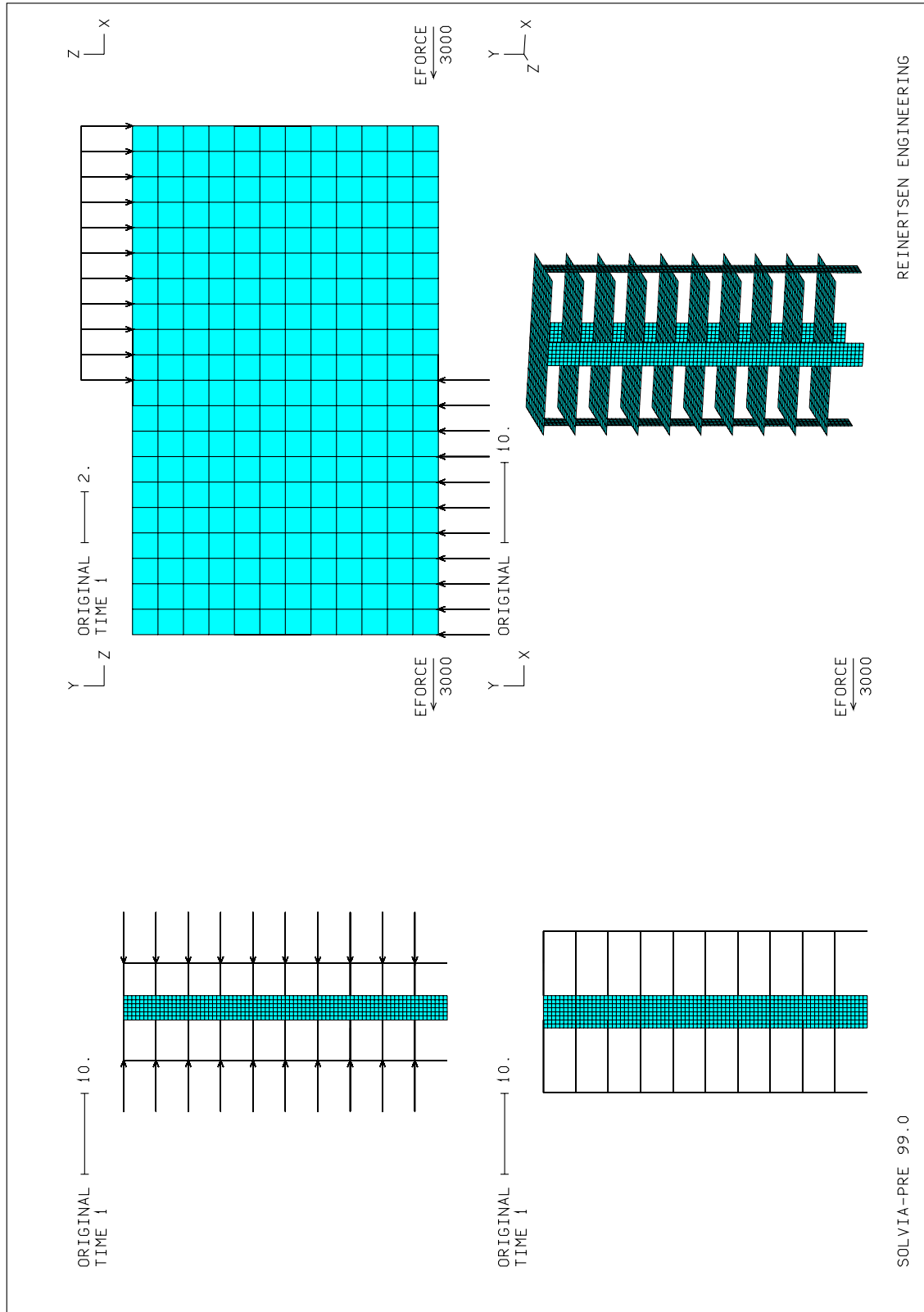
Floor slab: $E = 30 \text{ Gpa}$ $t = 0.3 \text{ m}$



APPENDIX D.4 Force distribution in a multi-storey structure

Load applications and figure illustrations. Case 2a – Twisting

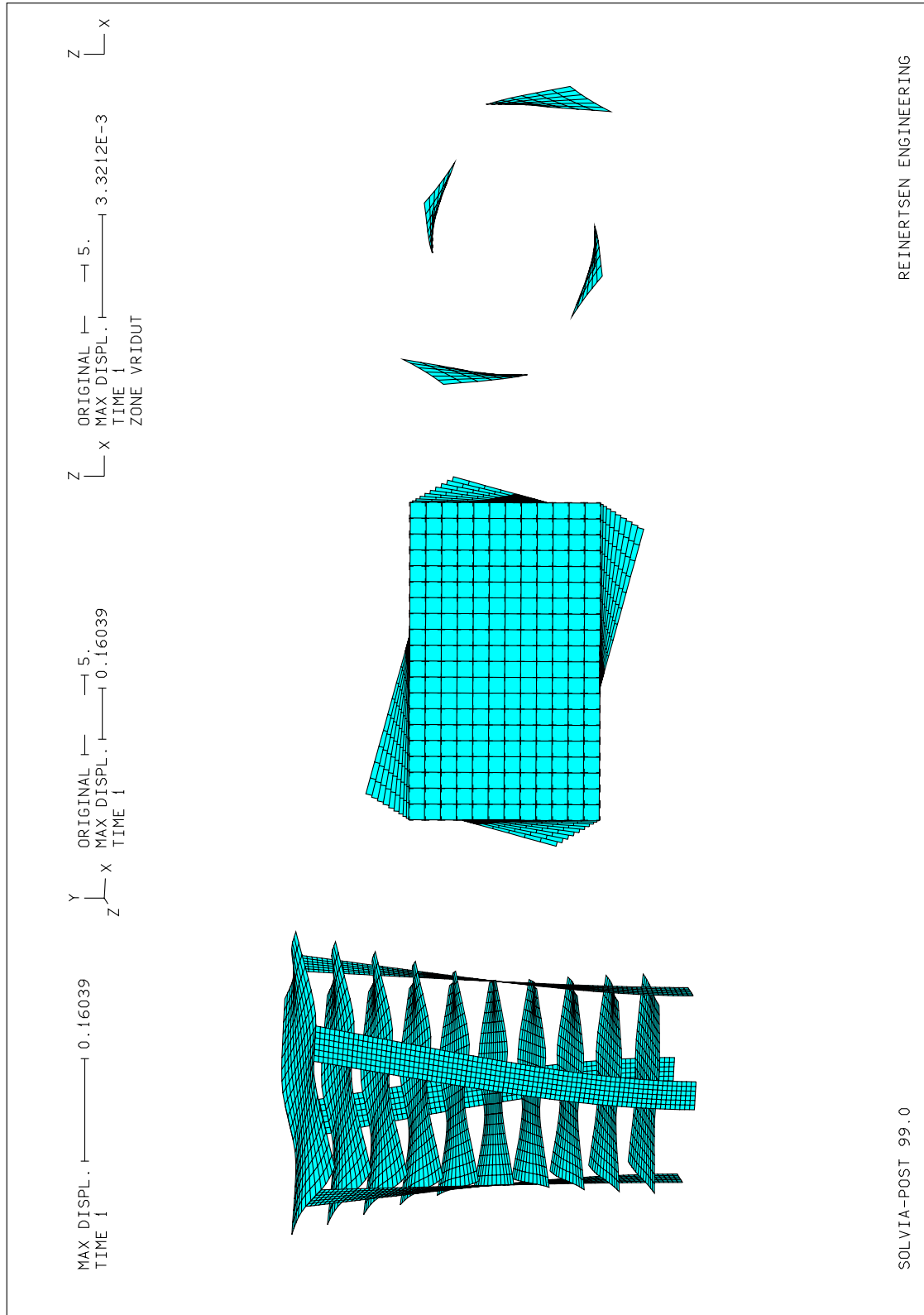
Floor slab: $E = 1 \text{ Gpa}$ $t = 0.1 \text{ m}$



APPENDIX D.4 Force distribution in a multi-storey structure

Deformation figures. Case 2a – Twisting

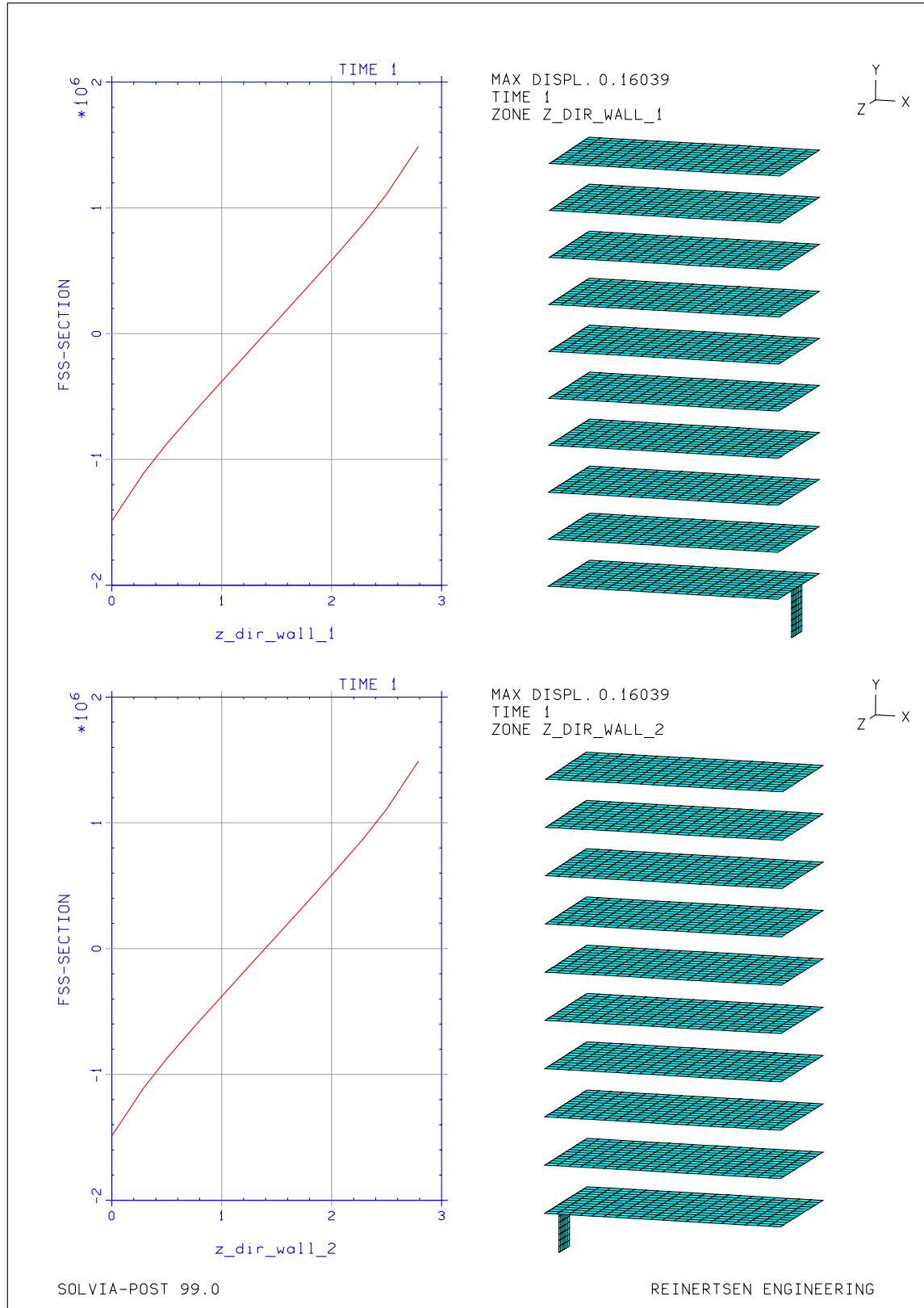
Floor slab: $E = 1 \text{ Gpa}$ $t = 0.1 \text{ m}$



APPENDIX D.4 Force distribution in a multi-storey structure

Force distribution in wall 1 and 2. Case 2a – Twisting

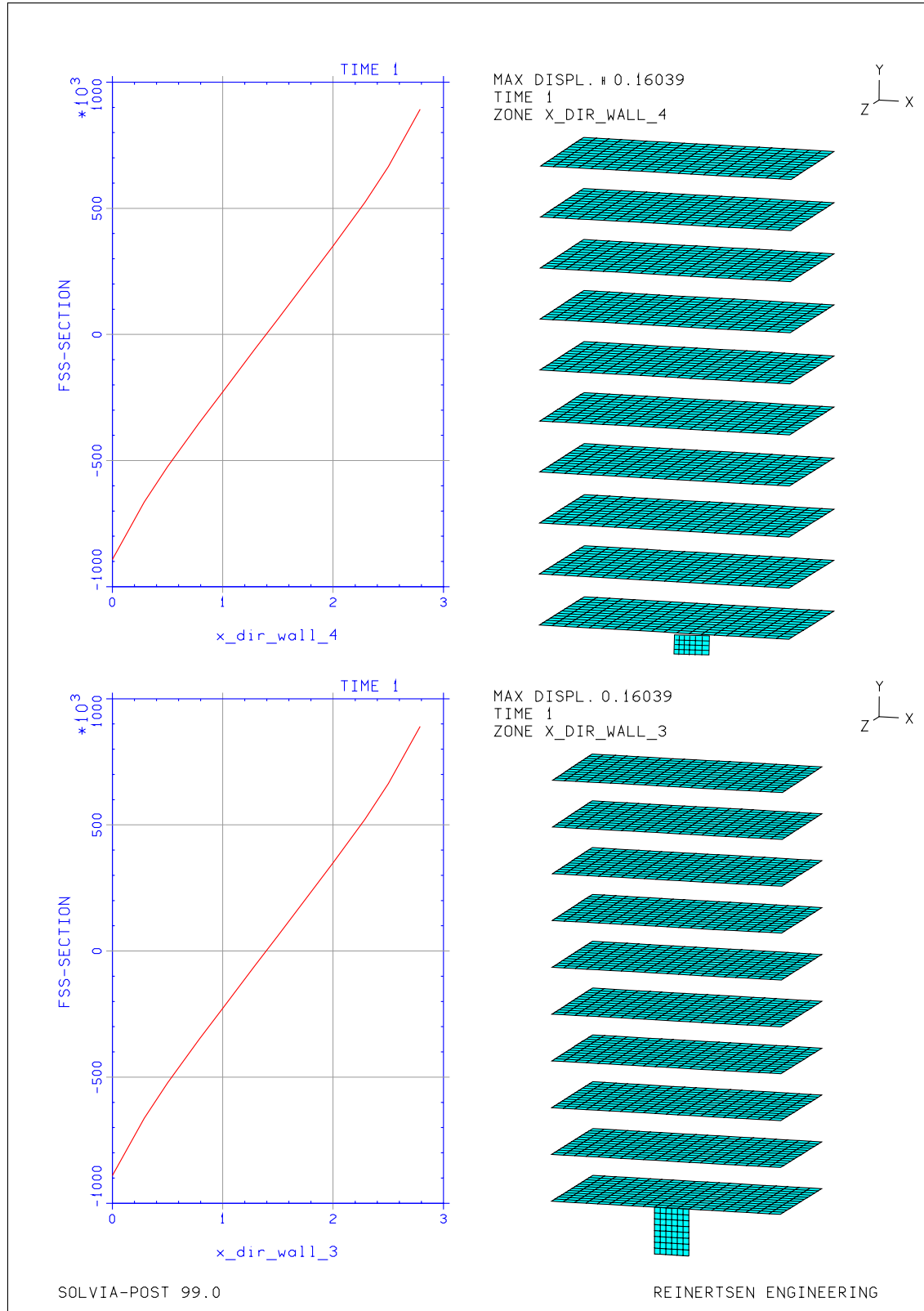
Floor slab: $E = 1 \text{ Gpa}$ $t = 0.1 \text{ m}$



APPENDIX D.4 Force distribution in a multi-storey structure

Force distribution in wall 3 and 4. Case 2a – Twisting

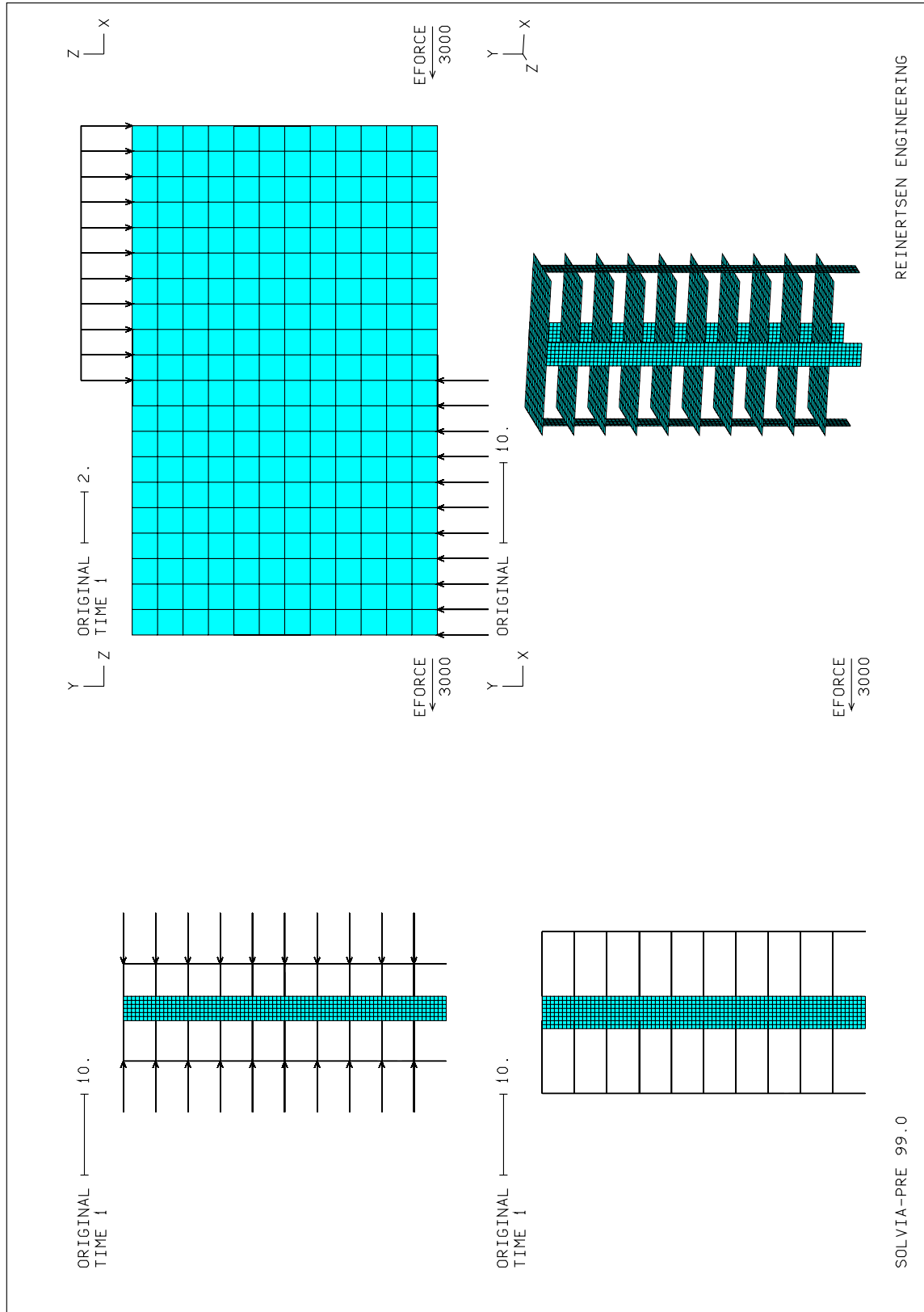
Floor slab: $E = 1 \text{ Gpa}$ $t = 0.1 \text{ m}$



APPENDIX D.4 Force distribution in a multi-storey structure

Load applications and figure illustrations. Case 2a – Twisting

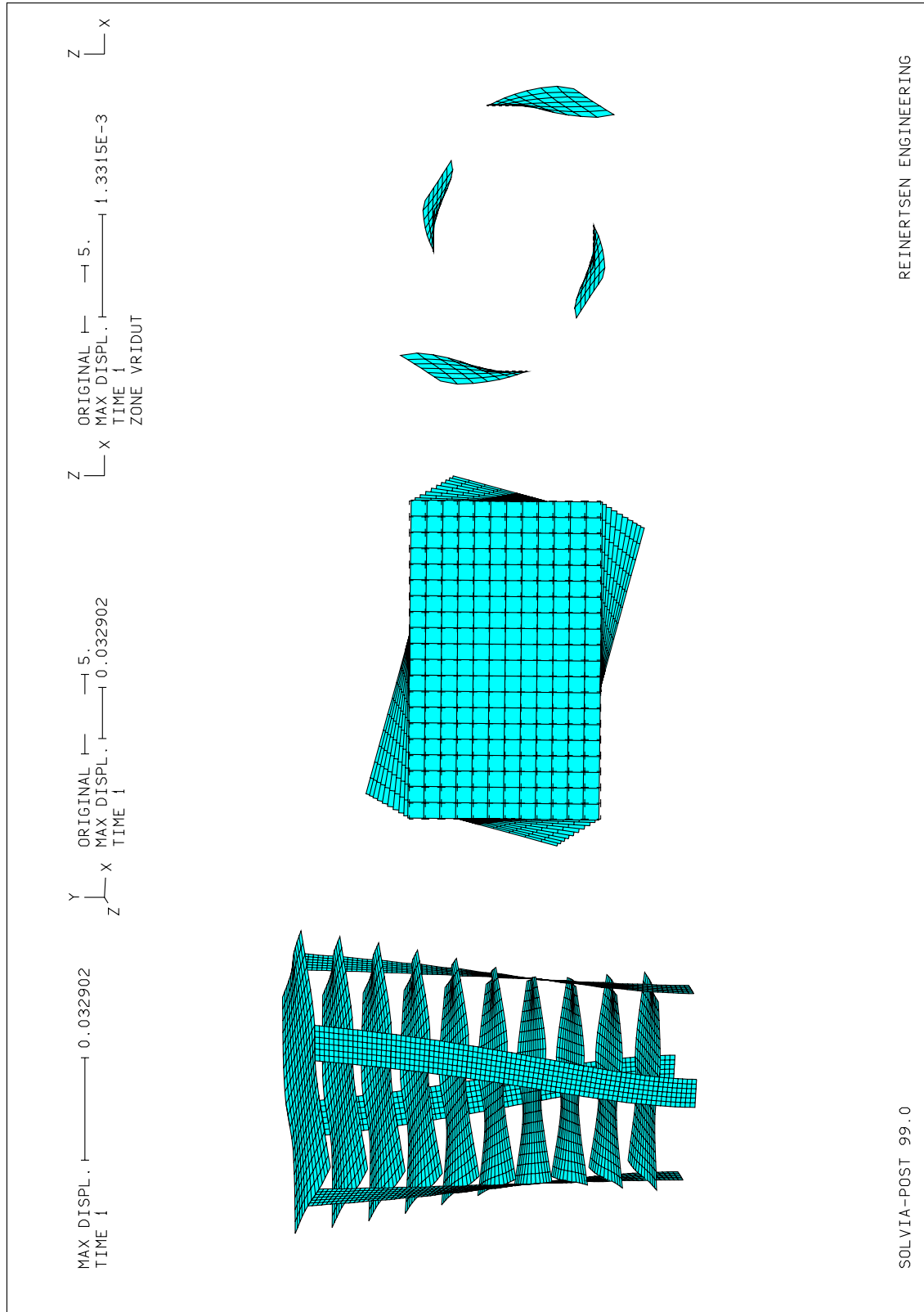
Floor slab: $E = 30 \text{ Gpa}$ $t = 0.3 \text{ m}$



APPENDIX D.4 Force distribution in a multi-storey structure

Deformation figures. Case 2a – Twisting

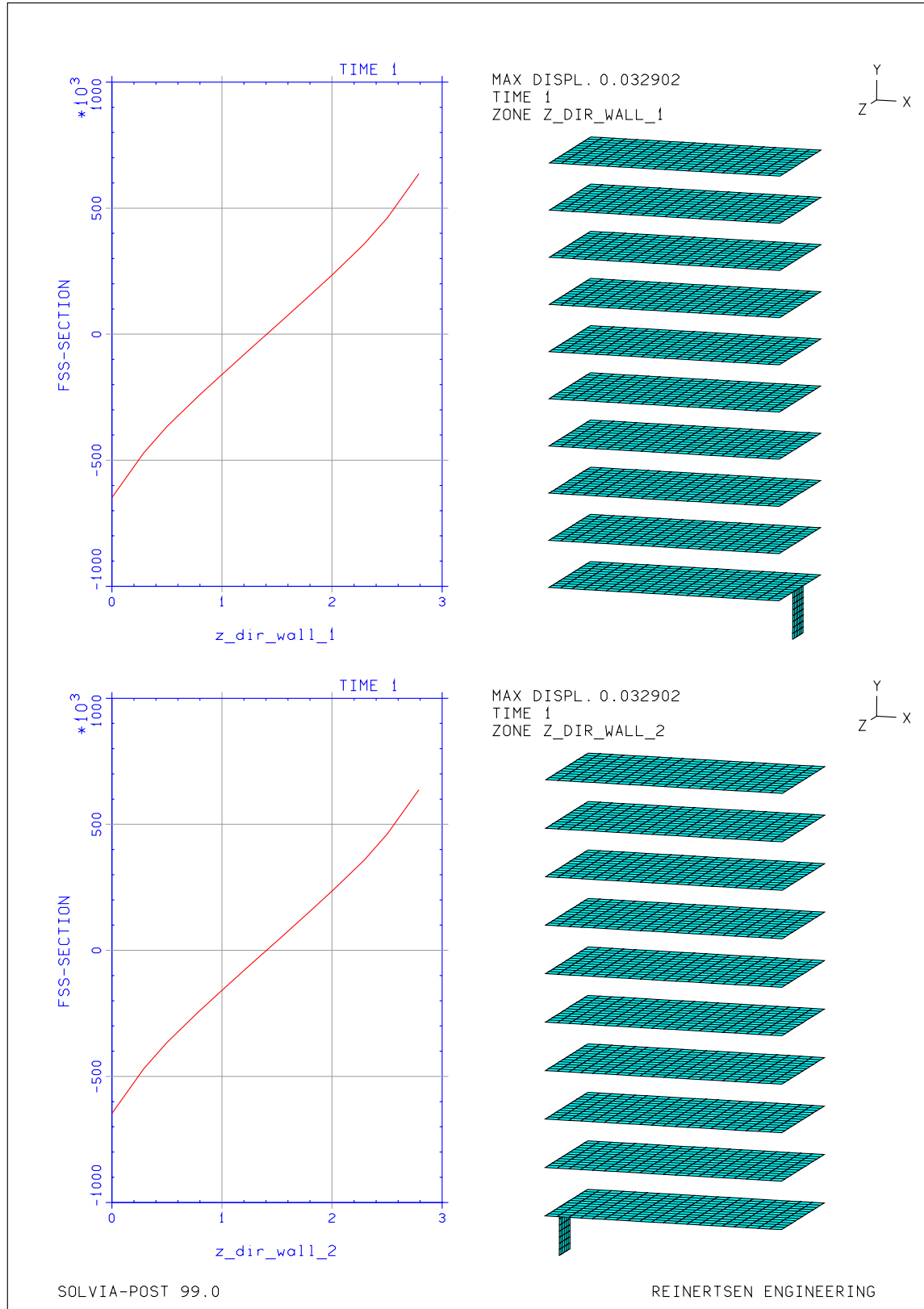
Floor slab: $E = 30 \text{ Gpa}$ $t = 0.3 \text{ m}$



APPENDIX D.4 Force distribution in a multi-storey structure

Force distribution in wall 1 and 2. Case 2a – Twisting

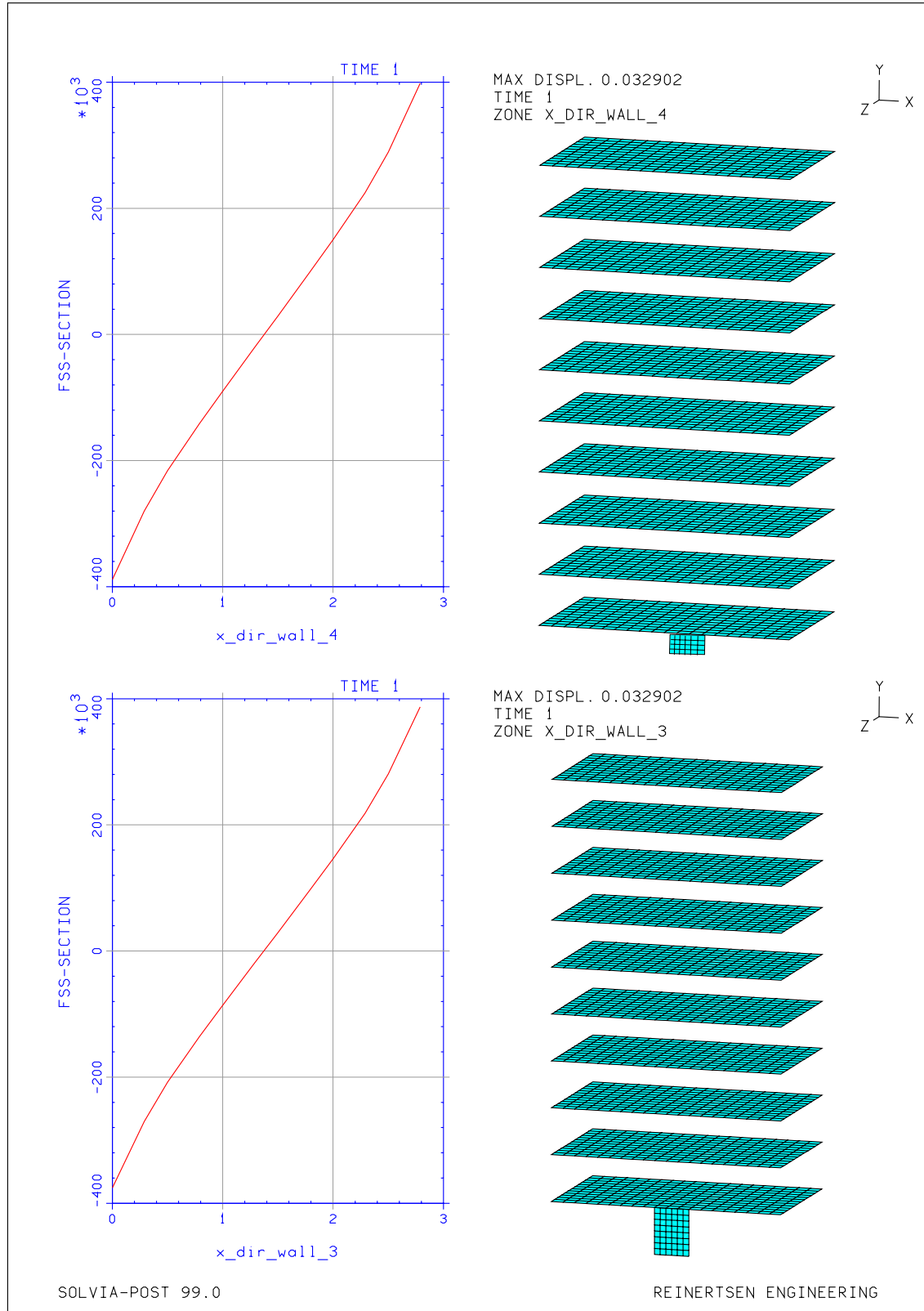
Floor slab: $E = 30 \text{ Gpa}$ $t = 0.3 \text{ m}$



APPENDIX D.4 Force distribution in a multi-storey structure

Force distribution in wall 3 and 4. Case 2a – Twisting

Floor slab: $E = 30 \text{ Gpa}$ $t = 0.3 \text{ m}$

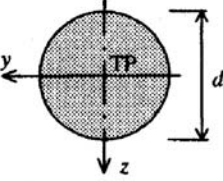
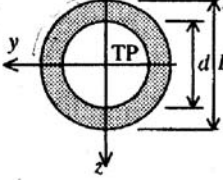
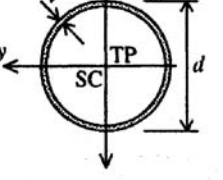
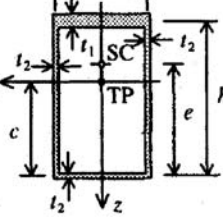
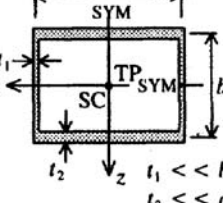


APPENDIX E Equations for coupled cross sections.

[Samuelsson & Wiberg (1995)]

c = distance to center of gravity [m]
 e = distance to rotation centre [m]
 I_y = moment of inertia around the y axis [m⁴]
 I_x = moment of inertia around the x axis [m⁴]
 K_v = factor of torsional resistance [m⁴]
 K_w = factor of warping resistance [m⁶]
 W_x = twisting resistance

	$I_y = I_z \approx \frac{2}{3}ta^3$	$e \approx \frac{5}{8}a$ $K_v \approx \frac{4}{3}t^3a$ $K_w \approx \frac{47}{96}ta^5 \approx 0,490ta^5$ $W_x \approx \frac{4}{3}t^2a$
	$c \approx b \frac{ht_h + bt_b}{ht_h + 2bt_b}$ $I_y \approx \frac{t_b b^3}{6} + 2t_b b \left(c - \frac{b}{2} \right)^2 + t_h h (b - c)^2$ $I_z \approx \frac{t_h h^3}{12} + \frac{1}{2} t_b b h^2$	$e \approx \frac{3b^2 t_b}{6bt_b + ht_h}$ $K_v \approx \frac{2t_b^3 b + t_h^3 h}{3}$ $K_w \approx \frac{t_b b^3 h^2}{12} \cdot \frac{3bt_b + 2ht_h}{6bt_b + ht_h}$ $W_x \approx \frac{2t_b^3 b + t_h^3 h}{3t_{\max}}$
	$c \approx \frac{a\sqrt{2}}{4}$ $I_y \approx \frac{ta^3}{12}$ $I_z \approx \frac{ta^3}{3}$	$K_v \approx \frac{2t^3 a}{3}$ $K_w \approx 0$ $W_x \approx \frac{2t^2 a}{3}$

	$I_y = I_z = \frac{\pi d^4}{64} = \frac{\pi r^4}{4}$	$K_v = \frac{\pi d^4}{32} = \frac{\pi r^4}{2}$ $K_w = 0$ $W_x = \frac{\pi d^3}{16}$
	$I_y = I_z = \frac{\pi(D^4 - d^4)}{64} = \frac{\pi(R^4 - r^4)}{4}$	$K_v = \frac{\pi(D^4 - d^4)}{32} = \frac{\pi(R^4 - r^4)}{2}$ $K_w = 0$ $W_x = \frac{\pi(D^4 - d^4)}{16D} = \frac{\pi(R^4 - r^4)}{2R}$
	$I_y = I_z \approx \frac{\pi d^3 t}{8} = \pi r^3$	$K_v = \frac{\pi d^3 t}{4} = 2\pi r^3 t$ $K_w = 0$ $W_x = \frac{\pi d^2 t}{2} = 2\pi r^2 t$
	$c = \frac{h^2 t_2 + b h t_1}{(2h + b)t_2 + b t_1}$ $I_y = \frac{t_2 h^3}{6} + 2t_2 h \left(\frac{h}{2} - c\right)^2 + b t_2 c^2 + b t_1 (h - c)^2$ $I_z = \frac{(t_2 + t_1) b^3}{12} + \frac{t_2 h b^2}{2}$	$e \approx \frac{1}{36 I_z} [6 h^2 b^2 t_1 + 3 h b^3 t_1 + 3 h^2 b^2 t_2]$ $K_v = \frac{4 b^2 h^2}{\frac{b}{t_1} + \frac{b}{t_2} + \frac{2h}{t_2}}$ $K_w \approx 0$ $W_x \approx 2 h b t_2$
	$I_y = \frac{t_1 b^3}{6} + \frac{1}{2} t_2 a b^2$ $I_z = \frac{t_2 a^3}{6} + \frac{1}{2} t_1 b a^2$	$K_v = \frac{2 a^2 b^2}{\frac{b}{t_1} + \frac{a}{t_2}}$ $K_w \approx 0$ $W_x \approx 2 a b t_1$

APPENDIX F Calculation of buckling load in MATHCAD

Variables :

$$t := 0.5 \quad b_0 := 6 \quad ht := 1.2 \quad c_0 := 2 \quad L := 3 \quad (\text{m}) \quad E := 30 \cdot 10^9 \quad \text{Pa} \quad \xi := 1.2$$

Calculations of variables:

$$b := b_0 - \frac{(b_0 - c_0)}{2} \quad b = 4 \quad \text{m} \quad c := c_0 + ht \quad c = 3.2 \quad \text{m} \quad G := 0.4 \cdot E \quad G = 1.2 \times 10^{10} \quad \text{Pa}$$

$$A_t := ht \cdot t \quad A_t = 0.6 \quad \text{m}^2 \quad A_v := t \cdot (b_0 - b) \quad A_v = 1 \quad \text{m}^2$$

$$I_t := t \cdot \frac{ht^3}{12} \quad I_t = 0.072 \quad \text{m}^4 \quad I_v := t \cdot \frac{(b_0 - b)^3}{12} \quad I_v = 0.333 \quad \text{m}^4$$

$$I_{\text{global}} := t \cdot \frac{b_0^3}{12} - t \cdot \frac{c_0^3}{12} \quad I_{\text{global}} = 8.667 \quad \text{m}^4$$

$$\text{styv} := \frac{(b - c)}{2} \quad \text{styv} = 0.4 \quad \text{m} \quad \text{Length of stiffed part}$$

Critical Buckling load due to Shear:

$$\gamma_{\text{tbend}} := L \cdot \frac{c^3}{12 \cdot b^2 \cdot E \cdot I_t} \quad \gamma_{\text{tbend}} = 2.37 \times 10^{-10} \quad \text{rad}$$

$$\gamma_{\text{vbend}} := \frac{L^2}{24 \cdot E \cdot I_v} \quad \gamma_{\text{vbend}} = 3.75 \times 10^{-11} \quad \text{rad}$$

$$\gamma_{\text{tshear}} := \xi \cdot L \cdot \frac{c}{b^2 \cdot G \cdot A_t} \quad \gamma_{\text{tshear}} = 1 \times 10^{-10} \quad \text{rad}$$

$$\gamma_{\text{vshear}} := \frac{\xi}{2 \cdot G \cdot A_v} \quad \gamma_{\text{vshear}} = 5 \times 10^{-11} \quad \text{rad}$$

$$\gamma_{\text{tot}} := \gamma_{\text{tbend}} + \gamma_{\text{vbend}} + \gamma_{\text{tshear}} + \gamma_{\text{vshear}} \quad \gamma_{\text{tot}} = 4.245 \times 10^{-10} \quad \text{rad}$$

$$N_{\text{crS}} := \frac{1}{\gamma_{\text{tot}}} \quad N_{\text{crS}} = 2.356 \times 10^9 \quad \text{N}$$

Critical buckling load due to bending:

$$\text{vant} := 10 \quad k := 6.8 \quad L_h := \text{vant} \cdot L \quad L_h = 30 \quad \text{m}$$

$$N_{\text{crB}} := k \cdot E \cdot \frac{I_{\text{global}}}{L_h^2} \quad N_{\text{crB}} = 1.964 \times 10^9 \quad \text{N}$$

Total critical buckling load:

$$N_{\text{crTOT}} := \frac{1}{\frac{1}{N_{\text{crB}}} + \frac{1}{N_{\text{crS}}}} \quad N_{\text{crTOT}} = 1.071 \times 10^9 \quad \text{N}$$

Critical buckling load for a solid wall with the same values:

Critical Buckling load due to Bending:

$$N_{crsolidb} := k \cdot E \cdot t \cdot \frac{b_0^3}{12 \cdot Lh^2} \quad N_{crsolidb} = 2.04 \times 10^9 \quad N$$

Critical Buckling load due to Shear:

$$N_{crsolids} := G \cdot b_0 \cdot \frac{t}{1.2} \quad N_{crsolids} = 3 \times 10^{10} \quad N$$

Total critical buckling load

$$N_{crsolidtot} := \frac{1}{\left(\frac{1}{N_{crsolidb}} + \frac{1}{N_{crsolids}} \right)} \quad N_{crsolidtot} = 1.91 \times 10^9 \quad N$$

Critical buckling load for two separate walls/towers:

$$b_{tower} := b_0 - b \quad b_{tower} = 2 \quad m \quad I_{tower} := t \cdot \frac{b_{tower}^3}{12} \quad I_{tower} = 0.333 \quad m^4$$

Critical Buckling load due to Bending:

$$N_{crtowerb} := k \cdot E \cdot \frac{I_{tower}}{Lh^2} \quad N_{crtowerb} = 7.556 \times 10^7 \quad N$$

Critical Buckling load due to Shear:

$$N_{crtowers} := G \cdot b_{tower} \cdot \frac{t}{\xi} \quad N_{crtowers} = 1 \times 10^{10} \quad N$$

Total critical buckling load:

$$N_{crtowertot} := \frac{1}{\frac{1}{N_{crtowerb}} + \frac{1}{N_{crtowers}}} \cdot 2 \quad N_{crtowertot} = 1.5 \times 10^8 \quad N$$

Comparisons :

Pierced wall : $N_{crTOT} = 1.071 \times 10^9 \quad N$

Solid : $N_{crsolidtot} = 1.91 \times 10^9 \quad N$

Seperate walls $N_{crtowertot} = 1.5 \times 10^8 \quad N$